Physical and Chemical Mechanisms of Direct and Controllable

Plasma Interaction with Living Objects

A Thesis

Submitted to the Faculty

of

Drexel University

by

Danil Dobrynin

in partial fulfillment of the

requirements for the degree

of

Doctor of Philosophy

May 2011

ACKNOWLEDGMENTS

I would like to thank my thesis advisors, Dr. Alexander Fridman and Dr. Gennady Friedman, for all their help and guidance throughout the time of my doctoral studies. My colleagues, coworkers, and friends were also an integral part of my development and without the help of all who surround me I would have never been able to complete this work.

I would especially like to thank Dr. Gregory Fridman, Dr. Alexander Gutsol, Dr. Andrey Starikovskii, Dr. Richard Rest, Dr. Ari Brooks, Graduate students: Kalyan Chakravarthy, Krishna Priya Arjunan, Natalie Shainsky, Yong Yang, Sin Park, Brian Dirks, Vladimir Ignakhin, Kirill Gutsol, Meghan Wynosky-Dolfi, Judy Rieger; Dr. Sameer Kalghatgi, Dr. Moogega Cooper, Dr. HalimAyan, Dr. Andrew Wu, Dr. David Staack, Dustin Doss, Dr. Mike Gallagher, Dr. Suresh Joshi, Kimberly Wasko, Dr. Yurii Mukhin, Dr. Alexander Rabinovich, Dr. Sreekant Murthy, Dr. Alisa Morss-Clyne, Dr. Young Cho, Dr. Alexandra Borisova, Dr. Kenneth Barbee; faculty and staff at Drexel University and Petrozavodsk State University, especially Dr. Valery Gostev, who introduced me into the field of plasma engineering and plasma medicine; and of course my encouraging family: Dr. Oksana Dobrynina, Valery Dobrynin, Kirill and Alexander.

TABLE OF CONTENTS

LIST OF TABLES

LIST OF FIGURES

ABSTRACT

Physical and Chemical Mechanisms of Direct and Controllable

Plasma Interaction with Living Objects

Danil Dobrynin

The number of potential applications of non-equilibrium atmospheric pressure discharges in biology and medicine has grown significantly in recent years; in fact, the activity in this direction lead to the formation of a new field in plasma chemistry titled `Plasma Medicine'. It is now clear that these plasmas can have not only physical (e.g. tissue cutting and cauterization), but medically relevant therapeutic effects — plasmas can trigger a complex sequence of biological responses in tissues and cells. To move ahead in further development of actual commercial tools that will enter the hospital, and in finding novel and perhaps even unexpected uses of these plasmas an understanding of mechanisms of interaction of non-equilibrium gas discharges with living organisms, tissues, and cells becomes essential.

This thesis is focused on understanding of the mechanisms of plasma interaction with living objects using a threefold approach: physical, chemical, and biological. First, a physical characterization of a novel microsecond spark discharge ignited in a pin-to-hole electrode configuration is performed. This provides ground for deeper understanding of the physical mechanisms of plasma effects of biological objects, and further adjustment of the discharge for specific applications. A series of *in vitro* and *in vivo* experiments on inactivation of bacteria and spores using various types of plasma discharges adds understanding of physicochemical plasma biodecontamination mechanisms. Based on the

results of this study, an initial model of such mechanisms is proposed. Results of i*n vitro* and *ex vivo* experiments show that plasmas are able to produce a number of various reactive species in gas phase, as well as deliver these species into liquid phase and into tissues. Depth of plasma effect penetration is shown to be on the order of several millimeters. Based on these results, an *in vitro* physicochemical model of tissue is proposed. Biological safety of plasma treatment is revealed through a series of differential skin toxicity trials on live mouse and rat skin tissue, live pig skin tissue, and in an open wound model on pigs. Plasma ability to coagulate blood, decontaminate and accelerate wound healing is shown in a series of *in vivo* experiments using live rat animal models. The first invasive plasma application for treatment of gastroenterological diseases is presented.

CHAPTER 1. PLASMA MEDICINE: BACKGROUND

Progress in various engineering technologies and physical sciences, for example, microelectronics, optics, material sciences, and nanotechnology, resulted in development of new methods and directions in life sciences. In the last decade, plasma technology is emerging worldwide as an independent medical field— Plasma Medicine, which now may be compared to the launch of laser technology into medicine years ago. Plasma medicine can be subdivided into three main fields: plasma-assisted modification of biorelevant surfaces, plasma-based biodecontamination and sterilization, and direct therapeutic plasma application.

Surface modification and decontamination are more or less indirect medical plasma applications where plasma technology is used to process material or devices for subsequent medical applications. In contrast to that, the aim of therapeutic plasma application as the central field of plasma medicine is to bring physical plasmas directly on or in a human (or animal) body. Particularly for this very innovative field, the fundamental knowledge of the mechanisms of plasma interaction with living cells and tissue is essential as a scientific basis. Worldwide, it is the aim of several research institutes and associations (INP Greifswald, Germany, Max-Plank Institute, Germany, McGill University, Canada, University of California, Berkley, CA, Montreal University, Canada, Osaka University, Japan, Old Dominion University, VA, Loughborough University, UK, and others) to put forward therapeutic applications of physical plasma in

different fields of medicine, like dermatology, dentistry, surgery, traumatology, internal medicine, oncology, and several others.

In the view of the field of Plasma Medicine, development of plasma sources and plasma-based medical devices becomes extremely important, and therefore an overview of major types of plasmas used for biomedical purposes will open this chapter. It will be followed by a review of the current states of the sub-fields of plasma biodecontamination and sterilization, plasma-cell interaction and therapeutic plasma applications.

1.1. Plasma sources for biomedical applications

Biomedical application of plasmas is not only a task for medicine; it is a challenge for plasma physics as well. Therapeutic applications of plasmas assume that the plasma discharges are ignited in open air atmospheres and thus at atmospheric pressures. Adjusted plasma sources for different applications are required, and the proposed selectivity of plasma action implies a thoughtful control of the performance parameters of the plasma sources. Widely used cold plasma discharges at atmospheric pressures are still a challenge for plasma diagnostic. Usually they are small-scale (due to the Paschen law with the pressure × distance scaling), constricted or filamentary (i.e., consisting of distinct microdischarges due to the streamer-breakdown process) and transient (due to high collision rates and quenching). Additional challenge occurs due to an input of nitrogen, oxygen, and water, implying complex plasma chemistry.

During recent years, a broad spectrum of plasma sources dedicated for biomedical applications has been reported, for example, plasma needle [1], atmospheric-pressure plasma plume [2], floating-electrode dielectric barrier discharge (FE-DBD) [3,4,5,6],

atmospheric-pressure glow discharge torch [7], microhollow cathode discharge air plasma jet [8], microwave plasma torch [9], helium plasma jets [10,11,12], dielectric barrier discharge (DBD) [13], and nanosecond plasma gun [14]. Although this list is far from being comprehensive, below we will focus on the following main types of the discharges: DBD and plasma jets.

1.1.1. Dielectric Barrier Discharges

Dielectric barrier discharges are characterized by the presence of at least one isolating layer in the discharge gap [15,16]. The classical configuration is the so-called volume barrier discharges (VBD), where one or two electrodes with an isolating layer form the discharge gap. The VBD enables direct treatment of the object to be treated, i.e., the object with stray capacity is the second electrode. Since the local current is limited by the capacity of the discharge configuration, a painless treatment is possible. Special configurations of the DBD are the so-called surface discharge and the coplanar discharge. In a surface barrier discharge (SBD), both electrodes are in direct contact with the isolator. In this geometry, the plasma is formed around the electrodes on the isolator surface.

Direct application of VBDs for skin and wound treatment has been demonstrated by means of so-called floating electrode DBD (FE-DBD) plasma [3,4,5,17,18,19] by Fridman et al (Figure 1). The discharge is operated in atmospheric air, without additives of noble gases. Usually the discharge is ignited as a number of microdischarges, they tipical characteristics are shown in Table 1.
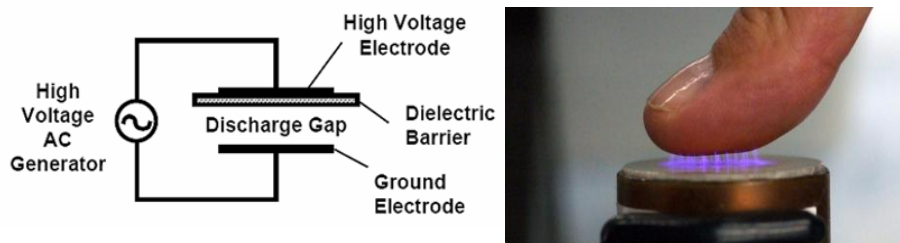
Figure 1 General schematic of a DBD setup (left), and a photograph of FE-DBD plasma in operation (right).

Uniformity of the plasma could be improved in two ways: 1) increasing uniform pre-ionization of the gas to initiate more avalanches or 2) shortening the voltage rise time [20,21] to avoid growth of highly inhomogeneous electric field that promotes growth of some avalanches at the expense of others. If the number of primary avalanches is high enough before the accumulation of the critical space charge, the discharge is likely to remain uniform even if streamers do occur. The resulting discharge will resemble 'pulsed avalanche' regime [22]. In addition, under these conditions, the shape of the electrodes does not affect the location of the avalanches and streamers making the discharge more independent of the topography. A fast rising driving voltage can also shift electron energy distribution function to higher values. Nanosecond-pulsed DBD with glass test tube electrode is shown in Figure 2. This discharge typically appears dim. Nevertheless, it can be seen in Figure 2(a-b) that plasma is spread all over the spherical tip of the electrode. Figure 2a is taken in the presence of background light and Figure 2b is taken in a dark room.

Table 1 Typical microdischarge parameters in a 1-mm gap in atmospheric-pressure air [23,24]

Lifetime	1 – 20 (100) ns	Filament radius	50 – 100 μm
Peak current	0.1 A	Current density	0.1 – 1 kA cm^{-2}
Electron density	10^{14} – 10^{15} cm^{-3}	Electron energy	1 – 10 eV
Total transported charge	0.1 – 1 nC	Overheating	5K
Total dissipated energy	5 μJ	Gas temperature	~300 K
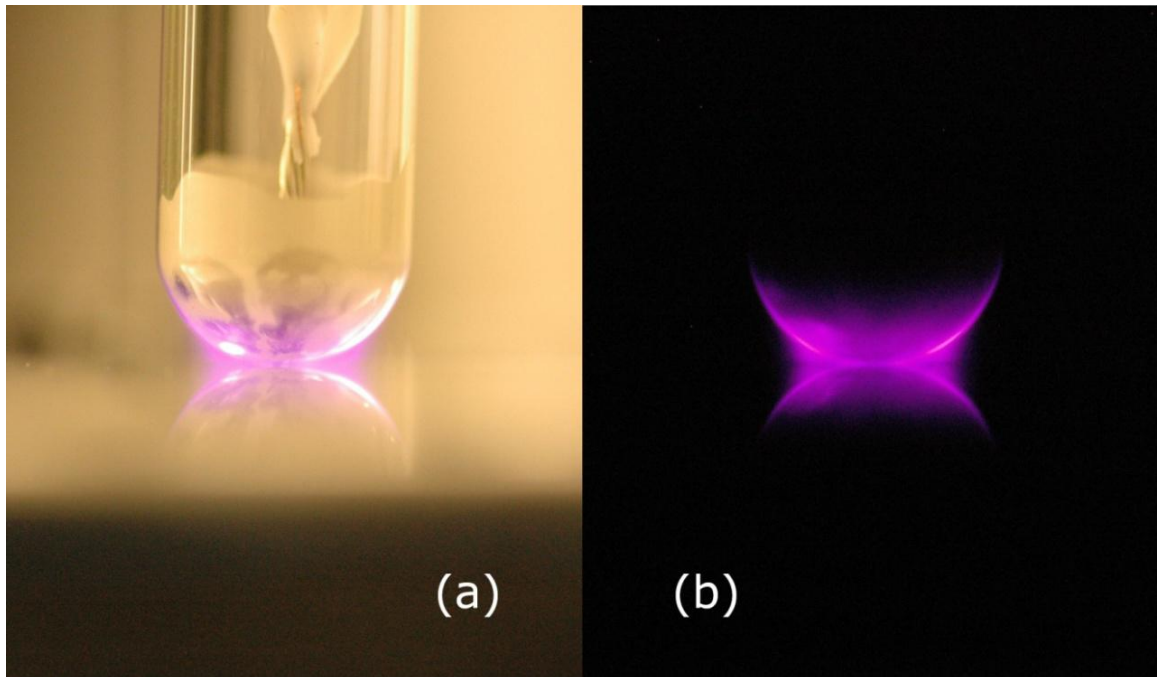
Figure 2 Side view of nanosecond-pulsed DBD between test tube electrode and ground metal electrode (a) with background light and (b) in a complete dark room for the same exposure time (bottom halves of the images are due to reflection from the ground plate electrode surface) [25,26,27]

1.1.2. Plasma jets

Plasma jets consist of a gas nozzle applied with one or two electrodes. The plasma is generated inside the nozzle and transported to the object to be treated by a gas flow. There are numerous plasma jets available and described in literature [8,10,12,28,29,30,31,32,33,34,35]. They mainly differ in electrode configuration, type of gas, and frequency of applied voltage. In general, one must distinguish between remote plasma jets (i.e., the plasma is potential free and consists of relaxing and recombining active species from inside the nozzle) and active plasma jets (i.e., the expanding plasma contains free and high energetic electrons). In the latter case, the substrate must be considered as a second or third electrode, i.e., the plasma is not potential free. Plasma jets enable direct and indirect treatment.

One of the first plasma jets, the so-called plasma needle, was used for a broad range of biomedical applications, including tissue treatment, cell manipulation, and dental applications [1,36,37,38,39,40,41,42,43] by Stoffels et al (Figure 3). Atmospheric plasma is generated by applying radio-frequency voltage to a tungsten wire (50 mm long, 1mm diameter) inserted in a quartz tube. Frequency generator (fixed 13.56 MHz frequency), matching network and power meter are home-built. The plasma is ignited in a gas mixture, directed through the tube at a flow rate of about $1 \, l \, min^{-1}$. Gas composition is determined from mass spectra; the feed gas contains 15% He, 12% O_2 and 73% N_2. The temperature in the plasma can rise up to 150 $\circ$C (Figure 4). These results are in very good agreement with previous measurements involving optical emission spectroscopy [1]. For medical applications, such a temperature is generally too high, unless tissue de-vitalization is desired. However, this problem can be solved by operating downstream,

increasing gas flowrate (only in external operations), reducing plasma power (using thinner electrodes) and shortening treatment times (e.g. pulsing the plasma). Plasma needle production of NO as measured by means of mass spectroscopy is shown on Figure 5. The density of NO may thus reach up to 20% of the ambient density. Besides nitric oxide, other reaction products must be present in this region. The product gases may contain N_2O and also some NO_2 due to NO oxidation.

Sakiyama and Graves presented various models of the plasma needle [44]. They used a fluid code in 1- or 2-D axially symmetric coordinates for the description of the atmospheric plasma needle interacting with different surfaces, and they modeled the transition between the unipolar and bipolar modes (Figure 3). The former was referred to as the "corona" and the latter as the "glow," and the transition corona-to-glow, with increasing plasma power, was studied. These simulation results were supported by the experimental observation of light emission spatial profiles, and a good qualitative agreement was obtained. Furthermore, ion fluxes toward and energy distributions at the grounded surface were simulated. Ion fluxes ranged from 10^{17} m^{-2} s^{-2} (corona) to 10^{22} m^{-2} s^{-2} (glow with a conductive surface). Typical ion energies at the considered power levels were up to 5 eV in the glow mode with conducting surfaces.
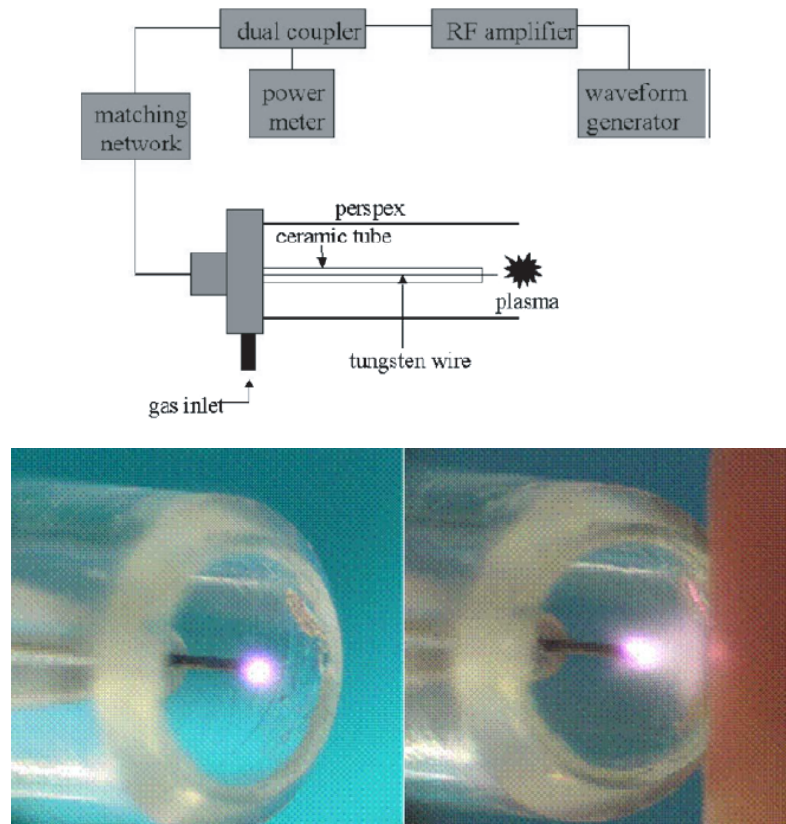
Figure 3 General schematic of the plasma needle setup (top), and two operation modes of the radio-frequency plasma needle (bottom): (Left) Unipolar "stand-alone" mode (corona). (Right) Bipolar plasma-to-surface mode (glow) [1,43]
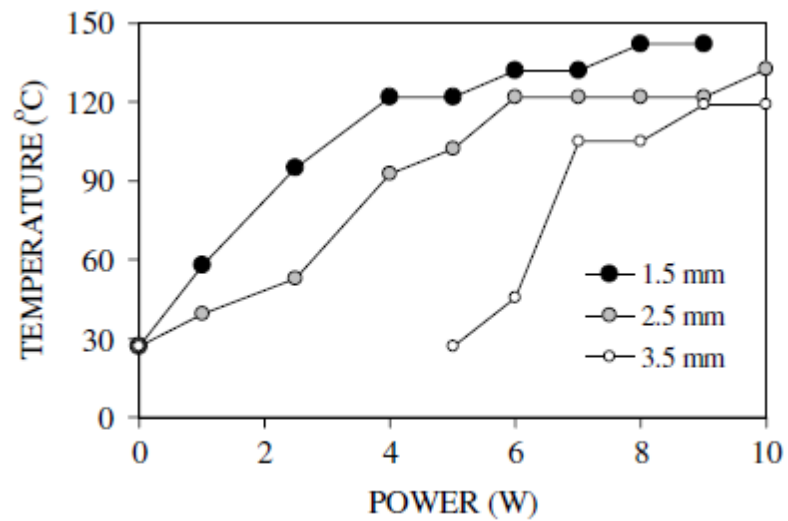
Figure 4 Gas temperature as a function of input power at various positions [45]
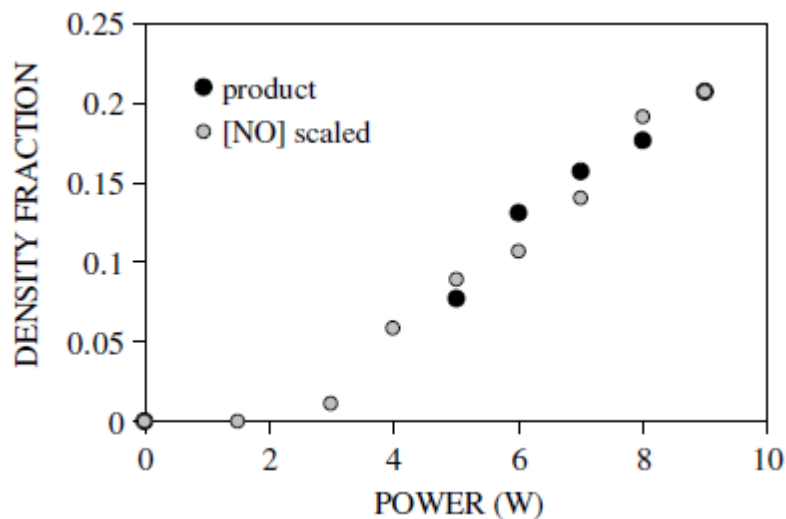
Figure 5 Scaled NO density and product gas density in fractions of ambient atmospheric density, at 1.5mm from the needle tip, as a function of plasma power [45]

Another plasma jet which is recently used for numerous biomedical investigation is the atmospheric pressure plasma jet (APPJ) which is shown in Figure 6. Recently, the device has got the CE marking, i.e., it fulfills the EU consumer safety, health or environmental requirements [46]. It consists of a hand-held unit (dimensions: length = 170 mm, diameter = 20 mm, weight = 170 g) for the generation of a plasma jet at atmospheric pressure, a DC power supply (system power: 8 W at 220 V, 50/60 Hz), and a gas supply unit. The principal scheme of the plasma source is shown in the right part of Figure 6. In the center of a quartz capillary (inner diameter 1.6 mm) a pin-type electrode (1 mm diameter) is mounted. In the continuous working mode, a high-frequency (HF) voltage (1.1 MHz, 2–6 kV_{pp}) is coupled to the pin-type electrode. The plasma is generated from the top of the centered electrode and expands to the surrounding air outside the nozzle. The whole system works with all rare gases (especially argon) with gas flow rates between 5 and 10 slm. Small admixtures (~1%) of molecular gases to the feed gas are

possible. At maximal input DC power of 3.5 W to the hand-held unit, the ignited plasma jet has a length of up to 12 mm.

Figure 6 Atmospheric-pressure plasma jet (APPJ; INP Greifswald, Germany) for experimental biomedical applications (left: CE approved device; right: schematic set-up) [46].

A detailed characterization of the macroscopic parameters of the plasma jet and profound analysis of the main risk factors is given elsewhere [29]. The axial temperature profile of the plasma jet revealed plasma jet temperatures between 63 and 46 °C. Radiation emitted from the plasma contains molecular bands of OH-radical and lines of excited argon atoms between 500 and 1000 nm. In the UV-A region between 350 and 400 nm, bands of nitrogen emission have been measured because of increasing mixing of the feed gas argon with the surrounding ambient air. There was no detectable emission in the UV-C range between 200 and 280 nm. The plasma jet emits significant amount of VUV radiation, mainly the 2nd continuum of the argon excimer Ar_2^* between 120 and 135 nm. Since the plasma jet is operated in its own argon atmosphere, considerable amount of

VUV radiation can reach the object to be treated. The irradiance in the 260–360 nm UV range was about 5 mW/cm^2 at minimal distance of 5 mm and maximum power of 6 W. With increasing distance from the capillary outlet, drastic reduction of irradiance was detected reaching values between 1 and 2 mW/cm^2. Thus, UV-caused problematic side effects of the plasma jet can be avoided in principle. The absolute VUV radiance of the APPJ reaches maximum values of 2.2 mW mm^{-2} sr^{-1}.

Besides (V)UV and heat radiation, the plasma jet provides a mixture of charged and non-charged reactive species, above all reactive oxygen species (ROS) and reactive nitrogen species (RNS) and other toxic gases. Maximum concentrations of ozone between 0.10 and 0.13 ppm have been measured in the close proximity of the plasma jet.

1.2. Plasma biodecontamination and sterilization

Plasma sterilization is one of the oldest and best established applications related to biomedical technology. The antimicrobial properties of plasmas have been thoroughly described in the literature [4,47,48,49,50,51,52,53,54,55,56,57,58]. Low-pressure as well as atmospheric sources have been used in direct and in indirect exposures, and chemical systems such as air, oxygen, nitrogen, and noble gases have been studied. Samples of different types, with various bacterial species (Gram positive and negative, aerobic and anaerobic [4,47,48,49,50,51,52,53,54,55,56,57,58]) and spores [59,60,61], have been subjected to plasma treatment. The nature of plasma interactions with bacteria is rather complex; the dose-dependent effects range from lethal (cell death, eradication [49]) through sublethal (bacteriostatic action due to slight damage followed by cell cycle arrest [41]) to nonlethal metabolic changes [62].

Obviously, plasma interactions with biological objects are very complex; the results depend on the manner of treatment and on the nature of the object (bacterium, cultured cell, tissue, etc.). From the physical point of view, one can distinguish between two manners of plasma exposure.

1) Direct: The active plasma is in direct contact with the surface [4,26,36,38,40,41]. In this arrangement, the (most reactive) short-living species have the highest chance to reach the surface. The energy transfer to the surface is optimal, and the fluxes of species are highest. A sheath is formed at the treated object, which allows surface bombardment with energetic positive ions. There is a physical current transfer to the object. Direct treatment is commonly acknowledged as the most effective one in regard to surface modification and sterilization. However, the effects can be quite drastic (cell necrosis or devitalization) when aggressive plasma sources are used.

2) Indirect: This is also called afterglow or postdischarge treatment [4,26,36,38,40,41]. In this arrangement, only the effluents from the plasma are directed onto the surface, usually by introducing a vigorous gas flow. Short-living particles such as charged species and certain radicals are unable to reach the treated objects; there is also no current transfer. The active factors are long-living products of plasma chemical reactions, e.g., in air plasmas, the afterglow is dominated by nitric oxide or ozone. Indirect plasma treatment is preferred for *in vivo* medical applications because of its relative safety. However, the efficacy is much lower than in case of direct exposure.

There are many factors that determine the efficacy of bacterial inactivation. First, direct treatment is always more effective than remote exposure; although in the latter case,

significant killing can be obtained as well [9,63]. From the plasma (chemical) point of view, agents that cause bacterial death or injury can be roughly classified as follows:

1) heat;

2) shear stress and desiccation;

3) UV radiation;

4) free radicals (OH, NO, ONOO, etc.);

5) charging (positive and negative ions, electrons).

Thermal damage is usually not an important mechanism of injury, considering that most cold atmospheric plasmas are designed to operate at ambient temperature. However, sample exposure to vigorous gas flows from several types of plasma jets may contribute to killing. Therefore, in such cases, it is always recommended to take control samples which are exposed only to gas jet without the ignition of the plasma. UV radiation is a very potent disinfectant [39,49,59,64], but its role in atmospheric plasma sterilization is said to be modest. Besides, UV poses a danger of cell injury (DNA damage), and therefore, many plasma sources are specially designed so as to limit the UV emission. Short-living free radicals, particularly the reactive oxygen species (ROS, e.g., O, , O_2^- OH), are considered to be the prime plasmaborne disinfectants [4,17,25,38,40,41,49,51,52,65,66,67]. The role of oxygen radicals in plasma sterilization has been also demonstrated: the rate of inactivation in air or oxygen plasmas is decades faster than in noble gases.

The aforementioned effects can contribute to cell death in cold atmospheric plasma treatment. As said before, the results depend on many factors, such as the sample type and bacterial species. However, one can make a few general statements with regard to the

efficacy of plasma inactivation. These statements are rather easy to predict *a priori*, keeping in mind the superficial nature of plasma action and the structure of bacterial cells.

1) Spores are more difficult to destroy than the vegetative forms.

2) Gram positive species are more difficult to deactivate than the Gram negative ones. This is easy to understand when chemical etching or charge-induced damage is taken as the prime injury mechanism. The membrane of G+ species is much thicker and harder to penetrate. However, the difference in the killing efficiency is not very large; the effects of the sample thickness seem to be of a higher order.

3) Anaerobic species are easier to kill than aerobes. This is because the anaerobes are more sensitive to ROS, and they generally cannot withstand oxygen-rich conditions.

4) Direct exposure is more effective than indirect treatment.

5) There may be a contribution of charged species in bacterial inactivation, but only in direct plasma treatment (no postdischarge) and only for the vegetative bacteria that are on or close to the sample surface.

1.3.   Plasma-cell interaction

The interactions of cold plasma with eukaryotic cells are much more complex than with bacteria, which are simply due to a greater complexity in the behavior and reactions of the cells. Just like bacteria, eukaryotic cells react to heat, shear stress, ROS, UV, and charged species. The effects on cells can be lethal (necrosis) or nonlethal (detachment [42,68,69]) but also triggeredlethal (programmed cell death, apoptosis [5,68,70]).

Considering that eukaryotic cells have much more advanced defense systems against hostile factors and much better repair possibilities, the induction of lethal effects in cells usually requires higher doses of treatment than in the case of killing bacteria. This is valid both for the administration of reactive chemicals (e.g., ROS; after all, inflammatory cells use ROS to inactivate bacteria in the body) and for UV irradiation. This means that a certain selectivity in plasma treatment can be obtained; the bacteria can be lethally harmed, whereas the damage to body cells remains tolerable. This natural selectivity is, of course, very favorable for all *in vivo* plasma applications, particularly for wound or dental treatment. In this sense, plasma can be seen as a "topical antibiotic."

1.3.1. *Reversible (repairable) DNA damage following plasma treatment*

If the plasma treatment is able to penetrate tissues and cells, what is the effect it has on the cells? The effect is, indeed, non-trivial, but does seem to involve DNA. We have measured the extent of DNA damage in mammalian cells using immunofluorescence and western blot techniques with hydrogen peroxide as a positive control as it is known to induce DNA damage. Experiments show that phosphorylation of γ-H2AX histone does occur following plasma treatment which is indicative of thymine cross-linking and DNA double strand breaks (DSBs) or DNA single strand breaks. The amount of DSBs depends on the plasma dose and it was shown that this effect is reversible for lower plasma doses (which are, interestingly, still high-enough for complete inactivation of high concentration of bacteria); in other words, at plasma doses below 1 J/cm^2 we observe minimal effects on DNA, at higher doses of 2 to 6 J/cm^2 we observe DBSs but they are repaired by the cell within 24 hours, and at doses above 7 J/cm^2 amount of DNA damage is sufficient for the cell to go into apoptosis[71]. These effects are somehow related to

reactive oxygen species generated in plasma as DSBs can be blocked by intracellular and extracellular anti-oxidants [72].

1.3.2. Cell proliferation and release of growth factors

Oxidative stress on mammalian cells may not be as detrimental as it initially seems. Indeed, ROS induce stress in mammalian cells and while in some cases it may lead to apoptosis in other cases this stress can actually promote or control angiogenesis, the growth of new blood vessels or repair/regeneration of existing ones [73,74,75]. In our experiments we show that plasma treatment increases proliferation of porcine aortic endothelial cells. Fold growth, determined by counting attached cells seven days following the treatment, shows a two-fold increase in proliferation compared to untreated cells. Initial results indicate that this phenomenon is due to release of fibroblast growth factor 2 (FGF-2) by these cells as was confirmed with FGF-2 inhibitors [76,77].

Plasma treatment can apparently have variable effect on cells. We can categorize these effects into non-damaging treatment where all cells survive, medium level treatment where cells are affected but some therapeutic effects are observed, and high doses where cell growth is impaired (Figure 7) [72,76,77,78,79].
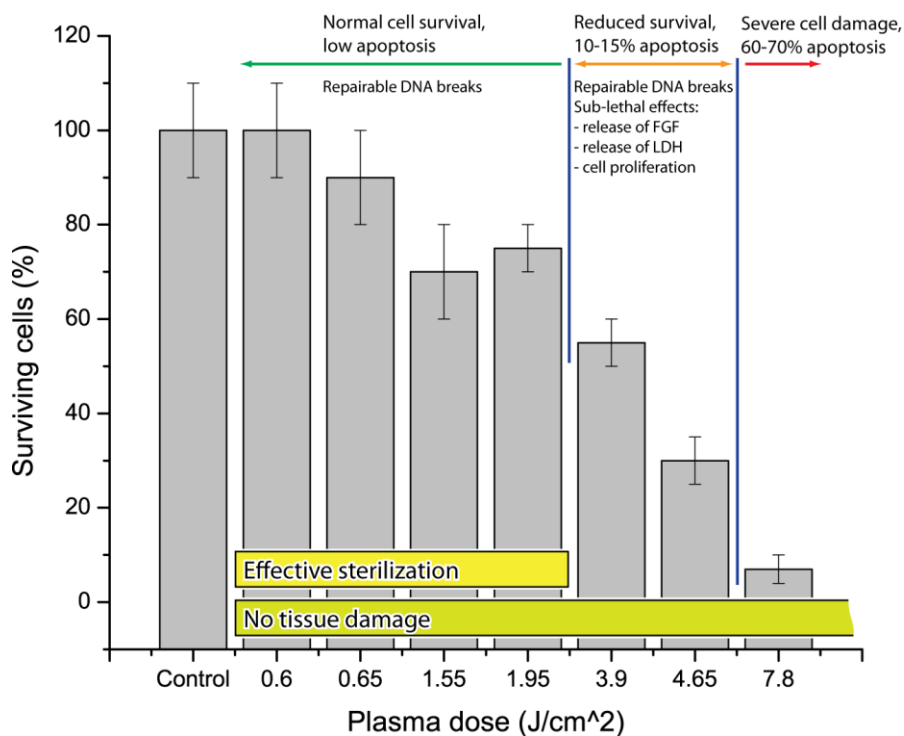
Figure 7. Summary of effects of varying doses of plasma on mammalian cells.

1.4. Therapeutic plasma applications

The most prominent effect of atmospheric plasmas on tissues is (blood) coagulation. Blood coagulation is readily achieved in a thermal way [80], but recently, it has been shown that cold atmospheric plasma treatment can produce this effect by pure chemical interactions, without heat. Recently, Fridman *et al. [3,17,81]* described a novel method of blood coagulation by means of a cold dielectric barrier discharge in air. Plasma treatment was shown to coagulate large bleeding areas (e.g., surgical cuts in human spleen) without inducing additional necrosis. This is an essential finding, because other methods (APC and coblation) always produce a necrotic zone around the treated spot. Nonthermal coagulation was ascribed to calcium-cation (Ca_{2+})-initiated release of thrombin that

induced precipitation of insoluble fibrin from soluble fibrinogen. The extra calcium cations were supplied by a charge exchange reaction with positive ions from the plasma; in other words, plasma shifted the pH toward more acidic. Acidic conditions are favorable for clot formation, because acids neutralize negatively charged colloidal protein suspensions and promote their precipitation (as in the case of bacteria, where acidic conditions reduced the negative charge on the cell and led to cell death).

A special micro-plasma jet system has been developed by Dr. Gostev at Petrozavodsk State University for local medical treatment of skin diseases, and especially for treatment of corneal infections (see [82,83,84,85,86,87,88]). Ability of the medical microplasma system to sterilize surface has been demonstrated by Misyn et al. [82,83,84,85,86,87,88] *Staphylococcus* cultures in liquid media (~10^6 cfu mL^{-1}) have been treated by the air plasma plume of 3 mm diameter, incubated for 24 h, and counted (Table 2).

A 6-log reduction in viable bacteria is achieved in 25 s of treatment; however the sterilization efficiency drops off with increase in volume of liquid which inhibits UV penetration and diffusion of active species generated in plasma. Nevertheless, the microplasma system should be a good solution for the treatment of living human and animal skin as the bacteria are normally at much lower concentrations on skin.

A series of in vitro experiments on bacterial cultures and in vivo experiments on rabbit eyes [83,85,86,88] affirm the strong bactericidal effect of the micro-discharge with minimal and reversible changes, if any, in biological tissues, even in such delicate tissues as cornea. During the investigation of plasma treatment of ulcerous dermatitis of rabbit cornea two important observations were made: 1) plasma treatment has a pronounced and

immediate bactericidal effect, and 2) the treatment has an effect on wound pathology and the rate of tissue regeneration and wound healing process.

Table 2 Results of *Staphylococcus* inactivation by air plasma

Culture volume, ml	Plasma exposure time, s			
	0 (control)	25	50	100
1	2×10^6 cfu	0 cfu	0 cfu	0 cfu
2	4×10^6 cfu	25 cfu	0 cfu	0 cfu
3	6×10^6 cfu	1×10^6 cfu	680 cfu	460 cfu

These results offered a strong ground for application of the medical micro-plasma system for treatment of human patients with complicated ulcerous eyelid wounds, which is shown in Figure 5 [84,88]. Necrotic phlegm on the surface of the upper eyelid was treated by air plasma plume of 3 mm diameter for 5 seconds once every few days. By the 5th day of treatment (two 5-second plasma treatment sessions) the eyelid edema and inflammation were reduced; and by the 6th day (third session) the treated area was free of edema and inflammation and granular tissue appeared. Three more plasma treatments were administered (six total), and the patient was discharged from the hospital six days following the last treatment. The micro-plasma treatment is being further developed for stimulation of reparative processes in various topical wounds, tropic ulcers, chronic inflammatory complications, and other diseases of soft tissues and mucous membrane [84,88,89].

Figure 8 Result of six sessions of plasma treatment of the complicated ulcerous eyelid wound.

Thesis outline

The thesis is organized in the following manner:

- first (Chapter 2), a physical characterization of a novel microsecond spark discharge plasma in pin-to-hole electrode geometry is presented;

- the second part is dedicated to the studies on plasma sterilization and biodecontamination via in vitro experimental work with bacteria (Chapter 3) and spores (Chapter 4) and in vivo inactivation of bacteria on skin surface (Chapter 5);

- the third part is related to the problem of plasma-tissue interaction studied by in vitro measurement of plasma delivery of active species into liquid media (Chapter 6) and wounds followed with development of a physicochemical model of tissue (Chapter 7), in vivo studies of plasma toxicity (Chapter 8), wound healing and blood coagulation (Chapter 9), and treatment of gastroenterological diseases (Chapter 10).

These findings on the mechanisms of plasma interaction with living objects are summarized in Chapter 11.

CHAPTER 2. MICROSECOND PIN-TO-HOLE SPARK DISCHARGE (PHD)

The first successful application of cold plasma for treatment of a eyelid wounds in human described in previous chapter offer a strong ground for further development of the newly formed field of Plasma Medicine. The discharge used by Dr. Gostev and colleagues was never physically characterized, and in order to understand the mechanisms of plasma interaction with living tissues, its role in wound healing and to optimize the efficiency discharge, an extensive study on plasma diagnostics has been performed.

2.1. Experimental setups

The microsecond spark discharge characterized in this study is ignited in a pin-to-hole electrode configuration (PHD, figure 1), and is based on the original schematic proposed by Gostev and colleagues [88]. A needle anode (1.5 mm diameter) is coaxially fixed in an insulator with gas inlet openings (air, ~0.5 L/min), which is surrounded by an outer cylindrical cathode (7 mm diameter) with an axial opening (2 mm diameter) for plasma outlet; the interelectrode gap was set to 1.6 mm, and the cathode wall thickness was 0.8 mm. Both electrodes are made of stainless steel. The plasma discharge was ignited by applying an 8 kV positive potential to the central electrode. To provide high discharge energy while keeping average gas temperature low (a little above room temperature), the electrode system was powered through a 0.33 μF capacitor. This formed a 35 μs dense energetic discharge with average energy of ~1.8 J/pulse.
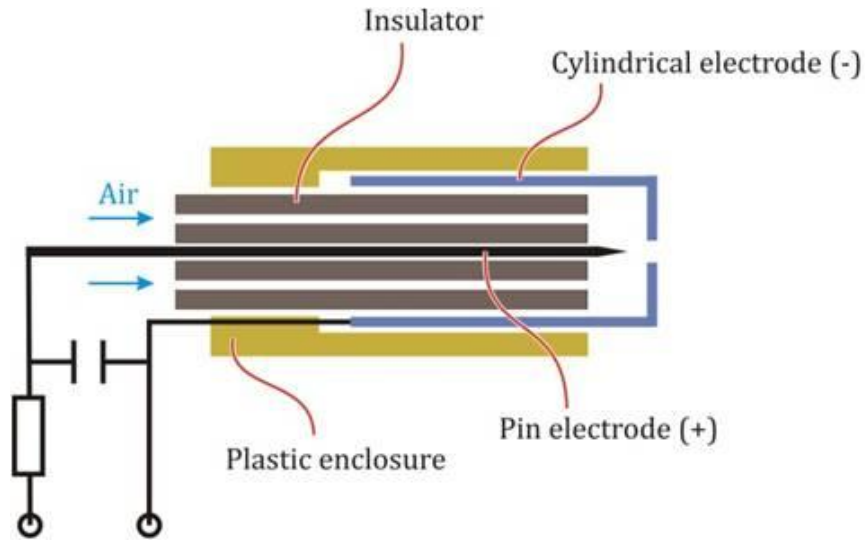
Figure 9 Pin-to-Hole spark Discharge (PHD) plasma system schematic and in operation, demonstrating that the plasma discharge is safe to the touch.

Typical PHD plasma voltage and current waveforms are shown in Figure 10, top. Due to lane inductance, the discharge appears as a series of microdischarges, in which the first one is the most energetic with ~1 μs duration and 0.6 J energy (Figure 10, bottom, where the current oscillations are numerically eliminated knowing line inductance of L=5.4 μH, and corresponding period of oscillations of T=7 μs). Measurements of the light intensity

at 310 nm wavelength using photomultiplier also showed the series of microdischarges (Figure 11).

The average gas temperature was measured using a K-type thermocouple as a function of distance from the cathode. Due to low frequency and short duration, the penetrating plasma temperature is relatively low, and can be decreased to be less than 50°C by introducing airflow through the discharge cell (Figure 12).
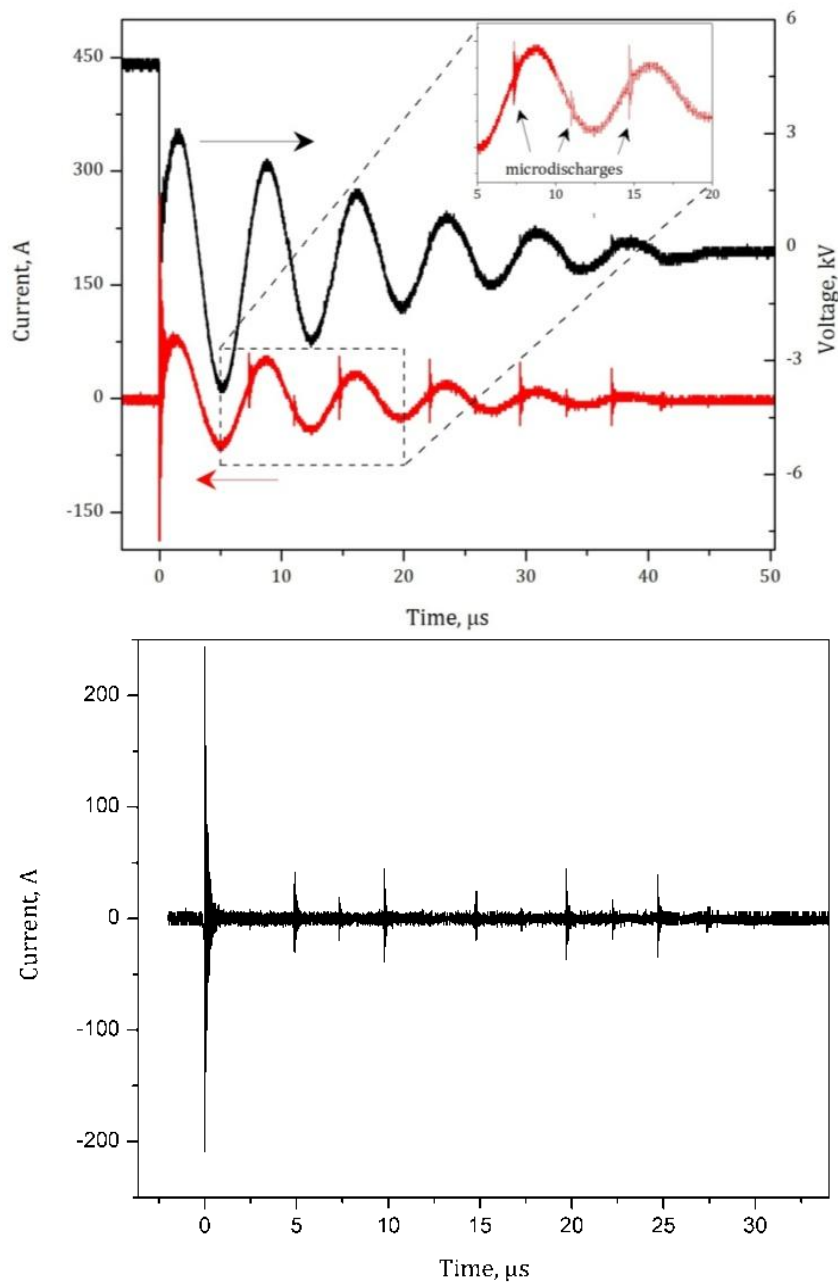
Figure 10 Typical PHD plasma voltage and current waveforms (top), and corrected current oscillogramm (bottom).
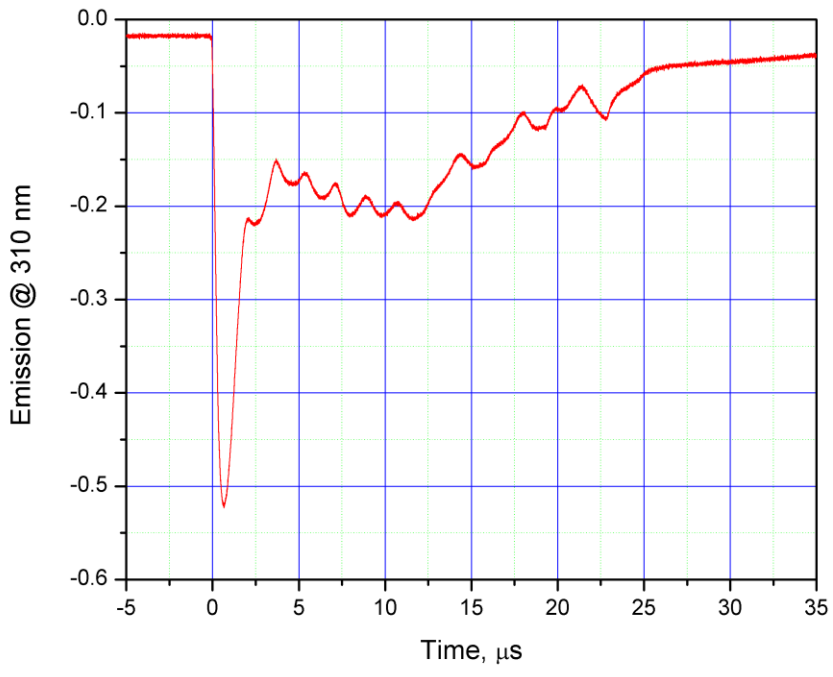
Figure 11 Discharge emission intensity at 310 nm wavelength measured with photomultiplier.
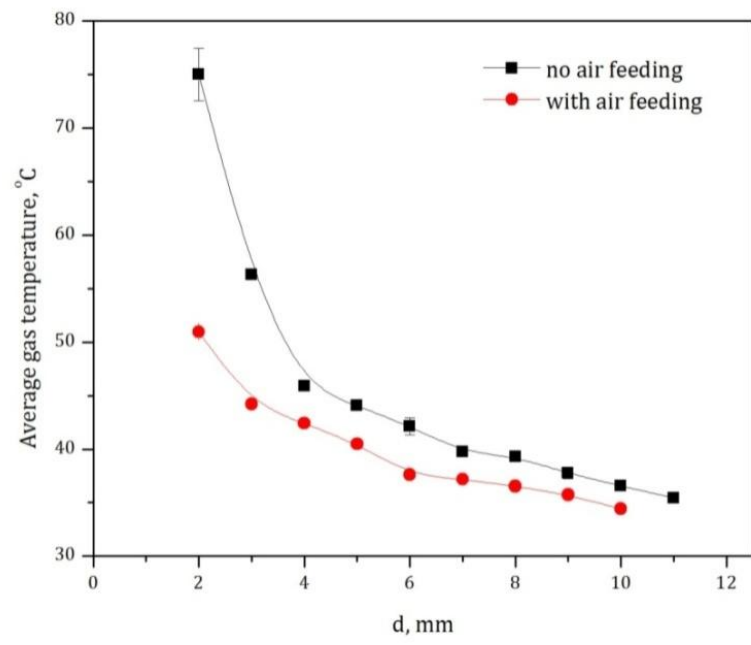
Figure 12 Penetrating plasma afterglow average gas temperature, with and without airflow, as a function of distance from the discharge.

In order to study the discharge development, a modified experimental setup which allows generation of a single discharge was used (Figure 13). Here, a 150 m long coaxial cable was used as a charging capacitor with capacitance of 0.33 µF. The discharge was initiated by separate air spark gap charged with 1.2 µF capacitor. Typical voltage and current oscillograms are shown on Figure 14: the peak discharge voltage was approximately 8 kV, and the peak current − 130 A with the pulse duration of about 140 ns.
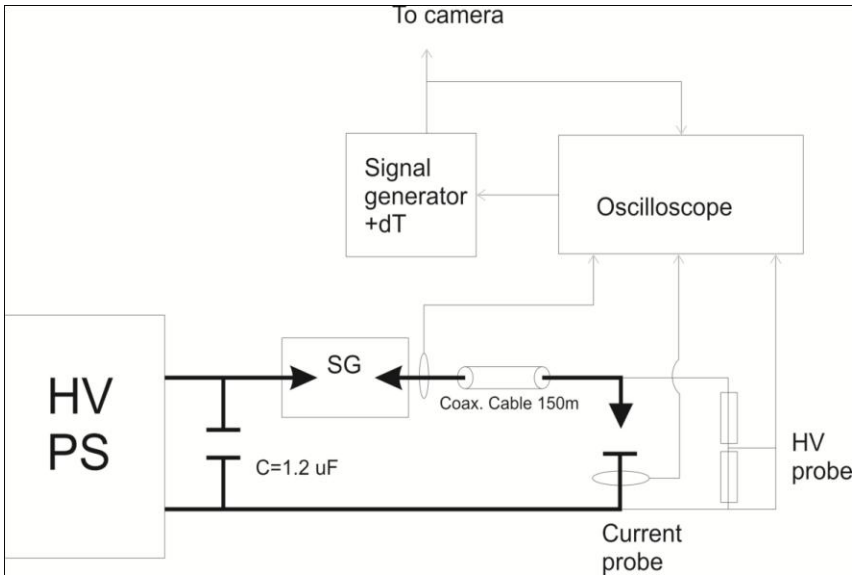
Figure 13 Modified setup for study of the discharge development.
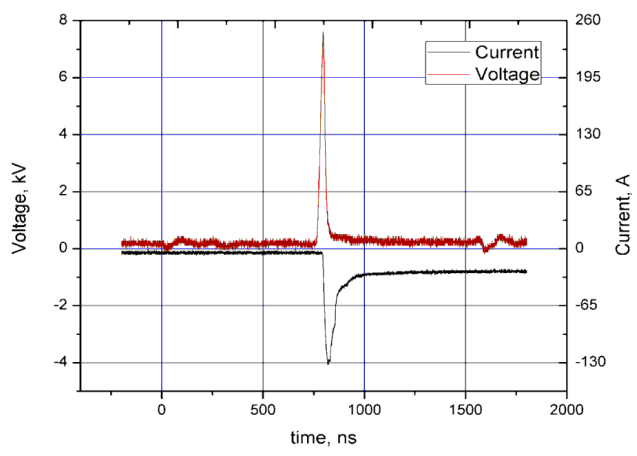
Figure 14 Typical waveforms of the discharge voltage and current.

2.2   Discharge characterization: OES

The spark discharge emission spectrum was measured using an Acton SpectraPro 500i
spectrophotometer (Figure 15). Plasma temperature was estimated using the Boltzmann
plot method, which uses the relative ratio of emission intensities on multiple spectra lines
to estimate the spark gas temperature. At local thermal equilibrium, the plasma
temperature can be derived from the following equation:

$$\ln\left(\frac{I\,\lambda}{A\,g_u}\right) = -\frac{1}{T}E_u + \ln C \, ,$$

where I is the relative emission intensity ratio, λ is the wavelength, A is the transition
probability, g_u is the upper level statistical weight, E_u is the upper level energy, and C is a
constant for various atoms. Iron and oxygen spectral lines were used to estimate the
temperature in the discharge center. Although the average gas temperature of the
penetrating plasma was slightly above room temperature, the discharge temperature itself
must be high to produce a significant amount of NO. A Boltzmann plot of iron and
oxygen spectral lines is shown in Figure 16. By this method, a time-averaged plasma
excitation temperature of 9030±320 K was estimated.
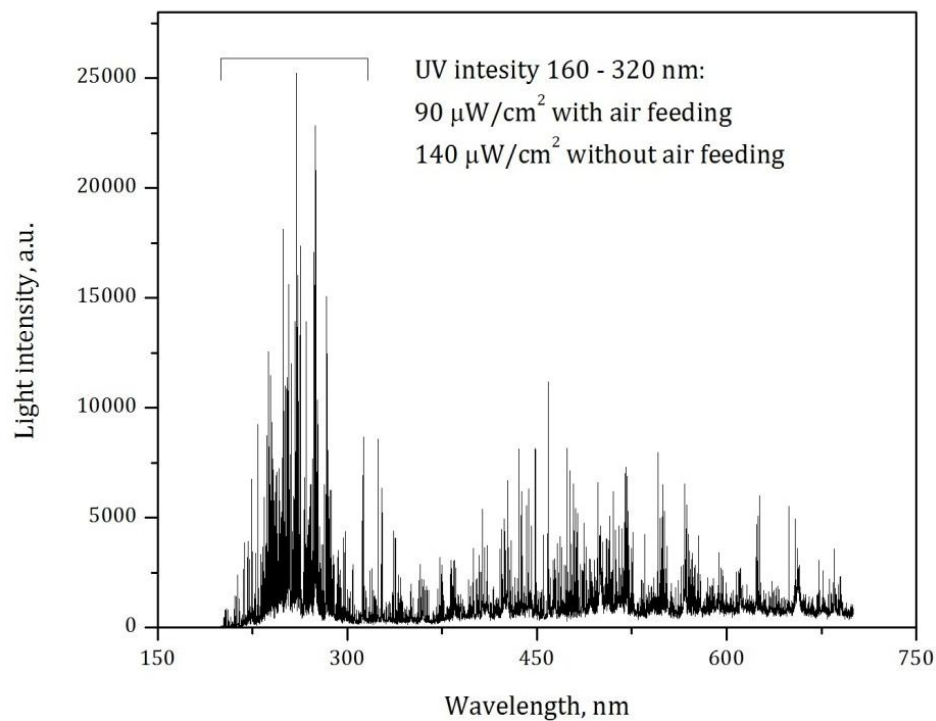
Figure 15 The spark discharge emission spectrum.
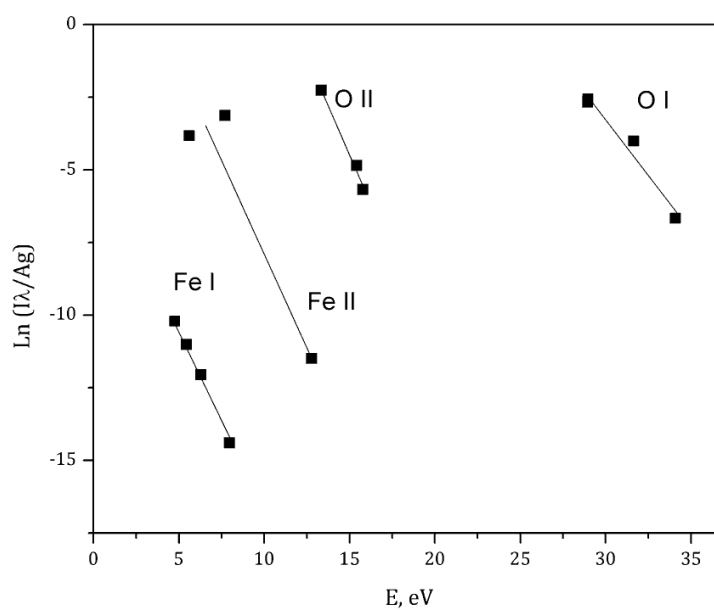
Figure 16 Boltzmann plot of iron and oxygen spectral lines

Plasma UV radiation with and without air flow was measured using an IL1700 photometer (International Light Technologies) with SED(SEL)220 detector (spectral

range 160-320 nm, 220 nm peak). The PHD plasma discharge radiates intensively in the UV range (Figure 15). The measured total plasma UV irradiation with and without gas feeding was 90 and 140 $\mu W/cm^2$ respectively. DNA damage by UV-C and UV-B radiation occurs after about 0.4 mJ/cm^2 and 10 mJ/cm^2 respectively.

By using the linear Stark effect of lines broadening it is possible to estimate electron concentration in the discharge. The determination of the electron density using Stark-broadening has the advantage of not requiring the validity of LTE conditions. LTE conditions require that the collision excitation and deexcitation processes predominate over the radiative processes, i.e. that the electron number density is sufficiently high. The corresponding lower limit of electron density is given by the criterion: *Ne ≥ 1.6·10^{12}·T$^{1/2}$·(ΔE)^3 = 1.3e15 cm^{-3}*. Here, broadening of hydrogen (656.2 nm) and oxygen (645, 926, 615 and 605 nm) lines were used. The hydrogen line profile is mainly broadened due to the linear Stark effect: $\Delta\lambda_{1/2} = 2.5\cdot10^{-9}\alpha_{H_\alpha}n_e^{2/3}$. Oxygen O I broadening: $\Delta\lambda_{1/2} = 0.2[1+1.75\cdot10^{-4}n_e^{1/4}\gamma(1-0.068n_e^{1/6}T_e^{-1/2})]\cdot10^{-16}wn_e$, where where *w is the electron impact width parameter and* γ is the ion-broadening parameter; both weak functions of temperature. Stark broadening parameters for the selected line were taken from Griem's tables. The average electron density was calculated to be n_e = (7.8 ± 4.2)E+16 cm^{-3} (Figure 17).
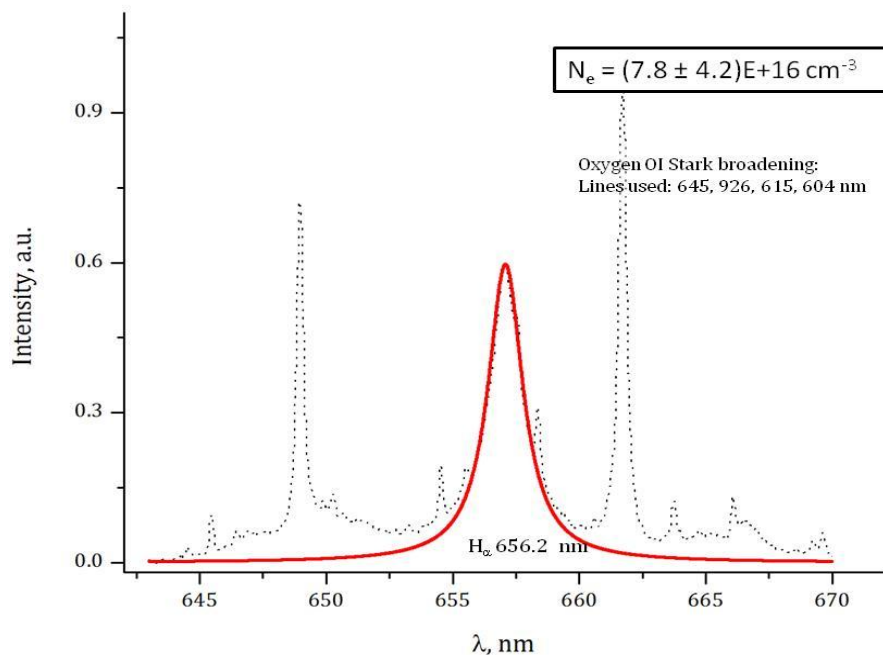
Figure 17 H_α line profile used for determination of electron density in the discharge using Stark broadening.

2.3 Discharge characterization: jet formation (imaging and gas dynamic modeling)

The measurements were performed using 4Picos ICCD camera and quartz lens with focal distance of 16 mm. Camera spectral response range was 220-750 nm. Camera gate was equal to 5 ns and was synchronized with the high-voltage current pulse with the accuracy of about 10 ns. These measurements allowed us to trace the spark stage of the discharge (Figure 18). Here one can notice, that the discharge is started as a classical high voltage arc, which then, as the energy stored in the capacitor is discharged, extinguished, and the plasma is propagating in both directions as a result of high temperature and pressure in the discharge cell with formation of the "plasma jet".

2.4   Discharge characterization: strimer and spark stages modeling

The numerical modeling of gas discharge development was made based on the fluid

model approximation. The motion of species is described by the balance equation within

hydrodynamic (drift-diffusion) approximation:

$$\frac{\partial N_s}{\partial t} + div j_s = Q_s$$

$$\vec{J_s} = \vec{V_s} N_s - D_s \nabla N_s$$

$$\vec{V_s} = \mu_s \vec{E}$$

Here, N_s is the species density; flux j_s consists of an advective part with drift velocity V_s

and diffusion part with coefficient D. The right part in the balance equation Q_s

corresponds to various plasma-chemical processes like ionization, recombination,

electron attachment, and photoionization, etc. Electron transport parameters, namely,

mobility and diffusion coefficients, are calculated with BOLSIG+ solver as a part of

ZDPlasKin module integrated into the code. These transport coefficients for other species

(ions mainly) have to be taken from somewhere. Electric field distribution E can be

expressed vie the electric potential ϕ which in its turn obeys Poisson's equation:

$$\Delta \varphi = -\frac{1}{\varepsilon \varepsilon_0} \sum q_s N_s$$

$$\vec{E} = -\nabla \varphi$$

Where ε and ε_0 are the dielectric permittivity of the media and of free space, respectively,

and q_s is the charge of species (s). In presence of an interface dielectric-gas or dielectric-

metal, the later relation has to be corrected due to for surface charge and different permittivity. Processes leading to production of electrons far from the region of discharge and close to surfaces have a great importance in the development of pulsed discharges, especially of positive polarity.

$$\frac{\partial N_e}{\partial t} = Q_{photo}$$

Emission of electrons from a metal or dielectric surface due to bombardment by ions is expressed as:

$$\vec{J_e} = -\gamma_s^{m,d}\vec{J_s}$$

Here, j is the transport flux of incident species (s) and emitted electrons (e). The coefficient of ionelectron emission γ depends not only on the type of ions but also on the material of the surface. At the present, two values are used in the code: γ^m and γ^d corresponding to emission from metal (m) and dielectric (d) surfaces for any positive ion. Identically, two coefficients of electron emission by photons from metal and dielectric surfaces are used.

The results of modeling experiments are shown in Figure 19 and Figure 20. Pulsed discharge develops in two stages. First stage is a streamer stage. During this stage the streamer crosses the gap and bridges the electrodes. Streamer starts when the voltage on the gap reaches 5-7 kV/cm at atmospheric pressure air. Electric field in the streamer head is several times higher than the breakdown threshold while the field in the channel is 5-6 times lower the breakdown limit. When streamer reaches the opposite electrode the reverse stoke re-distributes the potential across the gap. Electric filed becomes lower than

the breakdown threshold in all points of the gap and plasma recombination prevails on the ionization. Channel's plasma degradation occurs simultaneously with
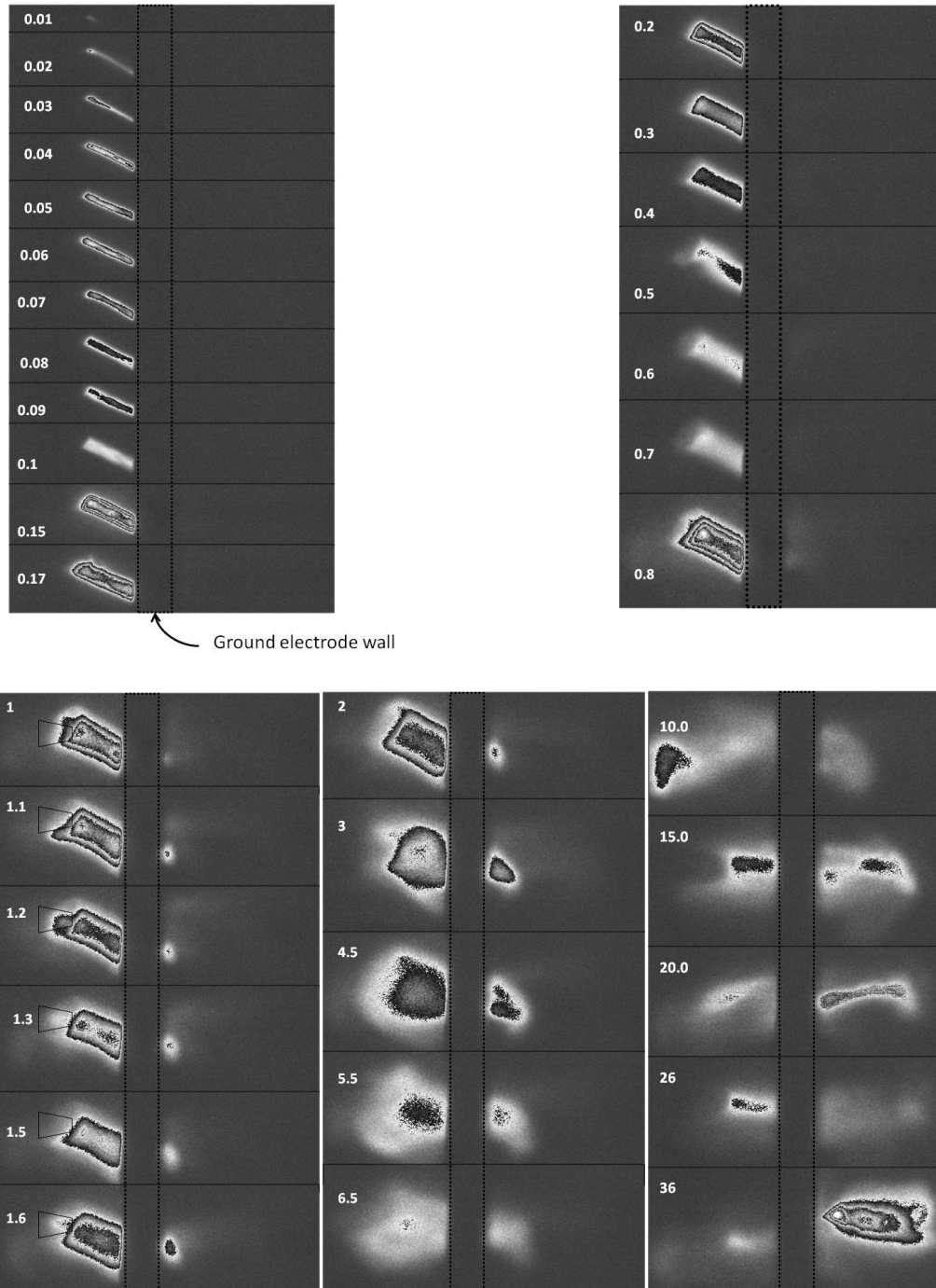
Figure 18. Here: number is time when picture is taken (in microseconds) after the discharge starts.

gas heating due to joule heating of the gas, and, more important, continuous voltage increase on the high-voltage electrode. As a result of gas density decrease and voltage increase, reduced electric field E/n reaches the breakdown threshold in all points of the gap and gas ionization starts again [90]. Now the gas ionization leads to fast formation of hot conductive channel. Discharge power reaches its maximum when the channel's conductivity is equal to the power supply's resistance. Further gas ionization leads to conductivity increase and decreases the voltage across the discharge gap. Hot pressurized channel formed during the discharge phase starts the gasdynamic expansion with shock waves formation. Gas dynamic motion in the discharge chamber leads to the hot jet formation through the nozzle. Let's consider this sequence of events in more details.

Streamer starts from the conical tip of the high-voltage electrode (Figure 19) and propagates across the gap with velocity u ~ 1 mm/ns. After 1.5 ns it reaches the central point of the gap (Figure 19, b). Typical channel diameter is d ~ 0.2 mm.

When streamer head becomes close to the low-voltage electrode, the electrical field ahead of the ionization wave becomes sensitive to the shape of the electrode (cylindrical hole on the axis). Streamer's shape changes (Figure 19, d) and the channel touches the edge of the low-voltage electrode (Figure 19,e). The streamer phase takes approximately 2 ns from the streamer start to the conductive bridge formation between the electrodes.

Continuous voltage increase leads to breakdown development (spark phase of the discharge). Energy release during this stage leads to formation of fast hot channel formation (Figure 20, a). Further modeling was performed using Euler's equations,

including mass, momentum and energy conservation equations, as well as the equation of state.
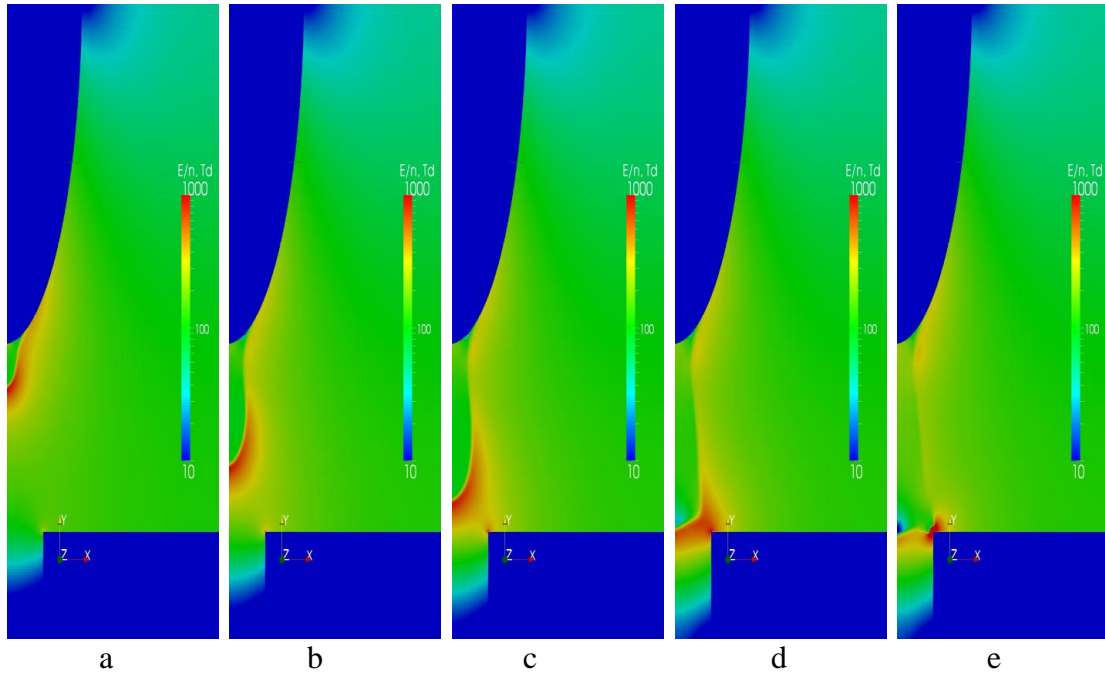
Figure 19 Air, P = 1 atm. U = 8 kV. a) – e): t = 1, 1.5, 1.7. 1.9 and 2 ns

The gas temperature in the pulsed spark channel can reach 10-20 kK because of high rate of energy release. Short time of the hot channel formation lead to pressure increase in the discharge. Hot gas from the spark channel expands from the region of discharge energy release, forming shock waves and complex gasdynamic motion in the discharge chamber (Figure 20, b,c). It should be noted that during initial stage of the expansion there is no gas motion along the discharge axis because of almost symmetrical conditions of gas expansion in both directions (Figure 20, d, e, f). At time t = 3.2 μs shock wave appears on the nozzle exit and starts to propagate into free space (Figure 20, f). Shock wave propagates also in the discharge chamber and after t = 7 μs reaches the closed end of the

chamber (Figure 20, g). Reflected shock wave appears and propagated toward the nozzle (Figure 20, h, t= 12.8 μs). Until this time only small portion of the gas from plasma channel penetrates through the hole. Reflected shock reaches the nozzle after t = 20 ms and increases the pressure near it (Figure 20, t = 25.6 μs). Gas acceleration through the nozzle forms the high-speed jet which propagates several centimeters from the nozzle (Figure 20, t = 51.2 μs). Almost all discharge products (O3, NO, etc) produced during the discharge stage are pushed away from the discharge chamber at this time. Inertia of the jet formed creates the negative pressure in the discharge chamber after t ~ 100 μs after the discharge. A suction stage appears and the discharge cavity fills with a fresh portion of air.

2.5   Bacteria inactivation *in vitro*

The efficiency of microsecond spark discharge in inactivation of bacteria was tested in vitro. In this study an *Escherichia coli* suspension in phosphate buffered saline (PBS) at initial concentration of about $3 \cdot 10^9$ cells/ml was used. Bacteria were treated on brain heart infusion (BHI) agar: 400 μl of bacteria solution were inoculated on BHI agar prepared Petri dishes and spread on agar surface to obtain uniform layer of bacteria. After inoculation plates were allowed to dry in room air for about 30 minutes to allow evaporation of excess water. To quantify the number of bacteria per unit area of agar, the bacteria solution was properly diluted, inoculated on agar surface as described above, and after incubation at 37°C for 15 hours resulting colonies were counted. In order to check the role of UV radiation produced by the discharge as a mechanism of bacteria inactivation, treatment was done either with or without 0.5 mm quartz glass placed in between the discharge and bacteria (Figure 21).
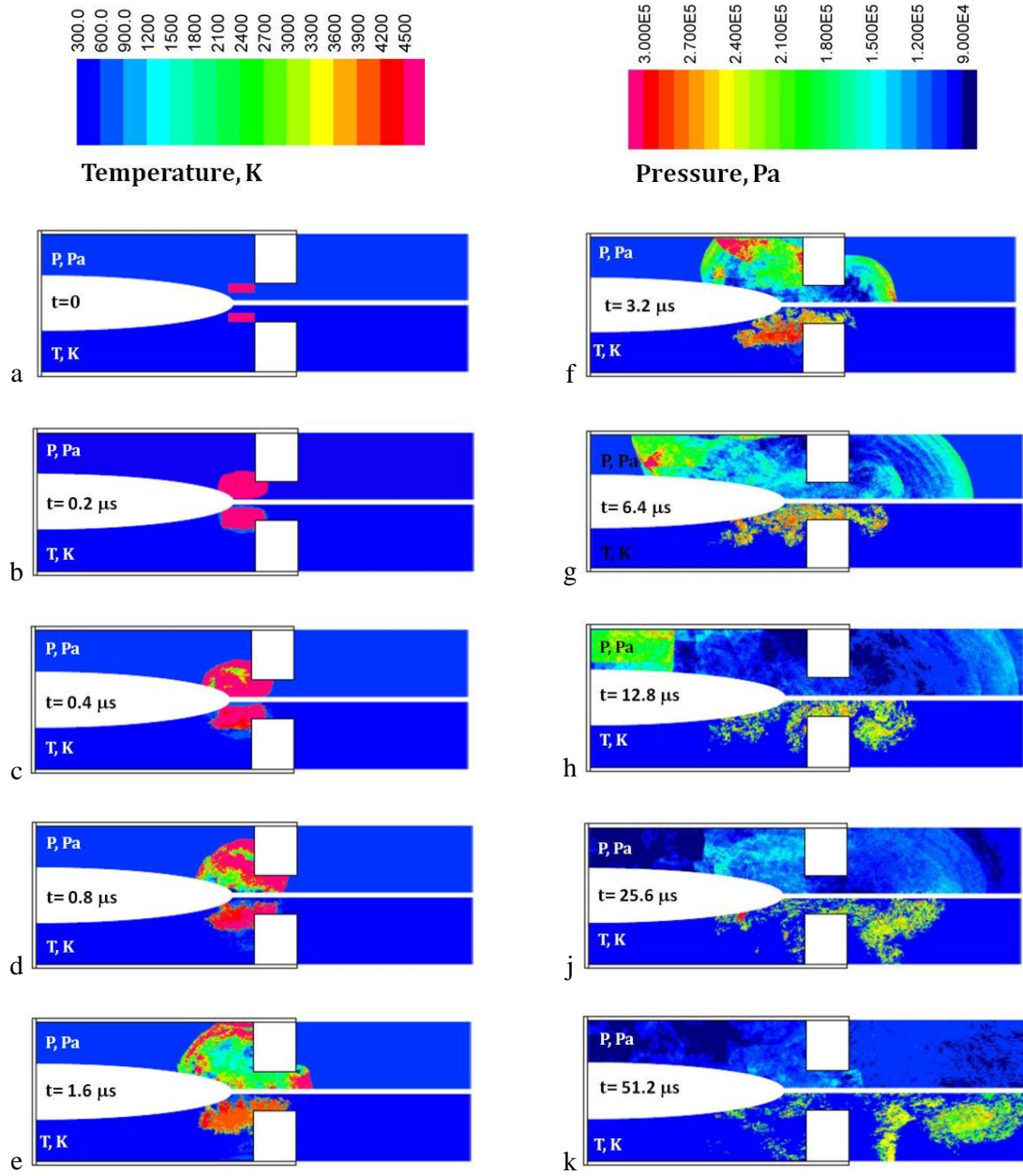
Figure 20. Spark channel expansion and plasma jet formation.
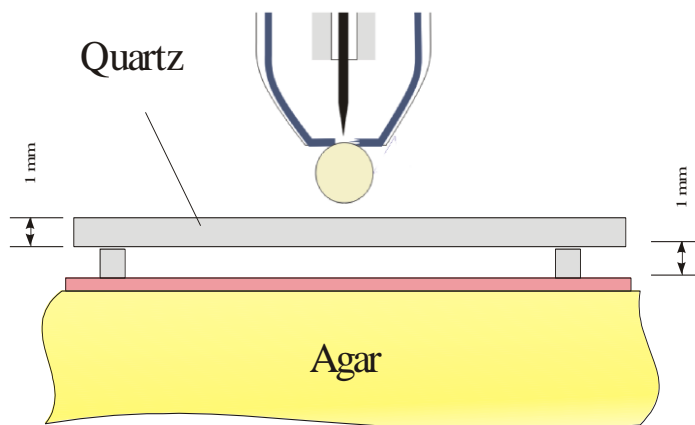
Figure 21. PHD treatment of bacteria on agar.

The results of experiments are shown on Figure 22: the clear circles correspond to absence of bacteria growth (inactivation area). Here we show, that even after 1 pulse (~35 µs) bacteria are inactivated (~10^7 cells). At the same time it is clear that the dominant mechanism of inactivation in the case of spark discharge is probably UV radiation.
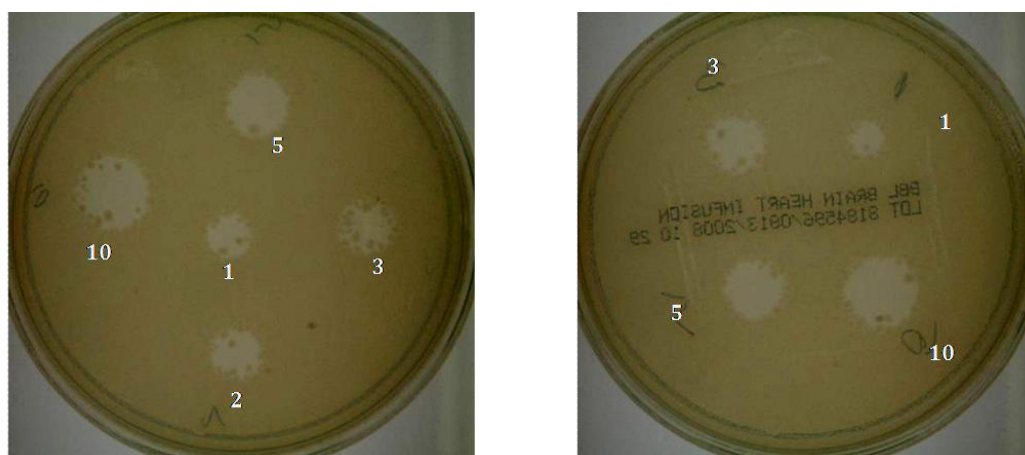
Figure 22. The results of PHD treatment of bacteria on agar: without (left) and with (right) quartz. Numbers indicate number of pulses used for treatment.

2.6 Microsecond spark in a pins-to-hole discharge cell configuration (PsHD)

As it was shown above, PHD plasma is a powerful source of UV radiation which plays the major role in the process of bacteria inactivation. The measured total plasma UV irradiation with and without gas feeding was 90 and 140 $\mu W/cm^2$ respectively. DNA damage by UV-C and UV-B radiation occurs after about 0.4 mJ/cm^2 and 10 mJ/cm^2 respectively. This means that the safe treatment dose for the PHD is on the order of 5 – 90 s. In order to decrease the amount of UV exposure produced by the discharge during treatment, the discharge was ignited in a different geometry (Figure 23). Measured UV was 5 $\mu W/cm^2$, i.e. 20 times lover than in the case of original PHD configuration.
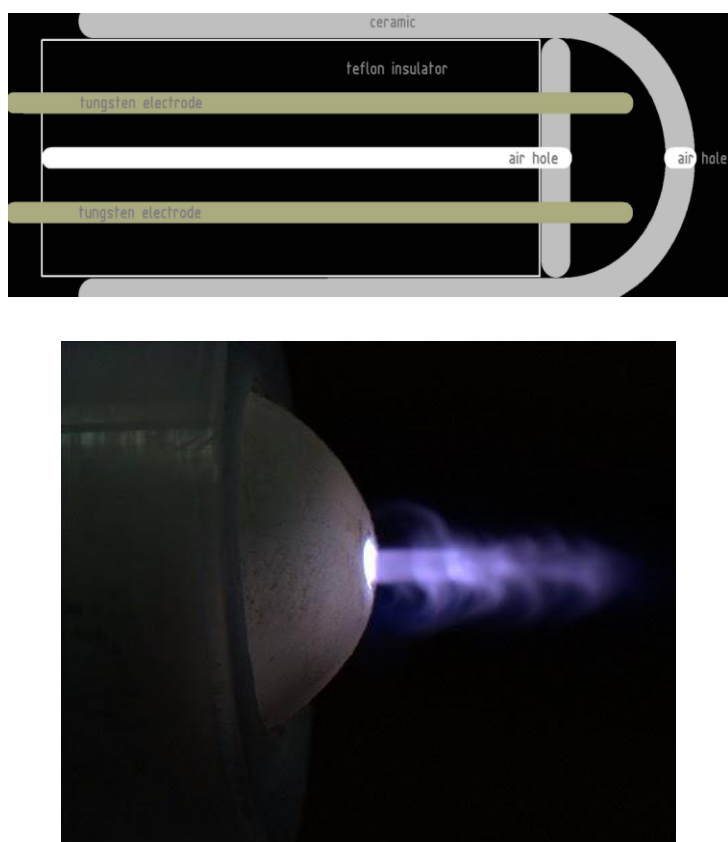
Figure 23. Spark discharge cell for reduced UV generation: discharge cell schematic (top), discharge in operation (bottom)

The bacteria inactivation experiment was conducted in the same way as described above. The results (Figure 24) show that although the efficiency of bacteria inactivation significantly decreased, the effect of UV no longer plays a significant role.
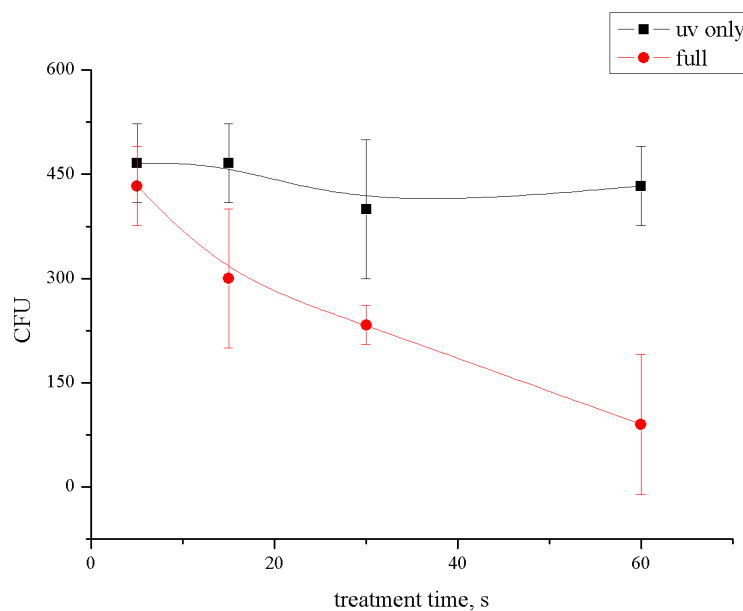
Figure 24. The results of bacteria inactivation by microsecond spark plasma in pins-to-hole discharge cell configuration.

CHAPTER 3. DIRECT PLASMA INACTIVATION OF BACTERIA: IN VITRO STUDIES

One of the first and probably the simplest from the point of view of practical realization application of atmospheric pressure plasmas is inactivation of bacteria on various surfaces, in air and liquids. In medicine, obviously, the primary focus would be decontamination and sterilization of tissues: skin and wounds, i.e. primary target is usually surface. Although a large number of experimental data has been obtained in last decade by researchers from various research centers and laboratories, the basic mechanisms of plasma inactivation of bacteria are still poorly understood. The main focus of this chapter is to indicate the role of major plasma components in the process of plasma "sterilization". For this purpose, two types of discharges were used as a plasma source: floating electrode dielectric barrier discharge (FE-DBD) and atmospheric pressure corona discharge. The spark discharge ("PHD") was not used since the major factor in this case is powerful UV radiation, and separation of other components seems to be rather difficult.

3.1 Role of charged species in direct plasma interaction with bacteria

Floating electrode dielectric barrier discharge (FE-DBD) system is based on a conventional dielectric barrier discharge and is basically a system driven by alternating current high voltage applied between two conductors where one or both are covered with a dielectric to prevent transition to arc. In this setup, amplitude and waveform of the high voltage signal are quite important. It is widely known that damage to a surface being treated is related to the temperature of the filaments, their density, and the energy per

filament [26,27,91,92]. Uniformity of FE-DBD treatment was discussed elsewhere and can range from a rather non-uniform continuous wave discharge to a uniform nanosecond pulsed plasma [27,93]. Continuous wave system can have different waveforms (sin, triangle, etc), 1 to 30 kHz, 10 to 40 kV peak-to-peak; microsecond pulse system: single polarity positive pulse, 2 μsec duration, 5 V per nsec rise time, 120 Hz to 4 kHz pulse frequency; nanosecond pulse system: 40 nsec duration, 1 to 3 kV per nsec rise time, single pulse to 2 kHz [26,27,78,94]. The continuous wave discharge has the lowest number of filaments while operating at highest power and temperature; and this was shown to significantly damage biological tissues being treated [26,94]. Electrical safety of application of plasma to living tissue has been discussed in detail previously [2,78,94,95]; however, toxicity of such treatment, or the extent of immediate or long term damage, remains an open question.

There are two modes of application of FE-DBD to the surface being treated: 1) where the tissue or cells are used as a second active electrode — plasma then is bound between the dielectric surface of the powered electrode and the surface of the tissue being treated; or 2) where plasma is separated from the tissue by a grounded metal mesh and gas is blown through the discharge to carry active species outside of the plasma. The first method is called a "direct" and the second - an "indirect" application of plasma to tissue. Fridman *et al.* have previously shown that direct application of plasma yields to roughly a two orders of magnitude improvement in rate of bacteria inactivation as compared to indirect application, even when the plasma is removed from the tissue by a fraction of a millimeter [79]. All the effects of direct plasma on bacteria are negligible compared to the effects of charges. In short, leaving only UV radiation (removing plasma by use of

quartz (UV) or magnesium fluoride (VUV) windows) removes the ability of plasma to sterilize. Global gas temperature and applied electric fields are also negligible as the gas temperature rise is insufficient to achieve sterilization and the frequency and waveform utilized is out of the range for effective electroporation (see [78,96,97,98] for further details). Effects of neutral active species cannot be ignored. Neutrals by themselves, given enough time, are able to sterilize as well as direct plasma treatment and they are also responsible for many interesting biological effects; e.g. effect of NO in tissue regeneration [78,99,100]. It is important to note here that the effect of plasma is on bacteria and not on the substrate: a) agar treated by plasma for up to 1 hour remains able to grow bacteria the same way untreated agar does and bacteria appear unaffected; and b) bacteria treated on one Petri dish and transferred to another one immediately following the treatment remain inactivated and do not grow.

3.1.1 *Comparison of direct plasma treatment to indirect treatment with and without ion flux*

In this section three sets of experiments are discussed: comparison of direct and indirect plasma treatment of bacteria, and investigation of the effect of ions of both polarities in the process of bacteria sterilization. In the case of direct plasma treatment the discharge is ignited on the treated surface with 1.5 mm discharge gap. For indirect plasma treatment a grounded metal mesh is used as a second electrode (22 wires per cm, 0.1 mm wire diameter, 0.35 mm openings, 60% open area, weaved mesh). The gap between the mesh and the quartz dielectric is set to 1.5 mm, just as in the case of the direct treatment setup. To ensure that both FE-DBD setups, with and without the mesh, produce the same amount of UV radiation, we correct for the UV transparency of the mesh using separate

measurements. The spectrum is measured using TriVista Spectrometer System with Princeton Instruments PIMAX intensified CCD camera with and without mesh. It turns out that the mesh cuts off only about 20-40% of UV light depending on UV wavelength (Figure 25).
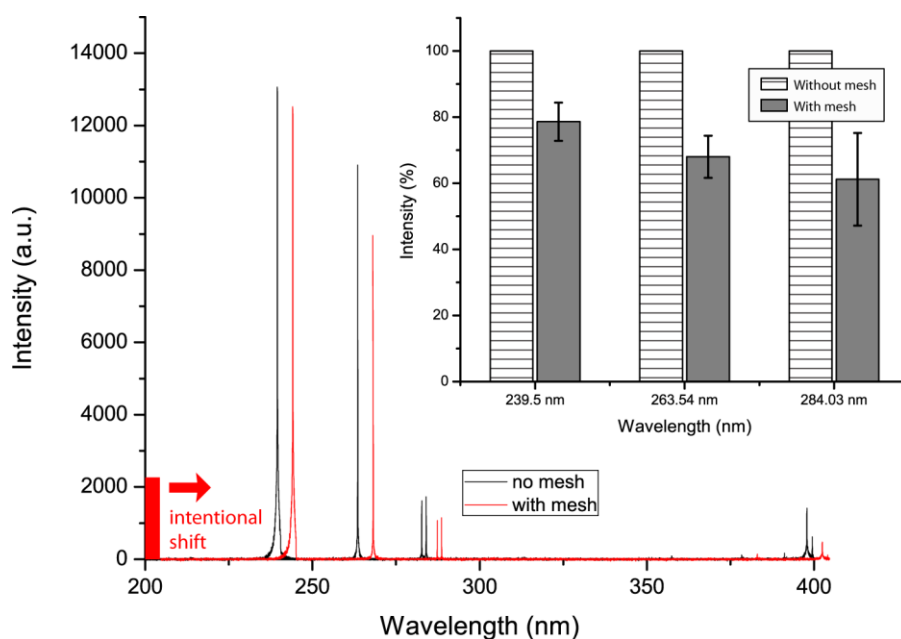
Figure 25 Results of measurement of light intensity from FE-DBD in the ultraviolet spectrum measured at three peaks (239.5 nm, 263.54 nm, and 284.03 nm) without mesh (taken as 100% for each wavelength) and with mesh: a representative spectra and averaged data for the three peaks.

To investigate the effect of charged species agar prepared in metal dishes was used. These dishes are then biased with unipolar potential to extract charges from the discharge. The fact of charge extraction is confirmed by current measurements in "dish – ground" circuit (Figure 26). The plasma is ignited in the same electrode-mesh configuration as in the indirect plasma treatment experiment. Distances between the powered electrode and the mesh, and between the mesh and the agar, both are set to 1.5 mm.
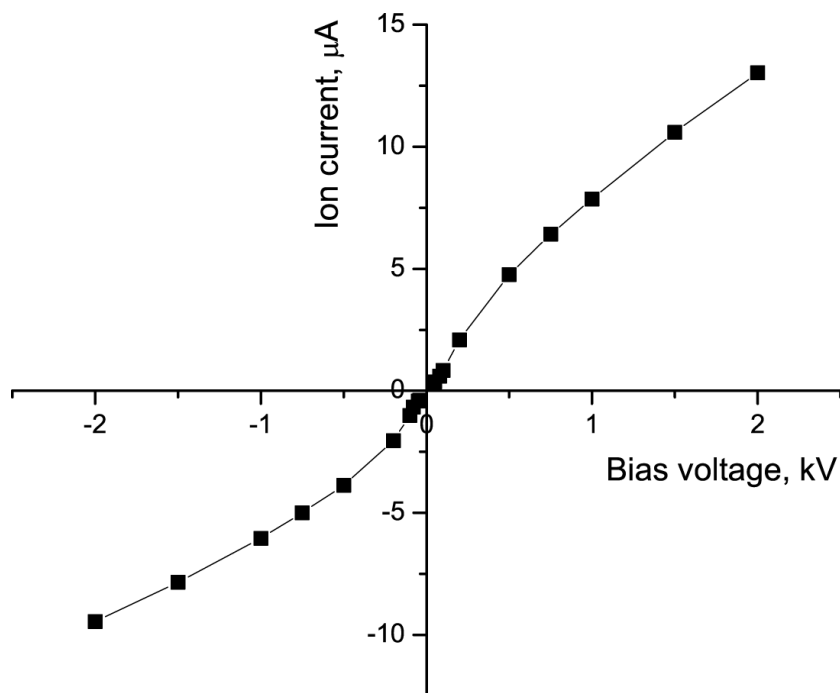
Figure 26 The results of current measurements in experiments with ion flow.

The results of direct, indirect, and bias experiments are shown in Figure 27. When *E. coli* are treated with plasma directly they are exposed simultaneously to charged particles, UV, and all active plasma components such as ozone (O_3), hydroxyl radicals (OH), and other excited molecular and atomic species, and thus maximum inactivation effect is obtained in this case. The results of indirect plasma treatment show that it is significantly less effective, probably due to absence of charged species in plasma afterglow as was previously reported with skin flora (mix of staphylococci, streptococci, and yeast) [79]. Applying bias potential to the agar leads to an increase in inactivation efficiency. These results show that presence of charged species may lead to a significant increase of plasma treatment efficiency. Although in Figure 27 it may appear that there is some observable

difference between positive and negative bias we did not observe this statistically. Careful quantitative analysis of these results will be discussed below.

(a) Direct, 2 J/cm²   **(c)** Indirect, 2 J/cm²   **(e)** Positive bias (1 kV), 2 J/cm²   **(g)** Negative bias (1 kV), 2 J/cm²

(b) Direct, 5 J/cm²   **(d)** Indirect, 5 J/cm²   **(f)** Positive bias (1 kV), 5 J/cm²   **(h)** Negative bias (1 kV), 5 J/cm²
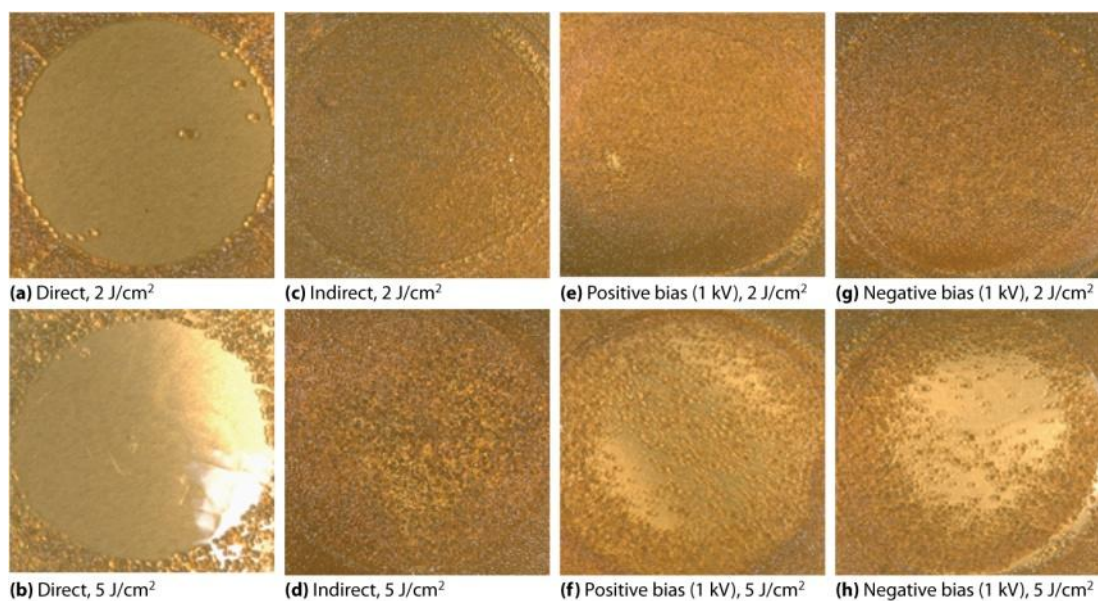
Figure 27. Results of inactivation of *E. coli* on agar surface by direct (a, b) and indirect (c-h) plasma treatment. In the case of indirect treatment the agar was either grounded (c, d) or DC-biased with 1 kV positive polarity (e, f) or 1 kV negative polarity (g, h). For all cases, the plasma dose was kept at 2 (a, c, e, g) and 5 J/cm² (b, d, f, h).

3.1.2 *Effect of positive and negative ions on inactivation of E. coli in nitrogen corona discharge*

To study the role of ions alone, we use DC corona discharge in flow of dry nitrogen at 0.5 slpm. A stainless steel needle electrode is placed inside of ceramic tube with inner diameter of 5 mm and is powered through a 10 MOhm resistor to produce ion flow with average current of approximately 20 µA for both positive and negative polarities; voltage is then varied around 1 kV to produce the same current for both polarities. Grounded metal dish of 60 mm diameter with agar and *E. coli* is then used as a second grounded electrode, completing the circuit. There is also a 2 mm gap between end of the tube and

agar surface to provide gas output from the system. Nitrogen (99.999% pure) is used to ensure that concentration of reactive oxygen species is reduced in the discharge. The results show that ions of both polarities are able to inactivate bacteria. The effect becomes visible after ~25 seconds of treatment for both cases and positive ions show slightly higher efficiency; however, the difference between positive and negative ions is no more than ~10-15% (Figure 28). No water evaporation was observed for treatment times below 1 hour and the effect of gas flow alone was analyzed and shown to have no effect on bacteria (results not shown, but see [79] for similar experiment). This experiment serves as a second indication of the potential importance of ions in the inactivation of bacteria; however it does not completely eliminate the role of UV and ROS since even in high purity Nitrogen minute amounts of water and oxygen are present.
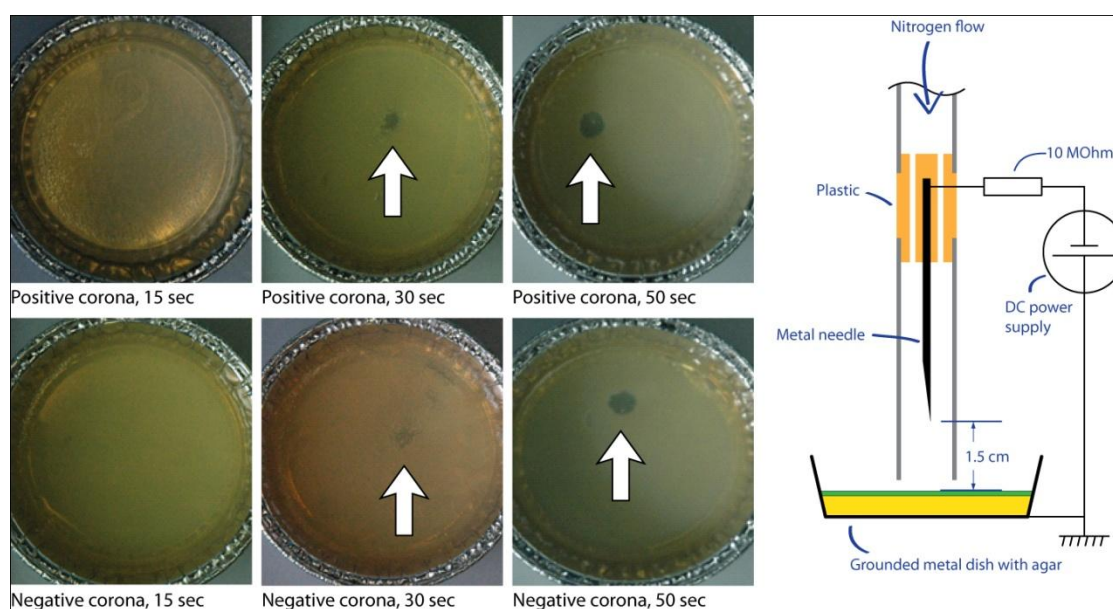
Figure 28. Schematic and results of *E. coli* inactivation on agar surface by negative and positive polarity corona discharge in nitrogen.

3.1.3 *Inactivation of bacteria using DC corona discharge: role of ions and humidity*

Here the results of an experimental study of the effect of ions produced in a DC corona discharge on inactivation of bacteria on the surface of agarose gel are discussed. Both positive and negative corona discharges in various gases at varied humidity were studied. The measurements in N_2-O_2-H_2O mixtures show that there is no inactivation in pure N_2, pure O_2, and N_2-H_2O mixture. The best results were achieved in the case of *direct* treatment when discharge was ignited in oxygen and water containing mixtures. It is shown that neither UV radiation, ozone, or H_2O_2, nor other neutral active species alone produced by corona have an effect on bacteria viability. It is shown that the main role of charged particles may be related to the faster transport of active peroxide species – cluster ions $OH^-(H_2O)_n$ and $H_3O^+(H_2O)_n$. The efficiency of these radicals is much higher, than of the oxygen radicals and ions (including O_2^-, O_4^+ and O_3) and of nitrogen and argon ions.

Corona discharge setup

Experiments were conducted using DC corona discharge at atmospheric pressure. Seventeen needles were uniformly fixed in cylindrical plastic enclosure with inner diameter of 5 cm (Figure 29, a). Grounded metal plates filled with agar or grounded metal coupons were placed 4 cm below the needles, and played the role of a second electrode. The corona needles were powered with either positive or negative DC voltage through a 10 MOhm resistor to produce ion flux. The current associated with the charge impinging on the agar plate was measured by an amperemeter connected in series with the grounding connection. By variation of applied voltage from 5 to 30 kV, the current of

ions was varied from 10 to 250 µA. In order to check inactivation efficiency of neutral active species generated by the discharge, a grounded metal mesh was introduces into the system in the same way as in [4,101]. Mesh was placed between the high voltage electrodes and the treated surface. In these set of experiments corona current was kept at 100 µA, while the distance between mesh and bacteria was 2 mm. In addition, effect of neutral radicals was studied by corona treatment in reverse room air flow (vacuuming the system) at rate of 1 slpm. The effects of gas composition and presence of water were studied by introducing either dry or wet (gases were bubbled through distilled water, which was boiled prior the experiment for ~20 min and then cooled to room temperature) air, O_2, N_2, Ar, and He into the discharge volume at rate of 10 slpm.

Preparation of bacteria

In this study an *Escherichia coli* suspension in phosphate buffered saline (PBS) at initial concentration of about $3 \cdot 10^9$ cells/ml was used. Bacteria were treated either on brain heart infusion (BHI) agar or on aluminum coupons after ~60 minutes of drying at room air. In the first case 400 µl of bacteria solution were inoculated on BHI agar prepared in aluminum plates (plate diameter 6.5 cm) and spread on agar surface to obtain uniform layer of bacteria. After inoculation plates were allowed to dry in room air for about 30 minutes to allow evaporation of excess water. In such a case, bacteria were never completely dry and were covered by a minute amount of water, a condition which we refer to as "moist" [101]. To quantify the number of bacteria per unit area of agar, the bacteria solution was properly diluted, inoculated on agar surface as described above, and after incubation at 37°C for 15 hours resulting colonies were counted (see Figure 29, b). For air-dried bacteria treatment experiments, 100 µl drops of bacteria solution were

placed on sterile aluminum coupons. Due to relatively low wetability of coupons, drops always had round shape at base with diameter of about 8 mm. Then, inoculated drops were dried at room air for about 1 hour, and treated with corona discharge or left untreated as controls. After the treatment, bacteria were washed out with ~1 ml of PBS, and incubated on BHI agar. Here it is necessary to mention that some number of *E. coli* after drying were probably killed and number of colonies observed after incubation decreased for about 90%. Therefore, this loss of bacteria was accounted in our further experiments, and actual number of treated bacteria was recalculated correspondingly.

a   b
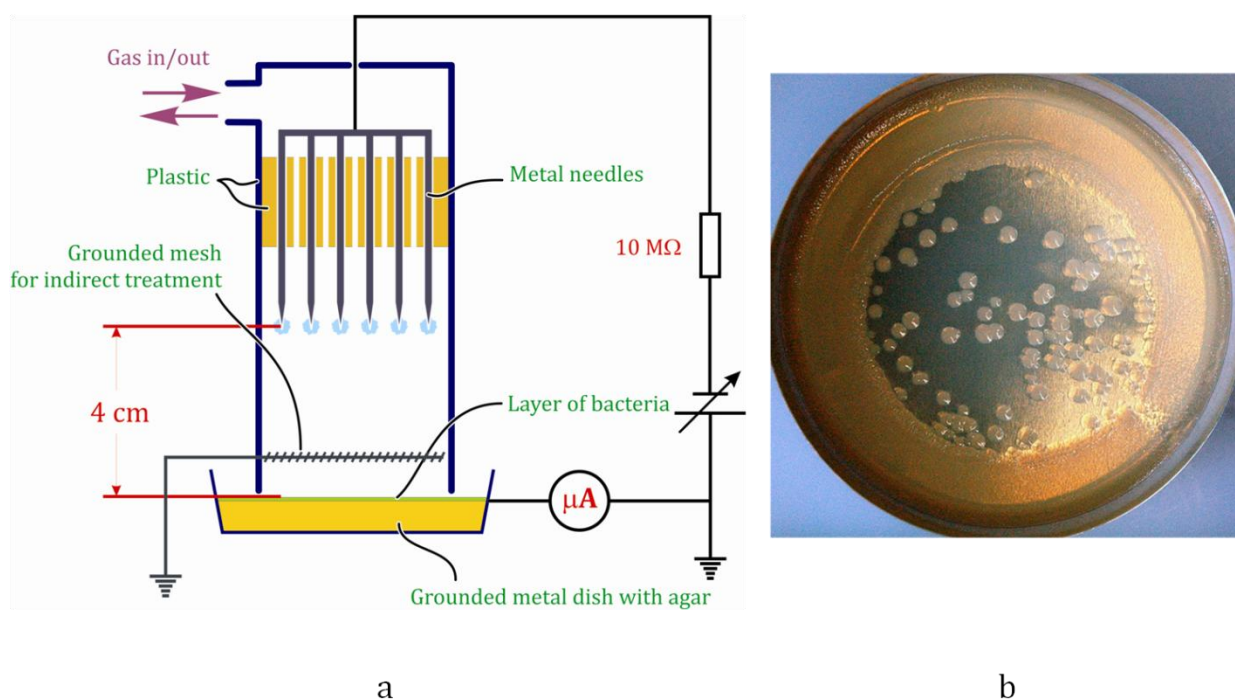
Figure 29 Schematic of the DC corona experimental setup (a), and representative picture of bacteria treated by corona discharge in air after incubation (b).

Results

Initial experiments were done with bacteria of various initial concentrations dried on agar ("moist" condition) utilizing corona discharge in room air (~60% humidity) with constant current of 100 μA. Resulting numbers of colonies on treated area after incubation were recalculated to a number of colony forming units (CFU) per cm^2 assuming that area of treatment was about 19.5 cm^2 . Because it is almost impossible to count relatively large number of colonies after the treatment with low doses, here we considered colony numbers less than ~150 CFU per treated area. To be able to study inactivation kinetics at lower doses we have used initial bacteria surface densities from 10^7 cm^{-2} to ~150 cm^{-2}. Results for corona of both positive and negative polarities of applied voltage are shown on Figure 30 in terms of colony number density as a function of dose, where exposure time of treatment area at constant current was recalculated to charge density ($\mu C/cm^2$). It is shown that positive corona discharge treatment of bacteria dried on agar surface at constant current of 100 μA permits up to about 6 log reduction of viable bacteria in about 90 seconds of treatment. Interestingly, negative corona has in general the same effect on bacteria viability, however the same level of inactivation may be achieved at 1.5 – 3 times higher doses of treatment.
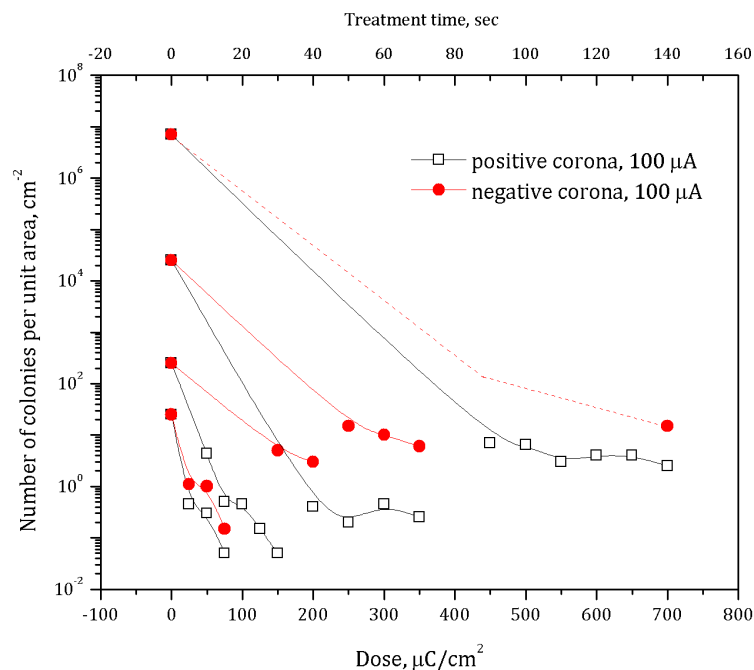
Figure 30 Bacteria inactivation on agar by positive and negative corona discharges in room air

Although corona discharge used in this study is expected to be relatively weak in terms of production of active neutral species, compared to, for example, dielectric barrier discharges (first of all, due to low discharge power), and to produce mostly ionic flows, here we also studied the effect of neutral radicals. In this set of experiments corona was ignited in room air between powered needle electrodes and grounded metal mesh placed 2 mm above bacteria layer dried on agar. The discharge current was kept at 100 µA. The results (Figure 31) show that, indeed, in the present discharge conditions neutral radicals alone probably do not play the major role: no visible effect was observed in the case of indirect treatment. Similar results (Figure 32) were achieved by introducing a reverse air flow through the discharge system (air flow direction was opposite to the ion flux). In this

case a large portion of neutral active radicals was carried out by the air flow, which did

not result in significant reduction of bacteria inactivation.
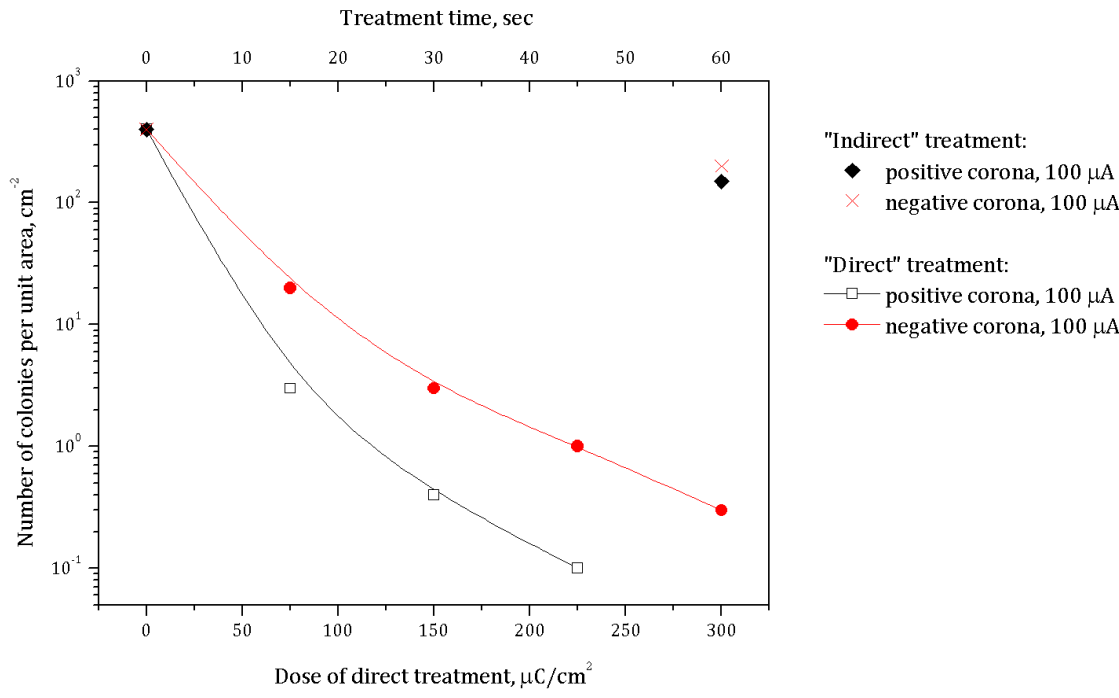
Figure 31 Bacteria inactivation on agar by direct and indirect treatment with positive and negative corona discharges in room air
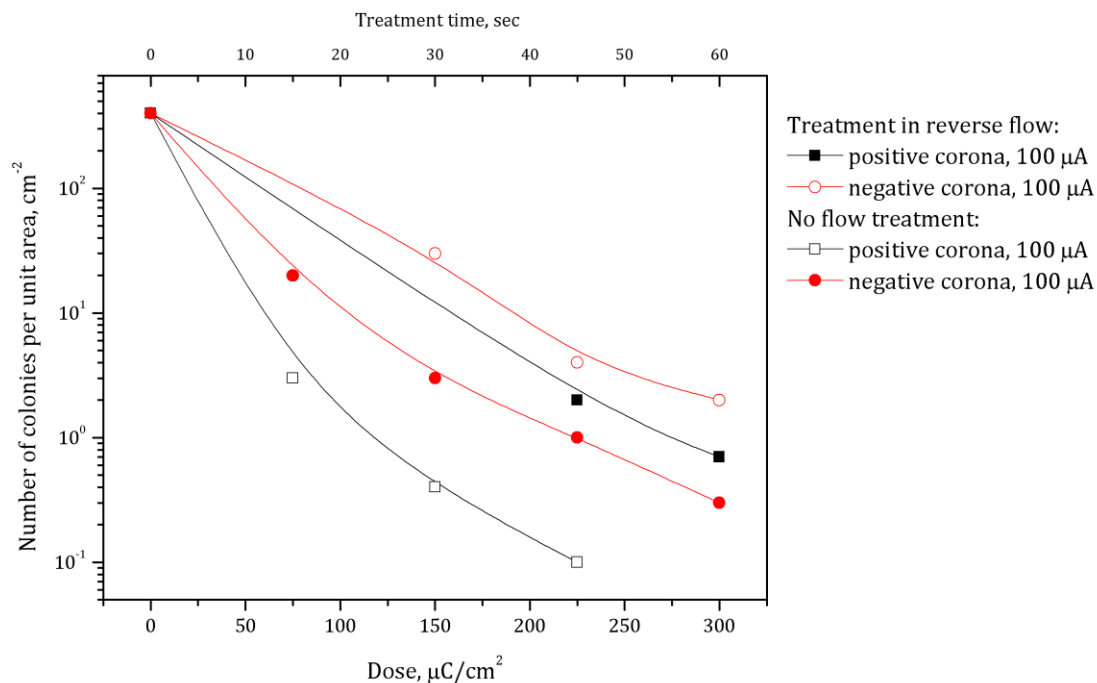
Figure 32 Bacteria inactivation on agar by positive and negative corona discharges in room air with and without reverse gas flow

In order to study the effects of different sorts of ions, a series of experiments on bacteria treatment dried on surface of agar was performed. Here we used He, Ar and N_2 flow through the system at rates of 10 slpm. High flow rates and ~60 second exposition prior to treatment (setup volume is ~0.2 l) ensured the full gas replacement before the experiment. Bacteria were treated with 100 μA corona for up to 60 seconds, and then immediately exposed to room air and incubated at standard conditions. After the incubation, no visible decrease in viability was noticed, as expected. Similar experiments were done using oxygen and dry air with the same treatment doses. Surprisingly, in these last two cases, no inactivation was observed also. Compared to room air, these experiments were done using dry gases at zero humidity, therefore next was to check the effect of water on inactivation efficiency of corona discharge. To do that, in three

separate experiments nitrogen, argon or oxygen was fed through bubbler contained distilled water at flow rate of 10 slpm. The results of the experiments are shown on Figure 33. Compared to room air (~60% RH), only in O_2/H_2O mixture the same inactivation efficiency was achieved, while no visible inactivation was observed in all other cases. These results show that neither UV radiation, ozone, H_2O_2, nor other *neutral active species alone* produced by corona in dry oxygen or other gases with water have an effect on bacteria viability. Also, it is clear that non-oxygen *charged species alone* or in combination with water do not provide any bacteria inactivation.
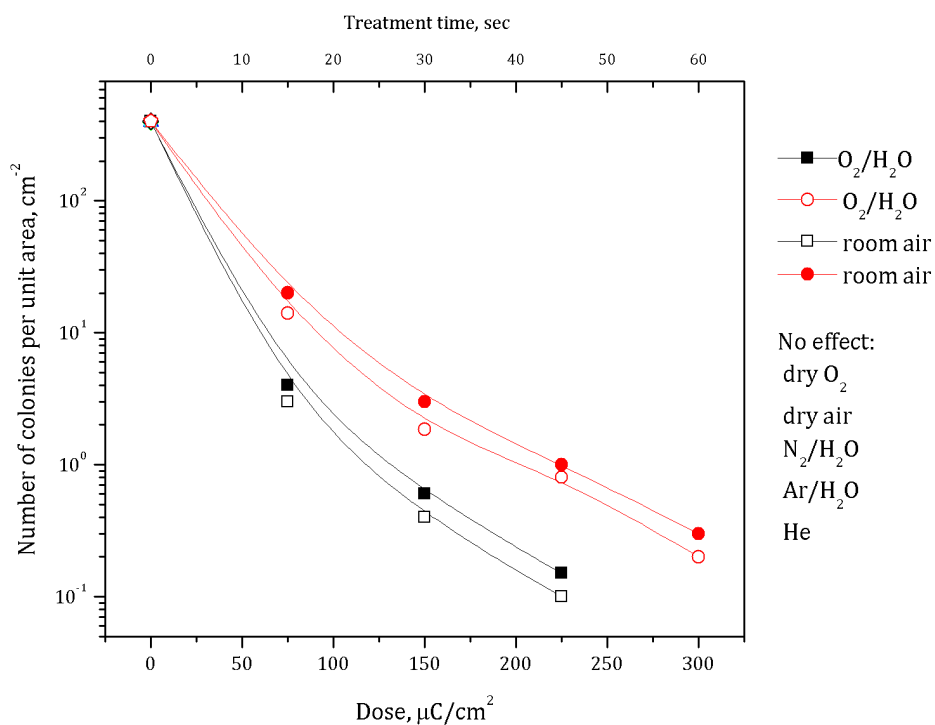
Figure 33 Effect of gas composition on bacteria inactivation on agar by positive and negative corona discharges

Possible effects of ions on bacteria inactivation may be divided in two groups: physical effect (e.g. membrane disruption due to accumulation of charges), and chemical (e.g.

catalysis of membrane peroxidation) [38,101,102]. In the first case, there should be a strong dependence on dose rate – time, which is required to accumulate certain number of charges on bacteria outer surface, probably should be relatively short, given that agar is a conductive media. In contrast, chemical mechanism is likely to be much slower. In order to separate these two possibilities, the following experiment was carried out. 400 µl of bacteria solution were dried on surface of agar and then exposed to positive corona discharge. Discharge current varied in the following ranges: 10, 50, 100 and 250 µA, with maximum treatment time from 700 to 30 seconds in order to provide same dose of treatment (number of charges). The results (Figure 34) make it possible to suggest, that inactivation mechanism is provided by chemical effects rather than physical.
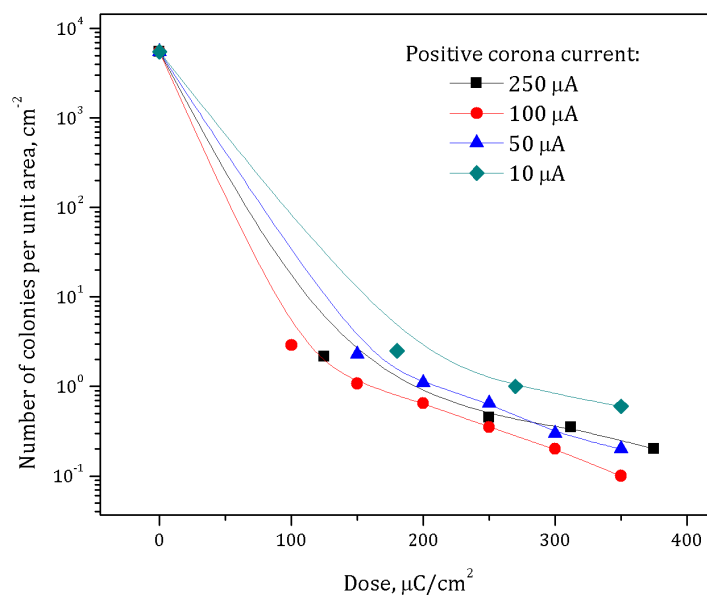
Figure 34 Effect of dose rate on bacteria inactivation on agar positive corona discharge in room air

Another important question is the role of water layer which covers bacteria: in all experiments described above, bacteria were dried on agar (hydrogel) at room air, and therefore were covered by minute amount of water ("moist"). To study the effect of this water layer, the experiment, similar to the first described in this paper, was performed. To minimize the layer of water covering bacteria, bacteria contained solution was dried on stainless-steel coupons as described in section above. Then bacteria were exposed to either positive or negative corona discharge at constant current of 100 µA. The results are shown on Figure 35, where it was taken into account that total treated area was 19.5 cm^2, but only 0.5 cm^2 were covered with bacteria. From these results one may conclude, that the actual difference between inactivation efficiency of "moist" bacteria is about 2-4 times higher than that of "dry" ones, which is in good correlation with our previous observations, when bacteria were treated with dielectric barrier discharge plasma [101]. However, given that the last experiment (treatment of "dry" bacteria) was done in humid room air, presence of water is still important, and optimal amount of water would lead to higher efficiency (as in a case of so-called "water chemistry"), and vice versa, excess water leads to dilution of the effect.
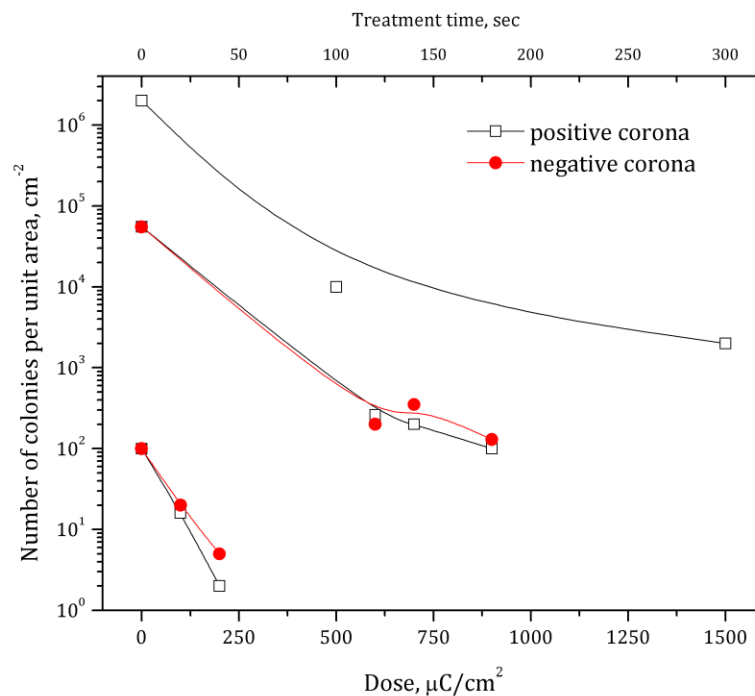
Figure 35 Inactivation of bacteria by positive and negative corona discharges dried on metal in room air

Using linear parts of inactivation curves from Figures 2 and 7, we have recalculated charge doses required for inactivation of "moist" and "dry" bacteria obtained for both positive and negative corona to obtain required dose per one log reduction and number of ions (assuming that each ion carries a single charge) per bacteria for different initial concentrations. These curves are shown in Figure 36.
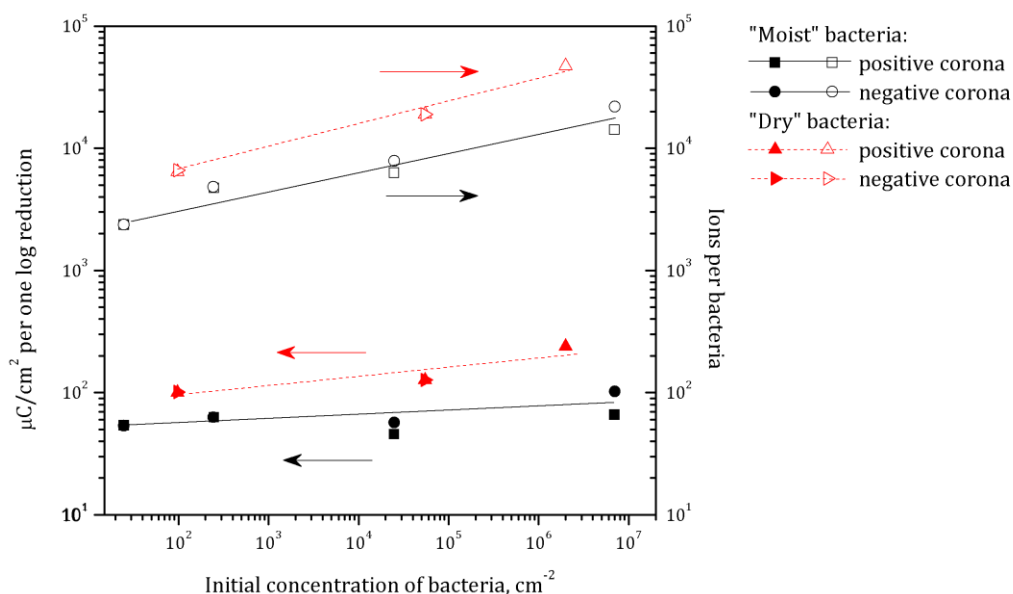
Figure 36. Dose per one log reduction and number of ions per inactivated bacteria for corona discharge treatment. Solid symbols – charge density, open symbols – specific charge per bacteria.

3.2 Role of ultraviolet light, hydrogen peroxide, and ozone on plasma inactivation

3.2.1 Effect of ultraviolet radiation in bacteria inactivation by direct dielectric barrier discharge

The mechanism of UV-based sterilization is widely studied, and indeed in many cases it plays major role [64,103], therefore experiment that analyzes the role of UV radiation produced by direct plasma was carried out. One way to protect bacteria from everything that is generated in plasma, except for the UV photons, is to place a quartz glass on top of the treated surface. In our experiments we have used quartz, which is transparent to UV photons of >200 nm wavelengths, and MgF_2, which is transparent to VUV photons of >140 nm wavelengths [92]. This way only UV/VUV photons generated in plasma reach bacteria. As can be seen in Figure 37, bacteria that are protected from direct discharge by

a 10 mm square MgF_2 slide are unaffected (highest dose used was 600 J/cm^2 with no observed difference between untreated bacteria and MgF_2-protected bacteria); thus we can conclude that the action of ultraviolet radiation for our case can be neglected. However, even though we observe no visible effect on bacteria by UV/VUV photons, it should not be discounted completely as UV, especially VUV, is known for its synergetic effect in interaction and destruction of model polymers [91,92,104].
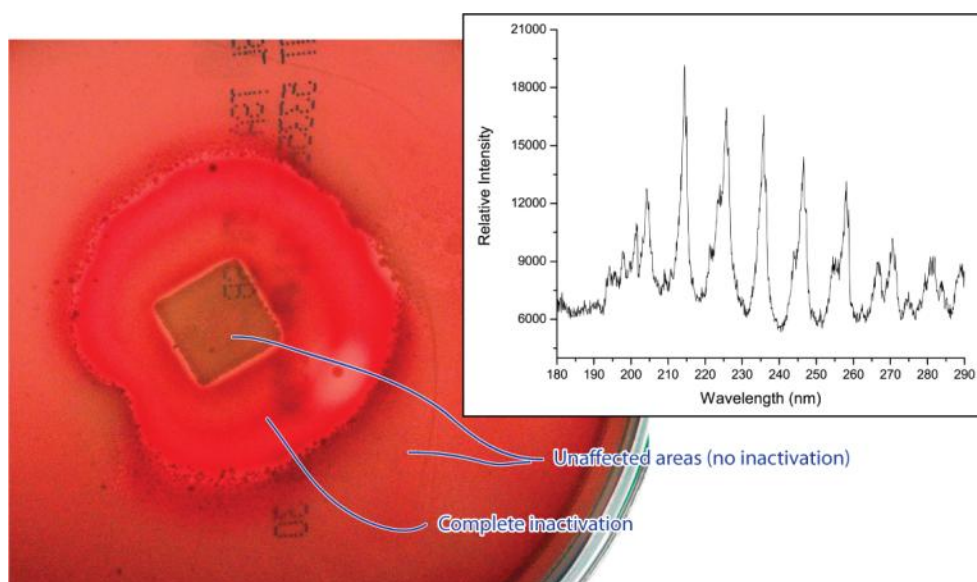
Figure 37. Emission from DBD plasma over the cell surface in UV range (right) and results of inactivation of bacteria by direct plasma contact compared with only UV (left). No effect on bacteria protected from plasma by MgF_2 slide (10 mm square in the center) is observed. In this image the plasma surface power density was 0.6 $Watt/cm^2$ and the treatment dose was 108 J/cm^2.

3.2.2   Effect of hydrogen peroxide produced by plasma on bacteria inactivation

In the presence of water molecules in room air, a certain amount of OH molecules is produced in DBD plasma. Although this highly reactive radical probably does not play a key role in inactivation process by itself, as was discussed above, the product of recombination of two polar OH molecules on charge centers, a hydrogen peroxide

molecule, may relatively easy pass cell membrane and later cause lethal effects (for example, fatal DNA damage [105,106]). The ability of hydrogen peroxide to sterilize is widely used and well studied, and therefore an experiment that helps analyze the role of hydrogen peroxide in DBD plasma inactivation of bacteria was carried out. Because measurement of H_2O_2 concentration on the surface of agar is a challenging problem, this concentration was estimated using approximation of the dependence of measured amount of H_2O_2 produced in liquid. Concentration of H_2O_2 was measured in distilled water and phosphate buffered saline (PBS) with H_2O_2 specific test strips (Emd Chemicals, No.:10081/1). Dependence of peroxide concentration on treated volume is almost linear, and increases approximately three times when amount of treated liquid is decreased 10 times (Figure 38). The estimated amount of liquid under the electrode (surface area of ~5 cm^2) in the case of "moist" agar is a few microliters; therefore, we can expect the concentration of peroxide is on the order of a few tens of mmol/L for plasma dose of several J/cm^2.
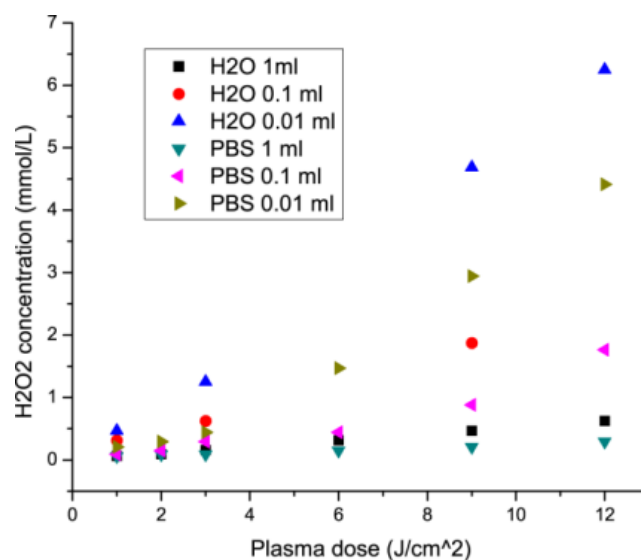
Figure 38. Dependence of peroxide concentration on volume of liquid for water and PBS.

To determine the concentration of H_2O_2 which causes the same sterilization effect on agar in direct plasma treatment, we use 50 volume percent water solution of H_2O_2, further diluted with distilled de-ionized water. The 0.1 ml droplet of the solution is poured onto bacteria dried on agar and spread over the whole agar surface. The results show that concentration of H_2O_2 that corresponds to 0.5 J/cm^2 of direct DBD plasma is more than 200 mmol/L (Table 3). As can be seen from Figure 38, in the best case direct DBD plasma produces 6.5 mmol/L H_2O_2 at plasma dose more than an order of magnitude higher than that required for inactivation by plasma; thus we conclude that while hydrogen peroxide may have some effect it is not the key mechanisms by which direct plasma inactivation occurs.

Table 3. Effect of hydrogen peroxide on inactivation of E. coli.

H_2O_2 volume %	H_2O_2 mmol/L	Inactivation result
50	20,000	Complete inactivation
5	2,000	
0.5	200	Some visible disinfection
$5 \cdot 10^{-2}$	20	No visible result
$5 \cdot 10^{-3}$	2	
$5 \cdot 10^{-4}$	0.2	

3.2.3. Effect of ozone produced in plasma on inactivation of bacteria

Bactericidal effect of ozone is well known and has already been utilized in industry for some time [107,108,109]. In room air, dielectric barrier discharge generates ozone which may be responsible for the observed bacterial inactivation. We assess the effect of ozone in two ways. First, dielectric barrier discharge in room air at ~60% relative humidity produces 28 ppm of ozone measured outside of the discharge zone (recorded by ozone-

specific spectrophotometer MedOzon 254/5, MedOzon, Russia). We then use ozone generator (~500 ppm max output, Quinta Inc) to produce same concentration of ozone in room air without plasma [50,51,52]. No inactivation effect was observed on *E. coli* and on skin flora (mix of streptococci, staphylococci, and yeast) in as much as 30 minutes of treatment. However, ozone meter measures ozone concentration downstream of plasma so the concentration inside plasma may be significantly different. For this reason we use nitric oxide to remove ozone [110,111,112]:

$$NO+O_3 \rightarrow NO_2^* + O_2$$

$$NO_2^* \rightarrow NO_2 + h\nu$$
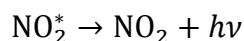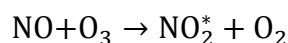
DBD plasma in gas produced by diluting a stock 700 ppm NO in N_2 with oxygen leads to the same inactivation efficiency as when pure N_2 with O_2 mixture is used while the measured ozone concentration is zero in the first case and 28 ppm in the second. Thus we can conclude that, as with UV and H_2O_2, ozone does not play a major role in inactivation of bacteria, at least in the case of *E. coli* or skin flora on agar surface.

3.3. The role of water in inactivation of bacteria

3.3.1 The role of water in direct plasma inactivation of bacteria

Water is present in all the plasma treatment cases discussed above. However, the effect of water and the amount required is not clear; and to analyze it we separate our treatment conditions into three groups: a) *dry* treatment, when a droplet with bacteria is placed on a glass slide and then dried in a desiccator in a biological hood until droplet appears completely dry (~1 hour); b) *moist* treatment, when droplet with bacteria is placed on agar surface and left to dry until agar appears dry (~1 hour); and c) *wet* treatment, when a

droplet with bacteria is placed in a cavity on a glass hanging drop slide and treated immediately, before water evaporates. Plasma treatment is then performed in direct or indirect conditions described above. There is a significant difference between these three cases: while on agar bacteria are covered with extremely thin, probably on the order of microns, layer of free water and the loss of charges in volume is small, in solution bacteria are covered with thick layer of water and therefore the effect of charged particles may be significantly diluted. In case of bacteria dried on glass slides, free water is evaporated almost completely, and bacteria are covered with layer of water molecules bound by van der Waals forces. In this last case, a priori, the result is not clear: the effect of plasma treatment may be enhanced due to energetic ion bombardment, or may be lowered due to the lack of free water which is required for effective oxidation processes.

Results of comparison of dry, moist, and wet treatment in direct and indirect setup are shown in Figure 39. For all the cases, a 0.2 ml of 10^8 CFU/ml *E. coli* solution was used and treated with plasma in ~1 J/cm^2 increments. It is clear that, as was previously shown by the authors [79], direct plasma treatment achieves inactivation at lower doses than indirect. Interestingly, this remains the case for all types of treatment regardless of the amount of water. While the difference in dose required for inactivation of bacteria in moist and wet conditions may be attributed to the amount of water protecting the organism, the case of dried bacteria is not as clear. The clear conclusion we can draw from this experiment is that presence of water and direct plasma treatment are both required to achieve fast inactivation and this inactivation is highly dependent on the amount of water.
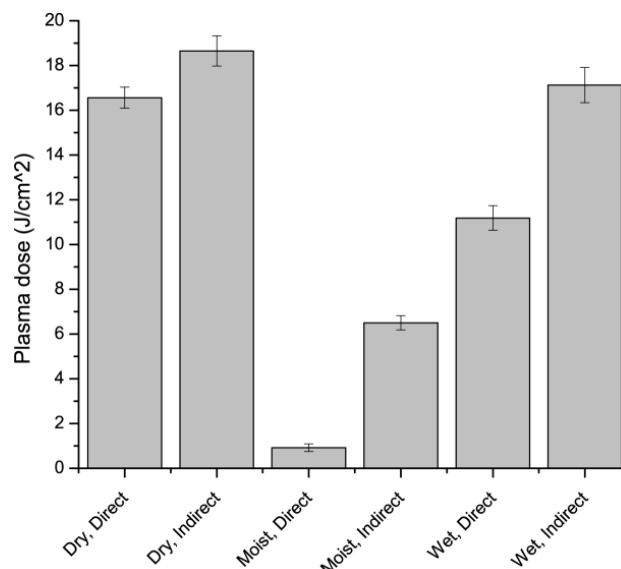
Figure 39. Results of comparison of dry, moist, and wet treatment in direct and indirect setup.

3.4. Discussion

In this chapter we address a problem of direct plasma interaction with bacteria, particularly, inactivation of viable bacteria. Plasma is a complex medium with the following major active components: charged particles (i.e. electrons and ions), electric fields (both global applied electric field and those associated with charges), photons (and first of all, energetic ones – UV photons), and neutral active species (free radicals, e.g. OH radical, and stable active products, e.g. O_3). It was noticed [4,38,101,102] that in the case of direct contact of plasma with the treated sample, i.e. when there is a physical charge transfer from plasma to surface, effect of plasma treatment is always the highest (here it is necessary to note, that this is true for treatment of surface, and not for treatment of liquid in volume [101]). In contrast, indirect plasma treatment, or treatment with afterglow, when only long-living species and in some cases active radicals are able to react with the sample, provides much lower efficiency. The mechanism of inactivation of microorganisms by cold atmospheric pressure plasmas is undoubtedly complex in nature,

and should be studied from both biological (i.e. processes that occur in microorganism after plasma treatment which lead to lethal or sub-lethal effects), and plasma-chemical (i.e. generation of active components in plasma, determination of major ones, an study of chemical and physical processes in water layer surrounding microorganism) sides. Here we are focused on inactivation of viable bacteria (not bacteria in spore form) using direct atmospheric pressure DC corona discharge and DBD plasma treatment because of possibility to separate the effects of different components.

In low pressure discharges UV radiation often plays a major role in sterilization, however in atmospheric pressure cold plasmas (such as DBD, corona, "plasma needle", etc.) it is usually not the case [36,38,41,101,102]. For corona discharge this suggestion is confirmed by the results of bacteria treatment in various gases, including dry air and oxygen (see Figure 33). Also, these results show that global electric fields in our experimental setup also have no effect on inactivation of viable *E. coli*.

A common hypothesis of bacterial inactivation mechanism by air plasmas is related to oxidative damage by neutral active species, either stable ones, e.g. ozone and hydrogen peroxide, or short living reactive oxygen species (ROS), like hydroxyl radical and atomic oxygen. These neutrals may be formed directly in plasma, in water layer surrounding bacteria, or inside of bacteria. DC corona discharges were studied to produce ROS, ozone, H_2O_2, etc., however, it was shown that ozone and H_2O_2 alone require much longer treatment times than direct plasma treatment (see, for example, [101]),. Our experiments show that the treatment of bacteria with corona discharge ignited in oxygen, where ozone is formed, resulted in no visible inactivation.

Hydroxyl radicals (and hydrogen peroxide as a result of recombination of two OH molecules) are formed in discharges ignited in humid atmosphere (for example, Ar/H_2O mixture):

$$M^+ + H_2O \longrightarrow M + H_2O^+$$

$$H_2O^+ + H_2O \longrightarrow H_3O^+ + \mathbf{OH},$$
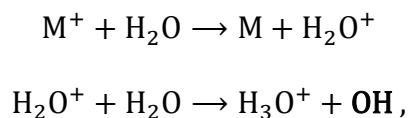
where M^+ is any ion. Hydroxyl radicals can then react with nearby organics leading to chain oxidation and thus damage of cellular membranes and other cell components (here R is any organic molecule):

$$OH + RH \longrightarrow \mathbf{R\cdot} + H_2O$$

$$\mathbf{R\cdot} + O_2 \longrightarrow RO_2$$

$$RO_2 + RH \longrightarrow RO_2H + \mathbf{R\cdot}$$
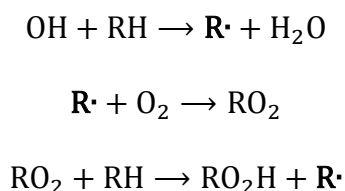
Hydrogen peroxide can travel trough liquid and relatively easy transferred though cell membrane, and at appropriate conditions inside the cell is converted back to hydroxyl radicals through a natural reaction chain termed Fenton mechanism:

$$H_2O_2 + Fe^{2+} \longrightarrow \mathbf{OH} + OH^- + Fe^{3+}$$

$$Fe^{3+} + O_2^- \longrightarrow Fe^{2+} + O_2$$
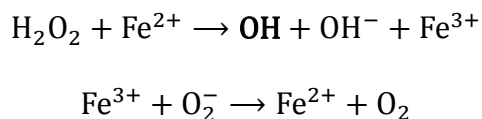
Bacteria are known to have protective mechanisms to "inactivate" hydrogen peroxide through enzymes, for example, catalase and peroxidase, which convert H_2O_2 into water and oxygen: $2H_2O_2 \rightarrow 2H_2O + O_2 . 2H_2O_2 \rightarrow 2H_2O + O_2$. Here we have experimentally shown that these two active species, OH and H_2O_2, alone do not play a major role in the process of bacteria inactivation.

Charged species were shown to have a great influence on efficiency of bacteria inactivation, and several hypotheses were proposed. First, it should be mentioned that energetic ions may be responsible for membrane etching, however, this probably happen mostly in low pressure plasmas or in streamers of direct DBD. Another possible effect of ions is traditionally associated with superoxide (O_2^-), which in presence of superoxide dismutase (SOD) is readily converted into hydrogen peroxide: $2O_2^- + 2H^+ \xrightarrow{[SOD]} H_2O_2 + O_2$, causing oxidative damage to the cell. Positive ions, as it was mentioned above, also may be converted into OH and hydrogen peroxide directly on the bacterial membrane. Third hypothesis is related to mechanical stress caused by electrostatic charging of bacteria [38,102]. It was considered, that bacteria charged in plasma (analogously to particle charging in "dusty" plasmas) under certain conditions may be ruptured due to mechanical stress. Although in this model only spherical gram-negative bacteria were considered, proposed electrostatic rupture mechanism possibly may be applied to nonspherical objects, which may be killed even easier. Another hypothesis is related to neutralization of bacteria surface charge which leads to cytoplasm leakage and cell death (analogously to surface disinfectants) [38]. These two last physical mechanisms of electrostatic inactivation of microorganisms may take place under condition of electrically isolated surface, where there is no leakage of transferred charge, but accumulation of these charges. In the present work, bacteria were placed on the surface of conductive agar which was grounded, and therefore no charge accumulation may be expected. The results of our study clearly show that inactivation of bacteria cannot be explained by the effect of only neutral active species or charged particles acting independently. Moreover, presence of oxygen and water molecules in the discharge is

absolutely necessary. Therefore a mechanism of peroxidation of bacterial membrane catalyzed by charges is proposed [101], where:

- both positive and negative ions have relatively the same effect;

- effect of charged species is *chemical* and not related to such physical phenomena as sheer stress, ion bombardment damage, or thermal effects;

- ions *catalyze* peroxidation processes of bacterial membrane composed of polysaccharides ;

- presence of *oxygen and water is necessary* and reactive oxygen species play a crucial intermediate role.

A multitude of ions may be produced in air plasma. Their concentration is lower than that of active neutral species but their effect may be stronger due to their ability to catalyze complex biochemical processes. Positive nitrogen or oxygen ions can be produced in a three-body collision: $e + 2N_2 \rightarrow N_4^+ + 2e$ or $e + 2O_2 \rightarrow O_4^+ + 2e$. Superoxide anion can be produced in a similar collision with another molecule, at the wall, or at a charge center: $e + O_2 + M \rightarrow O_2^- + M$. These ions are well known to create or catalyze chain oxidation processes in presence of organic molecules; for example, oxidation of aldehydes catalyzed by negative ions or oxidative hydrolysis catalyzed by positive ions (Figure 40) [113,114,115]:
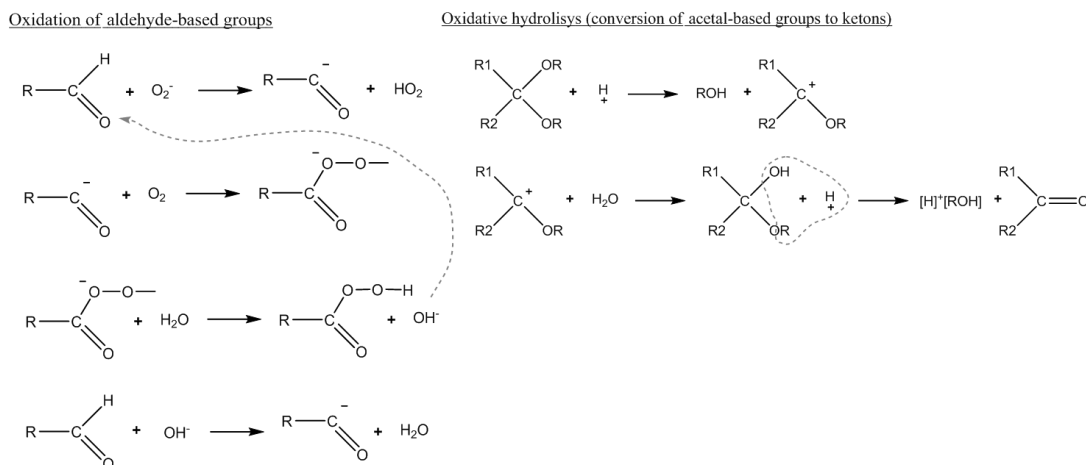
Figure 40. Oxidation reactions catalyzed by positive or negative ions that may take place in solution.

It is well known that these reactions can create long chains for both positive and negative ions and these chains may be much longer than the OH oxidation of organic molecules discussed in the previous section. In other words, charges may have an effect on bacteria and cells in solution due to the oxidation and peroxidation chain reactions they can catalyze; the same may be a reason for difference in doses required to inactivate bacteria versus achieve cellular damage which will be discussed in the next section.

The role of water vapors in the plasma system may be related to charged water clusters which carry both charge and radicals (e.g., OH and H_2O_2), resulting in simultaneous delivery of all active components to bacteria. Another possibility is related to production of highly reactive HO_2 ions which are effectively transported to the target inside of protective water clusters.

In summary, it is shown that for an effective and fast inactivation of bacteria on a surface by a plasma discharge simultaneous presence of oxygen and hydrogen contained

compounds (e.g. water vapor) is required. It is well known, that in a discharge ignited in this atmosphere highly biologically active peroxides, peroxide radicals and their ions (e.g. H_2O_2, HO_2, OH^-, H_3O^+) are produced. The significant difference in the inactivation efficiency observed in the experiments with the direct and indirect plasma treatment setups demonstrates the importance of charged particles. Through, the efficiency does not strongly depend on the polarity of ions: both positive and negative charges are important. In the O_2-H_2 system, these may be cluster ions $OH^-(H_2O)_n$ and $H_3O^+(H_2O)_n$. We show in experiments of pure oxygen (mainly O_2^- and O_4^+ ions) and pure nitrogen (electrons and N_4^+ ions) atmospheres that ions probably play a secondary role, and the chemical composition in the most important factor. Therefore we come to the conclusion that the role if charge in the process of bacteria inactivation is probably related to the active radical transport to the treated surface.

Our estimations show, that in an electric field of about $E/n \sim 30$ Td that is created in the discharge gap, the ion (mainly $OH^-(H_2O)_n$ and $H_3O^+(H_2O)_n$) drift time to the surface is about 100-200 μs. In contrast, convective transport with a typical speed of about 1 cm/s for the same distance of 4 cm requires about 4 seconds. Therefore, presence of charged particles provides about 4 orders of magnitude faster transport of active radicals to the treated surface, while the transport does not depend on polarity of ions. Thus, recombination losses are significantly reduced and the inactivation efficiency is increased.

This mechanism explains that the bacteria inactivation efficiency does not depend on the discharge polarity (in fact, the difference between positive and negative coronas is related to different peroxide radical ions – H_3O^+ and OH^-), the low effect of the treatment with

the discharge ignited in a dry atmosphere (the role of ions is related to fast radical transport to the surface), and the difference between direct and indirect treatment (charged radical clusters $OH^-(H_2O)_n$ and $H_3O^+(H_2O)_n$ are effectively trapped by the grounded metal mesh which prevents their transport to the bacteria).

CHAPTER 4. COLD PLASMA INACTIVATION OF *BACILLUS CEREUS* AND *BACILLUS ANTHRACIS* (ANTHRAX) SPORES

The mechanisms of non-thermal plasma inactivation of viable bacteria were discussed in the previous chapter. However, bacteria in spore form seem to be inactivated by plasma in a different way, first of all because of multiple protective layers and low metabolism. Here the results of experimental study on inactivation of *Bacillus* spores by FE-DBD plasma are presented and possible mechanisms are discussed.

Bacillus species, which are ubiquitous in the environment, are aerobic or facultative anaerobic, gram-positive bacteria [116,117,118]. The genus *Bacillus* is divided into three broad groups, depending, amongst other characteristics, on the morphology of the spore. *B. cereus*, *B. anthracis* (anthrax) and *B. thuringiensis* belong to the *B. cereus* group [116,119]. Moreover, morphological and chromosomal similarities between these species have prompted the view that *B. anthracis*, *B. thuringiensis*, and *B. cereus* are all varieties of a single species [116]. Bacilli can produce a dormant cell type called a spore in response to nutrient-poor conditions. Bacterial spores have little or no metabolic activity and can withstand a wide range of environmental assaults including heat, UV and solvents [120,121,122,123]. To kill or inactivate *Bacillus* spores one can apply 0.88 mol/l hydrogen peroxide, pH 5.0 for 3 hours to sterilize a spore suspension of 10^6 spores per ml, 5×10^7 μW/cm^2 of UV radiation for 30 hours to achieve 0.67 log reduction in 0.1 ml of 10^8 spores per ml placed on a wood carrier, or 10^6 rad of gamma irradiation to sterilize 10^6 spores per ml [123].

B. anthracis spores, as opposed to vegetative cells, are the infectious form and cause anthrax. Spores of *B. anthracis* represent a noteworthy bioterrorism agent, and can be easily distributed in dry form in parcels and letters via postal service, as occurred in 2001, when anthrax-contaminated letters sent through the US postal service killed five people and sickened 23 others [124], in aerosols or in contaminated water, for instance. In response to these possibilities, an effective, low-energy and cost effective method of spore inactivation or sterilization is required. An attractive method of spore inactivation is plasma treatment. Low temperature plasma at low pressure, arc discharge plasma, microwave plasma, and other plasmas are effective in sterilization of spores [59,61,125,126,127]. For example, Kuo et al. reported that a 3 to 5 log reduction of *B. cereus* spores in aqueous suspension can be achieved after several seconds of treatment with arc-seed microwave (2.45 GHz, 700W) plasma torch [61]. Several systems based on different types of discharge have been reported [59,61,126,127]. In most of these systems spores were treated either at low pressure, or with relatively high power discharges, and 1 to 5 log reduction of germinated spores was achieved within a few minutes of treatment.

In the present study we were interested in inactivating *Bacillus* spores in both dry form and suspended in water with use of atmospheric pressure Dielectric Barrier Discharge (DBD) plasma on surfaces, as well as inside of closed volumes, e.g. envelopes. We reported previously on sterilization of bacteria and yeast, including skin flora such as streptococcus and staphylococcus, on agar surfaces with atmospheric pressure DBD plasma [128]. It took 5 -10 seconds in the case of direct DBD treatment to achieve up to an 8 log reduction of a mixture of staphylococci, streptococci and Candida yeast species. The results of the present study show that inactivation of bacteria in spore form both in

liquid or air-dried on surface requires higher doses of DBD plasma treatment, and up to 5 log reduction can be achieved within a minute of exposure to plasma. It is also shown that the mechanisms by which direct plasma inactivates spores and vegetative bacteria may be quite different.

4.1. Materials and Methods

The atmospheric pressure DBD plasma was used to treat *Bacillus* spores at room temperature in air. The powered electrode was made of a 2.5 cm diameter solid copper disc covered by a 3.5 cm diameter 1 mm thick quartz dielectric. The discharge gap was kept at 1.5 mm. The microsecond-pulsed DBD discharge was ignited by applying AC pulsed high voltage of 30 kV in magnitude (peak to peak) and 1.3 kHz frequency between the electrodes. Current peak duration was 1.2 μs, and corresponding plasma surface power density was 0.3 W/cm^2.

Spores were treated in either dry form or in aqueous suspension on glass slides (Figure 41). The slides were placed on top of grounded metal and plasma was ignited directly between the powered electrode and treated spores. For treatment of spores in water, in order to avoid splashing of the solution due to charging during plasma treatment, we used hanging drop slides with well diameters of 15 mm and 20 μl capacity (Fischer Scientific). To prevent loss of spores due to disbursement during treatment of air-dried spores, spores were dried in a plastic chamber (Figure 42) placed on a grounded metal surface, and covered with a glass cover slide. The chamber was ventilated with air for faster drying of samples; and was washed with water to collect spores after treatment.
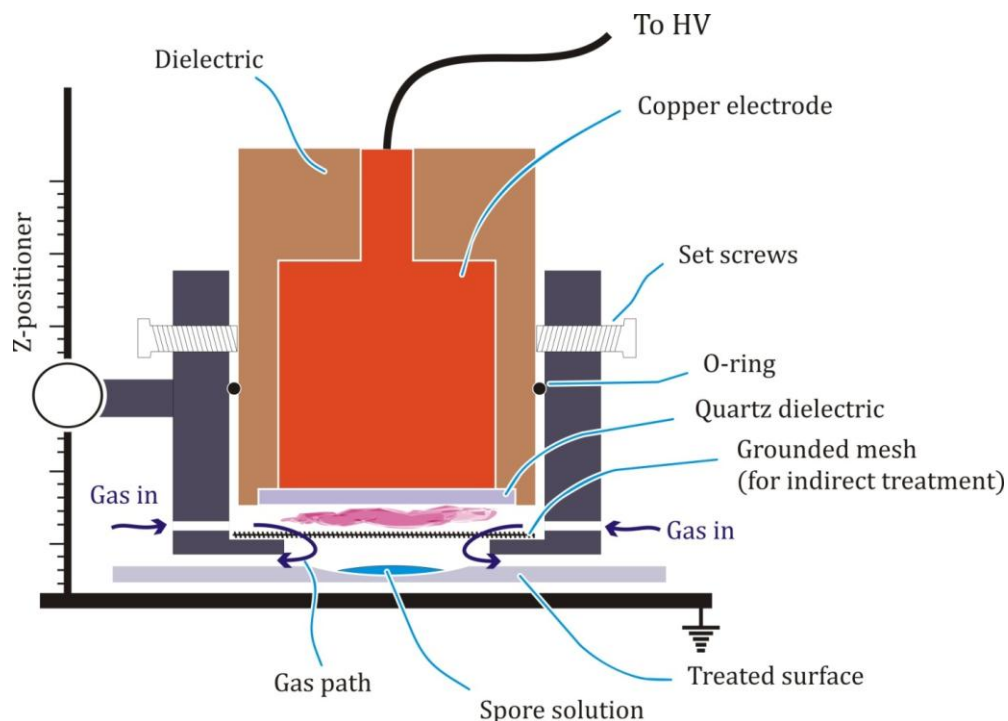
Figure 41 Principal schematic of the DBD plasma treatment setup with removable mesh, used for indirect treatment. Additional flow of ethanol vapor may be provided as shown by gas flow arrows.

Another set of experiments was carried out using indirect plasma treatment. In this case we used a modified plasma system (Figure 41), where grounded metal mesh (22 wires per cm, 0.1 mm wire diameter, 0.35 mm openings, 60% open area, weaved mesh) was used as a second electrode. The gap between the mesh and the second electrode was kept at 1.5 mm, the same in the direct treatment setup. The distance between mesh and treated surface was also kept at 1.5 mm.

In this study we used *B. cereus* (ATCC 6464, *B. cereus* Frankland and Frankland) and *B. anthracis* (Sterne strain 7702) spores suspended in distilled water at 10^5 to 10^8 spores per ml. These experiments were first done using *B. cereus* spores as a surrogate for *B. anthracis* spores, and then repeated with *B. anthracis* species. Spores were prepared

according to standard protocol [129], [130]. Each experiment was repeated three times. Treated spores were diluted and plated on Brain Heart Infusion (BHI, Fisher Scientific) agar, incubated at 37^0C overnight, and colony forming units (CFUs) were counted. All work with *B. anthracis* was done in BSL 2 laboratory, certified by Drexel University and by the CDC.
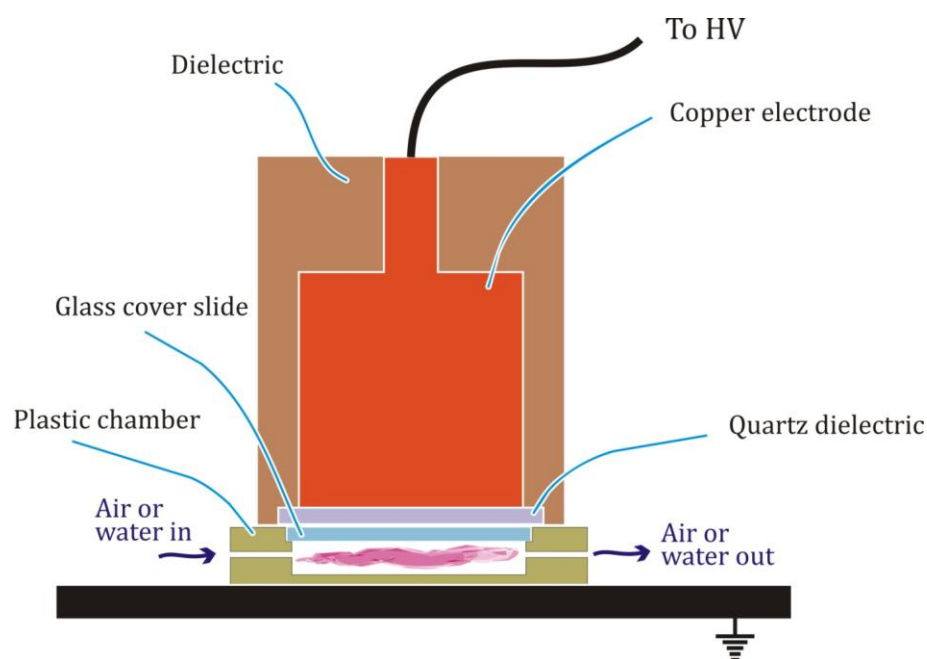
Figure 42 Schematic of the setup for treatment of air-dried spores with direct DBD plasma.

Treatment of spores in suspension

Ten μl of *B. cereus* or *B. anthracis* spores in distilled water at concentrations of 10^7, 10^6, and 10^5 spores per ml, were placed in hanging drop glass slide wells and treated for 5 to 45 sec with direct DBD plasma. After treatment, bacteria were appropriately diluted and plated, as above. Experiments were done in duplicate on 3 different days.

Treatment of dried spores in room air

Spores were placed inside a plastic chamber (see Figure 42), covered with a glass cover slide and dried for about 30 minutes with constant air flow of about 0.1 l/min (control experiments with only gas flow through the chamber showed no loss of collected spores). 10 µl of *B. cereus* at 10^8, 10^7, and 10^6 spores per ml in distilled water were used. Dried spores were treated with direct DBD plasma for 5 to 45 sec, and then washed out of the chamber with 30 ml of distilled water, appropriately diluted and plated, as above. Similar experiments were done using *B. anthracis* spores, except 10 µl of *B. anthracis* spores were placed inside of either plastic or paper envelopes, dried in room air for 1 hour and treated with DBD plasma. In these experiments, the discharge was ignited in the volume of either plastic chamber, or paper or plastic envelope (envelopes were slightly inflated to assure that walls are in contact with powered and grounded electrodes (Figure 43)).
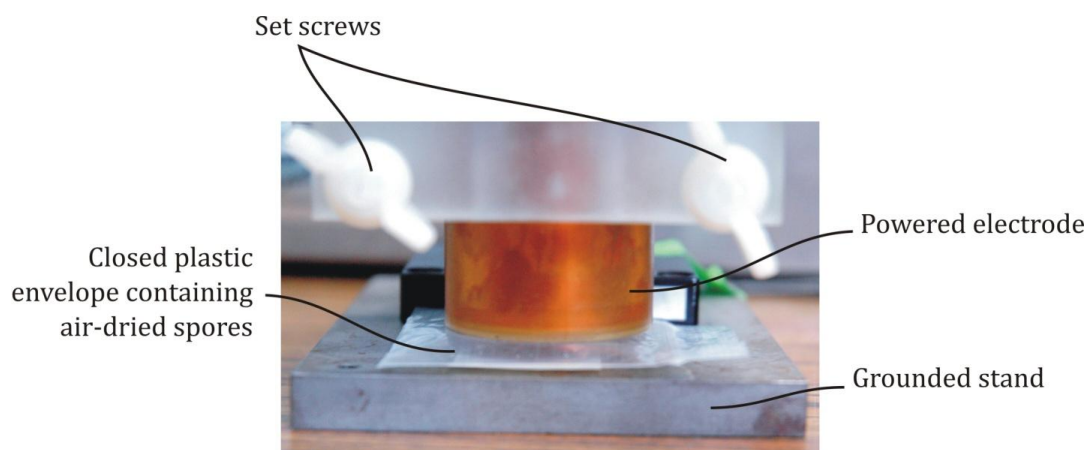
Figure 43 The setup for DBD plasma treatment of air-dried spores contained inside a closed envelope

Direct versus indirect treatment of spores in room air

We compared the effects of direct and indirect DBD plasma treatment on *B. cereus* spore viability. Ten μl of spores in water at 10^5 spores per ml were treated with direct or indirect plasma for 10 to 60 seconds, and appropriately diluted and plated.

4.2. Results and Discussion

In the first series of experiments, the spores of two *Bacillus* species, *B. cereus* and *B. anthracis*, were treated in water droplets on the surface of glass slides using atmospheric pressure DBD plasma in room air. The inactivation kinetics of these *Bacillus* spores of three different concentrations after DBD plasma treatment are shown in Figure 44. The number of colonies after treatment is plotted on a logarithmic scale as a function of treatment dose and time, which are directly related. Although spores of both species were effectively inactivated (up to 5 log reduction in less than a minute of treatment), log *N*, i.e., killing kinetics, was quite different for *B. cereus* vs. *B. anthracis* spores; 2-step vs. linear, respectively. In addition, anthrax spores appeared to be slightly more resistant to plasma treatment (see inset in Figure 44). These species have similar morphology, metabolism and physiology, and similar behavior of inactivation kinetics was reported previously, for example when aqueous spore suspensions were treated with UV_{254} irradiation (see Figure 6 in [131]). It was noted by the authors that this difference may be related to virulence plasmids that may influence UV sensitivity of *B. cereus* and *B. anthracis* spores.
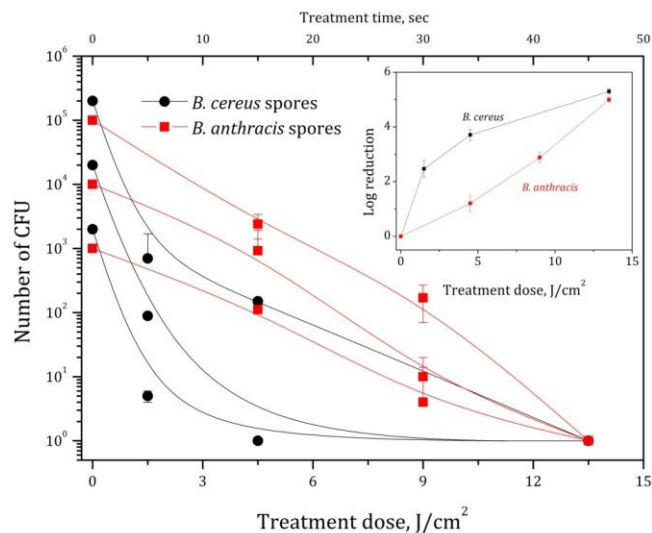
Figure 44 Inactivation of various concentrations of *B. cereus* (filled squares) and *B. anthracis* (filled circles) spores in water on glass slides using direct DBD plasma treatment.

In contrast to inactivation of spores suspended in distilled water, inactivation by plasma treatment of air-dried *B. cereus* and *B. anthracis* spores both appear to be linear. Figure 45 shows the results of plasma inactivation of three different concentrations of *B. cereus* spores dried inside a plastic chamber (see Figure 42). Inactivation of 10^7 per ml anthrax spores inside of a closed paper envelope is shown in Figure 46. Similar results were obtained in the case of plastic envelope (data not shown). These results are interesting, as they show the high efficiency of DBD-plasma based systems to sterilize within temperature sensitive materials. This is important in view of the 2001 bioterrorism attacks when anthrax spores in envelopes were distributed through the U.S. postal service, resulting in illness and death [124].
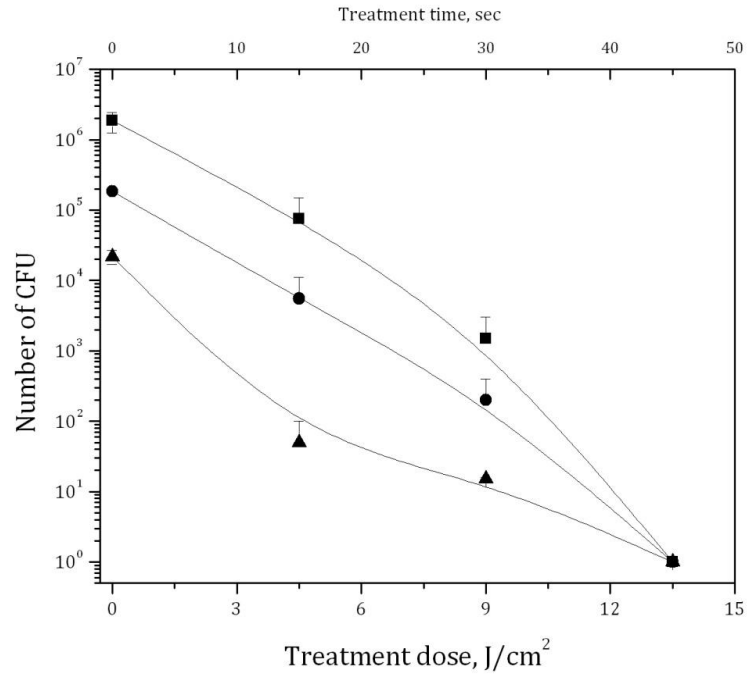
Figure 45 Inactivation by direct DBD plasma of various concentrations of dry *B. cereus* spores contained inside a closed plastic chamber.
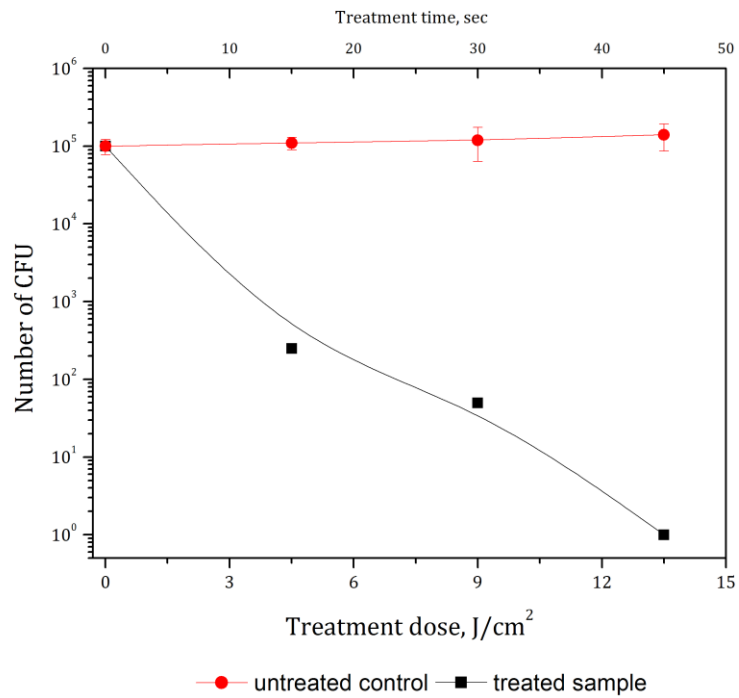
Figure 46 Inactivation by direct DBD plasma of dry *B. anthracis* spores contained inside a paper envelope.

Fridman *et al* [128] observed a significant difference (a few orders of magnitude) in killing of bacteria (streptococcus and staphylococcus) and yeast when charged species were excluded from plasma by introducing a grounded metal mesh between the powered electrode and the treated surface. In this case plasma is generated remotely (indirectly) and active neutral species and radiation are delivered to the object with the plasma afterglow. In our previous experiments [28] we observed that in the case of direct plasma treatment of bacteria on agar with an initial concentration of 10^8 CFU per ml in phosphate-buffered saline (PBS), complete sterilization was achieved in 5 to 10 seconds, and in more than 15 minutes in the case of indirect plasma treatment. To determine the role of charged species (electrons, ions and associated electric fields) on inactivation of spores we performed similar experiments using *B. cereus* spores in distilled water (Figure 47). The difference in spore inactivation, about 1.5 log, appears to be not as large as for vegetative bacteria, however, it is still significant. Moreover, in the case of indirect plasma treatment, the inactivation process clearly consists of 2 stages, with about the same inactivation rate in the first stage as we observed for direct plasma treatment. The effect of charged species, electron and ions, may be related to production of hydrogen peroxide in liquid phase (similar reactions may take place in the gas phase; all experiments were done in room air at about 60% relative humidity):

$$\begin{cases} e^-_{(H_2O)} + O_{2(H_2O)} \rightarrow O^-_{2(H_2O)} \\ 2O_2^- + 2H^+ \rightarrow H_2O_2 + O_2 \end{cases}$$

$$\begin{cases} M^+ + H_2O \rightarrow M + H_2O^+ \\ H_2O^+ + H_2O \rightarrow H_3O^+ + OH \\ OH + OH \rightarrow H_2O_2 \end{cases}$$
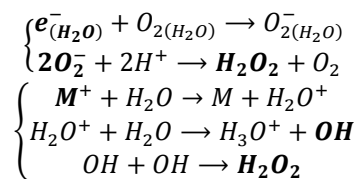
where M^+ is any positively charged ion. Hydrogen peroxide is readily soluble in water and is relatively easily transported through outer spore coats [132]. At appropriate

conditions, hydrogen peroxide may be converted inside of spores to hydroxyl radicals through a natural reaction chain termed Fenton mechanism:

$$\begin{cases} H_2O_2 + Fe^{2+} \longrightarrow OH + OH^- + Fe^{3+} \\ \quad\quad Fe^{3+} + O_2^- \longrightarrow Fe^{2+} + O_2 \end{cases}$$
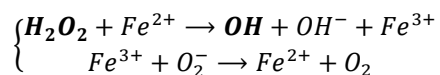
To determine the role of neutral OH radicals, which may react directly with spores due to their extremely high reactivity, or which may be converted into hydrogen peroxide, we introduced ethanol vapors into indirect DBD plasma discharge, and treated *B. cereus* spore suspensions in water (in plasma, ethanol is easily decomposed with formation of OH radicals and hydrogen peroxide [133], [134]). There was no decrease in spore viability in control experiments where only ethanol vapor flowed through the system (data not shown). The results (Figure 48) show that additional production of OH radicals allows greater inactivation of spores.
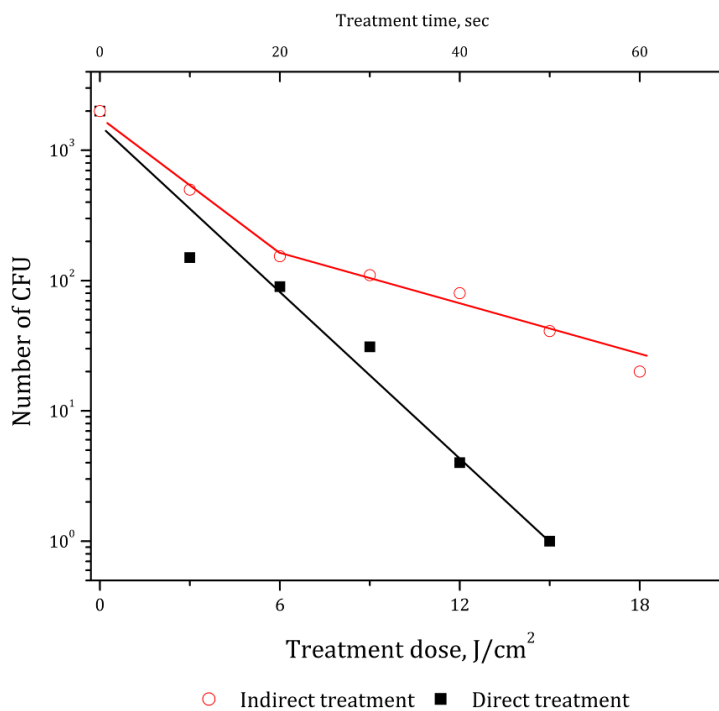
Figure 47 Inactivation of *B. cereus* spores in water using direct and indirect DBD plasma

To see if morphological differences occurred, we analyzed spore morphology before and after DBD plasma treatment. *Bacillus cereus* spores were deposited onto stainless steel coupons and were observed by scanning electron microscopy (SEM). Samples were then exposed to DBD plasma for 1 minute (corresponding to a dose of 18 J/cm^2), and SEM photomicrographs of the same spores were taken again. As can be seen when comparing the photomicrographs of spores before and after treatment (Figure 49), the inactivation mechanism is not erosion of the spores, since their protective coats appear to be undamaged. Therefore, we believe that diffusion of chemically active oxygen species (e.g. H_2O_2) into spores followed by damage of internal macromolecules or molecular systems may be the primary mechanism of spore inactivation.
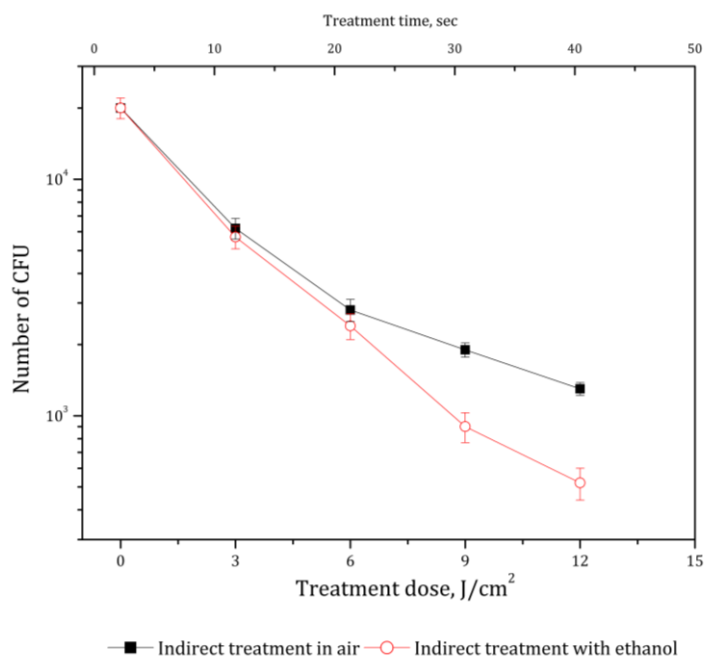
Figure 48 The effect of ethanol vapor on inactivation of aqueous suspensions of *B. cereus* spores by indirect DBD discharge.
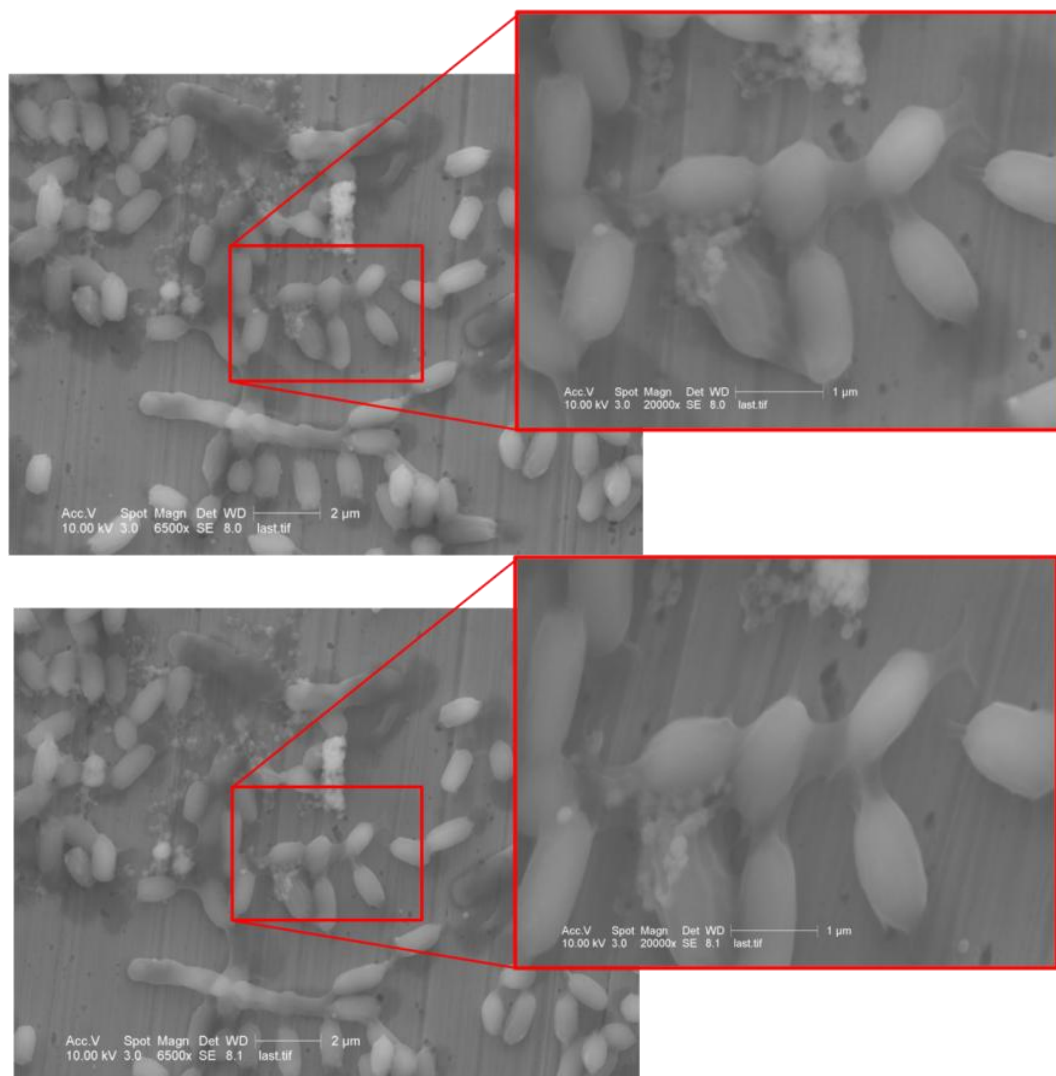
Figure 49 SEM photomicrographs of *B. cereus* spores on a stainless steel coupon before (top) and after (bottom) exposure to direct DBD plasma (same spot of one sample in both photos)

4.3. Conclusion

In summary, the mechanism by which DBD plasma kills *Bacillus* spores appears to be quite different from the mechanism by which it kills vegetative bacilli. As indicated above, a 2-stage process occurs in killing of spores by DBD plasma: the first stage, which is not sensitive to the presence of charged particles, may be dominated by the effect of UV radiation generated by the plasma. This supposition comes from the following observations: 1) the initial rate of inactivation of spores is about the same for direct and

indirect plasmas (slightly less for indirect, since the metal mesh allows less radiation to access the sample); 2) difference in inactivation rate of *B. cereus* and *B. anthracis* spores, which may be related to different sensitivity due to differences in, for example, plasmid and surface content. The second stage appears related to production of neutral reactive oxygen species that are transported inside the spore to cause damage to biomolecules critical to cell's survival or germination. One possible effect may be related to oxidation of germination proteins located in spore coats, or inactivation of germination receptors which are located on inner spore membrane [135,136]. Both germination proteins and germination receptors are required for successful germination [135,136]. Hydrogen peroxide is one possible agent responsible for such effects, as it is known to inactivate spores at low concentrations [120]. It was suggested that lethal action occurs through inactivation of enzymes which are mainly located in the spore protoplast, and of the germination apparatus, while no lysis of spores is noticed [120].

We have demonstrated that DBD plasma is able to effectively inactivate *Bacillus* spores both in liquid and in dry forms: up to 5-log reduction of spores was observed after less than a minute of treatment. We also showed that active oxygen radicals play a significant role in the inactivation process.

CHAPTER 5. PLASMA STERILIZATION OF LIVING TISSUE: IN VIVO STUDIES

One of the most widely discussed potential applications is plasma treatment of wounds for the purpose of reducing microbial load and enhancing healing processes [55,79,137,138,139]. Two major types of plasma treatment have been discussed in connection with wound disinfection (see Chapter 3). One is indirect treatment using gas flow through plasma which brings mostly neutral active species in contact with living tissue. The other is direct application of non-thermal plasma to living tissues. Indirect treatment permits to decouple plasma system design from constraints related to applying the treatment to living tissues. For example, it permits to employ thermal plasma for generation of active species including substantial quantities of NO [63,88,140,141]. Indirect plasma treatment of skin and wounds has been investigated over the last several years demonstrating a significant effect [137]. On the other hand, applying non-thermal plasma directly to living tissue makes it possible to employ charges and short living neutral species [94,142]. It has been demonstrated above that bacterial inactivation on surfaces of agar and even skin can be achieved significantly faster with direct exposure to non-thermal plasma such as the Dielectric Barrier Discharge (DBD). No significant toxicity was observed during relatively low power and duration plasma exposure which is typically sufficient to achieve significant reduction in the bacterial load [94,137,140,143]. However, effects of direct DBD plasma treatment on bacterial inactivation in real wounds have not been reported so far.

In this chapter, a study where open wounds contaminated with bacteria are treated with Floating Electrode DBD plasma directly is presented. Rat is employed as the animal model. Although bleeding is stopped and most of the excess wound fluid is removed prior to plasma application, the wound remains moist. The results demonstrate that over 3-log reduction (over 1000 times) of bacteria occur following only 1 min of DBD plasma treatment without any visible tissue damage.

5.1.   Materials and methods

Floating electrode dielectric barrier discharge

In this study we have used a floating electrode dielectric barrier discharge (FE-DBD) generated between an insulated high voltage electrode and the sample (FE) undergoing treatment. Half millimeter thick polished clear fused quartz (Technical Glass Products, Painesville, OH), was used as an insulating dielectric barrier. The setup and high voltage electrode schematic is shown in Figure 50. The discharge was generated by applying high voltage pulses with the following characteristics: 20 kV (p-p), 1.6 µs pulse duration, 1 kHz frequency. The average power density for the active area of the high voltage electrode was kept at the level of approximately 0.5 W/cm^2, i.e. 0.74 Watt for 15 mm electrode diameter. The electrode was specifically designed to fit into the Polycarbonate holder as is shown in Figure 50 and a set of spacers of 0.5 mm thickness was provided to the operator to allow for controlled application of plasma for every wound.
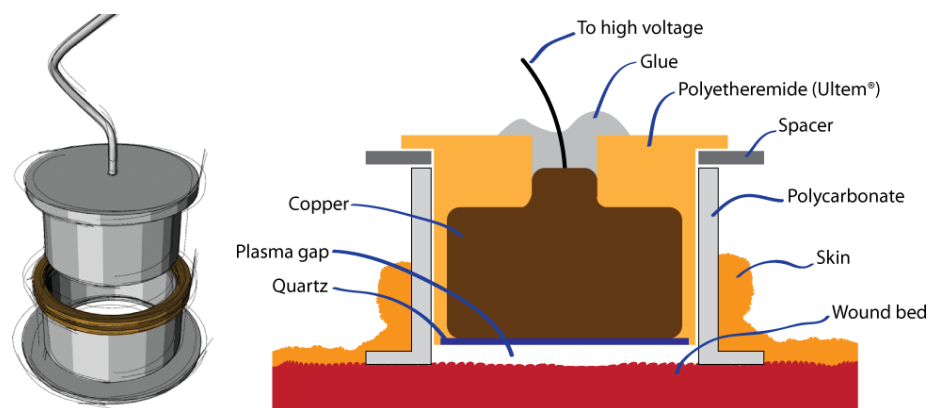
Figure 50. Schematic of the FE-DBD plasma electrode that fits into the plastic ring sutured to the wound.

All procedures were performed in compliance with the animal welfare and protection act following the Drexel University's Institutional Animal Care and Use Committee (IACUC) approval.

Animal model

Thirty hairless Sprague-Dawley rats, weighing approximately 250 g, arrived and acclimated for 3-5 days in the facility. Animals were transferred from the vivarium to the approved surgical suite. Animals were continuously anesthetized with inhalational gas anesthetic, Isoflurane (Vedco, St. Joseph, MO) at 2-3% induction plus oxygen 2L/min then 1.5-2% maintenance administered via a face mask for the appropriate length of time and placed in the supine position. Animals received analgesia (Meloxicam, Boehringer-Ingelheim, Germany) at 1 mg/kg, subcutaneous, Bupivicaine 25% (Hospira, Lake Forest, IL) 0.5 ml/site intradermally and Normosol R (Baxter, Deerfield, IL) crystalloid parenteral fluid therapy at 10ml/kg subcutaneous bolus at the onset of anesthesia but prior to surgery. The ventral surface of the rat was prepared in sterile surgical fashion: the surgical area was gently washed and sanitized with chlorhexidine

scrub solution; the area underwent an initial contact scrub of 5 minutes, rinsed with normal saline solution and repeated second time; a preparatory solution of diluted chlorhexidine with isopropyl alcohol (1:8) was lightly sprayed onto the surgical area. Approximately 2 cm incisions along the right and left side of the thoracic region were inflicted and plastic rings were inserted into the subcutaneous layer of the skin (ring size was equivalent to the size of the plasma probe) and restricted the bacteria to the affected area only, Figure 51). The skin was sutured with 3-0 nylon around the ring in a continous suture pattern. Twenty μl drops of PBS solution containing *S. aureus* at concentration of 10^5 or 10^6 ml^{-1} were applied to the wounds and covered and secured with sterile Tegaderm dressing (3M, St. Paul, MN). Animals were recovered from anesthesia in a pediatric warming incubator and bacteria incubated for four hours. Upon completion of bacterial incubation, animals were re-anesthetized, wounds were opened and treated with DBD or untreated controls. After treatment, wounds were swabbed using sterile technique and transferred into PBS for further dilution and plating and plated directly onto BHI agar. Bacteria inactivation efficiency by DBD plasma treatment was analyzed after 14 hours of incubation on BHI agar. Figure 51 shows the sequence of steps taken during the animal procedure.

Figure 51. Steps taken during the animal procedure: (a) a cut is made; (b) plastic ring is inserted into the skin and (c) sutured in place; (d) wound area is inoculated with known concentration of *S. aureus* and (e) covered with sterile dressing; 4 hours following inoculation the sterile covering is removed and (f) wound area is treated with plasma; after the treatment (g) the wound area is thoroughly swabbed and (h) plated for bacterial counts.

All data is reported with 95% confidence interval ($p < 0.05$) and the number of samples in each experiment is identified.

5.2.   Results and discussion

The results of viable *Staphylococcus aureus* inactivation in living tissue of experimental wound using FE-DBD plasma for initial concentration of bacteria of 10^5 or 10^6 cells per ml of PBS are shown in Figure 52. We observed a 3-log reduction of bacteria after a one minute exposure to plasma, and the results are similar for the both initial concentrations of bacteria.
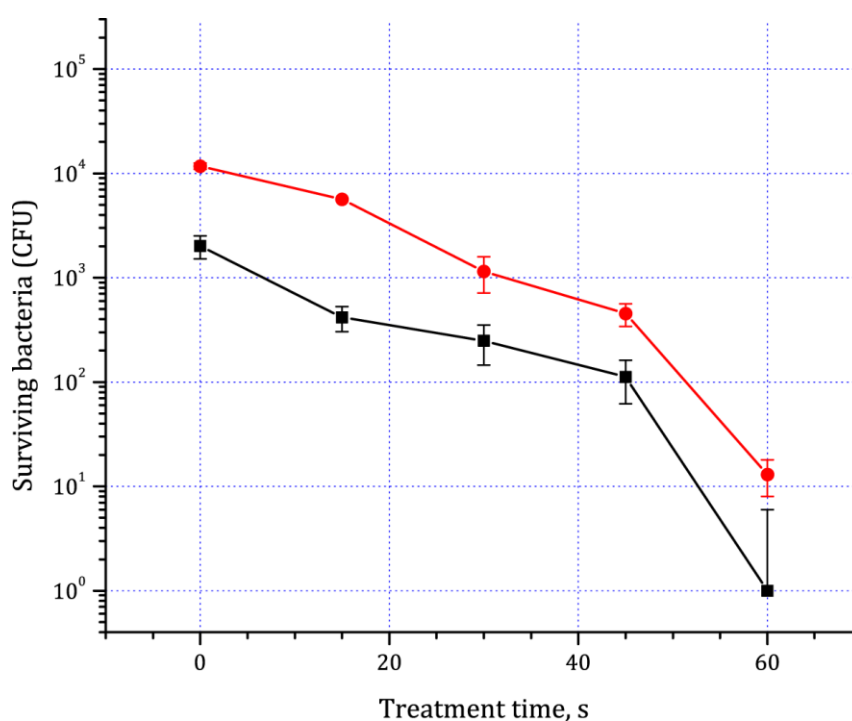
Figure 52. Results of wound sterilization with 10^3 and 10^4 starting bacterial load.

Interestingly, the inactivation efficiency of plasma treatment in the wound is about an order of magnitude less than that for the agar surface [94,137]. Here we propose two possible explanations of this effect. First, it is necessary to mention that even under assumption of discharge uniformity (i.e. discharge was covering the whole surface of the electrode, which in present setup was impossible to control), direct plasma exposure has provided only at ~75% of the wound surface due to presence of dielectric enclosure around central copper. Therefore, it is possible that the remaining ~25% of bacteria, which were relatively uniformly distributed over the wound, were treated indirectly. Indirect plasma exposure, i.e. when there is no direct exposure of the treated bacteria to charged species, was previously shown to be about an order of magnitude less effective in bacteria inactivation on agar than direct treatment. The second hypothesis is related to the presence of wound liquids – compared to almost dry, covered with a minute amount of water, "moist" surface of agar. Again, as we have previously shown, liquid water plays as a "protective" layer, preventing direct delivery of charges to the bacteria surface, and significantly dilutes the inactivation effect of active neutral particles [79,142]. At the same time, this wound liquid, which contains high amount of organic molecules, and wound itself may also react with plasma produced reactive species, resulting in decreased activity of plasma treated medium.

5.3. Conclusion

While we have previously shown effective inactivation of pathogenic organisms in many regimes of plasma and on various surfaces (see [137,142] for examples) we have not previously addressed sterilization of living open wound tissue such as would be present during surgery. Here, it is shown that sterilization is possible and is quite effective of an

open wound area of bacteria that was allowed to "settle" in the wound for 4 hours. While the treatment appears to not have any adverse or toxic effect on the wound tissue (as was previously the case with intact skin [94]) an open question remains of the effect of plasma on the wound itself and on the wound healing rate. Since plasma was previously shown in-vitro to generate reactive oxygen species (ROS) which were shown to promote cell proliferation [143] and in this work was confirmed in-vivo to produce bacterial inactivation similar to in-vitro studies we may assume that wound healing time will be reduced following the treatment. This, however, remains to be verified and is the subject of the follow-on studies.

CHAPTER 6. DIRECT AND CONTROLLABLE PRODUCTION AND DELIVERY OF ACTIVE SPECIES BY PLASMA

Cold atmospheric pressure plasma discharges have been shown to be effective when applied for wound sterilization and decontamination purposes and wound healing. Action of specific charged or neutral active species or radiation is frequently associated with the corresponding specific effect (e.g., anti-inflammatory effect of nitric oxide (NO), and highly oxidative hydroxyl radical and other reactive oxygen species (ROS)). Traditionally, production of these biologically extremely important reactive species has been measured in gas phase, i.e. at the production point – plasma itself or plasma afterglow. Although these measurements are undoubly necessary and useful, the real effect of plasma treatment is almost never "direct" (except for special cases of, for example, low pressure sterilization of surfaces or polymer treatment), and is often associated with so-called "water chemistry". Indeed, in the case of wounds, where a large amount of various biological liquids (e.g. blood, pus) is present, plasma produced reactive species are first react and diffuse in media, and then for successful activation of signaling pathways of healing mechanism have to be delivered even further – deep into tissues and cells. Therefore, measurements of production and delivery of plasma produced ROS, followed by numerical modeling of these processes linked to the plasma source, seem to be extremely important for the development of fundamental understandings of the plasma-tissue interaction.

In this chapter we discuss the results of experimental studies on plasma delivery of reactive oxygen and nitrogen species (ROS and RNS) into liquid media.

6.1. Detection and measurement of ROS and RNS produced in liquid media by microsecond spark discharge in a pin-to-hole electrode configuration (PHD)

Reactive oxygen and nitrogen species play an extremely important role in many biological processes, and depending on concentration of these species one may expect different effects on cells – from accelerated cell growth to apoptosis and necrosis. Therefore it is important to control amount of ROS and RNS produced by plasma in a treated biological object. Since almost always these objects (cells and tissues) are surrounded by certain liquid media, as a first step we chose detection and, if possible, measurement of ROS and RNS in a solution. One of the easiest way to do that is utilizing a widely used among biologists, well studied and readily available fluorescent technique, where a certain fluorescent dye reacts with a specific molecule of interest and as a result of this reaction its fluorescent properties are changed. One of drawbacks of this method is that it is difficult to synthesize a dye which would react only with specific specie of interest (because of highly reactive nature of these species), and usually manufacturers indicate "preferred" reactive specie. However, by blocking (scavenging) other possible reactants it is possible to measure the concentration of specie of interest with little error. Here we focused on detection and measurement of the following species: hydrogen peroxide, superoxide (O_2^-), peroxynitrite and "singlet" oxygen. It is necessary to mention, that although the manufacturer specifically indicated that it is possible to measure singlet oxygen, it is still not clear in which state exactly the molecular oxygen is detected.

6.1.1. Materials and methods

Microsecond spark discharge plasma in a pin-to-hole spark discharge configuration (PHD) was used in all experiments. Measurements of hydrogen peroxide (H_2O_2), superoxide (O_2^-), peroxynitrite ($ONOO^-$) and "singlet" oxygen produced by plasma were done in phosphate buffered saline (PBS), since according to the manufacturers' protocols fluorescent properties of dyes highly depend on pH of the solution, while PBS provides necessary pH buffer properties. Measurements of H_2O_2 were done using 100 mM Amplex UltraRed reagent (Invitrogen) fluorescent dye with addition of 200 U/ml horseradish peroxidase (MP Biomedicals) according to the manufacturer's protocol. The reagent is a fluorogenic substrate for horseradish peroxidase (HRP) that reacts with hydrogen peroxide (H_2O_2) in a 1:1 stoichiometric ratio to produce Amplex® UltraRed, a brightly fluorescent and strongly absorbing reaction product (excitation/emission maxima ~568/581 nm). To obtain calibration curves for hydrogen peroxide in the plasma treated samples a standard stabilized 3% H_2O_2 (Fisher) water solution properly diluted to obtain various concentrations was used. Superoxide (O_2^-) was measured indirectly by H_2O_2 concentration increase in presence of superoxide dismutase (SOD, 3 U/mL, Fisher): 2 O_2^- + 2 H^+ [+SOD] $\rightarrow$ H_2O_2 + O_2 [+SOD]. Peroxynitrite, which is not a free radical, but also a powerful oxidant and is product of reaction of superoxide with nitric oxide: $O_2^- \cdot + NO \cdot \rightarrow ONO_2^-$, was measured using 2,7-Dichlorodihydrofluorescein (DCDHF, Ex/Em: 502/523 nm) (Cayman Chem, 300 mM in DMSO). Singlet oxygen was measured using 10 mM Singlet Oxygen Sensor Green Reagent (Ex/Em: 504/525 nm, Invitrogen) solution in PBS. According to the manufacturer's protocol, the Singlet Oxygen Sensor Green reagent is highly selective for $^1O_2$; unlike other available fluorescent and

chemiluminescent singlet oxygen detection reagents, it does not show any appreciable response to hydroxyl radical or superoxide. To check that, we have used singlet oxygen and OH scavengers, sodium azide NaN_3 (Fisher Sci, 600mM in PBS) and D-mannitol (Fisher Sci , 300 mM in PBS) respectively, added to the dye containing solution right before the treatment. In order to ensure that UV radiation produced by the discharge does not result in increased fluorescence, the solutions were first treated through a 0.5 mm quartz glass placed in front of the discharge. Fluorescence was measured using an LS55 (Perkin Elmer) fluorescent spectrometer equipped with well plate reader accessory.

6.1.2. Results and discussion

H_2O_2 concentration in PHD plasma treated PBS (Figure 53) increased up to 60 µM with 30 seconds of direct plasma treatment, while no significant effect was measured due to UV radiation. In terms of H2O2 concentration, superoxide O_2^- radical was detected in about the same amount – roughly twice higher signal was detected in the presence of superoxide dismutase.
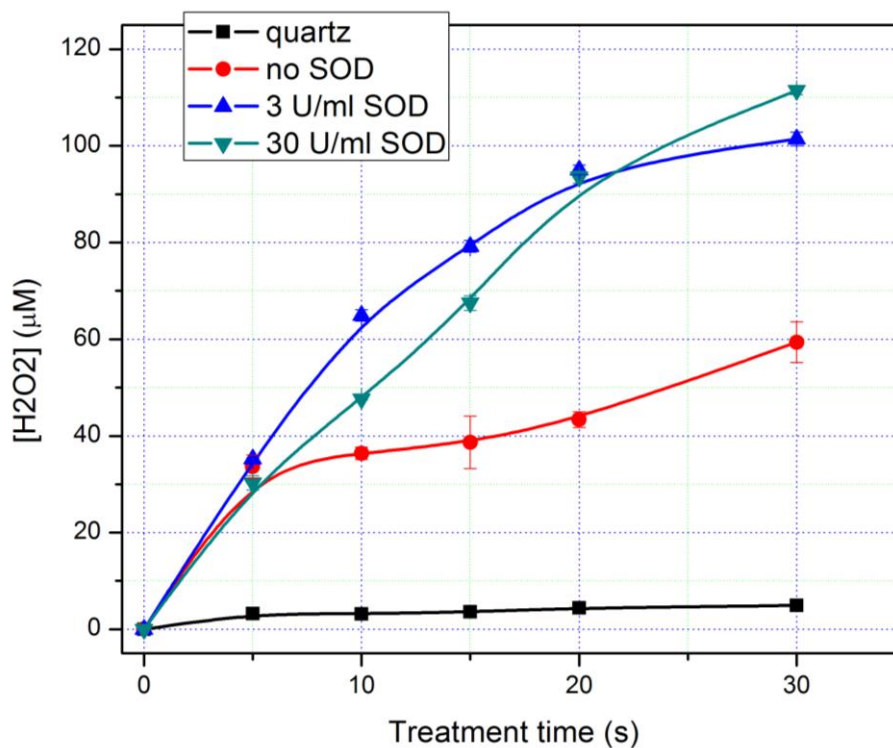
Figure 53 Measured H_2O_2 and O_2^- concentration in PHD plasma treated PBS

When measured singlet oxygen, the results obtained appear to be quite confusing: although there is definite dependence of the dye fluorescence on the distance from the plasma source (Figure 54), but addition of OH and singlet oxygen scavengers resulted in comparable fluorescent intensities. These results indicate that the Singlet Oxygen Sensor Green reagent may be sensitive to both of them and also depends on presence of other reactive species.
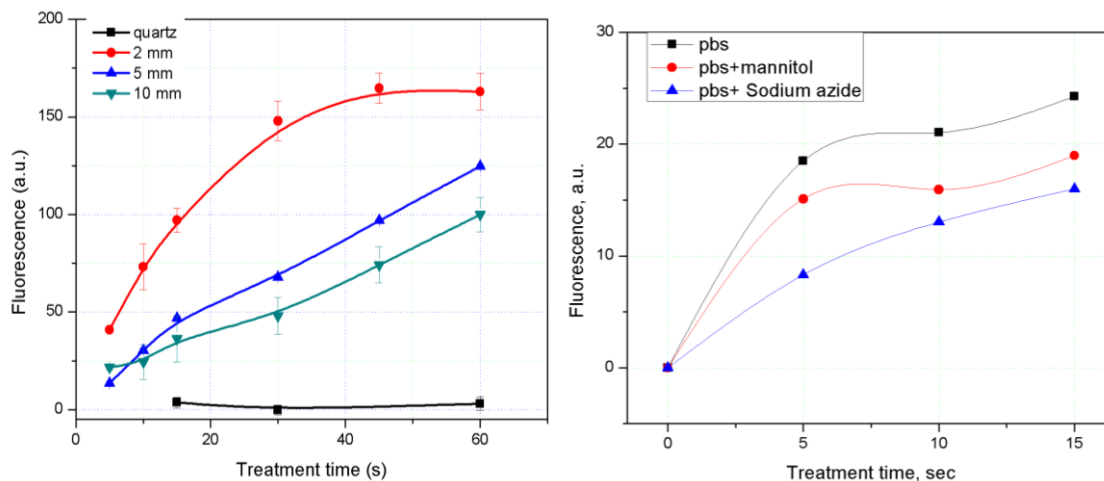
Figure 54 Detected "singlet" oxygen in PHD treated water (left), and effects of scavengers on "singlet" oxygen detection signal.

In contrast, measurements of peroxynitrite were fairly consistent (Figure 55), and addition of superoxide dismutase, which prevents formation of $ONOO^-$ by reacting with $O2^-$, resulted in significantly lower fluorescent signal.
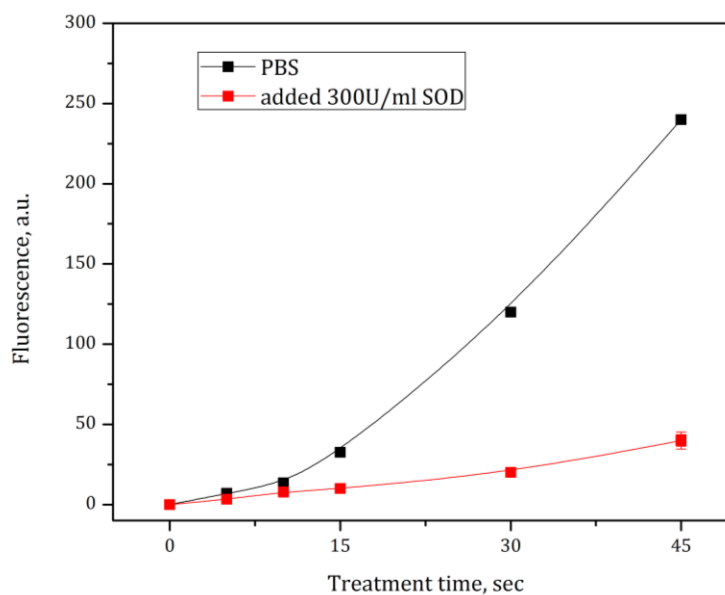
Figure 55 Detected peroxynitrite in PHD treated water.

6.2. Direct and controllable nitric oxide delivery into biological media and living cells by a pin-to-hole spark discharge (PHD) plasma

Nitric oxide (NO) is a short-lived bioactive molecule critical to inflammatory and vascular processes, in particular wound healing. In the early wound, high NO levels are produced by inflammatory cells such as neutrophils and macrophages to fight infection [144]. As the wound heals, endothelial cells, fibroblasts and keratinocytes produce lower sustained NO amounts to stimulate angiogenesis and new tissue formation. The critical role of NO in wound healing is evidenced by poor wound healing in animals with decreased NO production, which was reversed by exogenous NO application [145].

Various local topical NO delivery systems have been developed to promote wound healing in NO-deficient wounds, such as diabetic ulcers [145,146,147,148]. However, the success of these treatments was limited by short NO half-life, rapid or inconsistent NO release over a limited timeframe, and NO donor instability [145,149,150]. Any NO therapy for wound healing should have simple administration with minimal side effects. Ideally, the approach should address both the wound inflammatory and healing stages.

NO treatment from thermal plasmas has previously been shown to enhance wound and skin disease treatment. The "Plazon" system, a rapidly quenched hot air plasma jet, can provide a relatively high NO concentration with significant therapeutic effect [17,151]. This plasma device was used in two modes. In "hot mode," the plasma jet was used to rapidly coagulate and sterilize wound surfaces, as well as to remove, dissect, or desiccate dead tissue and pathologic growths. In "cold mode," the NO-rich plasma gas flow (20–40°C) was used to stimulate regenerative processes and wound healing. Additional NO

plasma sources include a pulsed arc discharge, a high frequency discharge, and an atmospheric pressure plasma jet [152,153,154].

An alternative NO producing plasma, a pin-to-hole spark discharge (PHD), has also been reported to sterilize liquids and surfaces (including living tissue) and may stimulate wound healing. The advantages of this plasma include that it is small and portable, uses a low voltage power supply, operates in room air, can be applied directly to tissue without measurable damage, and can deliver both reactive oxygen species (e.g., hydrogen peroxide) and UV radiation. However, this spark discharge and its cellular effects have never been characterized.

In this study, we measured the PHD plasma NO production in gas, and NO delivery into liquid and cells. We further investigated plasma NO effects on cell viability and intracellular signaling. It is shown that the PHD plasma effectively produces and delivers NO, which results in a functional cellular response with minimal cell toxicity.

6.2.1. Materials and methods

Spark discharge plasma in a pin-to-hole spark discharge configuration (PHD) was used in all experiments. To prevent cell effects due to plasma discharge UV emission and reactive oxygen species (ROS) production (e.g. hydrogen peroxide), either straight or curved 50 mm Tygon tube extensions were attached to the cathode (Figure 56).
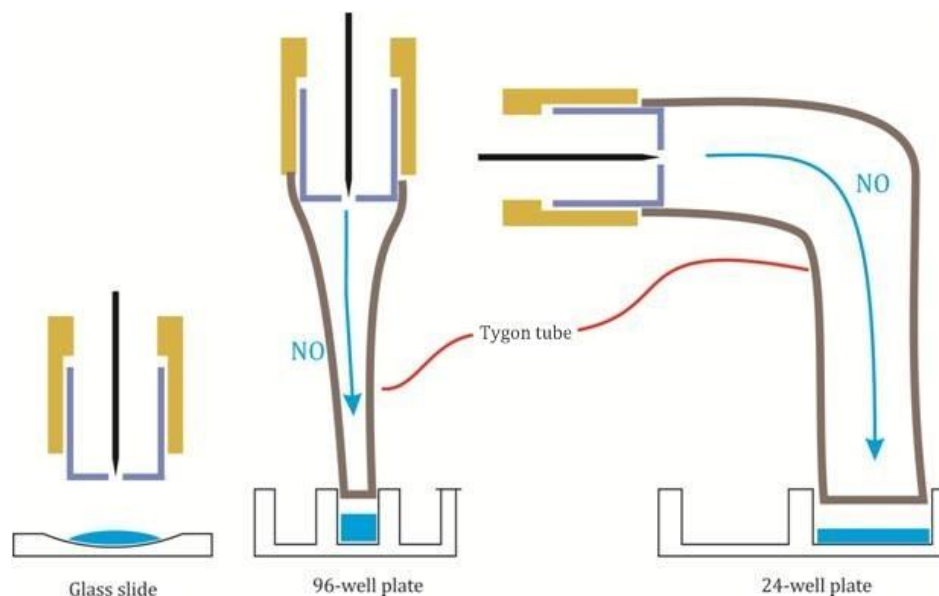
Figure 56 Probe extensions used in the study: direct treatment at 3 mm distance, straight and curved 50 mm tube extensions.

Endothelial cell culture and plasma treatment

Porcine aortic endothelial cells (PAEC) were isolated from swine aorta by the collagenase dispersion method [155]. Cells were cultured in low glucose Dulbecco's modified Eagle's medium (DMEM, Mediatech) supplemented with 5% fetal bovine serum (Hyclone), 1% penicillin-streptomycin, and 1% glutamine (Invitrogen). Cells between passages 4 and 9 were maintained in a humidified incubator at 37°C and 5% CO_2 with a media change every two days.

4,5-diaminofluorescein (DAF-2), 4,5-diaminofluorescein diacetate (DAF-2 DA), 3-isobutyl-1-methylxanthine (IBMX) and cGMP Enzyme Immunoassay (EIA) kit were purchased from Cayman Chemicals. Diethylamine NONOate (DEA NONOate, Cayman Chemicals) and sodium nitroprusside (SNP, Sigma) were used as NO donors. Sodium pyruvate (SP, Sigma) was used as the ROS scavenger.

Phosphate buffered saline (PBS) and endothelial cells were plasma treated with either the straight or curved tube extension. All NO measurements were carried out in PBS (pH 7.4) while cell viability assays were in both PBS and serum-free media. The cGMP assay was carried out in serum-free media.

Nitric oxide and hydrogen peroxide measurement in gas, liquid, and cells

NO production in gas phase was measured using a gas chromatograph (Agilent 3000 MicroGC) calibrated with 700 ppm NO balanced with nitrogen. The discharge cell was inserted inside a syringe tip, and plasma treated room air was collected by slowly pulling the plunger during plasma treatment. The collected air was then analyzed chromatographically.

The fluorescent dye DAF-2 is widely used for quantitative NO measurement in liquids and biological tissues. DAF-2 does not interact with reactive nitrogen and oxygen species, such as nitrates (NO_3^-) and nitrites (NO_2^-), superoxide (O_2^-), hydrogen peroxide (H_2O_2), or peroxynitrite ($ONOO^-$) [156]. DAF-2 detects NO by reacting with an active intermediate, N_2O_3, formed during oxidation of NO to nitrite, yielding a fluorescent compound DAF-2 triazole (DAF-2T) [156].

All reagents were freshly prepared prior to each experiment. 100 µl PBS containing 1 µM DAF-2 was added to a 96-well plate (Corning). The solution was treated with plasma for 0 - 240 pulses, using either the straight or curved tube extension. Fluorescence was measured at ex/em: 485/538 nm using an Infinite 200 Tecan microplate reader. Fluorescence was converted to NO concentration using a standard curve developed using the NO donor, DEA NONOate. DEA NONOate dissociates with a half life of 2 minutes

at 37°C to liberate 1.5 moles of NO per molecule NONOate [157]. To obtain the standard curve, DEA NONOate (0 − 667 nM) dissolved in 0.01 N NaOH was incubated with DAF-2 (1 µM) for 30 min at 37°C and fluorescence was measured using the microplate reader as described.

The cell permeant version of DAF-2, DAF-2 diacetate, was used to measure NO concentration in an endothelial cell monolayer. DAF-2 DA is a non-fluorescent cell permeable molecule, which upon entry into the cell is cleaved by cellular esterases into the less permeable DAF-2 [156]. PAEC were seeded near confluence in a 96-well plate (30,000 cells/well) and incubated for 24 h. Prior to plasma treatment, cells were loaded with DAF-2 DA (10 µM) for 45 min. The wells were washed once and 100 µl PBS was added. The cells were treated with plasma for 0 - 240 pulses, using the curved tube extension. Fluorescence was measured at ex/em: 485/538 nm in a microplate reader.

DAF-2T (fluorescent compound) stability was tested by plasma treating samples (60 pulses) and measuring fluorescence at regular intervals up to 30 min after treatment. The measured fluorescence was stable for up to 15 min, after which a 7% decrease was observed at 30 min. Hence, all plasma treatments and fluorescence measurements were carried out in less than 15 min for repeatability.

Hydrogen peroxide (H_2O_2) was measured in PBS after PHD plasma treatment using the fluorescent Amplex UltraRed probe (Invitrogen) according to the manufacturer's protocol. 75 µL PBS containing 100 µM Amplex UltraRed with 200 U/µL horseradish peroxidase (MP Biomedicals) was PHD plasma treated either directly at 3 mm distance or with straight or curved tube extensions. Calibration curves were obtained using

stabilized 30% hydrogen peroxide (Fisher Scientific) diluted in PBS. Fluorescence was measured at ex/em: 530/590 nm using an LS55 fluorescent spectrometer (Perkin Elmer).

NO concentrations in liquid and cells were numerically calculated based on measured NO gas concentration, with the assumption that only diffusion occurred and no NO was lost to reactions in the gas or liquid phase. The diffusion equations from the gas to the liquid are:

$$\frac{\mathrm{d}C_{\mathrm{gas/surf}}(t)}{\mathrm{d}t} = \frac{D_{\mathrm{gas}}S}{L}\left(C_0(t) - C_{\mathrm{gas/surf}}\right)$$

$$\frac{\mathrm{d}C_{H_2O}(t)}{\mathrm{d}t} = \frac{D_{H_2O}S}{L}\left(k_{\mathrm{h}}C_{\mathrm{gas/surf}}(t) - C_{H_2O}\right)$$

where C_o, $C_{gas/surf}$ and C_{H2O} are NO concentrations at the plasma discharge cell, at the liquid surface, and in the water respectively; D_{gas} and D_{H2O} are NO diffusion coefficients in gas and water; k_h is the Henry constant for NO in water, L is the tube length, and d is the liquid depth with surface area S. The plasma discharge NO production was simulated with a linear dependence on time until the saturation concentration was reached: $C_0(t) = \min(2000, 20t)$. A similar diffusion equation was used for calculation of NO diffusion into cells, assuming that cells uniformly covered the well bottom in a single layer. The values used for calculation are listed in Table 4.

Cell viability

Cell viability following plasma treatment was measured via cell counts and a Live/Dead assay (Invitrogen). PAEC were seeded near confluence in a 24-well plate (200,000

cells/well) and incubated for 24 h. Supplemented media in the wells was replaced with 200 µl serum-free media or PBS, and samples were treated with plasma for 0 – 240 pulses using the 50 mm curved tube extension. Following plasma treatment, PAEC were returned to supplemented media and incubated at 37°C for 3 or 24 hours. 5 mM SNP was used as the positive control. Cells were washed once in PBS to remove detached cells, trypsinized and counted using a Coulter counter (Beckman Coulter).

Table 4 Experimental parameters and constants used for numerical modeling of NO diffusion from gas into liquid and cells.

Quantity	value	Reference
Tube length, L	5 cm	
Liquid depth, d	0.3 cm	
Liquid surface area, S	0.3 cm^2	
NO diffusion coefficient in gas, D_{gas}	0.3 cm^2/sec	[158]
NO diffusion coefficient in water, D_{H2O}	$2 \cdot 10^{-5}$ cm^2/s	[159]
Henry constant for NO in water, k_h	$1.9 \cdot 10^{-3}$ M/atm	[160]
Cell membrane permeability	0.9 m/s	[161]
Intracellular NO diffusivity	$0.9 \cdot 10^{-9}$ m^2/s	[161]

For the Live/Dead assay, PAEC were seeded near confluence in a 96-well plate (30,000 cells/well) and incubated for 24 h. 100 µl serum-free media was added to each well, after which cells were treated with plasma for 0-240 pulses using the 50 mm straight or curved tube extension and incubated for 24 h. Cells were then washed to remove detached cells, labeled with 2 µM calcein AM and 4 µM ethidium homodimer-1 (EthD-1) and incubated for 45 min at room temperature. Live cells convert non-fluorescent cell permeant calcein AM into highly fluorescent calcein by intracellular esterase activity. EthD-1 binds to nucleic acids in membrane damaged cells to undergo a 40-fold increase in fluorescence, and is excluded by cells with intact membranes. Thus calcein is retained by live cells and produces green fluorescence (ex/em: 485/530 nm), while EthD-1 produces red fluorescence in dead cells (ex/em: 530/645 nm). Fluorescence was measured using a microplate reader as described.

For Live/Dead imaging using a fluorescent microscope, PAEC were seeded near confluence in a 24-well plate (200,000 cells/well) and incubated for 24 h. Supplemented media in the wells was replaced with 200 µl serum-free media, and samples were treated with plasma for 0-240 pulses using the 50 mm curved extension. Cells were then labeled with calcein AM and EthD-1 as described previously and imaged by fluorescent microscopy (Olympus) with a digital high performance CCD camera (Diagnostic Instruments).

NO intracellular cGMP induction

Nitric oxide diffuses freely through biological membranes into the cytoplasm [162], where it stimulates soluble guanylyl cyclase (sGC) to convert guanosine triphosphate (GTP) into 3, 5-cyclic guanosine monophosphate (cGMP) [163]. Many of the biological

effects of NO are mediated through the second messenger, cGMP. Hence, the cGMP assay is widely used for the indirect NO measurement. Guanylyl cyclase can be activated by nanomolar concentrations of intracellular NO [164].

Nitric oxide induced cGMP accumulation was measured using a cGMP competitive EIA. In this assay, a constant cGMP tracer concentration competes with free cGMP in the sample for cGMP-specific binding sites in the well. The sample cGMP concentration is therefore inversely proportional to the bound cGMP tracer amount (measured well color). PAEC were seeded near confluence in a 24-well plate (200,000 cells/well) and incubated for 24 h. Prior to plasma treatment, cells were incubated with IBMX (0.5 mM) for 30 min at 37°C to prevent cGMP degradation by phosphodiesterases [165]. Cell medium was then replaced with 200 μl serum-free medium containing IBMX, and cells were plasma treated for 0-240 pulses using the curved tube extension. Media was aspirated and 0.1 N HCl was added to each well. The cells were then scraped off the surface, samples were centrifuged at 1000g for 10 min, and the supernatant was assayed as per manufacturer's instructions.

Statistical analysis

Statistical analysis was performed using Prism software (Graphpad). Data are expressed as mean ± SD. Data were analyzed with one-way or two-way ANOVA. Individual groups were evaluated by Bonferroni's multiple comparison test and p values < 0.05 were considered significant.

6.2.2. Results and discussion

H_2O_2 concentration in PHD plasma treated PBS (Figure 57) increased up to 60 µM with 30 seconds of direct plasma treatment (210 pulses). However, the PBS H_2O_2 concentration was significantly reduced when either a straight or curved tube extension was used. In these configurations, H_2O_2 reached a stable concentration of 1.5 - 2 µM in 5 -10 seconds of treatment at 7 Hz (35-70 pulses), which was nearly 30 times lower than H_2O_2 measured in the direct treatment configuration. H_2O_2 is formed by water vapor in the air flow (relative humidity ~60%) around the discharge cell, as well as by interaction of ions with the liquid. These ions, which do not travel far, would not be able to reach the liquid in the tube configurations. Once formed, H_2O_2 in the gas may react with the Tygon tubing walls in the straight and curved tube extension configurations. This would dramatically reduce the amount of H_2O_2 that reaches the liquid.
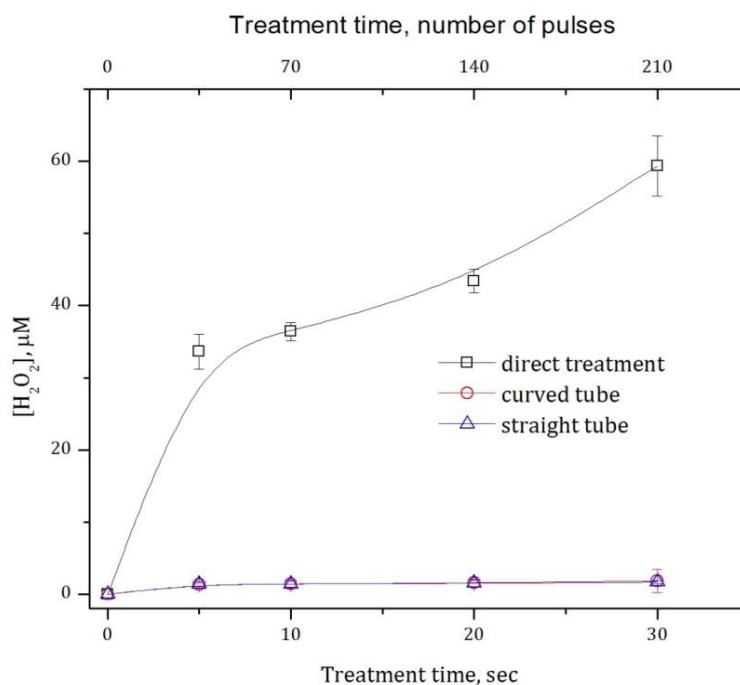
Figure 57 Hydrogen peroxide in PHD plasma treated PBS decreased in the straight and curved tube configurations, as measured by Amplex Ultrared probe.

PHD plasma H_2O_2 production is also of interest in wound healing applications. In early wound healing, H_2O_2 activates cell surface tissue factor to restore hemostasis and modulates both leukocyte adhesion and motility in inflammation [166,167,168]. Reactive oxygen species are also important in wound re-vascularization, since H_2O_2 induces vascular endothelial growth factor expression and is critical in its signaling [169,170]. Finally, in late wound healing, H_2O_2 promotes re-epithelialization by activating matrix metalloproteinases and promoting epithelial cell motility [171]. Thus a plasma device that can deliver defined doses of H_2O_2 and NO individually or in combination may be useful throughout the wound healing process.

Nitric oxide in gas, liquid, and cells after PHD plasma treatment

We determined NO concentrations in gas, liquid, and cells following PHD plasma treatment and compared experimental results to numerical simulations of NO concentrations in liquid and cells under diffusion-only conditions (Figure 58). In gas, NO concentration rapidly increased with plasma treatment and reached a stable level of 1980±50 ppm NO by around 50 seconds. In the liquid (PBS), NO concentration increased linearly up to 240 plasma pulses, as measured by DAF-2 dye. Approximately 75% of NO from plasma-treated PBS diffused through the cell membrane into the cytoplasm. A maximum 1000 nM NO was detected in endothelial cells immediately following 240 plasma pulses (Figure 58). The model closely predicted the experimental NO levels. However, since no losses were considered in the model, the theoretical NO levels were slightly higher than the experimental values.

While gas NO concentration saturated after 50 pulses, the NO level in liquid and cells continued to rise up to 240 pulses. This effect is likely related to diffusion time. NO diffusion through gas is relatively fast (D_{gas} = 0.3 cm^2/s), however NO diffusion through water is significantly slower (D_{H2O} = 2 x 10^{-5} cm^2/s). Plasma NO had to travel through a 50 mm tube filled with room air to reach the liquid surface, and it additionally traveled through 3 mm of PBS to reach the liquid bottom and the cells. While 240 seconds was inadequate to reach saturation, the model predicted that saturation would be reached after about 10 minutes. Lower NO concentration in cells as compared to PBS may be due to the short NO half-life in liquid, since NO diffuses freely across cell membranes. Similarly, while a maximum NO concentration of 1400 - 1600 nM was detected in PBS with the straight tube configuration, for the curved tube configuration, ~ 900 nM NO was detected in PBS for the same treatment duration. Decreased NO delivery with the curved tube was likely related to NO interaction with the tube surface.
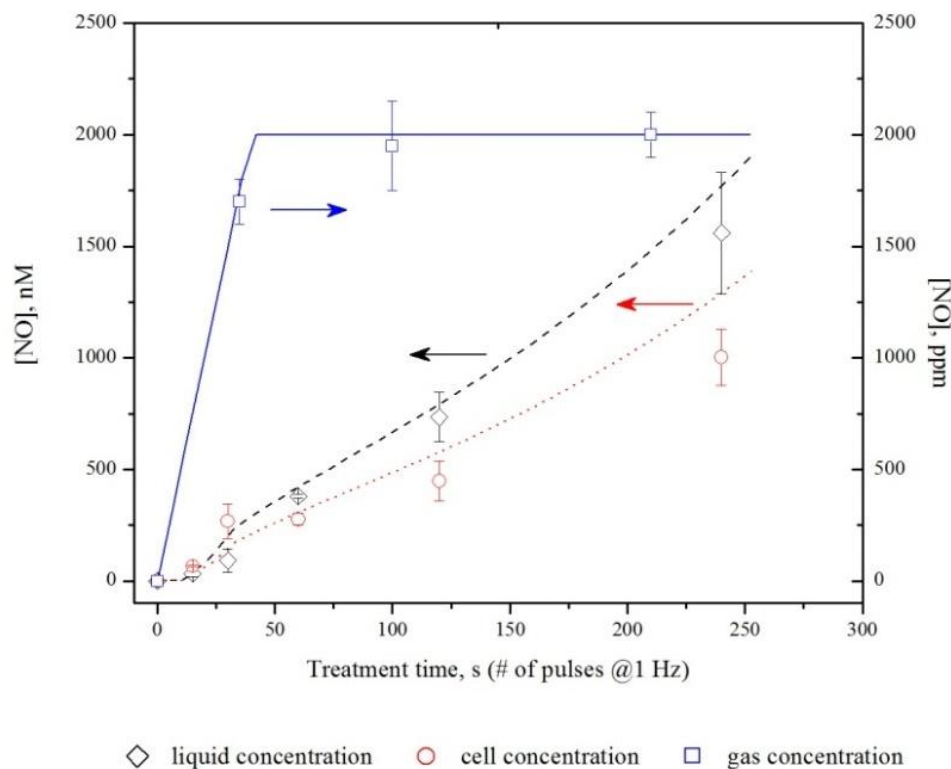
Figure 58 NO concentration in gas, PBS, and the endothelial cell monolayer following PHD plasma treatment with the straight tube configuration; dotted lines show numerically calculated NO concentration in PBS and endothelial cells.

Cell viability with plasma treatment

Cell viability after plasma treatment was measured to ensure that plasma was non-toxic to cells. For cell counts, PAEC were treated with plasma in both PBS and serum-free media, employing the curved tube configuration. For both fluids, no significant cell loss was observed 24 hours after plasma treatment up to 240 plasma pulses (Figure 59(a)). A Live/Dead assay was carried out to confirm the results from cell counts. Approximately 20% cell loss was observed for a treatment of 240 pulses in serum-free media in the straight tube configuration. No significant cell loss was observed for low treatment doses (Figure 59(b)). For similar treatment conditions employing the curved tube extension, no

significant cell loss was observed even at 240 pulses (Figure 59, (c)). Differences in cell viability between the straight and curved tube configurations may be related to NO dose, since the straight tube produced more NO. However the differences are more likely related to residual plasma UV reaching and killing the cells. These data suggest that plasma-derived NO and PHD plasma treatment are relatively non-toxic to endothelial cells.
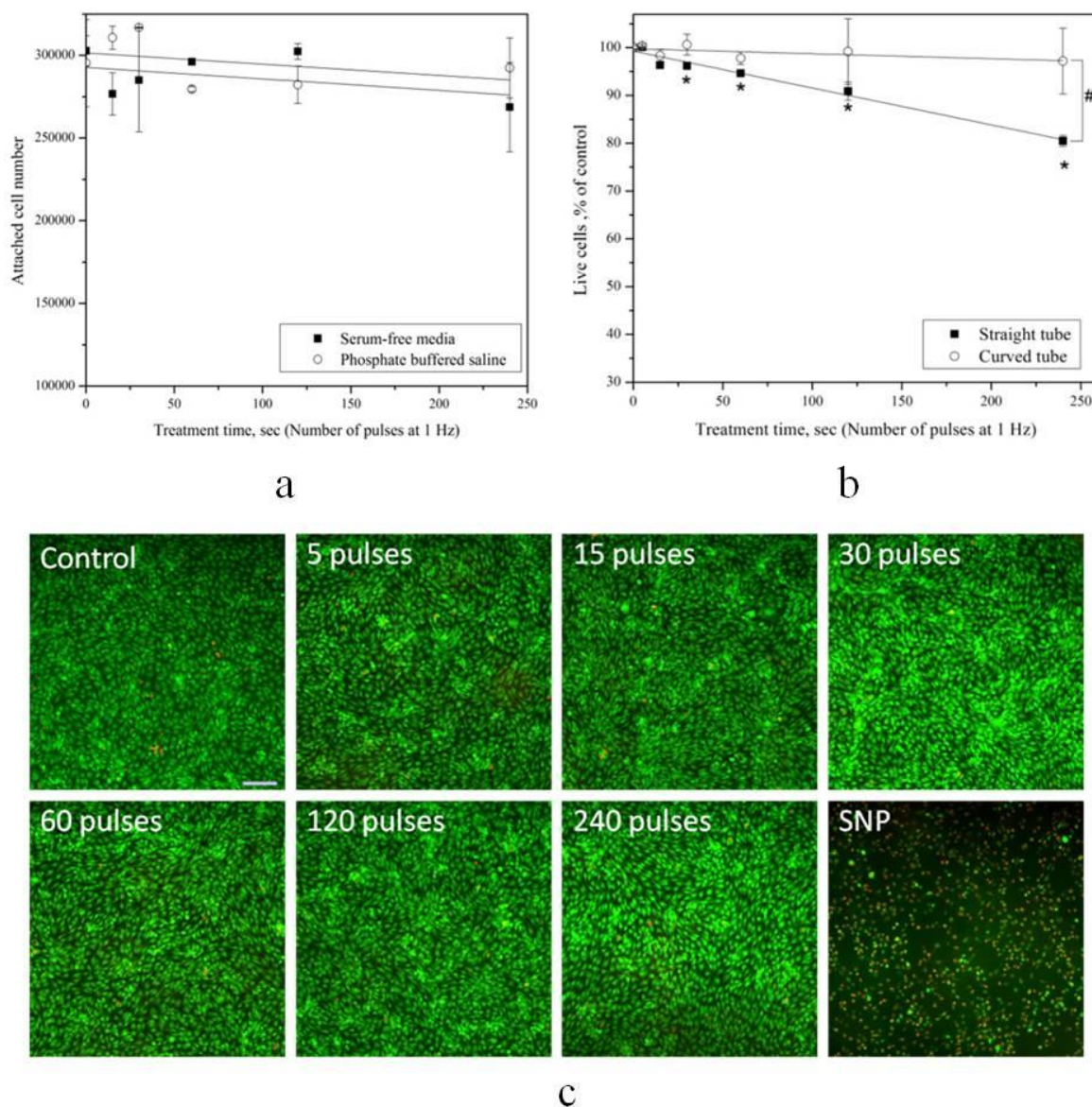
Figure 59 Endothelial cell viability was maintained following PHD plasma treatment. Viable endothelial cell number 24 hours post plasma treatment using (a) cell count and, (b) Live/Dead assay. * $p < 0.05$ compared to control, $^{\#}$ $p < 0.001$ comparing straight and curved tube for 240 pulse plasma treatment. Live/Dead assay images (c) show that almost all plasma treated cells are alive (green) whereas few are dead (red). Scale bar is 200 µm.

Intracellular cGMP in response to plasma-derived NO

NO biological activity was measured indirectly in cells by determining cGMP concentration. cGMP inside endothelial cells following plasma treatment was measured up to 240 pulses using the curved tube extension. A linear increase in cGMP was observed with plasma dose (Figure 60). The endothelial cGMP concentration for the

highest plasma treatment of 240 pulses increased approximately 4 times compared to control.
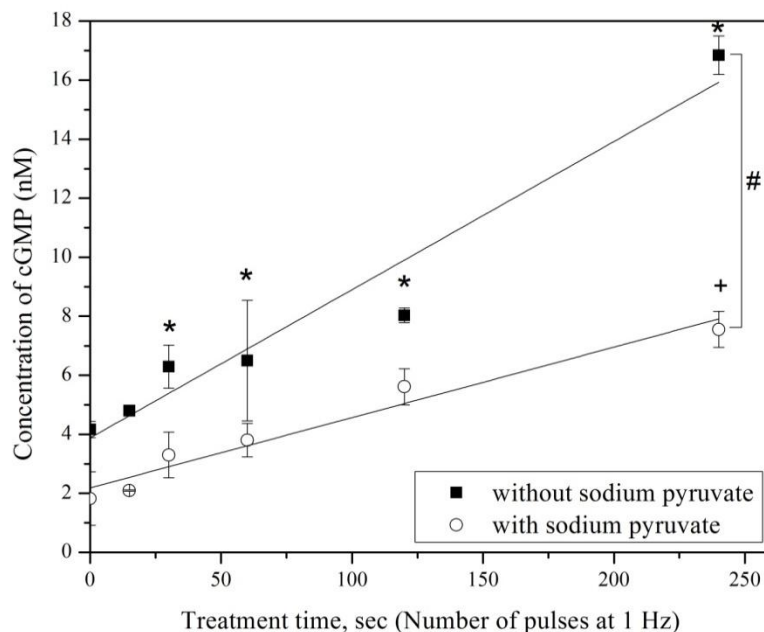
Figure 60 cGMP concentration increased linearly in response to plasma treatment. Plasma-induced cGMP decreased overall with addition of the ROS scavenger sodium pyruvate (10 mM), however levels continued to increase linearly with plasma dose. $^*p < 0.05$ compared to control without sodium pyruvate, $^+p < 0.05$ compared to control with sodium pyruvate, and $^\#p < 0.001$ comparing 240 pulses plasma treated samples with and without sodium pyruvate.

Hydrogen peroxide is known to increase NO-stimulated cGMP production [172]. Low production of H_2O_2, characteristic of hypoxia, decreases cellular cGMP level [173]. To determine the influence of plasma produced ROS on cGMP, the assay was carried out in the presence of the extracellular ROS scavenger sodium pyruvate. While plasma induced cGMP concentration decreased with addition of sodium pyruvate, the cGMP level continued to increase linearly with plasma dose. This suggests that NO produced by the PHD plasma resulted in endothelial cell cGMP production.

6.2.3. Conclusion

In summary, it shown that a microsecond spark discharge ignited in a pin-to-hole electrode geometry effectively produced both reactive nitrogen (NO, $ONOO^-$) and reactive oxygen (H_2O_2, O_2^-) species. In direct treatment mode, NO and H_2O_2 were delivered together with UV radiation. However, by adding a straight or curved tube extension to the plasma device, H_2O_2 was decreased 30 fold and UV was essentially eliminated. Since the curved tube also decreased NO delivery by a third, the plasma with the straight tube was used to directly and precisely deliver NO into cells and elicit a biological response. Although the discharge was designed to be thermal to produce a significant amount of NO, it was safely applied to cells without measureable viability loss. This plasma may therefore be used as a novel method for delivering NO locally and directly to wound sites. The different treatment configurations and consequent variation in delivered reactive species provide additional applications for this discharge. Simultaneous delivery of both NO and H_2O_2 may induce apoptosis in cancerous cells [174], inactivate bacteria [175], and form biologically important singlet oxygen [176]. On the other hand, results of "singlet" oxygen measurements are not conclusive, and this measurement technique should be significantly improved.

CHAPTER 7. A PHYSICOCHEMICAL IN VITRO MODEL OF TISSUE FOR STUDYING PLASMA PRODUCTION AND DELIVERY OF ACTIVE SPECIES

In the previous chapter it was experimentally shown that plasma acts as a source of a number of reactive species which may be in a controllable fashion delivered into a liquid media. Obviously, this media in most cases plays role of an intermediate layer between gas phase (plasma itself) and wound being treated, while all biochemical processes take place in tissue. Therefore the focus of this chapter is measurement of delivery of plasma produced active species into tissue *ex vivo*. Based on the results of these experiments, a corresponding physicochemical *in vitro* model of tissue based on agarose gel phantom is proposed.

7.1. Materials and methods

In this study we used atmospheric pressure dielectric barrier discharge (DBD) plasma at room temperature in air. DBD plasma was generated using an experimental setup similar to the one previously described elsewhere [3,4,5,17,101]. In short, the discharge was generated by applying alternating polarity pulsed (1 kHz) voltage of ~20 kV magnitude (peak to peak) and a rise time of 5 V/ns between the insulated high voltage electrode and the sample undergoing treatment. The powered electrode was made of a 1.5 cm diameter solid copper disc covered by a 1.9 cm diameter 1 mm thick quartz dielectric. The discharge gap was kept at 1.5 mm. Current peak duration was 1.2 μs, and corresponding plasma surface power density was 0.3 W/cm^2. In the case of ex vivo measurement in a rat tissue, a special pen-size electrode was used: one millimeter thick polished clear fused quartz (Technical Glass Products, Painesville, OH) was used as an insulating dielectric

barrier, where a handheld pen-like device with the quartz tip was used for treatment. In this case, the average power density for the active area of the high voltage electrode was kept at the level of approximately 0.74 Watt for 6 mm electrode diameter.

Agarose gels were prepared using standard procedure with pure agar powder (Fisher) in either distilled water or phosphate buffered saline (PBS, Fisher). In order to determine the best concentration of agarose gels which would closely represent tissue, we have used agar at concentrations of 0.6%, 1.5% and 3% weight percentage. These values were chosen for the following reasons. Agarose gels at 0.6% concentration were reported to closely resemble *in vivo* brain tissue with respect to several physical characteristics [177]. 4% agar phantoms are widely used as a tissue models for radiology studies [178]. The 1.5% concentration of agar was chosen as a median point which is often used as a microbiological substrate.

Measurements of H_2O_2 and pH penetration into agarose gels (0.6%, 1.5%, and 3% wt) and tissues were done using Amplex UltraRed reagent (Invitrogen, ex/em: 530/590 nm) and Fluorescein (Sigma Aldrich, ex/em: 490/514 nm) fluorescent dyes respectively. In the case of H_2O_2, 75μL PBS containing 100μM Amplex UltraRed with 200 U/μL horseradish peroxidase (MP Biomedicals) were placed in between 1 mm thick 4x4 cm agar slices and incubated for about 15 minutes before the treatment in order to provide presence of the dye in the agar volume; for the pH measurement, the agarose gels were prepared by adding fluorescein dye before its solidifying. In order to measure the H_2O_2 and pH in tissue, the dyes were injected using a syringe into a 1 cm thick 4x4 cm skinless chicken breast tissue samples at various points to the depth of up to 1 cm. *Ex vivo* measurements were done in a rat tissue: animal (hairless Sprague-Dawley male rat) was

euthanized right before the procedure. A 200 µl of dye solution (Amplex UltraRed) was injected subcutaneously using a sterile syringe, and the animal skin was treated with FE-DBD plasma for various time points after 5 minutes incubation period (Figure 61). Right after the treatment, skin tissue samples were extracted and analyzed as follows. Treated samples were sliced in a vertical direction with thickness of 1 mm, and fluorescence was measured using an LS55 (Perkin Elmer) fluorescent spectrometer equipped with XY reader accessory (Figure 62-Figure 63). To obtain calibration curves for hydrogen peroxide in the plasma treated samples a standard stabilized 3% H_2O_2 (Fisher) water solution properly diluted to obtain various concentrations was used.
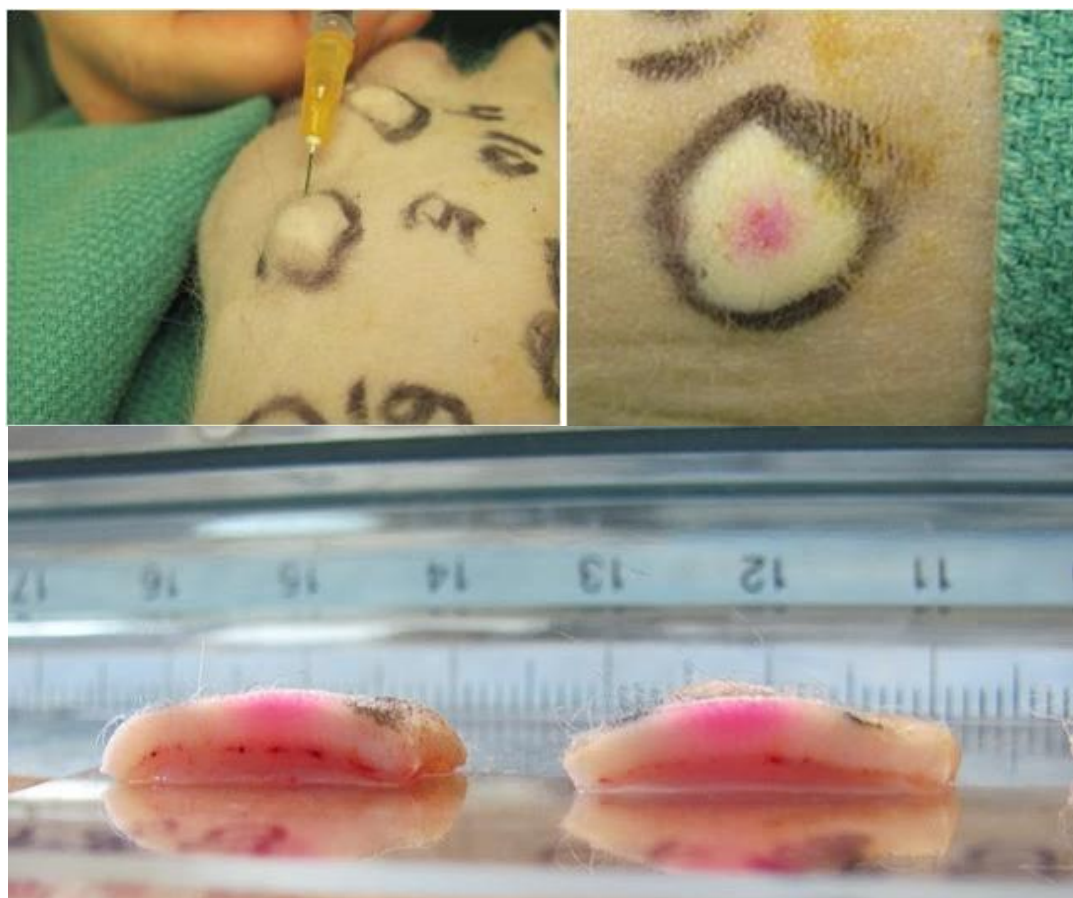
Figure 61 Subcutaneous injection of the fluorescent dye (euthanized rat, top left), the rat skin after the plasma treatment (top right), and the skin sample cross-section just before measurement (bottom).
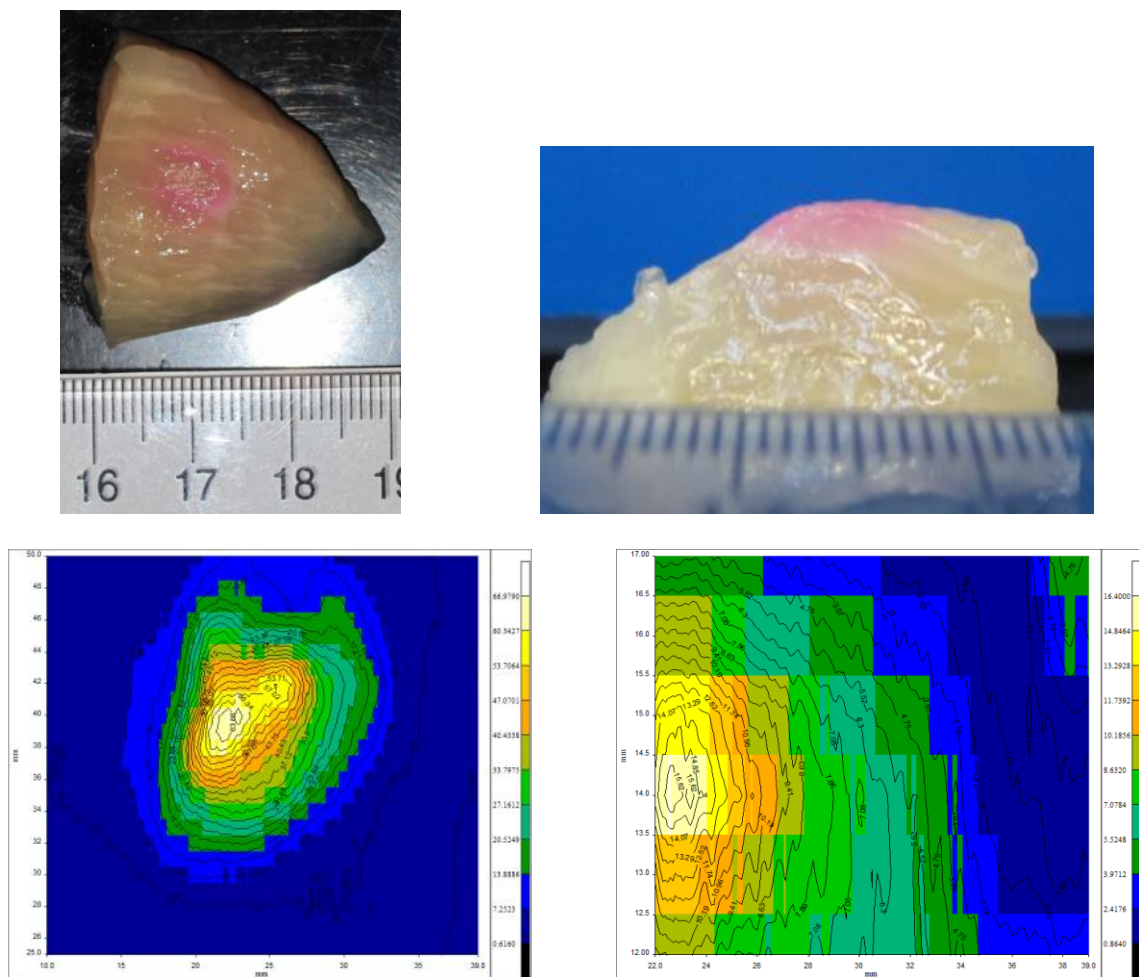
Figure 62 Chicken breast after plasma treatment with H_2O_2 fluorescent dye: photograph (top) and fluorescent images (bottom) from the top and side of the sample (arbitrary units).
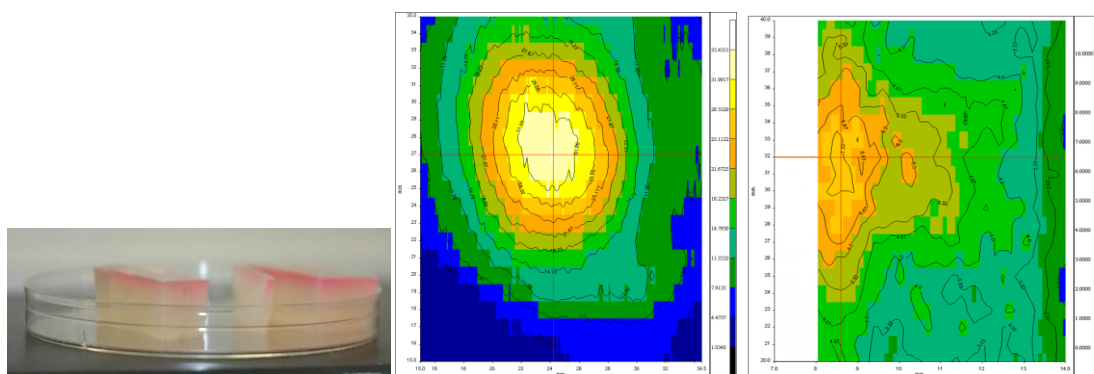
Figure 63 Agarose gel after plasma treatment with H_2O_2 fluorescent dye: photograph and fluorescent images from the top and side of the sample (arbitrary units).

7.2. Results

The results of H_2O_2 measurements in dead tissue are shown on Figure 64: with longer treatment time depth of penetration as well as concentration of hydrogen peroxide increases. In general, several millimoles of H_2O_2 are produced in tissue after plasma treatment, while it diffuses 1.5-3.5 mm deep. About the same tendency is observed in the case of tissue acidity change which is shown on Figure 65 (florescence intensity of fluorescein decreases with lower pH, and the data are presented in arbitrary units), however effect of pH lowering penetrates deeper – up to 4.5-5 mm.
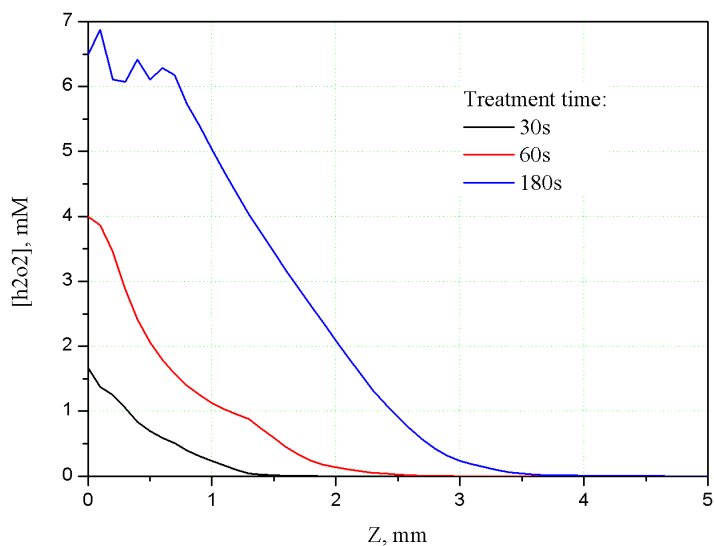
Figure 64The profiles of H_2O_2 in tissue after the plasma treatment.
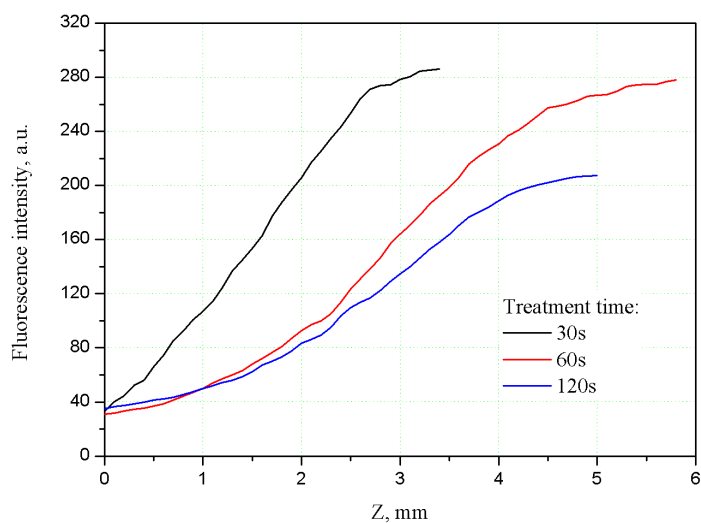
Figure 65 The profiles of pH in dead tissue after the plasma treatment.

In order to develop a simple realistic in vitro model of tissue that would have simple physicochemical characteristics, first of all from the point of view of depth of reactive species penetration, three concentrations of agarose media were used. The measurement results for H_2O_2 produced by plasma treatment in agar gels together with the results for dead tissues for the same treatment doses are shown on Figure 66. Hydrogen peroxide concentration on the agar gel surface was different for different agar densities: 0.5 mM for 0.6%, 0.7 mM for 3% and 1.9 mM for 1.5% gels after 1 minute of plasma treatment. The results of hydrogen peroxide penetration measurements in a euthanized rat skin tissues are shown on Figure 67, and compared to the dead chicken breast tissue, depth of penetration appears to be very similar – up to 4 mm after 2 minute treatment (although concentration is almost an order of magnitude higher due to corresponding 8 times higher power of the discharge). Surprisingly, depth of H_2O_2 penetration for all types of agarose

media was about the same: Figure 68 shows depths at which the same level of 0.05 mM

of H_2O_2 was detected in agar gels and tissue for different plasma exposure times.
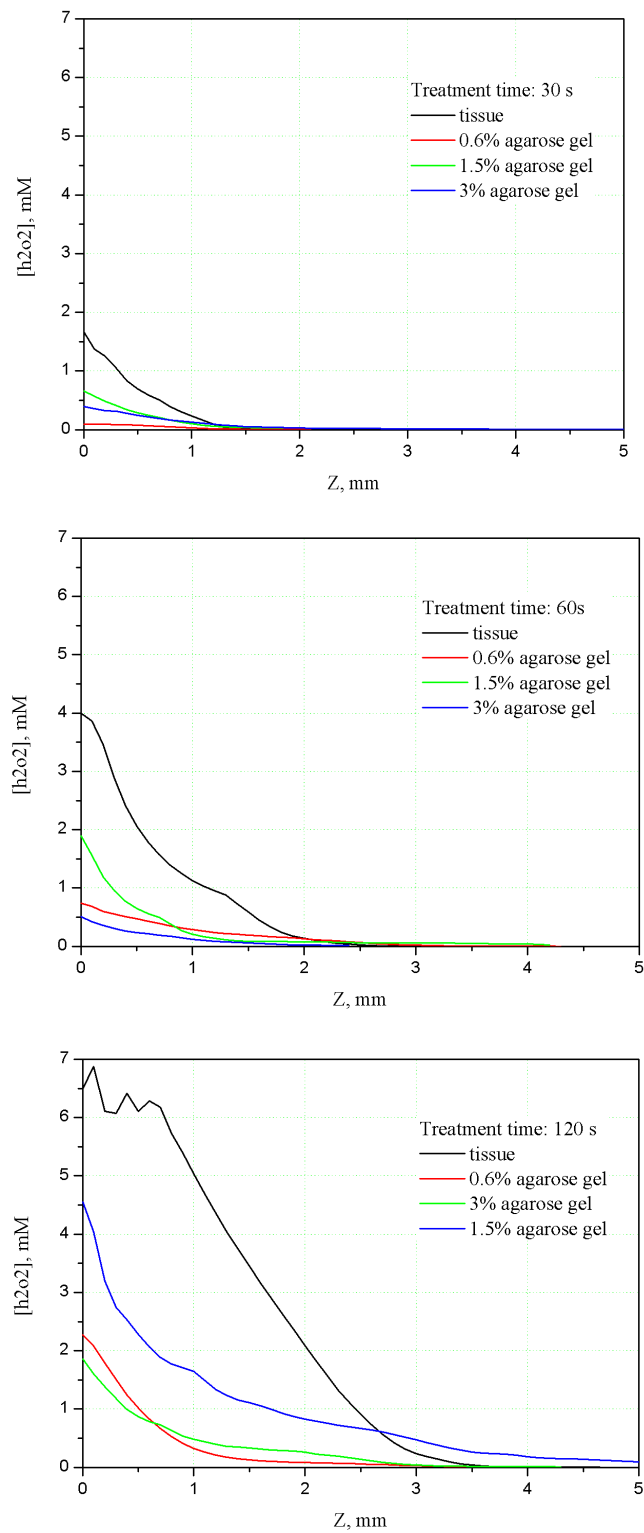
Figure 66 The profiles of H_2O_2 in non-buffered agarose gels and dead tissues after the plasma treatment.
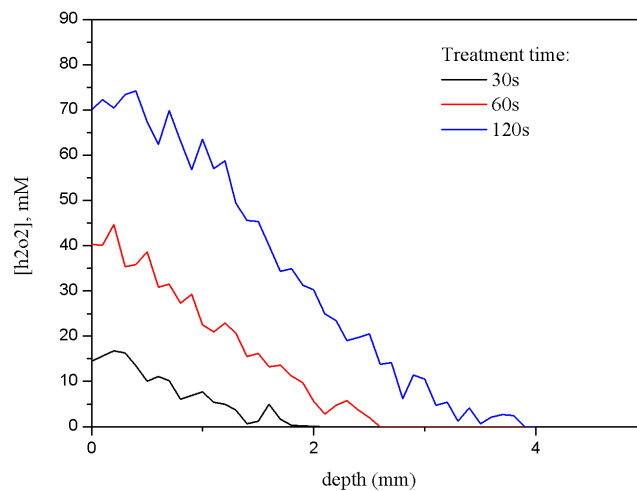
Figure 67 The profiles of H_2O_2 in euthanized rat tissue after the plasma treatment.
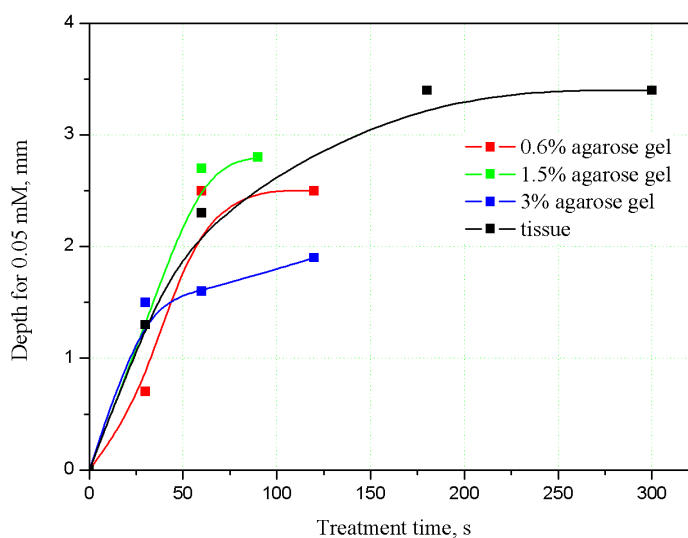
Figure 68 Depth of H_2O_2 penetration at concentration of 0.05 mM: comparison for agarose gels and dead tissue

In contrast to hydrogen peroxide, the dynamics of acidity change inside of agar gels was significantly different for different agar media compositions (Figure 69). Tissue appeared to have better buffer properties compared to non-buffered agarose gels. However addition of PBS into agar provides required similarities in terms of pH changes.
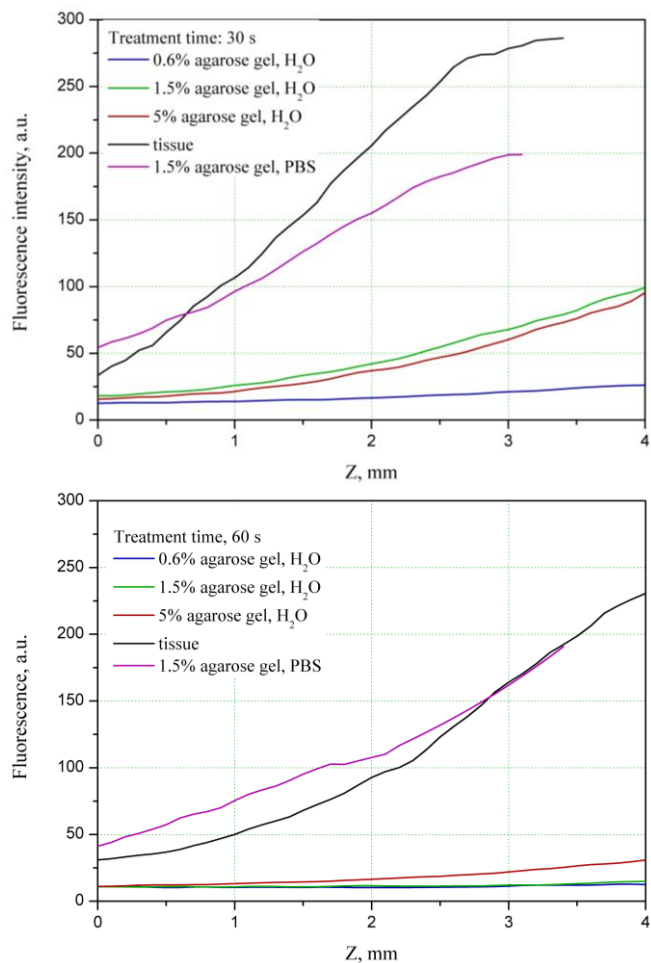
Figure 69 The profiles of pH in agarose gels and dead tissues after the plasma treatment.

7.3. Discussion

In this paper we address a problem of direct atmospheric pressure plasma interaction with tissues, particularly, delivery of neutral active components produced by plasma inside of tissues, and creation of a physical model of such interaction. Plasma is a complex chemically active medium, and a number of biomedical studies suggest that it can be successfully applied to various living tissues without damage [179,180,181], but providing a number of positive effects, such as blood coagulation [3,17,65,81], wound [17,65,69,182] and even cancer [5,183,184] treatment, for example. It was noticed that, for example in the case of experimental *subcutaneous* cancer tumor treatment in a mouse

model [184], the effect of plasma treatment is observed not only on the surface of treated tissue (skin), but also (and mainly) in volume, under the skin. In many cases, researchers report a significant change of pH of solutions and tissues after plasma treatment (see for example, [184,185]). On the other hand, hydrogen peroxide, which is almost always produced by plasma, is often considered to be important in bacteria inactivation [58,60,101,132,185] or wound healing processes [186]. Therefore, in the current study we focused on measurements of these two parameters – pH and H_2O_2 concentration, - as a function of treatment time and depth of penetration into a treated object.

The evaluation of measuring techniques on the effects of plasma treatment on tissues is complicated in direct experiments on actual biological objects due to a wide variation of morphological and biochemical parameters that are beyond the control of the experimenter. Therefore, a stable and reproducible test objects that mimic tissue physicochemical characteristics are needed. In the current study, we have used a custom-made agarose gel, similar to those used in microbiological studies, but modified to achieve certain similarities with dead tissue. Agarose phantoms are widely used as models of various tissues (see for example, [177,178,187,188].

The results we present in this paper show that, in the case of real tissue, active species produced by plasma on the surface may travel in tissue volume for up to several millimeters deep. Obviously, this depth of penetration is determined by diffusion and reaction rates, which would highly depend on type of tissue and its biochemical characteristics. A measurement of these parameters is extremely complicated task, and therefore creation of a simple model that would closely represent certain tissue is possible experimentally. We used agarose gels of various concentrations in order to mimic tissue

physical properties. For the case of hydrogen peroxide, as shown on Figure 66 and Figure 68, depth of diffusion is about the same for all types of agar, but the concentration of H_2O_2 varies, being the closest for the 1.5% agar weight percent case, and about 3 times lower for both 0.6% and 3% wt agar gels. This behavior may be possibly explained by both diffusion properties and reaction rates of H_2O_2 in agar.

Acidity of tissue, in contrast to the experimental *in vivo* data reported in [184] where authors observed a significant decrease of pH on the skin surface with a slight increase in subcutaneous tissue, in our experiments was measured to be consistently increased (lowering of pH) as a result of exposure to the discharge. Since the fluorescence of fluorescein highly depends not only on pH of a solution, but also on other parameters [189,190,191,192,193], we did not attempt to obtain calibration curves, and therefore the data are presented in arbitrary units. We show that tissue compared to agarose gels prepared in distilled water acts as a significantly better buffer, and the depth of pH changes inside such a gels is much greater. In fact, we observe significant drop in the whole volume of a phantom – up to a centimeter thick agar. This problem, as shown on Figure 69, may be addressed simply by adding a buffer into the agarose media – 1.5% wt agar was prepared in 1x PBS.

In summary, we show that plasma effects may be transferred several millimeters deep inside a tissue, as measured in an *ex vivo* chicken tissue and rat skin models. We have detected a penetration behavior of two simplest active components, namely hydrogen peroxide and pH, but other species may be detected and measured using other fluorescent dyes or techniques. In addition, we have shown that a simple agar gel model may express

similar physicochemical properties as a real tissue, resulting in comparable penetration effects of active species.

CHAPTER 8. TOXICITY OF PLASMA TREATMENT OF LIVING TISSUE

It is evident from the large number of recent reviews in the literature that there are many potential applications of non-equilibrium plasma discharges in biology and in medicine [66,67,137,138,140,142,194,195,196,197]. This is, in part, driven by the continued development of novel plasma sources and modification of existing ones [31,34,35,55,138,141,195,198,199,200,201,202,203] and by advances in modeling, simulation, and characterization of these sources, including characterization and quantification of biological effects [32,33,138,198,204,205,206,207,208,209,210,211,212,213,214]. The major focus in applications of plasma in medicine has been its antimicrobial effect, although some reports of wound healing applications have been presented [29,32,63,66,142,198,201]. In studying antimicrobial effects of plasma it is essential to evaluate the potential damage plasma can inflict on living tissues.

This chapter investigates toxicity in the direct application of two different types of plasma to living tissue: (a) Floating Electrode Dielectric Barrier Discharge which is an inherently non-thermal discharge that generates a multitude of reactive oxygen species (ROS) and (b) Pin-to-Hole spark Discharge which is a thermal discharge that generates ROS together with reactive nitrogen species (RNS). Both discharges have been considered before for antimicrobial treatment of living tissues. However, little work has been reported on the possible damage these discharges could inflict in the process. We show that low doses of plasma (previously reported to be quite sufficient for sterilization,

see [94,137] for example) do not cause any visible or microscopic damage to live pig skin and wound tissue. Higher doses do, in fact, cause damage and the damage appears to be related to the surface temperature of the tissue. Thus, if the plasma temperature is reduced (through shorter pulses, for example) this heating and thus the damage may potentially be avoided.

8.1. Materials and methods

8.1.1. Floating Electrode Dielectric Barrier Discharge (FE-DBD)

Non-thermal atmospheric pressure dielectric barrier discharge plasma was generated using an experimental setup similar to the one previously described by the authors [3,4,5,17,101]. In short, the discharge was generated by applying alternating polarity pulsed (500 Hz – 1.5 kHz) voltage of ~20 kV magnitude (peak to peak), 1.65 µs pulse width and a rise time of 5 V/ns between the insulated high voltage electrode and the sample undergoing treatment. One mm thick, polished clear fused quartz was used as an insulating dielectric barrier covering the 2.54 cm diameter copper electrode. The discharge gap between the bottom of the quartz and the treated skin or wound surface was fixed at 1.5 mm using a special electrode holder (Figure 70, a) or a modified planar electrode (Figure 70, b). Discharge power density was measured to be 0.13 W/cm^2 (at 500 Hz), 0.15 W/cm^2 (at 800 Hz), 0.17 W/cm^2 (at 1 kHz), and 0.31 W/cm^2 (at 1.5 kHz). Rotational and vibrational temperatures were measured to be 313.5 ± 7.5K and 3360 ± 50K respectively [25].
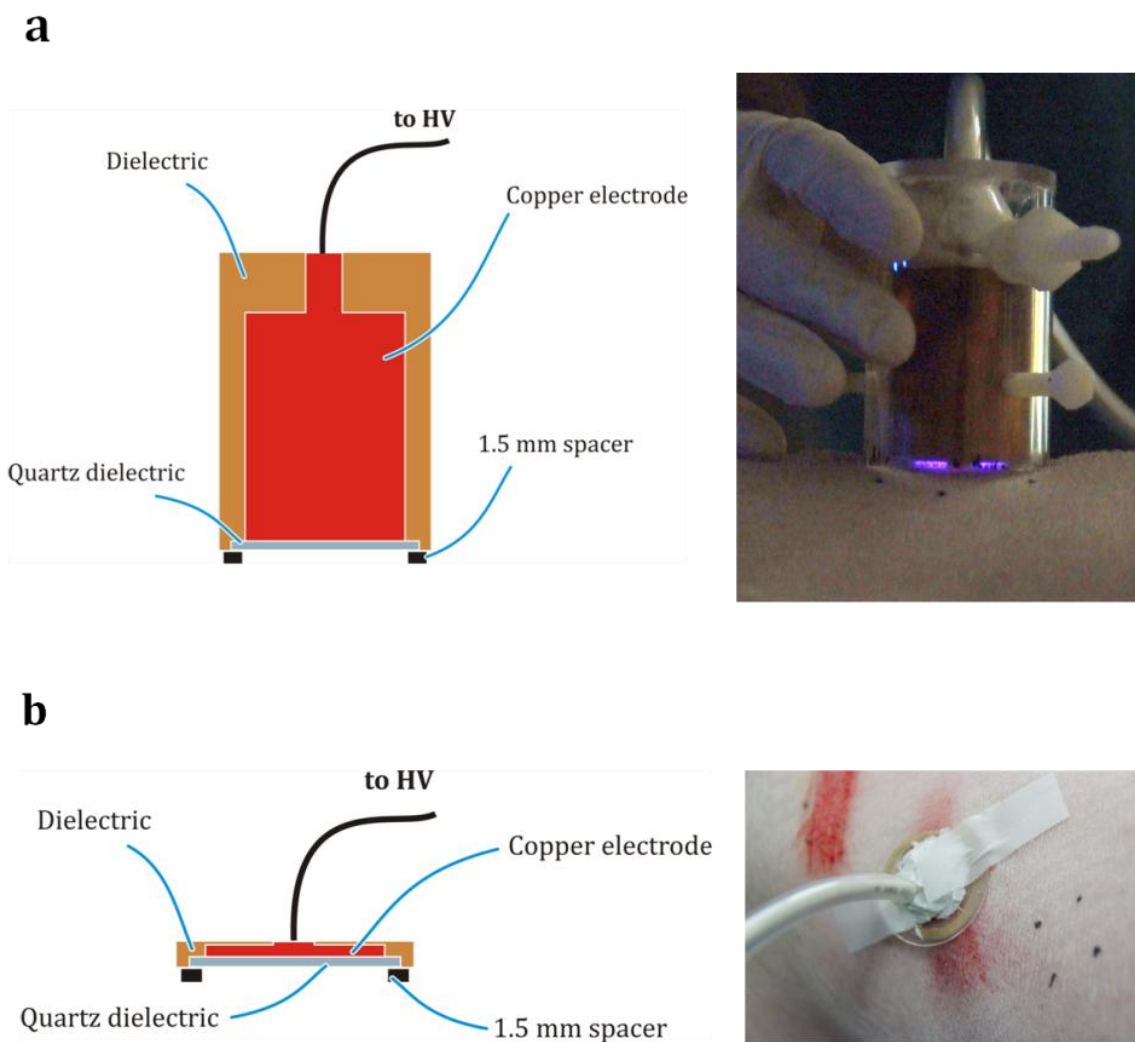
Figure 70. General schematics and photographs of the FE-DBD electrodes: conventional (a), and modified planar (b).

8.1.2. Microsecond Pin-to-Hole spark Discharge (PHD)

Atmospheric pressure spark discharge was generated in a pin-to-hole electrode, and is described in the Chapter 2

8.1.3. Animal model

We evaluated the potential toxic effects of the FE-DBD and PHD plasmas on both intact and wounded porcine skin in 12 Yorkshire pigs. Standard operative procedure included

the following: the pig was anesthetized and the dorsum of the pig was marked and divided for treatment areas (Figure 71, a). When intact skin toxicity was studied, the FE-DBD electrode was placed 1.5 mm above the skin, and plasma was applied for different doses by varying the power and time of treatment. Spark discharge was applied at fixed power at a 5 mm distance from the skin for various amounts of time. When wounded skin was studied, a dermatome knife was used to create a skin abrasion (Figure 71, b), removing about 2×3 cm of the epidermis and dermis (approximately 3 mm ± 1 mm deep), followed by plasma treatment. Pigs were then sacrificed immediately or 24 hours after the treatment. Tissue specimens from each treatment area were harvested and sent for histopathologic analysis.
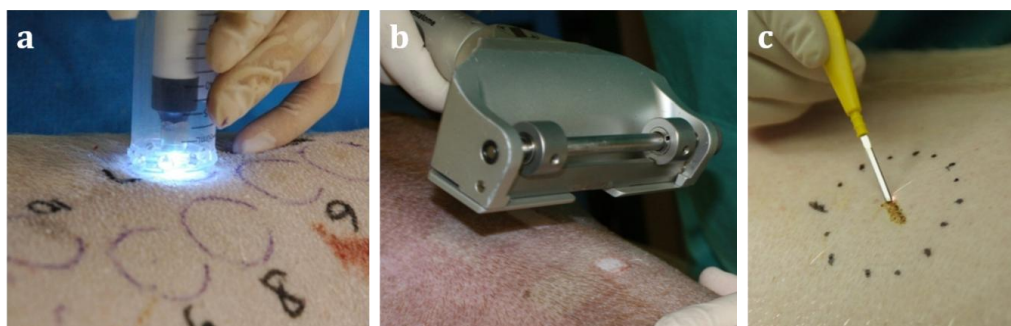
Figure 71. Marked treatment areas of the pig skin (a), creation of skin abrasion with dermatome (b), and skin treatment with a high frequency desiccator Bovie®, positive control (c).

For the intact skin model (3 pigs) of treatment with FE-DBD, we had a total of 85 treatment areas on the three pigs that were harvested 24 hours after surgery. One area of intact skin (n=3) was treated with a high frequency desiccator (positive control, Bovie®, Figure 71, c), and one area of intact skin (n=3) was left untreated (negative control). The

remaining 80 areas were treated with 4 discharge frequency (power) settings for different time points: from 30 seconds, and up to 15 minutes (Table 5).

Table 5. Number of areas for intact skin FE-DBD plasma treatment and corresponding exposure dose (in J/cm^2)

Treatment time, min	FE-DBD frequency, kHz (corresponding power density, W/cm^2)			
	0.5 (0.13)	0.8 (0.15)	1.0 (0.17)	1.5 (0.31)
0.5	-	-	3 (5.1 J/cm^2)	3 (9.3 J/cm^2)
1	-	4 (9 J/cm^2)	7 (10.2 J/cm^2)	9 (18.6 J/cm^2)
2	2 (15.6 J/cm^2)	4 (18 J/cm^2)	5 (20.4 J/cm^2)	7 (37.2 J/cm^2)
3	-	8 (27 J/cm^2)	4 (30.6 J/cm^2)	5 (55.8 J/cm^2)
5	-	5 (45 J/cm^2)	2 (51 J/cm^2)	5 (93 J/cm^2)
15	2 (117 J/cm^2)	2 (135 J/cm^2)	-	-

For the wounded skin model (4 pigs) treated with FE-DBD, we had a total of 56 treatment areas on 2 pigs harvested immediately after treatment, and 38 treatment areas on 2 pigs harvested 24 hours after procedure. Animals were treated with two discharge power settings for various amounts of time (see Table 6) using planar DBD electrode, with a high frequency desiccator (n=8), or left untreated as control (n=7).

For the intact and wounded skin model (5 pigs) treated with PHD, we had a total of 39 (intact skin) and 36 (wounded skin) treatment areas on 4 pigs that were harvested immediately after the procedure, and 48 (intact skin) and 36 (wounds) treatment areas on 4 animals that were harvested 24 hours after plasma exposure. Skin was treated with spark plasma at 5 mm for 5 to 300 seconds (see Table 7).

Table 6. Number of areas for wounded skin FE-DBD plasma treatment and corresponding exposure dose (in J/cm^2)

Treatment time, min	FE-DBD frequency, kHz (corresponding power density, W/cm^2)	
	0.5 (0.13)	1.5 (0.31)
0.5	6 (3.9 J/cm^2)	6 (9.3 J/cm^2)
1	8 (7.8 J/cm^2)	8 (18.6 J/cm^2)
3	9 (23.4 J/cm^2)	9 (55.8 J/cm^2)
5	9 (39 J/cm^2)	9 (93 J/cm^2)
15	6 (117 J/cm^2)	7 (279 J/cm^2)

8.1.4. Histological analysis

All specimens were analyzed with microscopic histological analysis. Specimens were longitudinally sectioned and fixed for 24 hours in formalin. Sections for histology were processed in a standard fashion and stained with hematoxylin-eosin. The pathologists were blinded to all specimens and categorized each specimen into a burn grading system for the intact and wounded skin data analysis. For intact skin, the specimens were either classified as normal, minimal change, epidermal damage, or full burn through the dermis. For wounded skin, the specimens were either classified as normal, presence of a clot or scab, and full burn through the dermis.

Table 7. Number of areas for intact and wounded skin PHD plasma treatment

Treatment time, s	5 mm, intact skin	5 mm, wounds
5	2 (non-survival) 4 (survival)	2 (non-survival) 2 (survival)
15	2 (non-survival) 4 (survival)	4 (non-survival) 4 (survival)
30	2 (non-survival) 4 (survival)	4 (non-survival) 4 (survival)
60	2 (non-survival) 4 (survival)	4 (non-survival) 4 (survival)
90	2 (survival)	-
120	6 (non-survival) 2 (survival)	-
180	5 (non-survival) 4 (survival)	4 (non-survival) 4 (survival)
240	2 (non-survival)	-
300	4 (non-survival)	-

8.1.5. pH and temperature analysis

In order to check the change of skin temperature and pH of the skin sample after plasma treatment, fresh pig skin samples with average thickness of about 1 cm were placed on aluminum foil and kept at constant initial temperature of about 37°C. Skin samples were

exposed to both discharges for the same amount of time as in-vivo study. These changes were monitored using infrared thermometer (OS53x-CR, Omega) and skin pH/temperature meter (HI 99181, Hanna).

All procedures were performed in compliance with the animal welfare and protection act following the Drexel University's Institutional Animal Care and Use Committee (IACUC) approval, Protocols #17030 (intact skin) and #17335 (wounded skin).

8.2. Results and discussion

Endpoints for toxicity analysis consisted of recording both gross and histological examination of the intact skin and wounded skin specimens. Gross observation was correlated with the histological grading system as mentioned previously.

8.2.1. Treatment of intact skin

FE-DBD plasma treatment was evaluated on 3 pigs with intact skin at 4 different frequency (power) settings, all harvested 24 hours after the procedure. The results for 3 discharge frequencies are shown on Figure 72 in terms of normalized number of observation of no or minimal changes in skin, epidermal damage, or burn after certain treatment dose. Untreated skin appeared normal on gross histological observation. With minimal change, there was a small area of erythema on the skin. With epidermal damage, there was mild erythema that resolved itself usually within 20 minutes. With full burn through the dermis, there was diffuse erythema that remained until time of harvest. Positive controls, i. e. samples treated with HF desiccator, all showed full thickness burn. Representative photographs and histological images are shown in Table 8. One can notice that resulting toxic effects (epidermal damage, burn) depends not only

on the exposure dose, but *dose rate* (frequency dependent): <u>the higher the frequency, the lower dose required for skin damage to occur</u>.

The results of intact skin treatment with spark discharge plasma at 5 mm distance from the skin are shown in Figure 73. In this case a burn was observed after 3 minutes of treatment, while, for example, inactivation of bacteria in liquid requires an exposure time of several seconds [82,180].

Overall results of the skin toxicity trials on pigs are similar to those on human cadaver skin and on SKH1 mice [3,17] – only rather high doses of plasma, those far greater than needed for sterilization or blood coagulation, are able to damage skin; while doses required to achieve desired medically relevant therapeutic effect are significantly below the damage threshold.
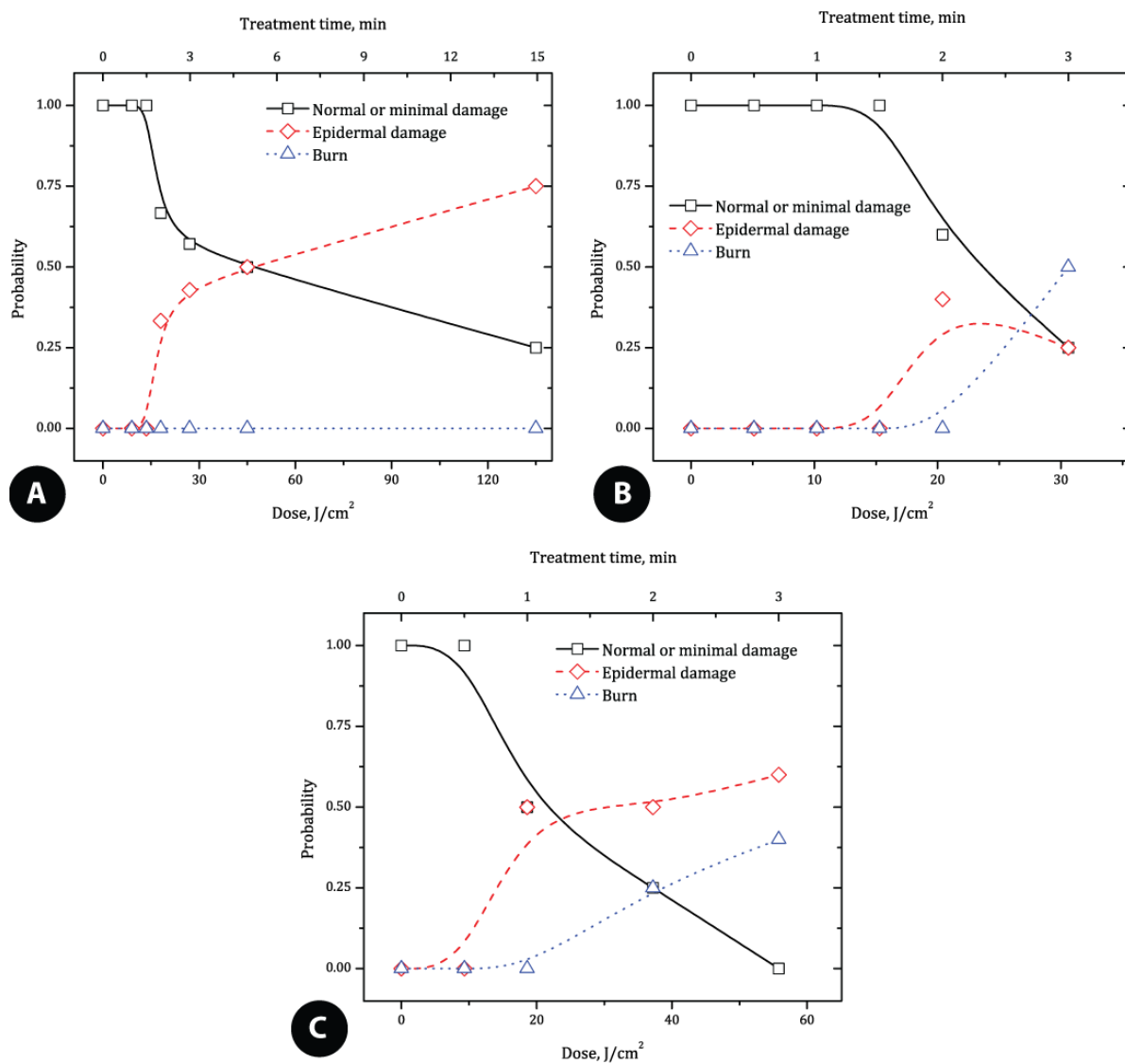
Figure 72. Results of the intact porcine skin treatment with FE-DBD plasma operated at 800 (a), 1000 (b) and 1500 (c) Hz frequency.
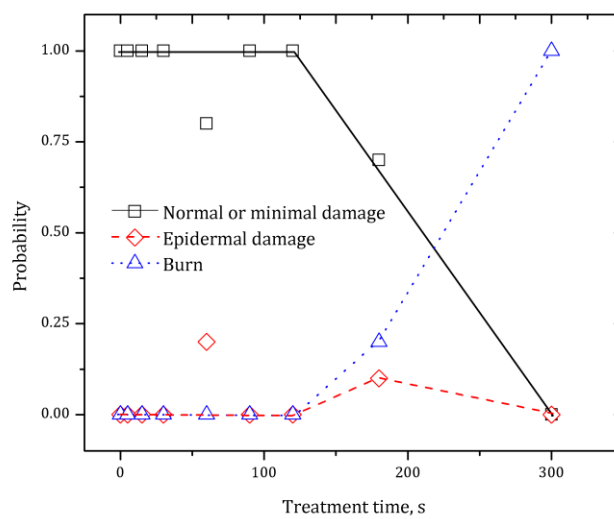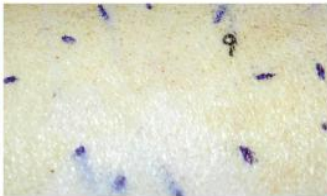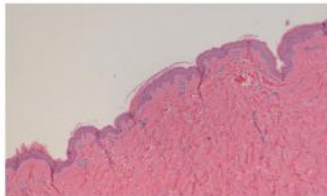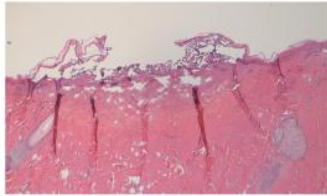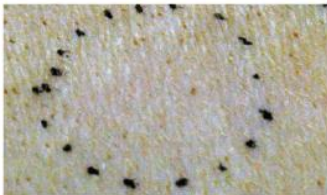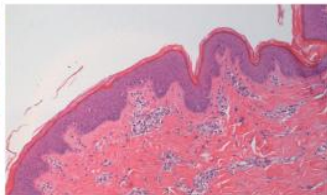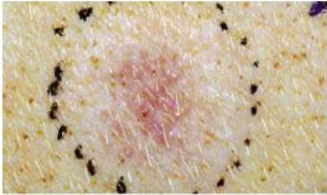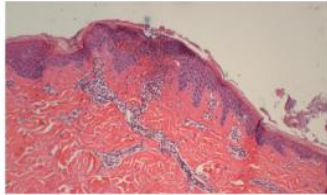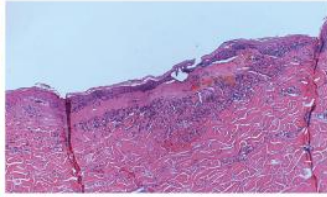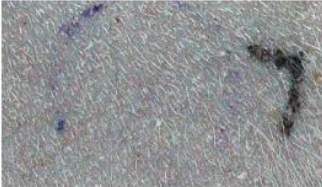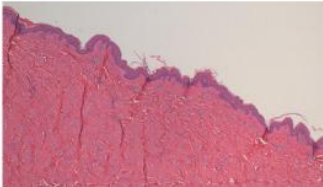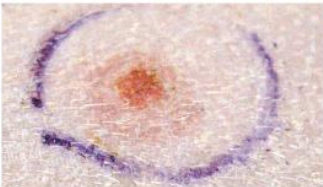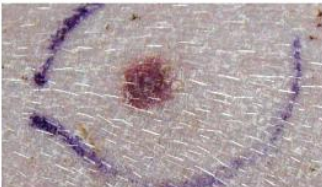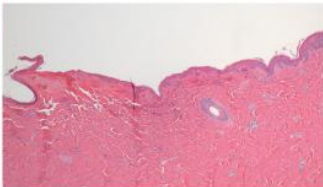
Figure 73. Results of the intact porcine skin treatment with PHD plasma operated at 5 mm distance from the skin surface.

Table 8 Representative photographs and histological images of the intact skin after treatment with FE-DBD and PHD plasmas

Treatment	Gross observation: right after treatment	24 hours after treatment	Histology
No treatment			

Appearance: Normal skin
Histology: Normal skin

Positive control Bovie®

Appearance: Burn: Immediate burning and charring of tissue
Histology: Disruption of epidermis and papillary dermis, areas of dermis coagulated, no dermal nuclei, hair follicles still intact

FE-DBD 45 J/cm² 5 min @ 0.8 kHz

Appearance: Normal skin
Histology: Normal skin

FE-DBD 135 J/cm² 15 min @ 0.8 kHz

Appearance: Epidermal damage; Diffuse redness with a distinct area of mild erythema
Histology: Small area of burn in epidermis

FE-DBD 37.2 J/cm² 2 min @ 1.5 kHz

Appearance: Burn Small Central area of increasing redness surrounded by erythema after 1 min treatment. Area of necrosis forming centrally surrounded by area of erythema
Histology: Similar to Bovie®, burn through to dermis

Treatment	Gross observation:		Histology
	right after treatment	**24 hours after** treatment	
PHD 60 s @ 5 mm			
	Appearance: Normal skin Histology: Normal skin		
PHD 180 s @ 5 mm			
	Appearance: Burn Histology: Similar to Bovie®, burn through to dermis		

8.2.2. *Ex-vivo treatment of porcine skin samples*

In order to estimate the effect of global increase of temperature and pH of skin after the plasma treatment on induction of tissue damage, we have measured these parameters on skin samples ex vivo. The results of temperature measurements (Figure 74, a) indicate, that after about 3 minutes of treatment by both plasmas, skin temperature increases by 11-14 degrees, which is the critical temperature for skin burn [215,216], and is in good agreement with our experimental observations (see Figure 72 and Figure 73). The effect of the decrease of pH due to plasma treatment is probably negligible for both discharges (Figure 74, b).
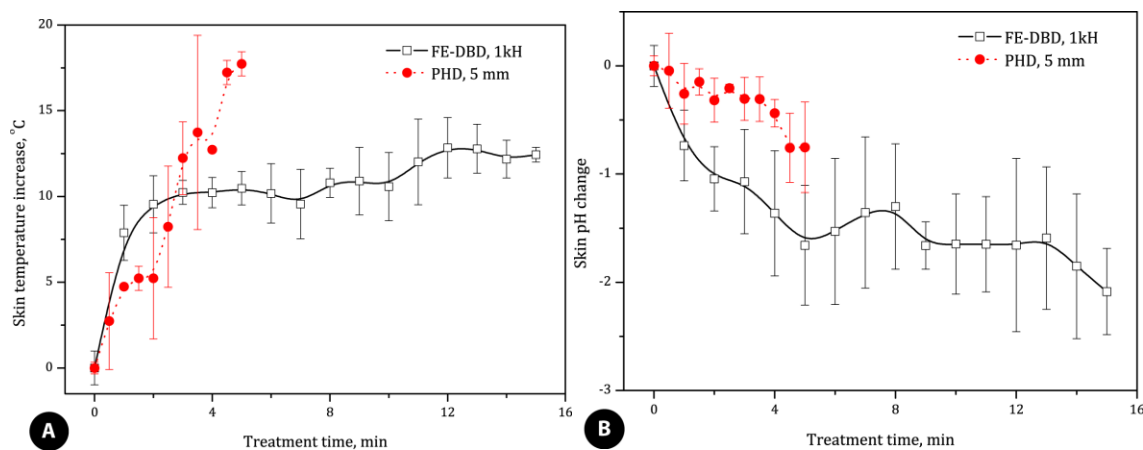
Figure 74. The results of temperature (a) and pH (b) measurements of the porcine skin ex-vivo treatment with FE-DBD and PHD plasmas.
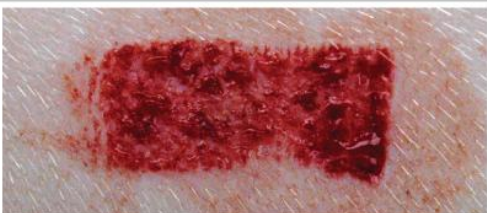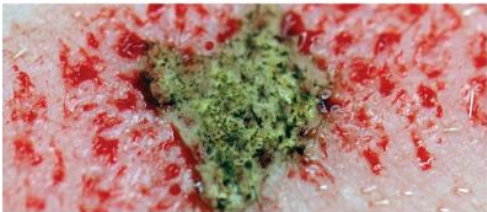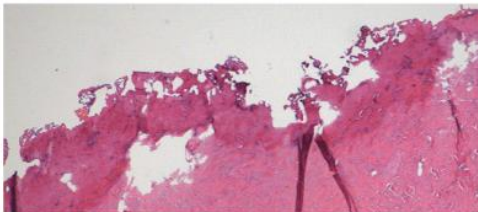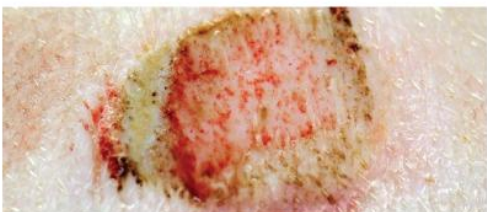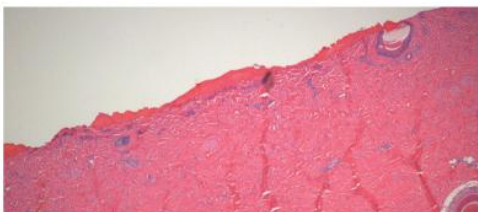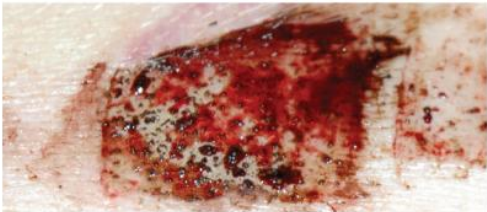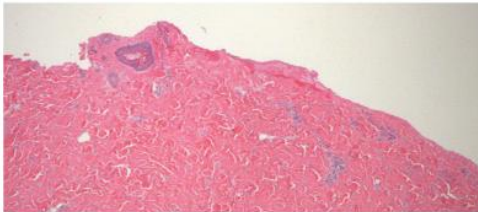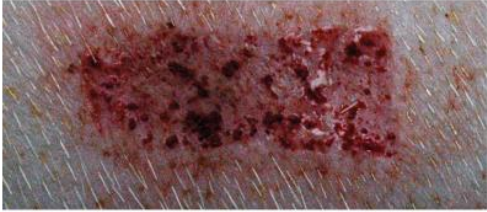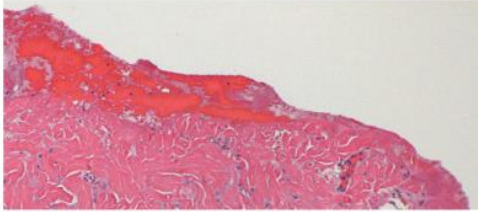
8.2.3. Toxicity of wound treatment

One of the potential applications of FE-DBD and spark plasma treatment is sterilization and healing of wounds and/or coagulation of bleeding capillaries. We were able to test the efficacy and toxicity of such treatment on a superficial partial thickness skin wound similar to that of scraping one's knee. Once the animal was anaesthetized the wound was made with a small hand-held dermatome knife (Zimmer, Franklin County, OH, USA) originally designed to remove precise-thickness skin grafts from a donor surface. These are partial thickness wounds with the blade set to cut no deeper than a millimeter into the skin. This exposes the top layer of skin and breaks capillaries located in the skin, but not the bigger vessels. Thus, the bleeding is slow and manageable. This is not a severe wound and the bleeding would normally self-terminate quickly. Immediately after the wound is made we proceed with the selected treatment.

Results of the various FE-DBD and PHD plasma treatments of wound surface and histological images of these skin samples are detailed in Table 9. Similar to the intact skin, treatment with Bovie® knife quickly coagulates blood and desiccates the tissue but

causes quite significant damage (see Table 9). Although the wound may be closed, there is a significant level of tissue damage which may prolong the wound healing process over that if the wound was simply left with no treatment in this case. While the Bovie[®] electrosurgery knife causes significant tissue damage, both plasma treatments can be applied to the tissue for up to 15 minutes with no or minimal damage to this tissue (Table 9). One other observation is that even after a short treatment, the blood appears to be coagulated and (although this is not visible on the photograph below) the wound looks to be covered with a thin layer of clear coagulum. We have seen such a thin transparent cork formation before with treatment of blood and blood plasma samples [3,17]. This film was claimed to be a thin layer of coagulated blood plasma – both FE-DBD and PHD seem to quickly form a layer of coagulated blood on the surface of the wound which protects the wound from further external disturbances.

Table 9. Representative photographs and histological images of the wounded skin after treatment with FE-DBD and PHD plasmas.

Treatment	Gross observation	Histology
No treatment	Appearance: Normal wound Histology: Normal wound	
Positive control Bovie®	Appearance: Eschar formation, burn formation immediately after treatment Instant blood coagulation Necrotic tissue Histology: Necrosis deep in the dermis. Disruption of the dermis. No dermal nuclei. Hair follicles still intact	
FE-DBD 117 J/cm² 15 min @ 0.5 kHz	Appearance: No burn. Blood clot formation Histology: Clot on surface. No damage to wound tissue. Intact hair follicles	
FE-DBD 93 J/cm² 5 min @ 1.5 kHz	Appearance: No burn. Coagulation. Histology: Clot on the surface of the wound. No damage to wound tissue.	
PHD 180 s @ 5 mm	Appearance: No burn. Coagulation Histology: Clot visible. No damage to dermis. Intact hair follicles.	

8.3. Conclusions

The purpose of this work was to determine the toxic doses of cold plasma treatment of living tissue for both intact and wounded skin. In this study we have used a well-established method for evaluation of tissue toxicity, where a Yorkshire pig intact or wounded skin was exposed to a plasma source and macroscopic toxic effects were studied histologically. In order to evaluate the possible source of plasma toxicity, we have used two plasma sources in which discharges are ignited and applied in completely different ways – direct non-thermal dielectric barrier discharge, and indirect thermal spark discharge. The results of our study show that, despite the fundamental differences of these two discharges, toxic effects (epidermal damage and tissue burn) are related to *global increase of temperature* of the treated skin, and are highly dependant not only on the dose of plasma exposure, but also on the *dose rate* – the lower the frequency of a discharge, the higher plasma dose may be applied to skin without damaging it. Plasma treatment of wounded tissue, on the other hand, did not result in any toxic effects to the tissue itself, but in effective and fast blood coagulation. This blood clot, apparently, protected underlying wound tissue from plasma damage. Overall, we have shown that plasma treatment is safe for living intact and wounded skin when applied for doses several times higher than required for effective inactivation of bacteria on surface of agar or in liquid.

CHAPTER 9. PLASMA WOUND HEALING AND PLASMA ASSISTED BLOOD COAGULATION: IN VIVO STUDIES

One of the most exciting, important and promising direction in the field of Plasma Medicine is shaping up to be plasma-assisted wound healing. Recent studies in this direction of biomedical applications of cold atmospheric pressure plasmas have shown a great potential of plasma discharges to become a new, safe and effective tool for everyday medical practice. Although still there is a limited number of reports, mostly very much preliminary, that it is possible to indicate the most general mechanisms of plasma action on wounds, specifically, acceleration of wound healing processes. The goal of this chapter is to propose an initial model of such mechanisms.

Wound healing is a complex and dynamic process of restoring cellular structures and tissue layers in damaged tissue as closely as possible to its normal state. Wound contracture occurs throughout the healing process, commencing in the fibroblastic stage whereby the area of the wound undergoes shrinkage.   It   has   3   phases: inflammatory, proliferative and maturational, and is dependent upon the type and extent of damage, the general state of the host's health and the ability of the tissue to repair.

We see three major effects of plasma treatment factors that affect healing efficiency:

- Oxidative stress
- Blood coagulation
- Anti-inflammatory effect of so-called "NO-therapy"

Below we will discuss these effects in detail.

9.1. Plasma induced oxidative stress.

Oxidative stress on mammalian cells may not be as detrimental as it initially seems. Indeed, ROS induce stress in mammalian cells and while in some cases it may lead to apoptosis in other cases this stress can actually promote or control angiogenesis, the growth of new blood vessels or repair/regeneration of existing ones [73,74,75]. Kalghatgi et al. showed that plasma treatment increases proliferation of porcine aortic endothelial cells. Fold growth, determined by counting attached cells seven days following the treatment, shows a two-fold increase in proliferation compared to untreated cells. Initial results indicate that this phenomenon is due to release of fibroblast growth factor 2 (FGF-2) by these cells as was confirmed with FGF-2 inhibitors [76,77].

In this section an experimental study of microsecond spark discharge treatment of erythrocytes in solution is discussed.

In order to investigate physiological and biochemical mechanisms of cold plasma affection changes in erythrocytes after plasma processing were studied in a series of *in vitro* experiments. Erythrocytes suspensions were prepared of human and mink blood. The concentration of red blood cells in the suspension was approximately $2 \cdot 10^7$ cells per ml. Cells were treated in suspension of 5 mm thickness at 3 mm distance from the plasma source. Treatment time varied from 5 to 60 s with constant mixing of the cell solution. The experiments with mink erythrocytes revealed hemolysis which was estimated by means of spectrophotometry. Percentage of destroyed cells was proportionate to exposition (Figure 75). Cell membranes are assumed to be damaged as a result of initiation of lipid peroxidation processes by ROS or directly in consequence of UV

irradiation. At the same time visible changes of hemoglobin in erythrocytes were not revealed.
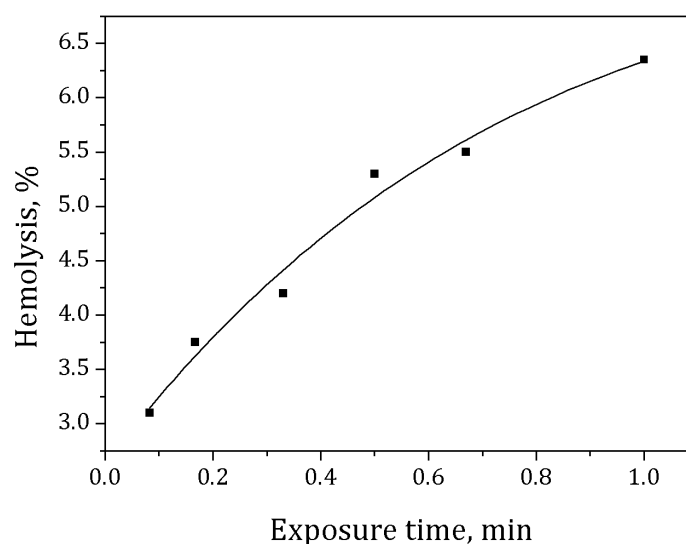
Figure 75 Hemolisys of mink red blood cells after spark plasma treatment.

Hemolysis was not observed in the experiments with human blood, but oxidation of intracellular hemoglobin took place. The concentration of MetHb and OxyHb were measured by absorption at 560, 576 and 630 nm wavelengths after the treatment. Concentration of forming methemoglobin depends on expositon. Rates of the reaction differ for the investigated samples (different individuals – Figure 76). This fact is supposed to be explained by means of different cells antioxidant status. The influence of UV radiation of plasma has been showed to be negligible by placing a quartz glass between the plasma source and treated solution (Figure 77).
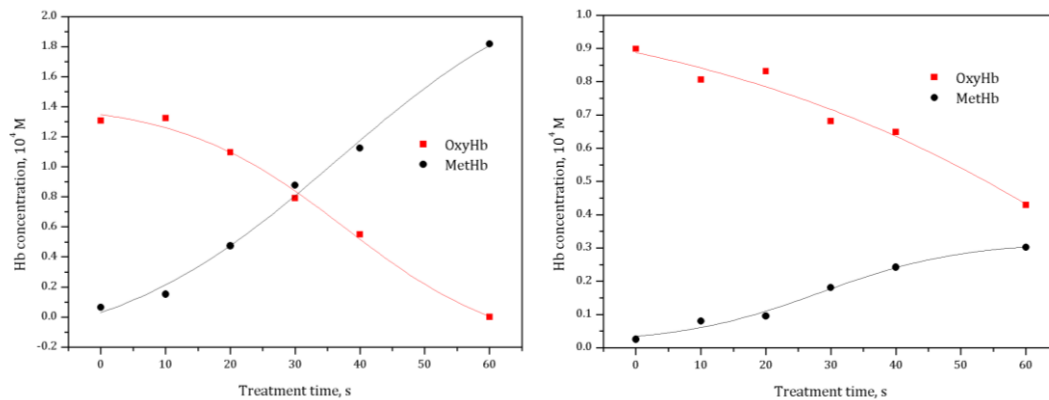
Figure 76 The concentration of MetHb and OxyHb in red blood cells in 2 samples after spark discharge treatment.

Thus, the obtained results are a point in favor of membrane-acting process, but specific mechanisms can be various. Particularly O_2^- is known to penetrate through cell membrane of a red corpuscle by anion channels or through lipidic double layer. O_2^- can be a predecessor of more toxic oxygen metabolites: $HbO_2(Fe^{2+}) + O_2^- + 2H^+ \rightarrow metHb(Fe^{3+}) + O_2 + H_2O_2$. As a conclusion, these results show that plasma effect penetrates inside the cell causing oxidation, while no cell lysis is observed.
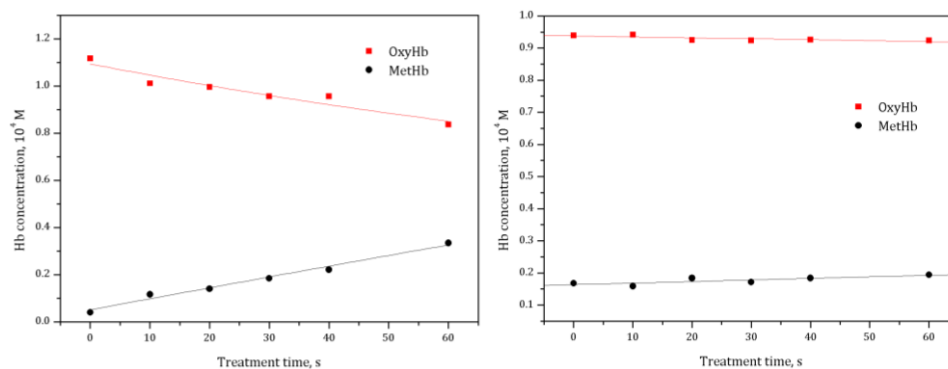
Figure 77 Oxidation of OxyHb in human red blood cells in presence (left) and absence (right) of UV produced by spark discharge.

9.2. Blood Coagulation by Plasma

Blood presents a challenging environment to every branch of science that studies it, from physiology [217] and biochemistry [218] of blood coagulation, to fluid dynamics of the process [219,220,221]. During the wound treatment process, for example, issues related to blood coagulation need to be addressed as blood provides the basis both for closing the wound and pre-forming matrix which is later used by cells and proteins to repair and close the wound, culminating in the re-formed tissue [222,223,224]. This section is concerned with the process of blood coagulation in a wound model where rat ear capillaries are cut and treated by cold plasma, promoting fast coagulation and closure of the wound. It is of interesting note that *electric plasma* was so named after the blood plasma by Irving Langmuir owing to the complexity and ionic nature of both mediums [225]. While thermal plasma is well-known to coagulate blood through thermal desiccation [226], authors and other groups have previously reported on ability of *cold plasma* treatment to coagulate stationary blood in-vitro and in explanted organs and tissues [78,94,227]. Some elucidation to the mechanisms of blood coagulation was made showing plasma's ability to interfere with the coagulation cascade, serving as a source of charged species that may catalyze the process [142], crosslinking blood plasma polymers, and activating platelets [227]. Cold plasma, in general, was shown to be an effective new tool with potential of use in the medical setting. Plasmas were shown to effectively sterilize various non-living surfaces such as medical instruments [28,51,53,56,103,228] as well as living human and animal tissues and cells [39,40,78,94,142,229]. Nitric oxide generated in plasma was shown to effectively promote wound closure and speedup

wound healing processes [78,84,89,140]. For these reasons it is important to show effective coagulation of capillary vessels in an *in vivo* model.

9.2.1. Materials and methods

Floating electrode dielectric barrier discharge, previously described [94], was used in this set of experiments and a standard rat ear bleeding model was modified for use of cold plasma as a treatment modality.

Floating electrode dielectric barrier discharge

In this study we have used a Floating Electrode Dielectric Barrier Discharge (FE-DBD) generated between the insulated high voltage electrode and the sample (FE) undergoing treatment. This setup was previously described in detail [94] so only a brief description is given here. One millimeter thick polished clear fused quartz (Technical Glass Products, Painesville, OH) was used as an insulating dielectric barrier. The setup and high voltage electrode schematic are shown in Figure 78 where a handheld pen-like device with the quartz tip was used for treatment. The discharge was generated by applying high voltage pulses with the following characteristics: 20 kV (p-p), 1.6 μs pulse duration, 1 kHz frequency. The average power density for the active area of the high voltage electrode was kept at the level of approximately 0.74 Watt for 6 mm electrode diameter measured electronically by integrating current and voltage signals as was previously described [94]. Of course, in the case of a hand-held electrode, as shown in Figure 78, the actual surface power density is difficult to estimate as it changes depending on the angle of application and distance to tissue; for this reason in this manuscript we report plasma treatment dose in seconds rather than J/cm^2 as the actual treatment area varies and is under the subjective control of the operator.
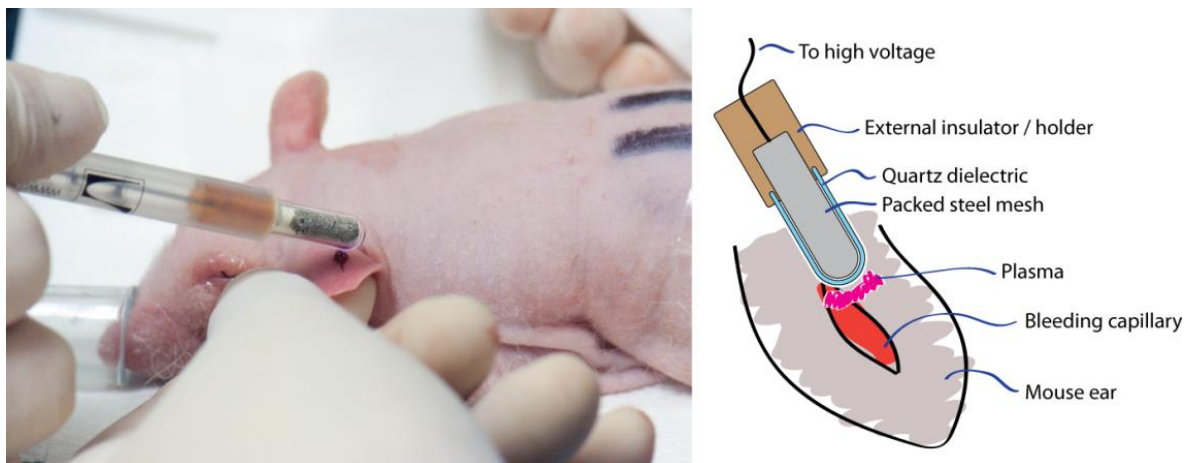
Figure 78. Photograph and schematic of the cold plasma treatment for capillary blood coagulation.

During the plasma treatment procedure operator was asked to hold the electrode steadily for a preset time interval. Training time for the operator was no more than a few minutes. All procedures were performed in compliance with the animal welfare and protection act following the Drexel University's Institutional Animal Care and Use Committee (IACUC) approval.

Animal model

Thirty hairless Sprague-Dawley rats, weighing approximately 250 g, arrived and acclimated for 3-5 days in the facility. Animals were transferred from the vivarium to the approved surgical suite. Animals were continuously anesthetized with inhalational gas anesthetic, Isoflurane (Vedco, St. Joseph, MO) at 2-3% induction plus oxygen 2L/min then 1.5-2% maintenance administered via a face mask for the appropriate length of time and placed in the supine position. Animals received analgesia (Meloxicam, Boehinger-Ingleheim, Germany) at the onset of anesthesia but prior to surgery at 1 mg/kg, subcutaneous. A full thickness wound of the auricular vein was inflicted on

bilateral pinnas with a sterile blade. One pinna served as the control experiment and coagulation allowed to occur naturally. Bleeding time commenced upon incision until hemostasis was achieved with no rebleeding within 30 seconds. FE-DBD plasma was applied to the opposing pinna upon onset of incision. Two techniques were applied to control blood coagulation using plasma. The first technique involved discharge treatment to the wound for 30, 20, 10 and 5 s increments. Blood coagulation was monitored without removal of the clot formed as the result of FE-DBD treatment. The second technique involved discharge treatment to the wound for 5 second increments during continuous removal of blood from the affected site until hemostasis was achieved. Control experiments were performed identical but without plasma treatment.

All data is reported with 95% confidence interval ($p < 0.05$) and the number of samples in each experiment is identified.

9.2.2. Results and discussion

Expected bleeding time for the type of wounds inflicted in this model is in the 1-2 minute range [230,231,232]. In our experiments, as expected, in the control wounds we observe typical bleeding times of approximately 2 minutes (Figure 79). As previously reported, there is no visible or microscopic adverse effect to tissue for long treatment times, over a few minutes [94,137,233] while blood clot formation was observed *in vitro* within approximately 15 seconds [94]. For this reason we have chosen 30 and 15 seconds as initial treatment points. Following the treatment, in all of the animals studied (n = 4 for each experiment) we observe clot formation with the same result achieved after 10 seconds of treatment both continuously and with 30 second intermission between 5 second treatments (Figure 79).

Plasma treatment without blotting
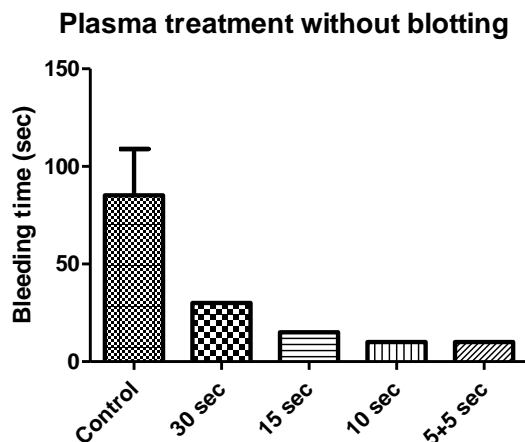
Figure 79. Results of observation of bleeding time in control groups and plasma treatment groups without continuous removal of blood clot.

Two conclusions can be drawn from this experiment. Either plasma significantly speeds up coagulation in bulk (as was previously suggested [94,227]) or there is a formation of solidified "corque" or thin film which creates sufficient pressure to stop blood from further flowing. This second possibility is less desirable in a medical setting since the formed solidified droplet of blood can be easily disturbed potentially leading to re-opening of the wound and further bleeding. Thus we have conducted a second set of experiments (Figure 80, here n = 16 for both control and plasma treatments). In this experiment we remove the forming droplet of blood, blot it off, with sterile gauze every 5 seconds. Removal of the droplet takes less than a second and the treatment is continued. This treatment, visually, closer represent an actual clinical setting than the original model. During surgery, excess blood is continually removed either by vacuum suction or by sterile gauze. As can be seen from Figure 81, the blotting process does decrease bleeding time in the control group by a few seconds; although, this small difference may

be attributed to statistical variation (n = 4 for first set and n = 16 for the second). Plasma treated wounds stopped bleeding, as before, in approximately 10 seconds (20 seconds was the highest, n = 1; and 5 or 10 seconds more typical, $n_5 = 4$ and $n_{10} = 7$).
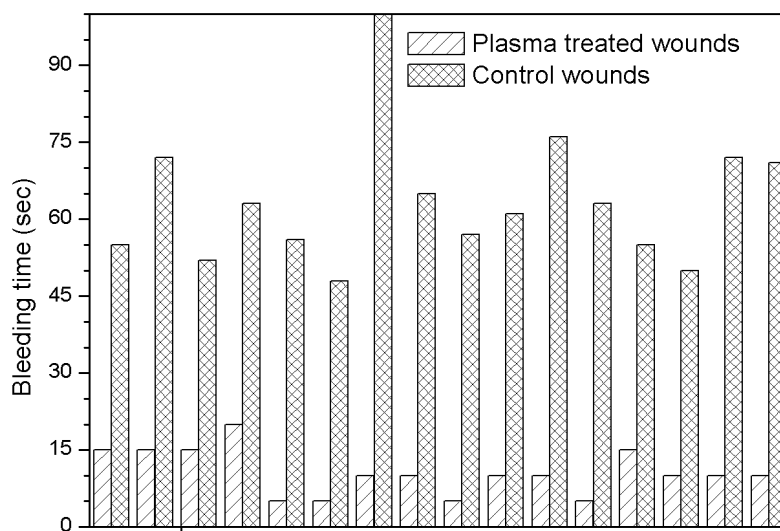
Figure 80. Results of observation of bleeding time with removal of blood clot every 5 seconds by sterile gauze.

Plasma treatment with blotting
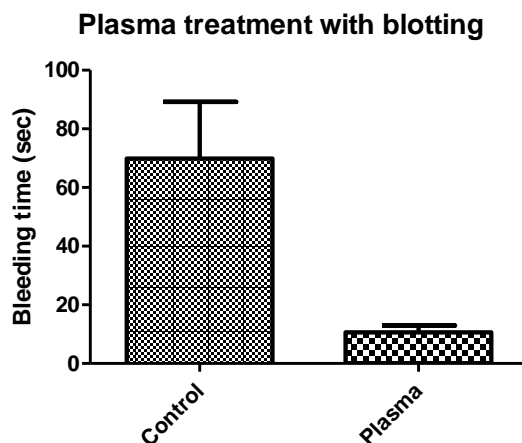
Figure 81. Summary of the results of observation of bleeding time with removal of blood clot every 5 seconds by sterile gauze.

9.2.3. Conclusion

In this section the results of verification of cold plasma interaction *in vivo* where blood coagulation of a wound model was shown on a rat ear are presented. These results further confirm a potential for cold plasmas to enter the medical field and serve as a new tool in treatment of wounds, in a surgical theatre, or possibly in treatment of diseases.

9.3. Anti-inflammatory effect of so-called "NO-therapy"

The Nobel Prize in medicine and biology was awarded in 1998 to R. F. Furchgott, L. J. Ignarro, and F. Murad for their work on the function of nitrogen oxide as a signal molecule. Today it is well known that in a human organism, NO serves a multitude of essential biological functions – it regulates blood vessel tone (via relaxation of flat epithelial cells) and blood coagulation, immune system and early apoptosis, neural communication and memory, relaxation of flat bronchial and gastrointestinal muscles, hormonal and sex functions, NO offers antimicrobial and anti-tumor defense, etc. In

pathology, NO plays a major role in adaptation, stress, tumor growth, immunodeficiency, cardiovascular, liver, gastrointestinal tract disease, etc. This explains wide possibilities of the plasma-generated exogenic NO in multiple medical applications.

Importance of exogenic NO in infection and inflammation processes is also well studied and is linked with anti-microbial effects; stimulation of macrophages; induction of cytokines, T-lymphocytes, and many immunoglobulins; interaction with oxygen radicals; and influence on microcirculation, cytotoxic and cytoprotective role in different conditions. During inflammation, macrophages and some other cells (i.e., aibroblasts, epithelial cells, etc.) produce NO via inducible NO-synthase (iNOS) in quantities significantly greater (two orders of magnitude) than normal when NO is formed via constructional NOS: endothelial (eNOS) and neuronal (nNOS).

Exogenic NO is also crucial in trauma wound processes. Activity of iNOS grows substantially in trauma wounds, burn wound tissues, bone fracture site tissues, and others in the inflammatory and proliferation phases of the healing process. Activation of iNOS was also discovered in the cultivation of wound fibroblasts. Macrophage activation in a wound, cytokine synthesis and proliferation of fibroblasts, epithelization, and wound healing processes are all linked with the activity levels of iNOS. In animal models, injection of iNOS inhibitors disrupts all of these processes and especially the synthesis of collagen, while NO synthesis promoters increase the rate of these processes.

Nitric oxide (NO) is a short-lived bioactive molecule critical to inflammatory and vascular processes, in particular wound healing. In the early wound, high NO levels are produced by inflammatory cells such as neutrophils and macrophages to fight infection

[16]. As the wound heals, endothelial cells, fibroblasts and keratinocytes produce lower sustained amounts of NO to stimulate angiogenesis and new tissue formation. The critical role of NO in wound healing is evidenced by poor wound healing in animals with decreased NO production, which can be abrogated by exogenous NO application [17]. Nitric oxide diffuses freely through biological membranes into the cytoplasm [18], where it stimulates soluble guanylyl cyclase (sGC) to convert guanosine triphosphate (GTP) into 3, 5-cyclic guanosine monophosphate (cGMP) [19]. The results of our study (see Chapter X) show that nitric oxide produced by microsecond spark discharge plasma may in direct and precise fashion be delivered into endothelial cells via liquid media with corresponding activation of cGMP production.

9.4. Plasma assisted wound healing: in vivo rat model

In this chsectionapter, a study where open wounds are treated with Floating Electrode DBD and microsecond spark discharge separately and in combination, and exogenous NO gas is presented. Rat is employed as the animal model.

9.4.1. Materials and methods

Plasma systems

In this study we have used a floating electrode dielectric barrier discharge (FE-DBD) generated between an insulated high voltage electrode and the sample (FE) undergoing treatment. In the first stage of the experiment the same electrode with the same plasma parameters as described in Chapter 5 was used. For the second stage, the same electrode system described in this chapter, section 2 was used. The microsecond spark discharge (PHD) described in detales in Chapter 2 was used for treatment of wounds on both stages.

All procedures were performed in compliance with the animal welfare and protection act following the Drexel University's Institutional Animal Care and Use Committee (IACUC) approval.

Animal model

Thirteen hairless Sprague-Dawley rats, weighing approximately 250 g, arrived and acclimated for 3-5 days in the facility. Animals were transferred from the vivarium to the approved surgical suite. Animals were continuously anesthetized with inhalational gas anesthetic, Isoflurane (Vedco, St. Joseph, MO) at 2-3% induction plus oxygen 2L/min then 1.5-2% maintenance administered via a face mask for the appropriate length of time and placed in the supine position. Animals received analgesia (Meloxicam, Boehringer-Ingelheim, Germany) at 1 mg/kg, subcutaneous, Bupivicaine 25% (Hospira, Lake Forest, IL) 0.5 ml/site intradermally and Normosol R (Baxter, Deerfield, IL) crystalloid parenteral fluid therapy at 10ml/kg subcutaneous bolus at the onset of anesthesia but prior to surgery. The ventral surface of the rat was prepared in sterile surgical fashion: the surgical area was gently washed and sanitized with chlorhexidine scrub solution; the area underwent an initial contact scrub of 5 minutes, rinsed with normal saline solution and repeated second time; a preparatory solution of diluted chlorhexidine with isopropyl alcohol (1:8) was lightly sprayed onto the surgical area. Approximately 2 cm incisions along the right and left side of the thoracic region were inflicted and plastic rings were inserted into the subcutaneous layer of the skin (ring size was equivalent to the size of the FE-DBD plasma probe) and restricted the bacteria to the affected area only, Figure 50. Schematic of the FE-DBD plasma electrode that fits into the plastic ring sutured to the wound.). The skin was sutured with 3-0 nylon around the

ring in a continous suture pattern. Animals were recovered from anesthesia in a pediatric warming incubator and then plasma treated in the following fashion. Each rat had a control wound (untreated), and the other one was used as an experimental wound. Experimental wounds were treated according to the following scheme (2 wounds per experimental point): FE-DBD treatment for 30 and 60 s, PHD treatment for 15 and 30 s, combination of 15 s FE-DBD and 30 s PHD treatment, and 15 s of treatment with 8000 ppm NO gas (balanced with N_2, Airgas) from the tank at rate of 1 slpm. After the treatment, wounds were covered with Tegaderm® dressing. The treatment procedure was repeated daily for 14 days until animals were sacrificed.

There were 2 stages of the study. On the first one, which last for 9 days, wounds were restricted from closure by rings (wounds on rats heal by contraction mechanism) covered with the Tegaderm® dressing every day in order to prevent their drying and access of oxygen, thus creating a chronic wound. On the 9th day rings were removed and wounds were allowed to heal naturally or were treated with plasmas or gaseous NO.
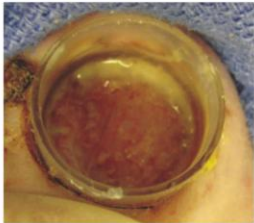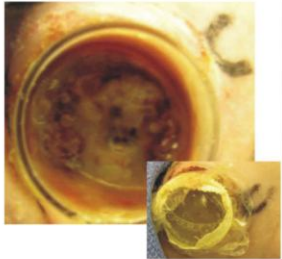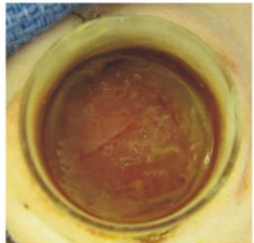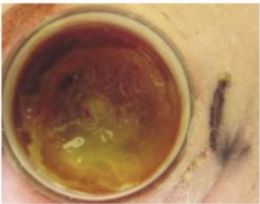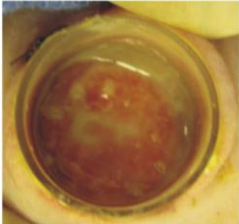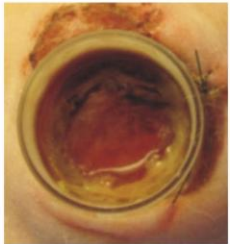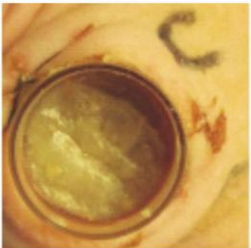
9.4.2. Results and discussion

On the first stage of the study, a chronic wound model was created. Representative pictures of wounds are shown in Table 10. Comparing plasma treated wounds to control one, the ones that were exposed to DBD or PHD plasmas looked healthier, probably due to some antibacterial action of plasma treatment, and in control wounds there was accumulation of significant amount of fluid (up to 1.5-2 ml) with fibrin on the bottom of the wound. There was no significant difference between plasma and NO gas treated wounds. The wounds treated with combination of DBD and PHD plasmas also were not significantly different from other treatment cases. These results, although a little

difference was observed, may be indication of a somewhat positive effect of plasma and NO treatment. This may be related to the fact, that gas flows in the case of NO gas and PHD discharge, and slightly elevated temperature of the treated surface in the case of DBD and PHD plasmas, helped in removing the excess liquid from the wounds while providing more oxygen to the tissue.

On the second stage of the study, rings were removed from the wounds (9th day), and wounds were allowed to close. Again, the treatment (Figure 82) was administrated every day until animals were sacrificed. Wound surface area was measured every day before treatment. The pictures of wounds are shown in Table 11. On Figure 83 graphs showing the progress of wound healing process for all 4 types of treatment by each animal compared to controls are presented. Figure 84 summarizes the result by comparing the average wound area by type of treatment relatively to control wounds. We show, that plasma treatment, both FE-DBD and spark discharge, result in almost 2 times faster wound closure. It is interesting to notice, that NO gas treatment has almost the same efficiency compared to plasma. At the same time, the fact that both discharges have relatively the same effect, although the physical nature of these plasmas are completely different, may indicate that both oxidative stress (DBD) and NO therapy (PHD) may be successfully applied for acceleration of wound healing processes. However, the most surprising and interesting result is related to combine treatment method: when both DBD and PHD plasmas are used, wound healing process is significantly, in about 2.5 times, suppressed. This effect may be related to over production of reactive oxygen species in the tissue, or negative effect of simultaneous action of reactive nitrogen species (PHD) and significantly lower pH (as a result of DBD plasma treatment).

Table 10 Representative pictures of chronic wounds

Figure 82 Plasma treatment of wounds with FE-DBD (top left), PHD (top right) and NO gas (bottom).

Table 11 Photographs of wound healing progress by days
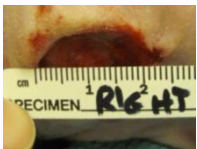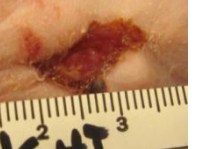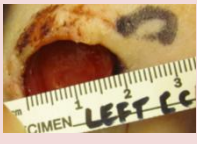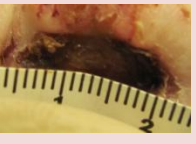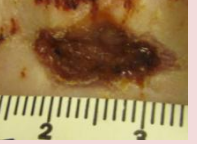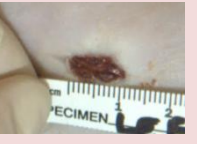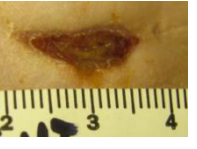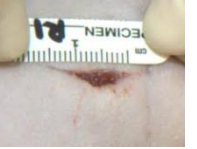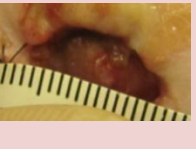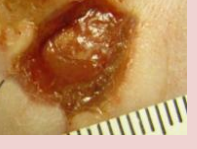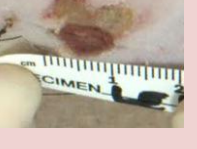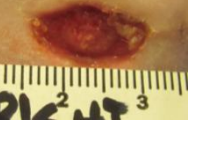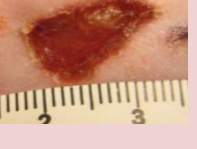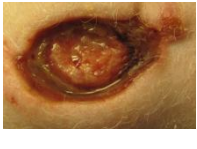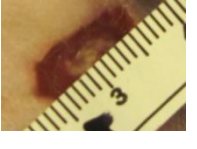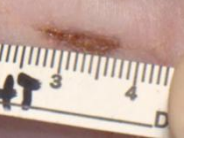
	Day #			
	1	2	3	5
DBD, 30s / Control				
DBD, 60s / Control				
PHD, 15s / Control				
PHD, 30s				

Table 11 (continued)

PHD, 30s Control				
NO, 15s / Control				
DBD 30s + PHD 15 s / Control				
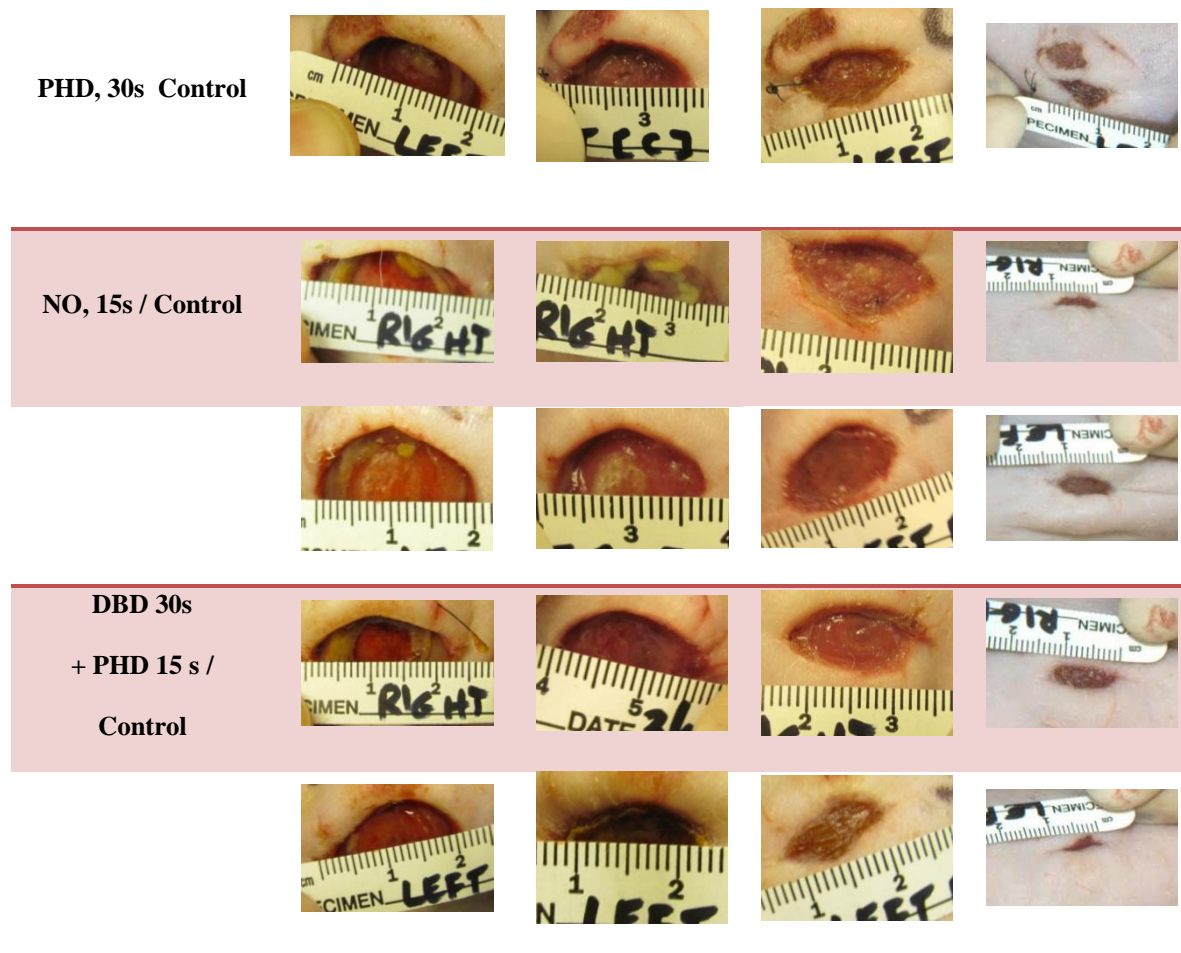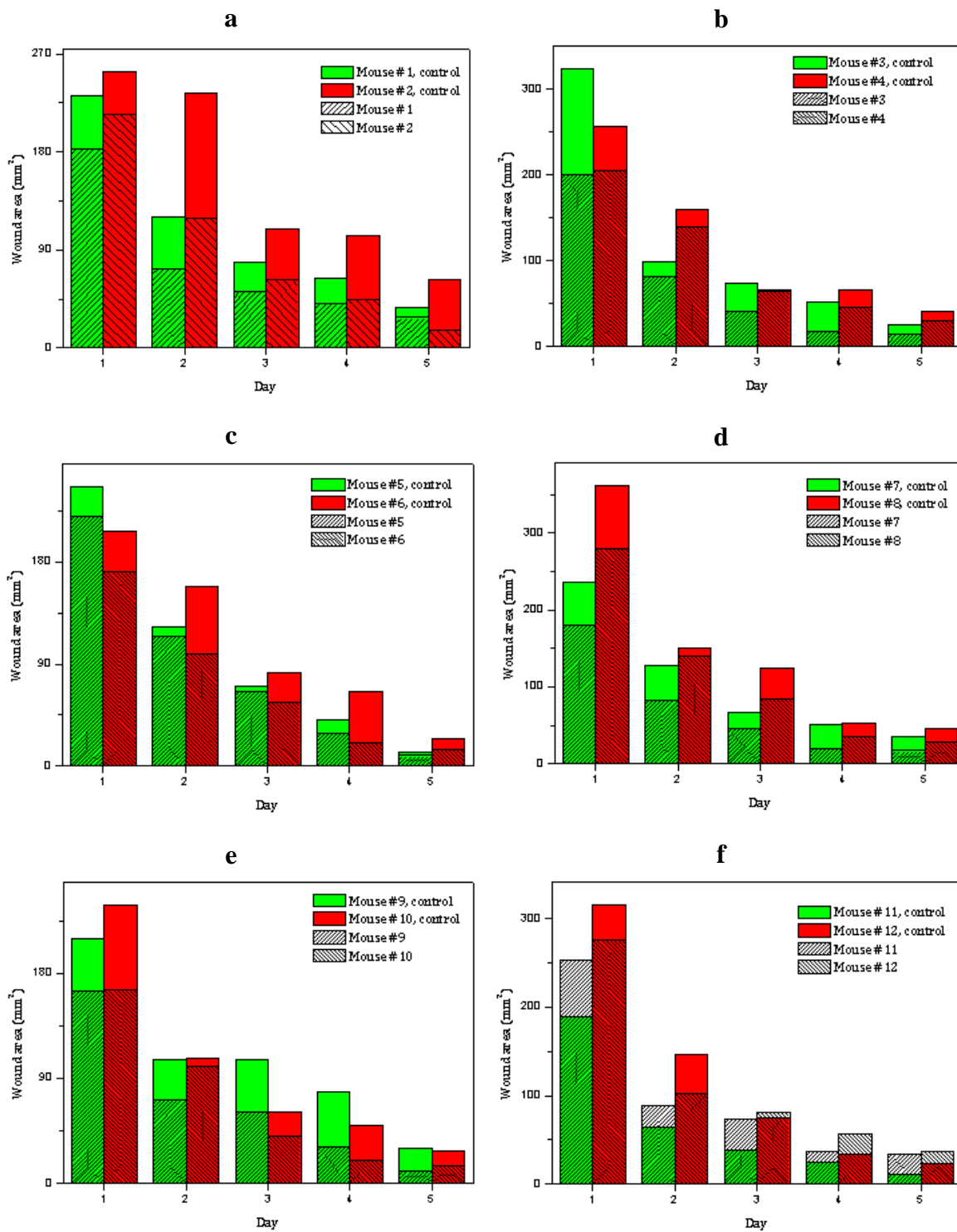
Figure 83 Progress of wound healing process for all 4 types of treatment by each animal compared to controls: FE-DBD 30 s treatment (a) and 60 second treatment (b), PHD 15 second treatment (c) and 30 second treatment (d), NO gas 15 second treatment (e), and combination of 30 second FE-DBD and 15 second PHD treatment (f).
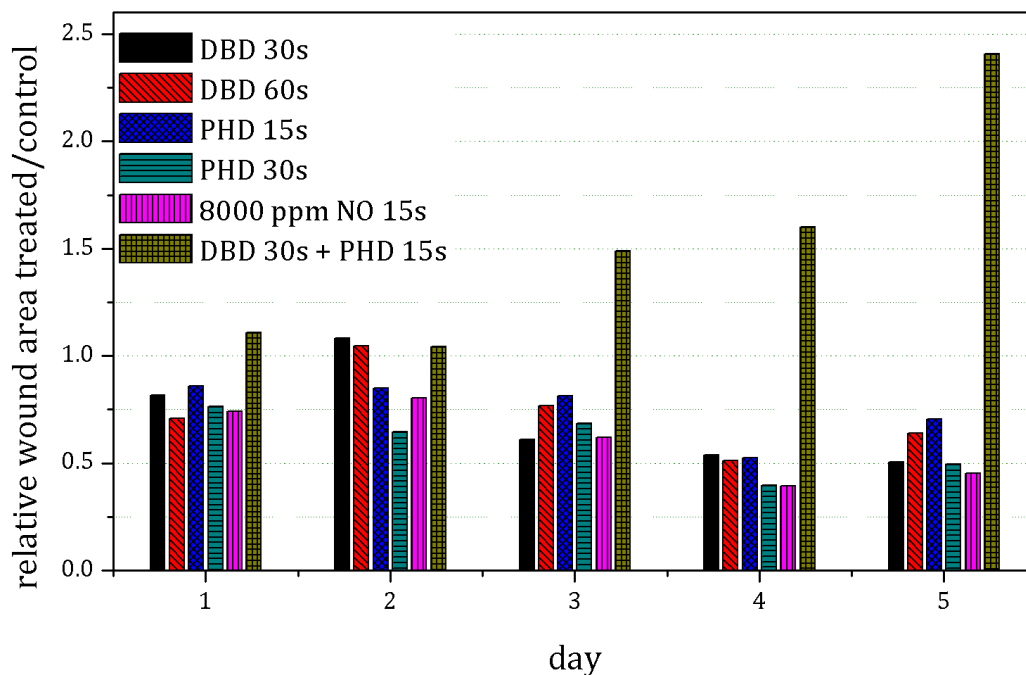
Figure 84 Summary of the wound healing process by treatment method.

9.4.3. Conclusions

In this section the results of the first *in vivo* experimental study of cold plasma wound treatment are presented. We show, that plasma treatment of chronic wounds do not cause adverse effects in general, and possibly may be beneficial. The effect of plasma treatment is shown to be positive: wound contracture was accelerated almost 2 times after treatment by either DBD of microsecond spark discharge, and was similar to the effect of NO treatment. Contrary, we show that effect of combined treatment by DBD and PHD plasmas is negative, resulting in 2 times slower wound healing. These results, although promising, are still very preliminary, and detailed careful study is required. The rat model used in this study must be further developed in *in vivo* studies involving larger animals (rabbits, pigs) where wound healing mechanisms are similar to those in humans.

CHAPTER 10. PLASMA TREATMENT OF GASTROENTEROLOGICAL DISEASES

Recently, non-thermal atmospheric pressure plasmas have emerged as a promising new tool in medicine. Compared to conventional thermal plasma [80,234,235,236,237], cold plasma is selective in its treatment and is safe since it does not burn tissue. Non-thermal plasmas generate free radicals, charged species, and ultraviolet radiation, which may be used for targeted chemical modification and catalysis [238,239] unlike thermal plasmas which employ high temperature that causes significant thermal tissue desiccation, burning, and scar formation. An example of thermal plasma is the Argon Beam or Argon Plasma Coagulator (APC) developed mainly to cauterize wounds [240]. On the other hand, cold plasma discharges have many potential medical applications that include sterilization of living tissue without damage [65], blood coagulation [81], induction of apoptosis in cancer and other cells [5,241], and control of cell attachment [242]. Another promising field of cold plasma applications in medicine is gastroenterology, where strong antibacterial effect can be successfully combined with healing and anti-inflammatory effects. Thus, the focus of this study is to evaluate whether cold plasma *in vivo* is detrimental to gastrointestinal tissue in health and disease conditions and whether cold plasma provides any therapeutic benefit in an animal model of murine experimental colitis. The disease in this model produces experimental colitis reminiscent of human ulcerative colitis, which is a form of inflammatory bowel diseases. Inflammatory bowel diseases (IBD) consist of two major chronic, relapsing and debilitive forms of diseases known as ulcerative colitis and Crohn's disease that affect the gastrointestinal tract. The

etiology of these diseases remains a mystery though genetic, environmental and immunological factors are found to play a major role in the induction, chronicity and relapses of these diseases. Crohn's disease may appear in any part of the gastrointestinal tract from the mouth to anus and affects the entire thickness of the bowel wall. On the contrary, ulcerative colitis is an inflammatory disorder affecting colonic mucosa and sub-mucosa [243]. There are no known curative therapies for these diseases; however , recent advances in IBD therapeutics have shown that certain biological therapies have been successful in maintaining remission particularly in Crohn's disease [244,245].

This study was designed to evaluate the effects of cold plasma treatment of both healthy colon tissue and experimentally-induced ulcerative colitis disease in a live animal model. The goals of the study were to examine whether cold plasma treatment adversely affects the mucosa in normal condition, and to evaluate if cold plasma treatment results in acceleration or worsening of the disease during its induction phase. Additional pilot experiments were conducted to study whether cold plasma discharges provide therapeutic effects, and whether these effects are comparable to a standard therapy, or cold plasma treatment enhances the beneficial effect of a standard therapy.

10.1. Materials and methods

10.1.1. Cold Pin-to-Hole Spark Discharge (PHD) Plasma

Currently, the primary reason of gastroenterological inflammatory diseases, and particularly ulcerative colitis, is still unknown; however, two major candidates are bacterial infections and autoimmune disorders. In order to be able to address these problems using plasma, the treatment should meet several conditions, namely:

- average plasma temperature should be low, i.e. close to room temperature, when there is no or minimal thermal damage due to contact of plasma with tissues;

- have strong bactericidal effect;

- be able to provide anti-inflammatory effect.

Another set of criteria which are important in the present mouse model experiments refer to plasma system engineering problems:

- electrode system ("plasma probe") should be small (maximum outer diameter is approximately 2 mm) in order to cause minimal mechanical damage to colon tissue of a mouse;

- plasma should be easily ignited inside of a colon, and should not be sensitive to the distance between electrode and inner colon wall.

All these conditions may be satisfied if one is using cold spark discharge plasma. Dr. Gostev and colleagues reported that this cold discharge [82,180] (there, a large-scale system of about 10 times greater in size has been used) is extremely effective in sterilization of bacteria both in liquid [246] and on tissue surface [247], and due to production of significant amount of nitric oxide (NO) has pronounced "healing" effect through faster tissue regeneration, and other beneficial effects [82,83,85,180]. The pin-to-hole electrode configuration makes the discharge ignition process not sensitive to the presence of surrounding tissues in contrast to arc, dielectric barrier, or corona discharges. Also, PHD treatment allows operator to provide relatively high energy input resulting in shorter treatment time and less discomfort to an animal.

In this study we have used modified PHD system which consists of central copper needle covered by dielectric material which is inserted into a grounded stainless steel cylindrical electrode (Figure 85). In order to cause minimal mechanical damage to colon tissues external electrode is covered by polyethylene sleeve. The discharge was ignited by applying high positive potential to the central electrode. In order to provide high discharge energy while keeping average gas temperature low, the electrode system was powered through a capacitor. This resulted in a formation of dense energetic spark which exists for about 3.5 µs. Due to low repetition frequency of about 7 Hz and short pulse duration, the average gas temperature did not exceed room temperature.
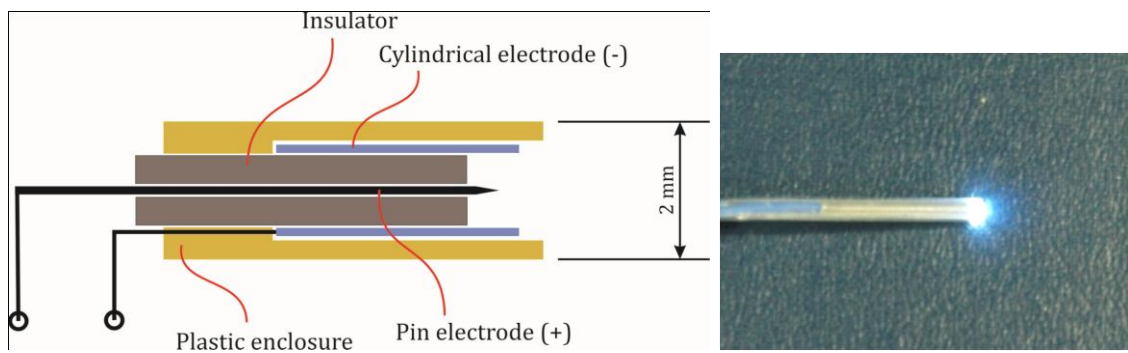
Figure 85 Pin-to-Hole spark Discharge (PHD) plasma system general schematic and photograph of the discharge in operation.

Main average PHD plasma characteristics are the following:

- peak voltage: 3.2 kV;

- pulse duration: 3.5 µs;

- frequency: 7 Hz;

- energy per pulse: 0.1 J;

- plasma diameter: ~2 mm;

- typical waveforms are shown in Figure 86.
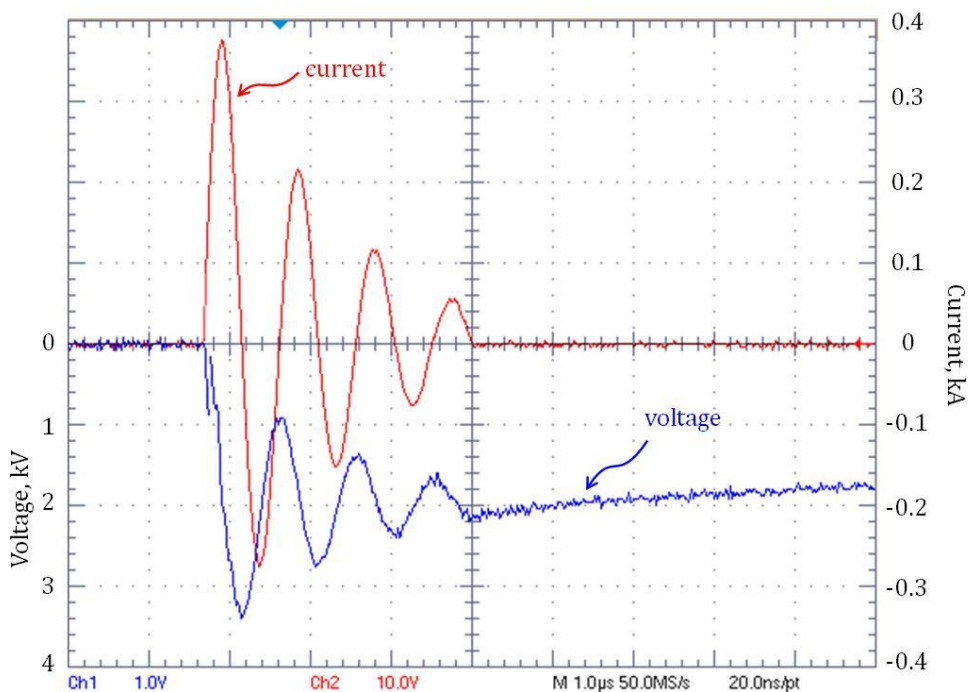
Figure 86 Typical voltage and current waveforms of cold Pin-to-Hole spark Discharge (PHD) plasma.

Lastly, it was necessary to check if miniaturized PHD plasma system indeed produces significant amount of NO, thus delivering the therapeutic effect (so-called, "NO-therapy" [17,248,249,250]). The NO production was measured using gas chromatograph Agilent 3000 MicroGC, calibrated with 700 ppm NO balanced with nitrogen. The discharge cell was inserted inside of a syringe tip, and plasma treated room air was collected with slow plunger pulling during plasma treatment. Then, collected air was analyzed chromatographically. The results of our measurements (see Figure 87) show that NO concentration is varied from 900 to 1200 ppm depending on plasma treatment dose, which allow us to expect that plasma treatment of colon ulcer may cause "healing" effect.
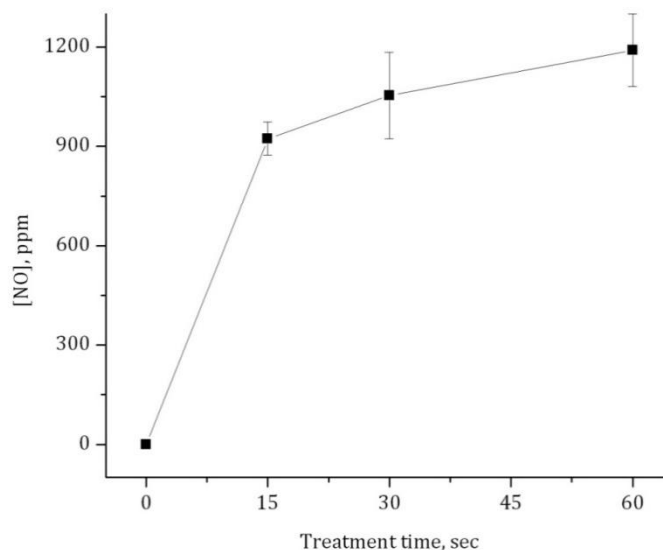
Figure 87 Nitric oxide production by PHD plasma

Although one can argue that plasma characterizations mentioned above were made in different atmosphere (room air), and therefore the results could differ from real experimental situation when plasma is ignited inside of intestine, we do not expect qualitative difference between these two conditions. This assumption is based on data on gas composition inside of a colon, which is mostly consists of air-like mixture (up to 80% of N_2 and 2.3% of O_2) with small additives of hydrogen, methane, and carbon dioxide [251]. Moreover, before the treatment procedure, the colon was cleansed with saline, and also room air was introduced into the colon during probe insertion. Therefore, air is expected to be a dominant plasma-forming gas.

10.1.2. Dextran Sodium Sulphate (DSS)-induced experimental colitis in Mice

The DSS model was used in the current study to produce ulcerative colitis in mice which is representative of human ulcerative colitis [33, 34]. The disease is induced in an animal

through a daily oral administration of 2.5% DSS dissolved in drinking water at concentration of 2.5%. Animal develops an acute form of inflammation beginning on the third day and they have a full blown colitis on the day of DSS feeding cycle. The primary characteristics of acute inflammation are the increased number of neutrophils in the mucosal layer, shortening of the epithelial crypts, hyalination in the lamina propria, accompanied by severe weight loss, diarrhea, and blood in the stool. This form of the disease gives an opportunity to use it as a model in efficacy studies of drugs and compounds [34]. The most striking feature of this model is that it works using a very simple pathway to produce the disease as DSS overcomes the barrier of the epithelium to expose the mucosa to the flora present in the intestine resulting in an inflammatory response; this in turn leads to activation of macrophages and monocytes. The model also shows close links to the disease in human beings and it is simple to induce and reproduce [33-35].

To quantify the disease induced by the DSS model a Disease Activity Index (DAI) have been used [252]. A scale of 0 to 4 is used to quantify the disease with 4 being the lethal stage of the disease. DAI is scored on the parameters of weight loss, consistency of the stool and presence of blood in the stool. This index has been shown to be in a linear correlation with the histology score based on changes in the architecture of the crypt [33].

10.1.3. *Animal study design*

All experiments were done on live animals. The study consisted of 3 stages:

1. Toxicity study of plasma treatment of a colon.
2. Study DSS model disease progression after plasma treatment.

3. Comparison of effectiveness of plasma treatment with conservative therapy

In all the experiments Female Swiss Webster mice approximately aged six to eight weeks of 25 to 30 grams in weight were used. Prior to plasma treatment animals were anesthetized with 0.4 ml Nembutal[®]. The effect of the anesthetic was checked using the toe relax by pinching. The colon was cleansed with saline before inserting the probe.

10.2. Results and discussion

10.2.1. Toxicity of plasma treatment of colon tissue

The primary objective of the study was to ascertain if cold plasma treatment would cause any damage, to colon tissue or to the animal itself. To ascertain this effect, 12 mice were divided into 4 groups of three animals in each group.   The first group was a control group which did not receive any treatment and the other three groups remained as experimental groups. In experimental groups a laparotomy was performed and the colon was exposed and kept moist covered with a saline gauze. The plasma probe was introduced through the anal verge up to 4 cm into the colon (Figure 88). Plasma treatment was administered for 0, 4, 30 and 60 seconds in the respective group. To check colon tissue damage, mice were intravenously injected with 30 mg/kg of Evans Blue (EB), ten minutes after the administration colon was washed with 1 ml physiological saline and EB presence was analyzed spectrophotometrically. Animals were euthanized with an over dose of Nembutal[®] and colon tissue samples were surgically removed and were preserved in formalin for further histopathological analysis.
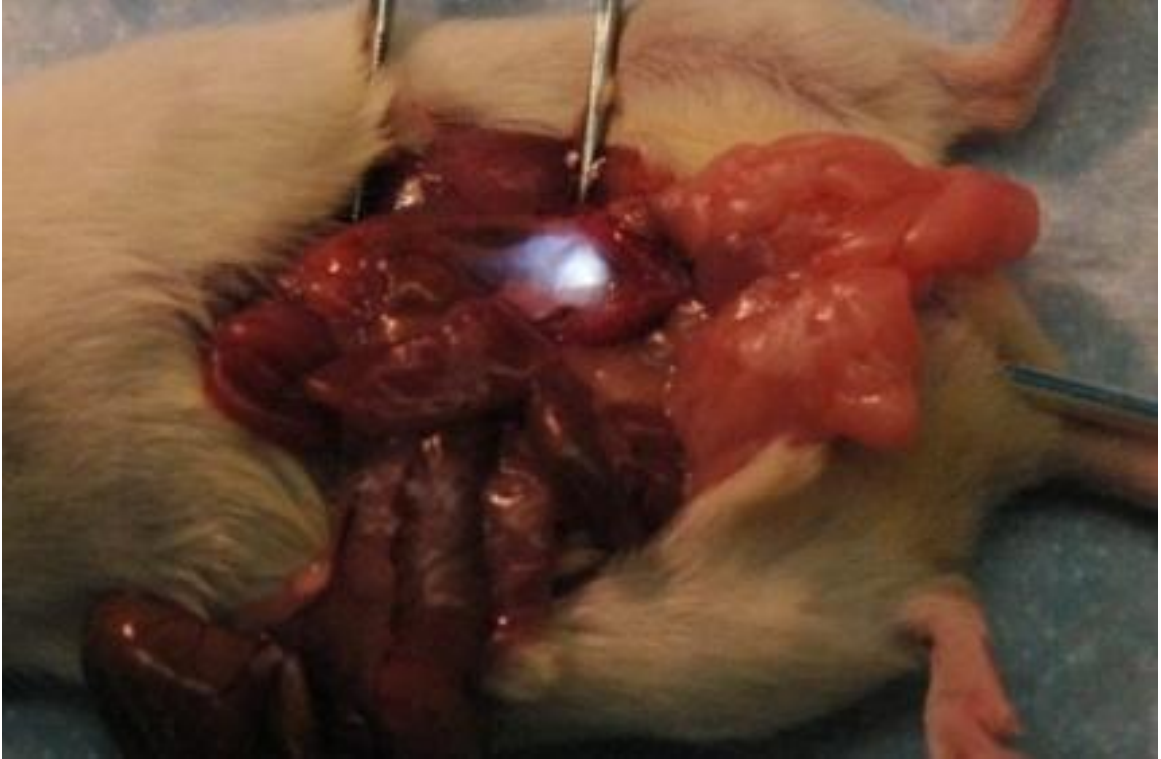
Figure 88 Photograph of cold spark plasma inside of the mouse colon: the colon here is not punctured and the light generated by plasma is seen through the thin tissue.

Spectrophotometrical analysis of the saline fluid collected from the colon showed no traces of EB, indicating that plasma did not affect the tissue integrity. Histology analysis also showed that no damage was induced to the colon tissues by plasma treatment or probe manipulation (Figure 89).
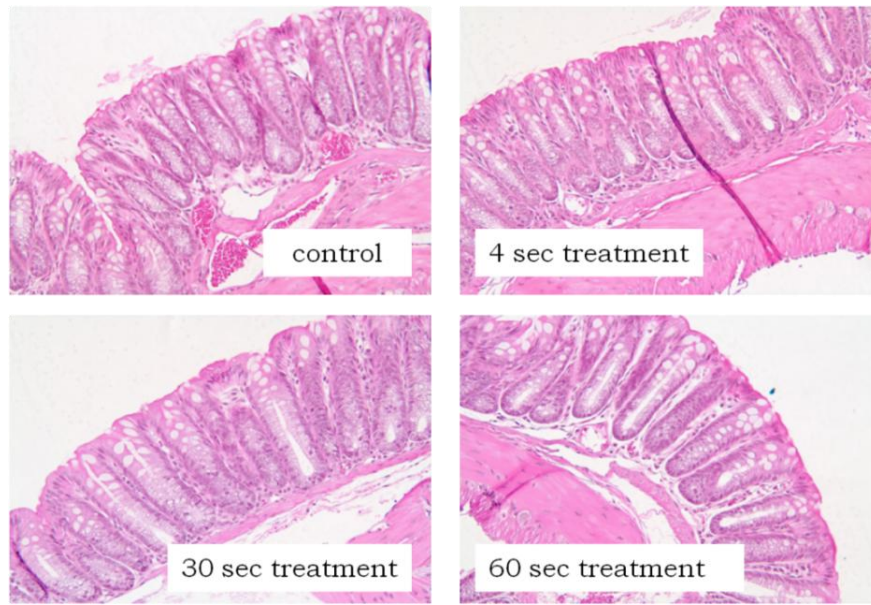
Figure 89 Colon tissue histology shows no detectable damage

10.2.2. DSS model disease progression after plasma treatment

The next step was to check the response of the disease progression to plasma treatment; hence 24 animals were divided into 4 groups each receiving 0, 4, 30 or 60 seconds of plasma treatment every alternate day for 7 days. All animals were fed 2.5% DSS for 7 days in parallel with plasma treatment. DAI was scored everyday to see which dosage of plasma was most effective in controlling the progression of the disease. For the plasma probe to be inserted and to go through the colon, the colon has to be cleansed of stool specks. To do so, the animals were fed a polyethylene glycol based laxative along with DSS one day before plasma treatment. However, the stool consistency on the next day was compromised as the laxative made the stool consistently loose. Hence, data extracted from the study were bifurcated and were analyzed using a three pronged approach considering:

a. Weight, stool consistency, and presence of blood in the stool.

b. Weight, and presence of blood in the stool (without stool data)

c. Mean hemoccult (visible blood in the stool)
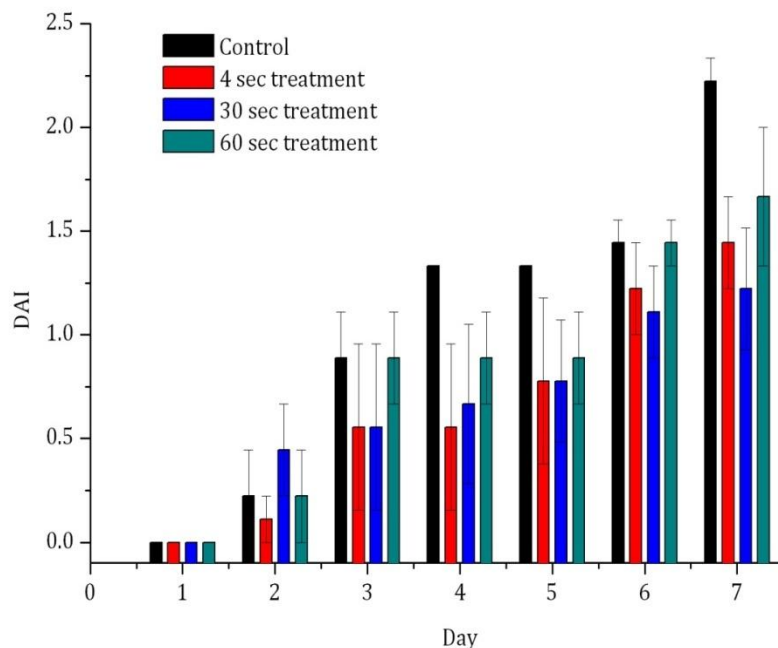
Figure 90 Progress of colitis, mean DAI: results of the second stage of the study (considering weight, stool consistency and hemmocult)

Results of the experiment (Figure 90) show that, in the control group the DAI scored using weight, stool consistency, and blood visibility in the stool reaches a value of 2.3 by the end of 7 days. The group which received 60 seconds of plasma treatment reached a DAI of 1.6 on day 7. Hence, the disease is not controlled very well in the 60 second plasma group; on days 3, 4 and 5 one minute of plasma treatment stabilized the disease and prevented it from progression. However, as the severity of the disease increased the plasma treatment effectiveness ceased. 4 seconds of treatment resulted in disease reduction during the end stage of the study and it is comparatively better than the 60 second treatment. Here the disease was well controlled through the course of the study. The most efficient dosage of plasma as shown by the study is 30 seconds exposure. This

group showed high resilience against the progression of the disease, and as compared to the control, showed great ability in stopping the progression of the disease even when DSS is being fed in parallel. The maximum DAI in this group was 1.2 as observed on day 7, the day of maximum disease prevalence.
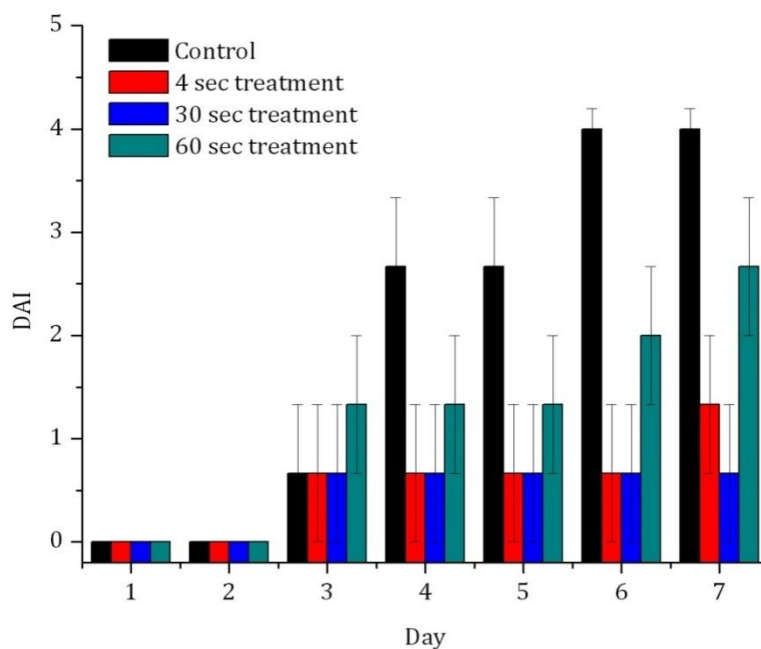
Figure 91 Progress of colitis, mean DAI: results of the second stage of the study (considering hemoccult only)

The laxative that was administered to the animals on days prior to plasma treatment might have compromised the score based on stool consistency as this makes the stool comparatively loose, and therefore on Figure 91 only hemoccult data have been considered as one of expected effects of plasma treatment is blood coagulation inside the inflammed colon. As the prime facet of tissue degradation of colitis is through bleeding out of the tissue which can be observed on the stool study. Hence this data is critical to check if plasma can actually clot and coagulate the blood inside the colon. Data shows that a statistically significant difference was obtained between untreated animals in

control group and animals treated with plasma for 30 seconds. On the final days of study hemoccult reached DAI of 4 in the control group while the "30 seconds" group had a DAI of just over 0.5. It can be inferred from the data that the "30 seconds" and "4 seconds" groups are showing blood coagulation inside the colon.

10.2.3. Comparison of effectiveness of plasma treatment with conservative therapy of ulcerative colitis

The goal of the last stage of the study was to investigate the effectiveness of plasma treatment as an adjuvant to conventional antioxidant drug (5-amino salicylic acid (5-ASA)) treatment. Based on previous results, where it was shown that 30 seconds of plasma treatment gives the best results in controlling and reducing the disease progression compared to all other groups, this treatment dose was selected for the next step. In this set of experiments 24 animals were divided into 4 groups: control group 1, where no plasma or drug treatment was performed, and groups where mice were treated either with plasma alone (group 2), 5-ASA alone (group 3), or drug and plasma together (group 4). All four groups of animals were fed with DSS for six days. On days 2, 4, and 6 they received 2.5 % DSS dissolved in water and for days 1, 3, and 5 (one day before plasma treatment) they received 2.5% DSS dissolved in 15% poly ethylene glycol based laxative to clean the colon. Plasma probe was introduced into the colon 4 cm from anal verge in groups 2 and 4, where group 2 received 30 second dose of plasma treatment only, while group 4 received same dose of plasma treatment in together with 0.1 ml of 5-ASA treatment. Animals in groups 3 and 4 were treated with 0.1 ml of 5-ASA. The DAI was scored everyday during the tenure of the study. On the seventh day of DSS

treatment and final plasma treatment DAI was measured and animals were euthanized with an over dose of Nembutal®.
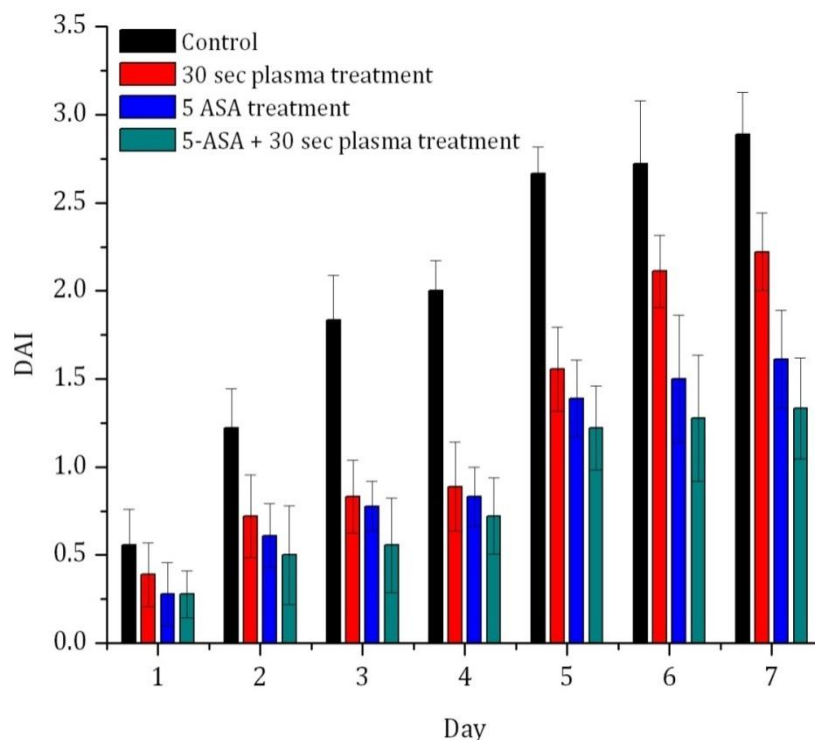
Figure 92 Progress of colitis, mean DAI: results of the third stage of the study (considering weight, stool consistency and hemmocult)

The disease progression for all four experimental groups is shown on Figure 92. The control group showed a steady increase through the course of seven days with the DAI reaching an expected 2.7 on day 7. The plasma treatment group was administered 30-second plasma treatment and obtained data are in direct correlation with the data acquired in the previous study and also show a constant increase of disease progression. However, the disease curtailed to near 1.8 on the DAI scale. The group 4 showed very positive

results as both in combination proved to be effective in controlling the disease and keeping the DAI on a level of 1.2 on the DAI scale.
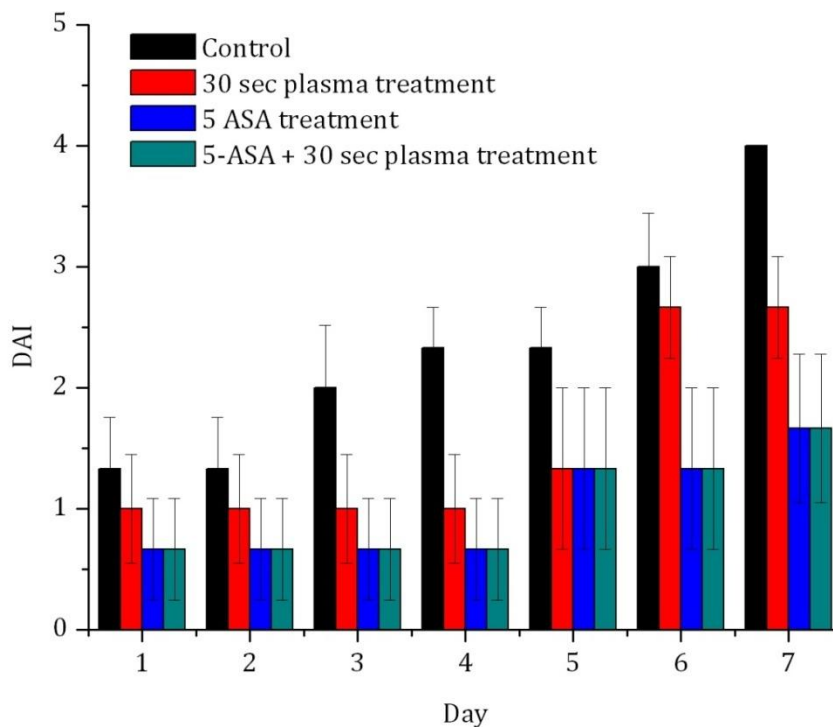
Figure 93 Progress of colitis, mean DAI: results of the third stage of the study (considering hemoccult only)

Figure 93 is designed to express the mean hemoccult charted on a scale of 0 to 4 with 4 being the advanced stage of the disease. The plasma treatment resulted in a significant drop on the hemoccult scale as compared to the control. This shows that plasma actually was working in clotting the blood that was being pumped out of the inflammed region in the colon. The combination treatment further reduced the hemoccult score as a two pronged approach is taken against the disease.

The most important aspect of the study is to verify the hypothesis that plasma can be used as an add-on to the conventional drug treatment to cure the disease faster and with

renewed vigor. Experimental results show that in the group which received combination treatment, disease progression was further decreased as compared to the groups which received the drug or plasma alone. The bars show a statistical significance in the two groups as plasma and 5-ASA reduce the disease as compared to the control group on days 5 and 7.

10.2.4. Plasma Assisted Blood Coagulation and Antioxidant Effect of Plasma Treatment

The results of our first invasive in-vivo experiments of cold plasma treatment of colon tissue in case of ulcerative colitis mouse model show that plasma can significantly reduce severity of the disease progression. In fact, while untreated (control) animals undergo weight loss, loss of stool consistency, and excessive bleeding, showing disease progression up to DAI number 3.1 (when 4 corresponds to lethal stage of the disease), plasma treated ones appeared to have significantly lover disease progression rate with reduced reaction to inflammation.

Cold plasma treatment apparently has positive effect on inflammed colon tissue when applied for ulcerative colitis treatment. First, analyzing contribution of hemmocult level to the DAI, it is shown that plasma may cause effective blood coagulation in colon ulcers. Indeed, Fridman et al. have experimentally shown that treatment of normal whole blood both in in-vitro and in-vivo cases with floating electrode dielectric barrier discharge (FE-DBD) plasma leads to initiation of natural coagulation cascade followed by fast, on the order of seconds, formation of blood clot [17,81]. However, contribution of various plasma species and detailed mechanism of this effect remain unclear.

Another possible effect of cold spark plasma is related to nitric oxide production. It is well known today, that NO plays an important role in wound healing and tissue regeneration by regulation of blood vessel tone and blood coagulation, immune system and early apoptosis, etc. [17] Exogenic delivery of NO-donors (compounds that contain and release or synthesize nitric oxide upon contact with tissue) to the wound promotes and speeds up healing processes [17].

Additionally, the role of NO may be related to "deactivation" of oxidants with formation of acidic environment. One possible explanation of pathogenesis of ulcerative colitis is given by so-called "Radical Induction Theory", which suggests that the main cause of inflammation is excess un-neutralized H_2O_2 [253]. Hydrogen peroxide is produced within colonic epithelial cells, and then easily diffuses through cell membranes, and through formation of highly reactive hydroxyl radical extensively causes oxidative damage to the cells. In this situation, increased acidity may play an important role in process of inhibition of inflammation: currently used drugs, for example, 5-ASA, which is acid, probably acts as an "antioxidant". To check this hypothesis, we have treated 100 μl of H_2O_2 water solution with initial concentration of about 30 mg/l with spark discharge plasma (Figure 94). In order to simulate closed environment of the treated colon, discharge cell and solution holder were incased using tygon tube.
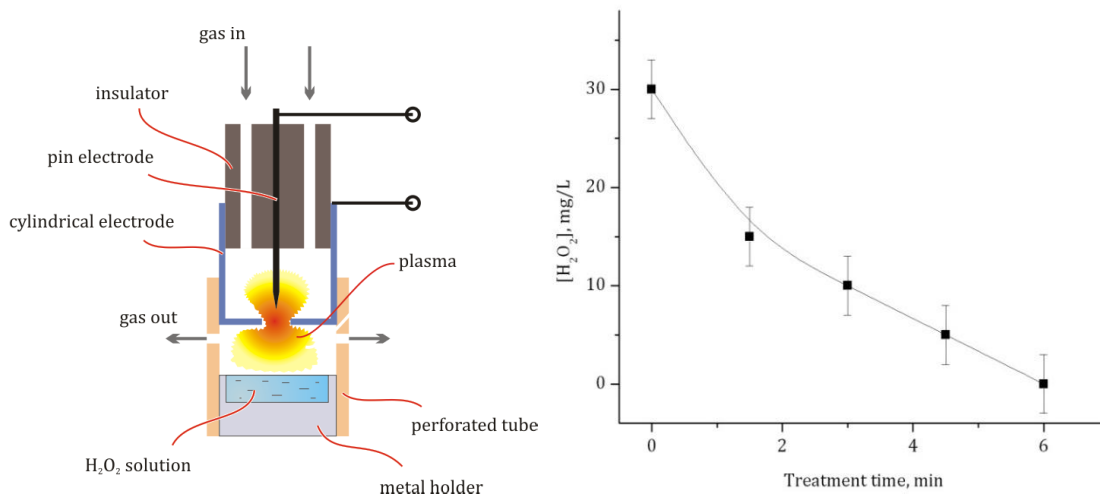
Figure 94 Scheme of the experimental setup and the results of hydrogen peroxide PHD plasma treatment

The result of the experiment shows that hydrogen peroxide was decomposed completely within 6 minutes of treatment. Possible mechanism of the destruction may be related to chemical reaction of H_2O_2 with NO with formation of nitric acid:

$$H_2O_2 + NO \rightarrow H_2O + NO_2,$$

$$H_2O + 3NO_2 \rightarrow NO + 2HNO_3.$$
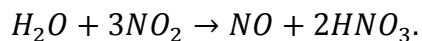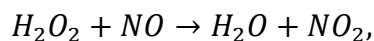
10.3. Conclusions

Major results may be summarized as follows:

1. In the first stage of the plasma study, the primary goal was to understand the interaction of cold plasma with a living animal. The study showed that the cold plasma alone in graded doses did not cause any damage to the colonic tissue or the animal based on Evan's Blue extravasation and histological analysis.

2. The second stage of the plasma study posed the challenge of ascertaining the graded dose at which the progress of the disease (ulcerative colitis) can be controlled. It is concluded

that plasma did not adversely affect the animals and did not *increase* the progress of the disease. Surprisingly, it *reduced* the disease from progressing rapidly as compared to the control. The exact mechanism by which cold plasma induced its beneficial effect remains unknown.

3. The final stage of the plasma study was designed to evaluate and check the activity of plasma as an adjuvant to the industry standard drug 5-ASA in controlling the disease. Combination therapy of 5-ASA and cold plasma showed that there is a significant therapeutic relevance when it comes to adding plasma to the drug in controlling colitis in the DSS model during the induction phase.

4. Possible explanations of observed positive effects of plasma treatment were proposed. First, it was noticed, that plasma treatment caused significant decrease of blood oozing from ulcerated colon tissues. Also, reduced progression rate of the disease may be related to "antioxidant" and "healing" effects of plasma produced nitric oxide.

Although presented results are very promising, many questions remain unanswered and further development of the model and accurate extensive study are both needed. However, this study clearly demonstrates feasibility that the cold plasma treatment may be safely applied not only for sterilization of living tissues, but also to achieve a medically relevant therapeutic effect(s), which opens new possibilities of cold plasma applications in the field of medicine.

CHAPTER 11. OVERVIEW OF THE MECHANISMS OF PLASMA INTERACTION WITH LIVING OBJECTS

It is shown in previous chapters that cold atmospheric pressure plasmas can have not only physical (e.g. burning the tissue), but medically relevant therapeutic effects — plasmas can trigger a complex sequence of biological responses in tissues and cells. To move ahead in further development of actual commercial tools that will enter the hospital, and in finding novel and perhaps even unexpected uses of these plasmas an understanding of mechanisms of interaction of non-equilibrium gas discharges with living organisms, tissues, and cells becomes essential. The goal of this chapter is to propose an initial model of such mechanisms.

Clearly, the interaction mechanisms depend on the way the plasma is generated, the way it is delivered, and the organism it is applied to; e.g. radiofrequency discharge in helium will likely have somewhat different mechanisms of interaction than afterglow from a nitrogen arc [9,42]. It is shown that not only reactive species generated in plasma are responsible for achieving a desired effect but also the charged species (electrons and ions) are. Below, an attempt to classify different types of species created in plasma and to assess their importance in achieving bacterial inactivation and other biological effects is taken.

The mechanism of interaction of plasma with living systems is complex owing partly to the complexity of plasma and mainly to the overwhelming complexity of biology. In our current understanding, we see three distinct paradigms for plasma interaction 1) with bacteria, 2) with mammalian cells, and 3) with tissues. In all three cases, mechanisms may and often prove to be significantly different. Further complexity is added by

presence of liquid or physisorbed water which is always present in our treatment. Regardless of the overall complexity, below we proposed a general scheme of interaction of direct discharges with biological systems.

A general schematic summarizing the plasma-cell interactions is shown on Figure 95. Here a direct cold plasma discharge, a Floating Electrode Dielectric Barrier Discharge, is considered as an example of direct cold plasma discharge. We show that charges produced in plasma and coming in direct contact with the treatment target play a key role in the biological mechanisms through initiation and catalysis of peroxidation processes. Primary target of the direct plasma treatment is the cell membrane, the phospholipid (eukaryotes) or polysaccharide (prokaryotes) layer where we observe all initial effects. Past the membrane, plasma-related mechanisms cease and biochemistry takes over. We show activation of complex biochemical pathways following plasma treatment, e.g. formation of malondialdehyde (MDA) which participates in formation of DNA adducts. MDA is a good example as it is also one of the examples of *selectivity* of plasma treatment as these DNA adducts are easily repaired by mammalian cells but not by bacteria. Other examples of selectivity of plasma treatment include selective development of apoptosis in cancer cells, difference in cellular metabolism for eukaryotes and prokaryotes, etc.
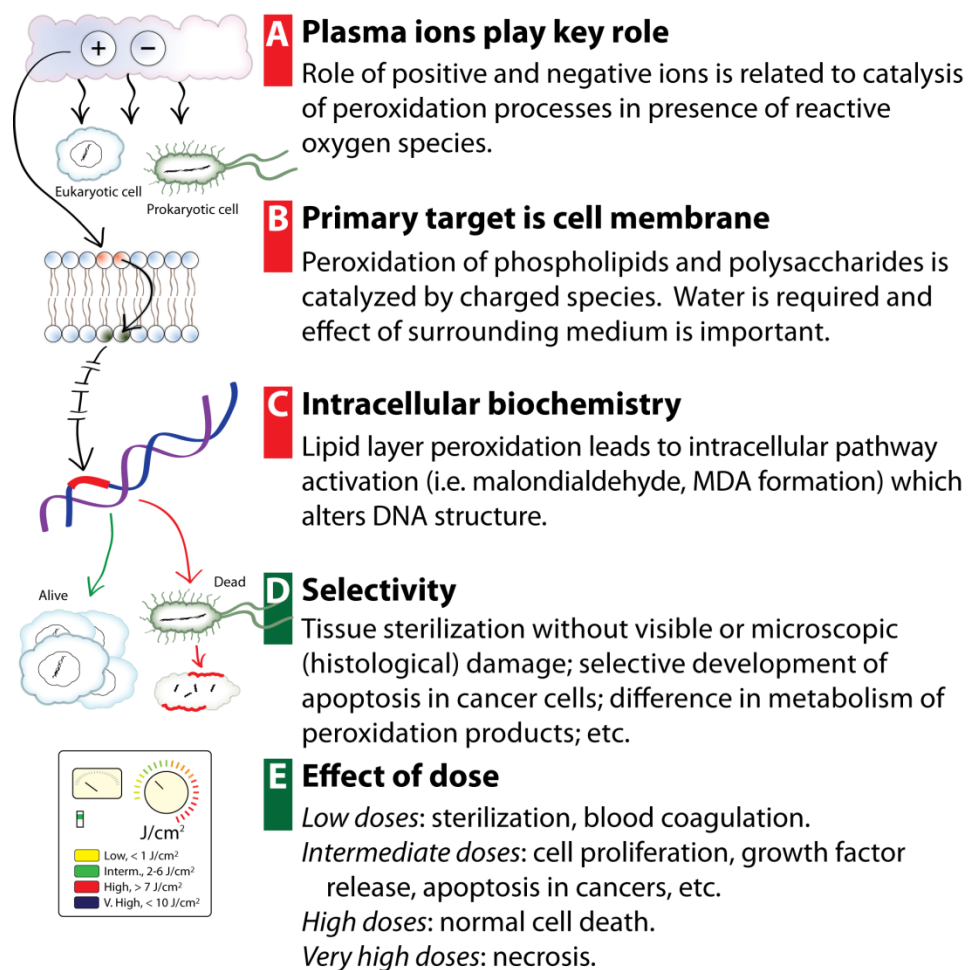
Figure 95 Summary of key findings on plasma interaction with biological organisms.

The key factors will now be examined in detail.

A. Plasma ions play key role

We show that plasma that comes in direct contact with a biological organism achieves the desired effect orders of magnitude faster than the same dose of indirect application where plasma is separated from treatment target even by a fraction of a millimeter. We show that this effect can be primarily attributed to charged species in plasma. Thus, the key role in plasma-cell interaction is played by ions, specifically:

- both positive and negative ions have relatively the same effect;
- effect of charged species is *chemical* and not related to such physical phenomena as sheer stress, ion bombardment damage, or thermal effects;
- ions *catalyze* peroxidation processes both inside and outside of the biological organism which explains why they are able to have greater effect than neutral active species;
- presence of *oxygen is necessary* and reactive oxygen species play a crucial intermediate role.

B. Primary target is cell membrane

Careful investigation of the target of these charges reveals that most processes occur on the cell membrane, e.g. the phospholipid bilayer of a mammalian cell or the polysaccharide membrane of bacterial cell. Key processes occurring on the membrane are:

- peroxidation of lipids and polysaccharides catalyzed by charges;
- effect is chemical and highly dependent on amount of water:
  - o dry organism — low effect,
  - o "moist" organism (minute amount of non-liquid water) — highest effect,
  - o and "wet" organism (suspended in liquid) — diluted effect;
- effect is strongly dependent on chemical composition of the medium surrounding the cells: complete inhibition or control over the plasma effects is possible, e.g. with addition of antioxidants to the media or intracellularly.

C. Intracellular biochemistry

The above mechanisms are related closer to plasma than to biology as they are biochemically controlled by plasma-generated species. However, there are biological consequences of plasma treatment where plasma initiates, catalyzes, or helps sustain a complex biological response, e.g.:

- compromised *membrane structure* (e.g. peroxidation), or change in *membrane-bound proteins* and/or enzymes (e.g. ion channel proteins) leads to complex cell responses and may affect many cells as the affected cell signal others;

- plasma treatment may *activate intracellular signaling pathways* (e.g. turn on secondary messenger systems to amplify and transport plasma effect);

- initiation of subtle *secondary effects*, like formation of malondialdehyde (MDA) which participated in DNA damage following lipid peroxidation, a process that is easily repaired by mammalian cells but not by bacteria.

D. Selectivity

Plasma effects can be quite selective, meaning tunable between damage to pathogenic organisms without damage to the host, or activation of different pathways in different organisms. Selectivity discussed in this thesis can be summarized to:

- sterilization of living tissue is achieved at two orders of magnitude lower plasma doses than required for damage as confirmed both visually and by histological stains;

- bacteria are much smaller than mammalian cells and selectivity may be achieved simply though size/volume differences;

- biochemical differences in the organisms, e.g. polysaccharides are easier to peroxidize than lipids;

- difference in metabolic rates between, for example, cancer cells, normal cells, and bacteria may lead to difference in uptake rate of toxins generated by plasma;

- cell cycle differences: frequently replicating cancer cells and bacteria have exposed DNA compared to static mammalian cells which do not, and thus in cancers and bacteria it is easier to get to the unfolded DNA.

E. Effect of dose

The effects of dose and dose rate is quite important:

- low plasma doses (< 1 J/cm^2): inactivation/sterilization of bacteria, normal cell survival;
- intermediate doses (2-6 J/cm^2): repairable DNA damage, release of cell growth factors, increase in proliferation and migration, controlled development of apoptosis in cancers;
- higher doses (> 7 J/cm^2): normal cell death;
- very high doses (> 10 J/cm^2): cell necrosis.

This concludes the general overview of interaction of non-equilibrium discharges with tissues, mammalian cells, and bacteria.

CONCLUDING REMARKS

The main novel contributions of this thesis are:

- Development and characterization of a cold microsecond spark discharge which can be safely and effectively applied for biomedical applications;

- Experimental study of the physical and chemical mechanisms of plasma interaction with microorganisms – bacteria and spores. A hypothesis of such mechanisms is proposed;

- Experimental study of plasma production and delivery of reactive species into liquid media, tissues and cells;

- Development of an *in vitro* physicochemical model of tissue based on agar hydrogel phantom;

- Experimental study of plasma treatment toxicity of intact and wounded skin *in vivo*

- Demonstration of high efficiency of plasma blood coagulation, wound decontamination and acceleration of wound healing *in vivo*;

- Demonstration that cold plasma may be safely applied for treatment of gastroenterological diseases *in vivo*.

Mechanisms of plasma interaction with living tissues and cells can be quite complex, owing to the complexity of both the plasma and the tissue. Therefore the physicochemical mechanisms of these interactions proposed in this thesis should be further investigated from the biochemical and biological stand points. A careful analysis of plasma treatment effects on cells, tissues and organs is required. Nevertheless, this work clearly

demonstrates the very basic effects of plasma on biological objects, and their relations with plasma parameters.

REFERENCES

1   E. Stoffels, *et al.*, "*Plasma Needle: A Non-Destructive Atmospheric Plasma Source for Fine Surface Treatment of (Bio)Materials*," Plasma Sources Science and Technology 11 (4), 383-388 (2002).

2   M. Laroussi and X. Lu, "Room-temperature atmospheric pressure plasma plume for biomedical applications," Applied Physics Letters 87 (11) (2005).

3   G. Fridman, et al., "Blood coagulation and living tissue sterilization by floating-electrode dielectric barrier discharge in air," Plasma Chemistry and Plasma Processing 26 (4), 425-442 (2006).

4   G. Fridman, A.D. Brooks, M. Balasubramanian, A. Fridman, A. Gutsol, V.N. Vasilets, H. Ayan, and G. Friedman, , "*Comparison of Direct and Indirect Effects of Non-Thermal Atmospheric Pressure Plasma on Bacteria*," Plasma Processes and Polymers 4, 370-375 (2007).

5   G. Fridman, A. Shereshevsky, M. Jost, A. Brooks, A. Fridman, A. Gutsol, V. Vasilets, and G. Friedman, "*Floating Electrode Dielectric Barrier Discharge Plasma in Air Promoting Apoptotic Behavior in Melanoma Skin Cancer Cell Lines*," Plasma Chemistry and Plasma Processing 27 (2), 163-176 (2007).

6   M. Cooper, Y. Yang, D. Dobrynin, H. Ayan, A. Fridman, A. Gutsol, V. Vasilets, and G. Fridman, "Observations of Filament Behavior and Plasma Uniformity in Continuous and Pulsed Dielectric Barrier Discharges", in *Drexel University Ninth Annual Research Innovation Scholarship and Creativity (RISC) Day* (Philadelphia, USA, 2007).

7   S. Coulombe, V. Léveilleé, S. Yonson, and R. L. Leask, "Miniature atmospheric pressure glow discharge torch (APGD-t) for local biomedical applications," Pure Appl. Chem. 78 (6), 1147–1156 (2006).

8   J. F. Kolb, A.-A. H. Mohamed, R. O. Price, R. J. Swanson, A. Bowman, R. L. Chiavarini, M. Stacey, and K. H. Schoenbach, "Cold atmospheric pressure air plasma jet formedical applications," Appl. Phys. Lett. 92 (24), 241501-241501–241501-241503 (2008).

9   T Shimizu, B Steffes, R Pompl, F Jamitzky, W Bunk, K Ramrath, M Georgi, W Stolz, HU Schmidt, and T Urayama, "Characterization of Microwave Plasma Torch for Decontamination," Plasma Processes and Polymers 5 (6), 577-582 (2008).

10   A. Shashurin, M. Keidar, S. Bronnikov, R. A. Jurjus, and M. A. Stepp, "Living tissue under treatment of cold plasma atmospheric jet," Appl. Phys. Lett. 93 (18), 181501-181501–181501-181503 (2008).

11   H. J. Lee, C. H. Shon, Y. S. Kim, S. Kim, G. C. Kim, and M. G. Kong, "Degradation of adhesion molecules of G361 melanoma cells by a non-thermal atmospheric pressure microplasma," New J. Phys. 11, 115026 (115013 pp.) (2009).

12   S. Rupf, A. Lehmann, M. Hannig, B. Schäfer, A. Schubert, U. Feldmann, and A. Schindler, "Killing of adherent oral microbes by a non-thermal atmospheric plasma jet," J. Med. Microbiol. 59 (2), 206–212 (2010).

13   M. Kuchenbecker, N. Bibinov, A. Kaemling, D. Wandke, P. Awakowicz, and W. Viöl, "Characterization of DBD plasma source for biomedical applications," J. Phys. D, Appl. Phys. 42 (4), 045212 (045210 pp.) (2009).

14   E. Robert, E. Barbosa, S. Dozias, M. Vandamme, C. Cachoncinlle, R. Viladrosa, and J. M. Pouvesle, "Experimental study of a compact nanosecond plasma gun," Plasma Process. Polym. 6 (12), 795–802 (2009).

15   Ulrich Kogelschatz, "Dielectric-Barrier Discharges: Their History, Discharge Physics, and Industrial Applications," Plasma Chemistry and Plasma Processing 23 (1), 1-46 (2003).

16   H. E. Wagner, R. Brandenburg, K. V. Kozlov, A. Sonnenfeld, P. Michel, and J. F. Behnke, "The barrier discharge: basic properties and applications to surface treatment," Vacuum 71 (3), 417-436 (2003).

17   G. Fridman, A.B. Shekhter, V.N. Vasilets, G. Friedman, A. Gutsol, and A. Fridman, "Applied Plasma Medicine," Plasma Processes and Polymers 5 (6), 503-533 (2008).

18   Gregory Fridman, presented at the First International Conference on Plasma Medicine (ICPM-1), Corpus Christi, Texas, 2007 (unpublished).

19   G. Fridman, S. Kalghatgi, R. Sensenig, A. Shereshevsky, R. Stoddard, G. Friedman, A. Gutsol, V. Vasilets, A. Fridman, and A.D. Brooks, "Non-Equilibrium Dielectric Barrier Discharge Plasma Promoting Apoptotic Behavior in Melanoma Skin Cancer Cells", in *NATO Advanced Study Institute (ASI), Plasma Assisted Decontamination of Biological and Chemical Agents* (Çesme, Turkey, 2007).

20   S.M. Starikovskaia, Anikin N.B., Pancheshnyi S.V., Zatsepin D.V., and Starikovskii A.Yu., "Pulsed breakdown at high overvoltage: development, propagation and energy branching," Plasma Sources Sci. Technol. 10, 344 (2001).

21   B. Qi, Ren C., Wang D., Li SZ., Wang K., and Zhang Y., "Uniform glowlike plasma source assisted by preionization of spark in ambient air at atmospheric pressure," Applied Physics Letters 89, 131503 (2006).

22   J.I. Levatter and Lin S.-C., "Necessary conditions for the homogeneous formation of pulsed avalanche discharges at high gas pressures," J. Appl. Phys. 51 (1) (1980).

23   A. Fridman, Chirokov A., and Gutsol A., "Topical Review: Nonthermal atmospheric pressure discharges," J. Phys. D: Appl. Phys. 38, R1–R24 (2005).

24   U. Kogelschatz, "Applications of Microplasmas and Microreactor Technology," Contrib. Plasma Phys. 47 (1-2), 80-88 (2007).

25   D Staack H Ayan, G Fridman, A Gutsol, Y Mukhin, A Starikovskii, A Fridman and G Friedman, "Application of nanosecond-pulsed dielectric barrier discharge for biomedical treatment of topographically non-uniform surfaces," J. Phys. D: Appl. Phys. 42, 125202 (2009).

26   H. Ayan, G. Fridman, D. Staack, A. Gutsol, V. Vasilets, A. Fridman, and G. Friedman, "Heating Effect of Dielectric Barrier Discharges for Direct Medical Treatment," IEEE Transactions on Plasma Science 37 (1), 113-120 (2009).

27   H. Ayan, G. Fridman, A. F. Gutsol, V. Vasilets, A. Fridman, and G. Friedman, "Nanosecond-Pulsed Uniform Dielectric-Barrier Discharge," Plasma Science, IEEE Transactions on 36 (2), 504-508 (2008).

28   Z Cao, JL Walsh, and MG Kong, "Atmospheric plasma jet array in parallel electric and gas flow fields for three-dimensional surface treatment," Applied Physics Letters 94, 021501 (2009).

29   K. D. Weltmann, E. Kindel, R. Brandenburg, C. Meyer, R. Bussiahn, C. Wilke, and T. von Woedtke, "Atmospheric Pressure Plasma Jet for Medical Therapy: Plasma Parameters and Risk Estimation," Contributions to Plasma Physics 49 (9), 631-640 (2009).

30   C. Cheng, P. Liu, L. Xu, L. Zhang, R. Zhan, and W. Zhang, "Development of a new atmospheric pressure cold plasma jet generator and application in sterilization," Chinese Physics 15 (7), 1544 (2006).

31   J. Choi, K. Matsuo, H. Yoshida, T. Namihira, S. Katsuki, and H. Akiyama, "Double-Layered Atmospheric Pressure Plasma Jet," Japanese Journal of Applied Physics 48 (8) (2009).

32   Q. Xiong, X. Lu, Y. Xian, J. Liu, C. Zou, Z. Xiong, W. Gong, K. Chen, X. Pei, F. Zou, J. Hu, Z. Jiang, and Y. Pan, "Experimental investigations on the propagation of the plasma jet in the open air," Journal of Applied Physics 107 (7) (2010).

33   N. Jiang and Z. X. Cao, "Experimental studies on an atmospheric pressure He plasma jet," Acta Physica Sinica 59 (5), 3324-3330 (2010).

34   J. L. Walsh, F. Iza, N. B. Janson, V. J. Law, and M. G. Kong, "Three distinct modes in a cold atmospheric pressure plasma jet," Journal of Physics D-Applied Physics 43 (7) (2010).

35   Q. Y. Nie, Z. Cao, C. S. Ren, D. Z. Wang, and M. G. Kong, "A two-dimensional cold atmospheric plasma jet array for uniform treatment of large-area surfaces for plasma medicine," New Journal of Physics 11 (2009).

36   E. Stoffels, "Biomedical applications of electric gas discharge," High Temperature Material Processes 5 (2), 191-202 (2000).

37   Eva Stoffels, presented at the First International Conference on Plasma Medicine (ICPM-1), Corpus Christi, Texas, 2007 (unpublished).

38   Yukinori Sakiyama Eva Stoffels, and David B. Graves, "Cold Atmospheric Plasma: Charged Species and Their Interactions With Cells and Tissues," IEEE TPS 36 (4) (AUGUST 2008).

39   E. A. Sosnin, E. Stoffels, M. V. Erofeev, I. E. Kieft, and S. E. Kunts, "The effects of UV irradiation and gas plasma treatment on living mammalian cells and bacteria: A comparative approach," Plasma Science, IEEE Transactions on 32 (4), 1544-1550 (2004).

40   E. Stoffels, R. E. J. Sladek, and I. E. Kieft, "Gas Plasma Effects on Living Cells," Physica Scripta 107, 79 (2004).

41   E. Stoffels, "Gas plasmas in biology and medicine," Journal of Physics D: Applied Physics 39 (16) (2006).

42   E. Stoffels, I. Kieft, R. Sladek, L. Bedem, E. Laan, and M. Steinbuch, "Plasma needle for in vivo medical treatment: recent developments and perspectives," Plasma Sources Science and Technology 15 (4), S169 (2006).

43   R. E. J. Sladek, E. Stoffels, R. Walraven, P. J. A. Tielbeek, and R. A. Koolhoven, "Plasma treatment of dental cavities: A feasibility study," Plasma Science, IEEE Transactions on 32 (4), 1540-1543 (2004).

44   Y. Sakiyama and D. B. Graves, "Finite element analysis of an atmospheric pressure RF-excited plasma needle," J. Phys. D, Appl. Phys. 39 (16), 3451–3456 (2006).

45   E Stoffels, Y Aranda Gonzalvo, T D Whitmore, D L Seymour, and J A Rees, "A plasma needle generates nitric oxide," Plasma Sources Sci. Technol. 15, 501–506 (2006).

46   Klaus Dieter Weltmann, Eckhard Kindel, Thomas von Woedtke, Marcel Hähnel, Manfred Stieber, and Ronny Brandenburg, "Atmospheric-pressure plasma sources: Prospective tools for plasma medicine," Pure Appl. Chem. 82 (6), 1223–1237 (2010).

47   M. Moisan, J. Barbeau, S. Moreau, J. Pelletier, M. Tabrizian, and L. 'H. Yahia, "Low-temperature sterilization using gas plasmas: A review of the experiments and an analysis of the inactivation mechanisms," Int. J. Pharm. 226 (1/2), 1–21 (2001).

48   M. Laroussi, "Nonthermal decontamination of biological media by atmospheric-pressure plasmas: Review, analysis, and prospects," IEEE Trans. Plasma Sci. 30 (4), 1409–1415 (2002).

49   M. Laroussi and Leipold F., "Evaluation of the roles of reactive species, heat, and UV radiation in the inactivation of bacterial cells by air plasmas at atmospheric pressure," International Journal of Mass Spectrometry 233 (1-3), 81-86 (2004).

50   MJ Gallagher, A Gutsol, A Fridman, G Friedman, and A Dolgopolsky, presented at the International Conference on Plasma Science, Baltimore, Maryland, 2004 (unpublished).

51   A Gutsol, N Vaze, K Arjunan, M Gallagher, Y Yang, J Zhu, V Vasilets, and A Fridman, presented at the NATO Advanced Study Institute (ASI), Plasma Assisted Decontamination of Biological and Chemical Agents, Çesme, Turkey, 2007 (unpublished).

52   M. J. Gallagher, N. Vaze, S. Gangoli, V. N. Vasilets, A. F. Gutsol, T. N. Milovanova, S. Anandan, D. M. Murasko, and A. A. Fridman, "Rapid Inactivation of Airborne Bacteria Using Atmospheric Pressure Dielectric Barrier Grating Discharge," Plasma Science, IEEE Transactions on 35 (5), 1501-1510 (2007).

53   R. Pompl, T. Shimizu, H.U. Schmidt, W. Bunk, F. Jamitzky, B. Steffes, K. Ramrath, B. Peters, W. Stolz, T. Urayama, R. Ramasamy, S. Fujii, and G.E. Morfill, presented at the 6th Int. Conf. Reactive Plasmas, Matsushima, Japan, 2006 (unpublished).

54   T. Shimizu, B. Steffes, R. Pompl, F. Jamitzky, W. Bunk, K. Ramrath, B. Peters, W. Stolz, H.U. Schmidt, T. Urayama, K. Fujioka, R. Ramasamy, S. Fujii, and G.E. Morfill, presented at the 6th Int. Conf. Reactive Plasmas, Matsushima, Japan, 2006 (unpublished).

55   E. Martines, M. Zuin, R. Cavazzana, E. Gazza, G. Serianni, S. Spagnolo, M. Spolaore, A. Leonardi, V. Deligianni, P. Brun, M. Aragona, and I. Castagliuolo, "A novel plasma source for sterilization of living tissues," New Journal of Physics 11 (2009).

56   S. Lerouge, M. R. Wertheimer, and L. H. Yahia, "Plasma Sterilization: A Review of Parameters, Mechanisms, and Limitations," Plasmas and Polymers 6 (3), 175-188 (2001).

57   R. Ben Gadri, J. R. Roth, T. C. Montie, K. Kelly-Wintenberg, P. P. Y. Tsai, D. J. Helfritch, P. Feldman, D. M. Sherman, F. Karakaya, and Z. Y. Chen, "Sterilization and plasma processing of room temperature surfaces with a one atmosphere uniform glow discharge plasma (OAUGDP)," Surface & Coatings Technology 131 (1-3), 528-542 (2000).

58   Masateru Nishioka Mitsuo Yamamoto, Masayoshi Sadakata, "Sterilization by H_2O_2 droplets under corona discharge," Journal of Electrostatics 56, 173–187 (2002).

59   M Moisan M K Boudam, B Saoudi, C Popovici, N Gherardi and F Massines, "Bacterial spore inactivation by atmospheric-pressure plasmas in the presence or absence of UV photons as obtained with the same gas mixture," J. Phys. D: Appl. Phys. 39, 3494–3507 (2006).

60   Gregory Fridman Danil Dobrynin, Yurii V. Mukhin, Meghan A. Wynosky-Dolfi, and Richard F. Rest Judy Rieger, Alexander F. Gutsol, and Alexander Fridman, "Cold Plasma Inactivation of Bacillus cereus and Bacillus anthracis (Anthrax) Spores," IEEE TPS 38 (8), 1878-1884 (2010).

61   Olga Tarasenko Spencer P Kuo, Said Nourkbash, Assya Bakhtina and Kalle Levon, "Plasma effects on bacterial spores in a wet environment," New Journal of Physics 41 (8) (2006).

62   M. Laroussi, J. P. Richardson, and F. C. Dobbs, "Effects of nonequilibrium atmospheric pressure plasmas on the heterotrophic pathways of bacteria and on their cell morphology," J. Appl. Phys. 81 (4), 773–774 (2002).

63   G. Isbary, G. Morfill, H. U. Schmidt, M. Georgi, K. Ramrath, J. Heinlin, S. Karrer, M. Landthaler, T. Shimizu, B. Steffes, W. Bunk, R. Monetti, J. L. Zimmermann, R. Pompl, and W. Stolz, "A first prospective randomized controlled trial to decrease bacterial load using cold atmospheric argon plasma on chronic wounds in patients," British Journal of Dermatology 163 (1), 78-82 (2010).

64   M. K. Boudam, M. Moisan, B. Saoudi, C. Popovici, N. Gherardi, and F. Massines, "Bacterial spore inactivation by atmospheric-pressure plasmas in the presence or absence of UV photons as obtained with the same gas mixture," Journal of Physics D: Applied Physics 39 (16), 3494 (2006).

65   D. Dobrynin S. Kalghatgi, G. Fridman, M. Cooper, G. Nagaraj, L. Peddinghaus, M. Balasubramanian, K. Barbee, A. Brooks, V. Vasilets, A. Gutsol, A. Fridman, and G. Friedman, presented at the *NATO Advanced Study Institute on Plasma Assisted Decontamination of Biological and Chemical Agents*, *Cesme-Izmir, Turkey, 2007* (unpublished).

66   G. Lloyd, G. Friedman, S. Jafri, G. Schultz, A. Fridman, and K. Harding, "Gas Plasma: Medical Uses and Developments in Wound Care," Plasma Processes and Polymers 7 (3-4), 194-211 (2010).

67   V. N. Vasilets, A. Gutsol, A. B. Shekhter, and A. Fridman, "Plasma medicine," High Energy Chemistry 43 (3), 229-233 (2009).

68   I.E. Kieft, M. Kurdi and E. Stoffels "*Reattachment and Apoptosis after Plasma-Needle Treatment of Cultured Cells* " Plasma Science, IEEE Transactions on 34 (4), 1331-1336 (2006).

69   E. Stoffels, "*Cold atmospheric plasma for wound healing: in vitro assessment.*", in *First International Conference on Plasma Medicine (ICPM-1)* (Corpus Christi, Texas, USA, 2007).

70   S. Kalghatgi, D. Dobrynin, G. Fridman, M. Cooper, G. Nagaraj, L. Peddinghaus, M. Balasubramanian, K. Barbee, A. Brooks, V. Vasilets, A. Gutsol, A. Fridman, and G. Friedman, presented at the NATO Advanced Study Institute on Plasma Assisted Decontamination of Biological and Chemical Agents, Cesme-Izmir, Turkey, 2007 (unpublished).

71   S. Kalghatgi, C. Kelly, E. Cerchar, R. Sensing, K. Priya-Arjunan, G. Fridman, A. Fridman, G. Friedman, and J. Clifford-Azizkhan, "Non-Thermal Plasma Induces DNA Damage Through the Generation of Long-lived Reactive Oxygen Species", in *Drexel University College of Medicine Discovery Day* (Philadelphia, USA, 2008).

72   S Kalghatgi, C Kelly, E Cerchar, R Sensing, K Priya-Arjunan, G Fridman, A Fridman, G Friedman, and J Clifford-Azizkhan, presented at the Drexel University College of Medicine Discovery Day, Philadelphia, USA, 2008 (unpublished).

73   D Gerald, E. Berra, Y. Frapart, D. Chan, A. Giaccia, D. Mansuy, J. Pouysségur, M. Yaniv, and F. Mechta-Grigoriou, "JunD reduces tumor angiogenesis by protecting cells from oxidative stress," Cell 118 (6), 781-794 (2004).

74   BL Bader, H Rayburn, D Crowley, and RO Hynes, "Extensive vasculogenesis, angiogenesis, and organogenesis precede lethality in mice lacking all alpha v integrins," Cell 95 (4), 507-519 (1998).

75   NS Brown, A Jones, C Fujiyama, AL Harris, and R Bicknell, "Thymidine Phosphorylase Induces Carcinoma Cell Oxidative Stress and Promotes Secretion of Angiogenic Factors 1", (AACR, 2000), Vol. 60, pp. 6298-6302.

76   S Kalghatgi, G Fridman, A Fridman, G Friedman, and A Morss-Clyne, presented at the 30th Annual International Conference of the IEEE Engineering in Medicine and Biology Society (IEEE EMBS), 2008 (unpublished).

77   S Kalghatgi, G Fridman, A Fridman, G Friedman, and A Morss-Clyne, presented at the Tenth Annual Research Day at Drexel University, Philadelphia, USA, 2008 (unpublished).

78   G. Fridman, A. B. Shekhter, V. N. Vasilets, G. Friedman, A. Gutsol, and A. Fridman, "Applied Plasma Medicine," Plasma Processes and Polymers 5 (6), 503-533 (2008).

79   G. Fridman, A.D. Brooks, M. Balasubramanian, A. Fridman, A. Gutsol, V.N. Vasilets, H. Ayan, and G. Friedman, "Comparison of Direct and Indirect Effects of Non-Thermal Atmospheric Pressure Plasma on Bacteria," Plasma Processes and Polymers 4, 370-375 (2007).

80   Zenker M Raiser J, "Argon plasma coagulation for open surgical and endoscopic applications: state of the art," J Phys D: Appl Phys 39 (16), 3520 (2006).

81   S.U. Kalghatgi, G. Fridman, M. Cooper, G. Nagaraj, M. Peddinghaus, M. Balasubramanian, V.N. Vasilets, A. Gutsol, A. Fridman, and G. Friedman, "*Mechanism of Blood Coagulation by Nonthermal Atmospheric Pressure Dielectric Barrier Discharge Plasma*," IEEE Transactions on Plasma Science 35 (5, Part 2), 1559-1566 (2007).

82   V. Gostev, presented at the NATO Advanced Study Institute (ASI): Plasma Assisted Decontamination of Biological and Chemical Agents, Cesme, Turkey, 2007 (unpublished).

83   F.A. and V.A. Gostev Misyn, ""Cold" plasma application for curing of eyelid phlegmon " Diagnostics and treatment of infectious diseases, Petrozavodsk, Russia (2000).

84   F.A. Misyn and V.A. Gostev, presented at the Diagnostics and treatment of infectious diseases, Petrozavodsk, Russia, 2000 (unpublished).

85   F.A. Misyn, E.V. Besedin, A.M. Obraztsova, and V.A. Gostev, "Experimental curing of bacterial ulcerous keratitis with "cold" plasma " Diagnostics and treatment of infectious diseases, Petrozavodsk, Russia (2000).

86   Besedin EV Misyn FA, Komkova OP, Gostev VA, "Experimental Investigation of Bactericidal Influence of ''Cold'' Plasma and Its Interaction with Cornea", in *Diagnostics and treatment of infectious diseases* (Petrozavodsk, Russia, 2000).

87   Besedin E Misyn F, Gostev V, Komkova O, "Experimental Studying of Bactericidal Action of Cold Plasma", in *Diagnostics and treatment of infectious diseases* (Petrozavodsk, Russia, 2000).

88   V. Gostev and D. Dobrynin, presented at the 3rd International Workshop on Microplasmas (IWM-2006), Greifswald, Germany, 2006 (unpublished).

89   V. Gostev, "Cold Plasma in Biological Investigations", in *NATO Advanced Study Institute (ASI): Plasma Assisted Decontamination of Biological and Chemical Agents* (Çeşme, Turkey, 2007).

90   Eduard M. Bazelyan and Yuri P. Raizer, *Spark Discharge*. (CRC-Press, 1998).

91   V. N. Vasilets, L. A. Tikchomirov, and A. N. Ponomarev, "The study of continues HF low pressure discharge plasma action on the polyethylene surface," High Energy Chemistry 15 (N1), 77-81 (1981).

92   Y. P. Baydarovtsev, V. N. Vasilets, and A. N. Ponomarev, "The influence of gas nature on the rate of radical accumulation in teflon during low pressure glow discharge treatment," Russian Journal of Chemical Physics 4 (N1), 89-96 (1985).

93   M. Cooper, Y. Yang, G. Fridman, H. Ayan, V. N. Vasilets, A. Gutsol, G. Friedman, and A. Fridman, presented at the NATO Advanced Study Institute on Plasma Assisted Decontamination of Biological and Chemical Agents, Cesme-Izmir, Turkey, 2007 (unpublished).

94   G. Fridman, M. Peddinghaus, H. Ayan, A. Fridman, M. Balasubramanian, A. Gutsol, A. Brooks, and G. Friedman, "Blood coagulation and living tissue sterilization by floating-electrode dielectric barrier discharge in air," Plasma Chemistry and Plasma Processing 26 (4), 425-442 (2006).

95   Sabrina Pesnel, Marc Vandamme, Stéphanie Lerondel, Alain LePape, Eric Robert, Sébastien Dozias, Emerson Barbosa, and Jean-Michel Pouvesle, "Antitumor effect of plasma exposure: preliminary results in a mouse model", in *2nd International Conference on Plasma Medicine (ICPM-2)* (San Antonio, Texas, 2009).

96   K. Schoenbach, R. Barker, and S. Liu, "Special issue on nonthermal medical/biological treatments using electromagnetic fields and ionized gases," Plasma Science, IEEE Transactions on 28 (1), 2-5 (2000).

97   Y. A. Kotov and S. Y. Sokovnin, "Overview of the application of nanosecond electron beams for radiochemical sterilization," Plasma Science, IEEE Transactions on 28 (1), 133-136 (2000).

98   J. F. Kolb, M. G. Kong, and P. F. Blackmore, "Special Issue on Nonthermal Medical/Biological Applications Using Ionized Gases and Electromagnetic Fields," Plasma Science, IEEE Transactions on 34 (4), 1250-1252 (2006).

99   A. B. Shekhter, R. K. Kabisov, A. V. Pekshev, N. P. Kozlov, and Y. L. Perov, "Experimental and clinical validation of plasmadynamic therapy of wounds with nitric oxide," Bulletin of Experimental Biology and Medicine 126 (2), 829-834 (1998).

100   A. B. Shekhter, V. A. Serezhenkov, T. G. Rudenko, A. V. Pekshev, and A. F. Vanin, "Beneficial effect of gaseous nitric oxide on the healing of skin wounds," Nitric Oxide-Biology and Chemistry 12 (4), 210-219 (2005).

101   G Fridman D Dobrynin, G Friedman and A Fridman, "Physical and biological mechanisms of direct plasma interaction with living tissue " New J. Phys. 11 (2009).

102   and Leipold F. Laroussi M., "Evaluation of the roles of reactive species, heat, and UV radiation in the inactivation of bacterial cells by air plasmas at atmospheric pressure," International Journal of Mass Spectrometry 233 (1-3), 81-86 (2004).

103   M. Moisan, J. Barbeau, M. C. Crevier, J. Pelletier, N. Philip, and B. Saoudi, "Plasma sterilization. Methods mechanisms," Pure and Applied Chemistry 74 (3), 349-358 (2002).

104   A. N. Ponomarev, A. I. Maksimov, V. N. Vasilets, and V. M. Menagarishvily, "Photo-oxidation of polyethylene and polyvinyl chloride in the process of simultaneous action of ultraviolet and active oxygen," High Energy Chemistry 23 (3), 231-232 (1989).

105   JA Imlay, SM Chin, and S Linn, "Toxic DNA damage by hydrogen peroxide through the Fenton reaction in vivo and in vitro," Science 240 (4852), 640-642 (1988).

106   Ernst S. Henle and Stuart Linn, "Formation, Prevention, and Repair of DNA Damage by Iron/Hydrogen Peroxide," J. Biol. Chem. 272 (31), 19095-19098 (1997).

107   CG Faddis, (1993).

108   T Ohmi, T Isagawa, T Imaoka, and I Sugiyama, "Ozone decomposition in ultrapure water and continuous ozone sterilization for a semiconductor ultrapure water system," Journal of the Electrochemical Society 139, 3336 (1992).

109   WT Broadwater, RC Hoehn, and PH King, "Sensitivity of three selected bacterial species to ozone," Applied and Environmental Microbiology 26 (3), 391-393 (1973).

110   Arthur Fontijn, Alberto J. Sabadell, and Richard J. Ronco, "Homogeneous chemiluminescent measurement of nitric oxide with ozone. Implications for continuous selective monitoring of gaseous air pollutants," Analytical Chemistry 42 (6), 575-579 (1970).

111   MAA Clyne, BA Thrush, and RP Wayne, "Kinetics of the chemiluminescent reaction between nitric oxide and ozone," Transactions of the Faraday Society 60, 359-370 (1964).

112   PN Clough and BA Thrush, "Mechanism of chemiluminescent reaction between nitric oxide and ozone," Transactions of the Faraday Society 63, 915-925 (1967).

113   DW Crabb, M Matsumoto, D Chang, and M You, "Overview of the role of alcohol dehydrogenase and aldehyde dehydrogenase and their variants in the genesis of alcohol-related pathology," Proceedings of the Nutrition Society 63 (01), 49-63 (2007).

114   DT Richens, *The chemistry of aqua ions: synthesis, structure and reactivity: a tour through the periodic table of the elements*. (Wiley Chichester, 1997).

115   BS Bal, WE Childers, and HW Pinnick, "Oxidation of α, ß-un saturated aldehydes," Tetrahedron 37 (11), 2091-2096 (1981).

116   Francis A. Drobniewski, "*Bacillus cereus* and Related Species," Clinical Microbiology Reviews 6 (4), 324-338 (October 1993).

117   Corbett W. and Grindem C. Hunter L., "Anthrax," *J. Am. Vet. Med. Assoc* 8, 1028–1031 (1989).

118   Matthew Meselson Terry C. Dixon, Jeanne Guilemin, and Philip C. Hanna, "Anthrax," The New England Journal of Medicine 341 (11), 12 (1999).

119   Agron PG Radnedge L, Hill KK, Jackson PJ, Ticknor LO, Keim P and Andersen GL, "Genome differences that distinguish *Bacillus anthracis* from *Bacillus cereus* and *Bacillus thuringiensis*," Appl. Environ. Microbiol 69 (2003).

120   Simon J. Foster Abdelmadjid Atrih, "Bacterial endospores the ultimate survivors," International Dairy Journal 12 217-223 (2002).

121   P. J. Setlow, "Mechanisms for the prevention of damage to DNA in spores of Bacillus species " Annu. Rev.Microbiol. 49 (1995).

122   P. J. Setlow, "Mechanisms which contribute to the long-term survival of spores of Bacillus species " Appl. Bacteriol. 176 (1994).

123   Mark E. Beatty Ellen A. Spotts Whitney, Thomas H. Taylor, Jr., Robbin Weyant, Jeremy Sobel, Matthew J. Arduino, and David A. Ashford, "Inactivation of Bacillus anthracis Spores," Emerging Infectious Diseases 9 (6), 623-627 (June 2003).

124   Mary Cooper James A. Higgins, Linda Schroeder-Tucker, Scott Black, David Miller, Jeffrey S. Karns, Erlynn Manthey, Roger Breeze, and Michael L. Perdue, "A Field Investigation of Bacillus anthracis Contamination of U.S. Department of Agriculture and Other Washington, D.C., Buildings during the Anthrax Attack of October 2001," Applied and Environmental Microbiology 69 (1), 593-599 (January 2003).

125   et al. Hury S., "A parametric study of the destruction efficiency of Bacillus spores in low pressure oxygen-based plasmas " Letters in Apll. Microbiology 26 (1998).

126   T. Akan A. Morris, G. B. McCombs, W. L. Hynes, M. Laroussi, presented at the 28th ICPIG, Prague, Czech Republic, July 15-20, 2007 (unpublished).

127   Joseph G. Birmingham, "Mechanisms of Bacterial Spore Deactivation Using Ambient Pressure Nonthermal Discharges," IEEE TPS 32 (4), 1526-1531 (August 2004).

128   Ari D. Brooks Gregory Fridman, Manjula Balasubramanian, Alexander Fridman, Alexander Gutsol, Victor N. Vasilets, Halim Ayan, Gary Friedman, "Comparison of Direct and Indirect Effects of Non-Thermal Atmospheric-Pressure Plasma on Bacteria," Plasma Process. Polym. 4, 370–375 (2007).

129   C. B. Thorne, "Transduction in *Bacillus cereus* and *Bacillus anthracis*," Bacteriol Rev 32, 358-361 (1968).

130   L. S. Tisa, T. Koshikawa, and P. Gerhardt. , "Wet and dry bacterial spore densities determined by buoyant sedimentation," Appl Environ Microbiol 43, 1307-1310 (1982).

131   Anne Meeusen; Arthur I. Aronson Ernest R. Blatchley, and Lindsay Brewster, "Inactivation of Bacillus Spores by Ultraviolet or Gamma Radiation," Journal of Environmental Engineering 131 (9) (September 1, 2005).

132   E. Melly, Cowan, A.E., and Setlow, P. , "Studies on the mechanism of killing of Bacillus subtilis spores by hydrogen peroxide," Journal of Applied Microbiology 93, 316-325 (2002).

133   A. Yanguas-Gil, Hueso, J. L., Cotrino, J., Caballero, A., and González-Elipe, A. R., "Reforming of ethanol in a microwave surface-wave plasma discharge," APPLIED PHYSICS LETTERS 85 (18) (2004).

134   M. A. Almubarak, and Wood, A., "Chemical Action of Glow Discharge Electrolysis on Ethanol in Aqueous Solution," *J. Electrochem. Soc.:* ELECTROCHEMICAL SCIENCE AND TECHNOLOGY 124 (9) (1977).

135   Anne Moir, "Bacterial spore germination and protein mobility," TRENDS in Microbiology 11 (10) (October 2003).

136   Peter Setlow, "Spore germination," Current Opinion in Microbiology (6), 550-556 (2003).

137   Gregory Fridman, Gary Friedman, Alexander Gutsol, Anatoly B. Shekhter, Victor N. Vasilets, and Alexander Fridman, "Applied Plasma Medicine," Plasma Processes and Polymers 5 (6), 503-533 (2008).

138   K. D. Weltmann, E. Kindel, T. von Woedtke, M. Hahnel, M. Stieber, and R. Brandenburg, "Atmospheric-pressure plasma sources: Prospective tools for plasma medicine," Pure and Applied Chemistry 82 (6), 1223-1237 (2010).

139   M. Vandamme, E. Robert, S. Pesnel, E. Barbosa, S. Dozias, J. Sobilo, S. Lerondel, A. Le Pape, and J. M. Pouvesle, "Antitumor Effect of Plasma Treatment on U87 Glioma Xenografts: Preliminary Results," Plasma Processes and Polymers 7 (3-4), 264-273 (2010).

140   MG Kong, G Kroesen, G Morfill, T Nosenko, T Shimizu, J Dijk, and JL Zimmermann, "Plasma medicine: an introductory review," New Journal of Physics 11, 115012 (2009).

141   G. E. Morfill, T. Shimizu, B. Steffes, and H. U. Schmidt, "Nosocomial infections-a new approach towards preventive medicine using plasmas," New Journal of Physics 11 (2009).

142   Danil Dobrynin, Gregory Fridman, Gary Friedman, and Alexander Fridman, "Physical and biological mechanisms of direct plasma interaction with living tissue," New Journal of Physics (11), 115020 (2009).

143   S Kalghatgi, G Friedman, A Fridman, and AM Clyne, "Endothelial Cell Proliferation is Enhanced by Low Dose Non-Thermal Plasma Through Fibroblast Growth Factor-2 Release," Annals of Biomedical Engineering 38 (3), 748-757 (2010).

144   Barbul A. Witte M. B., "Role of nitric oxide in wound repair," Am. J. Surg. 183, 406–412 (2002).

145   Ridnour L A Isenberg J S, Espey M G, Wink D A and Roberts D D, "Nitric oxide in wound healing," Microsurgery 25, 442-451 (2005).

146   Tantry U Schaffer M R, Efron P A, Ahrendt G M, Thornton F J and Barbul A, "Diabetes-impaired healing and reduced wound nitric oxide synthesis: a possible pathophysiologic correlation," Surgery 121, 513–519 (1997).

147   Kiyama T and Barbul A Witte M B, "Nitric oxide enhances experimental wound healing in diabetes," Br. J. Surg 89, 1594–1601 (2002).

148   Lee Y L and Ping I, "Controlled nitric oxide delivery platform based on s-nitrosothiol conjugated interpolymer complexes for diabetic wound healing," Molecular Pharmaceutics 7 (1), 254–266 (2009).

149   Ignarro L J, "Biosynthesis and metabolism of endothelium-derived nitric oxide," Annu. ReV. Pharmacol. Toxicol. 30, 535–560 (1990).

150   Wang P G and Cai T B (eds), *Nitric Oxide Donors* (Wiley-VCH, Weinheim, 2005).

151   Shekhter A B, Kabisov R K, Pekshev A V, Kozlov N P, and Perov Y L, "Experimental and clinical validation of plasmadynamic therapy of wounds with nitric oxide," Bulletin of Experimental Biology and Medicine 126 (2), 829-834 (1998).

152   Namihira T, Sakai S, Matsuda M, Wang D, Kiyan T, Akiyama H, Okamoto K, and Toda K, "Temperature and Nitric Oxide Generation in a Pulsed Arc Discharge Plasma," Plasma Science and Technology 9 (6) (2007).

153   Kuhn S, Bibinov N, Gesche R, and Awakowicz P, "Non-thermal atmospheric pressure HF plasma source: generation of nitric oxide and ozone for bio-medical applications " Plasma Sources Sci. Technol. 19 (2010).

154   Pipa A V, Bindemann T, Foest R, Kindel E, Ropcke J, and Weltmann K-D, "Absolute production rate measurements of nitric oxide by an atmospheric pressure plasma jet (APPJ)," J. Phys. D: Appl. Phys. 41 (2008).

155   and A. I. Gotlieb Wong M.K.K., "In vitro reendothelialization of a single-cell wound-role of microfilament bundles in rapid lamellipodia-mediated wound closure," Lab. Invest. 1 (51), 75-81 (1984).

156   Naoki Nakatsubo Hirotatsu Kojima, Kazuya Kikuchi, Shigenori Kawahara, Yutaka Kirino,Hiroshi Nagoshi, Yasunobu Hirata, and Tetsuo Nagano, "Detection and Imaging of Nitric Oxide with Novel Fluorescent Indicators: Diaminofluoresceins," Anal. Chem. (70), 2446-2453 (1998).

157   Deborah Morley Chris M. Maragos, David A. Wink, Tambra M. Dunams, Joseph E. Saavedra, Aaron Hoffman, Alfred A. Bove, Lawrence Isaac, Joseph A. Hrabie, and Larry

K. Keefer "Complexes of .NO with Nucleophiles as Agents for the Controlled Biological Release of Nitric Oxide. Vasorelaxant Effects," J. Med. Chem (34), 3242-3247 (1991).

158   Manish Keshive Bo Chen, and William M. Deen, "Diffusion and Reaction of Nitric Oxide in Suspension Cell Cultures," Biophysical Journal 75, 745–754 (1998).

159   Ian G. Zacharia and William M. Deen, "Diffusivity and Solubility of Nitric Oxide in Water and Saline," Annals of Biomedical Engineering 2 (33), 214–222 (2005).

160   S.E.; White Schwartz, W.H., "Solubility equilibria of the nitrogen oxides and oxyacids in dilute aqueous solution", in *Advances in Environmental Science and Engineering*, edited by J. R. Pfafflin and E. N. Ziegler (Gordon and Breach Science Publishers, NY, 1981), pp. 1-45.

161   Daniel R. Hyduke Tae H. Han, Mark W. Vaughn, Jon M. Fukuto, and James C. Liao, "Nitric oxide reaction with red blood cells and hemoglobin under heterogeneous conditions," PNAS 99 (11), 7763-7768 (2002).

162   Jennifer L. Caulfield Samar Burney, Jacquin C. Niles, John S. Wishnok, Steven R. Tannenbaum, "The chemistry of DNA damage from nitric oxide and peroxynitrite," Mutation Research (424), 37–49 (1999).

163   Attila Cziraki Andreas Papapetropoulos, Joseph W. Rubin, Christopher D. Stone, and John D. Catravas, "cGMP Accumulation and Gene Expression of Soluble Guanylate Cyclase in Human Vascular Tissue," Journal of Cellular Physiology (167), 213-221 (1996).

164   V.M. Darley-Usmar H. Rubbo, B.A. Freeman, "Nitric oxide regulation of tissue free radical injury," Chem. Res. Toxicol (9), 809–820 (1996).

165   Rhona Baxendale Lindsay Fawcett, Peter Stacey, Collette McGrouther, Ian Harrow, Scott Soderling, Joanna Hetman, Joseph A. Beavo, and Stephen C. Phillips, "Molecular cloning and characterization of a distinct human phosphodiesterase gene family: PDE11A," Proc.Natl.Acad.Sci.USA 7 (97), 3702-3707 (2000).

166   C.V. Patel M.S. Penn, M.Z. Cui, P.E. DiCorleto and G.M. Chisolm, "LDL increases inactive tissue factor on vascular smooth muscle cell surfaces: hydrogen peroxide activates latent cell surface tissue factor," Circulation 99, 1753–1759 (1999).

167   G.N. Semenkova A.A. Krjukov, S.N. Cherenkevich and V. Gerein, "Activation of redox-systems of monocytes by hydrogen peroxide," Biofactors 26, 283–292 (2006).

168   M.C. Capogrossi and J.L. Zweier B.S. Bochner, "Hydrogen peroxide and superoxide modulate leukocyte adhesion molecule expression and leukocyte endothelial adhesion," Biochim. Biophys. Acta 1310, 251–259 (1996).

169   S. Khanna C.K. Sen, B.M. Babior, T.K. Hunt, E.C. Ellison and S. Roy, " Oxidant-induced vascular endothelial growth factor expression in human keratinocytes and cutaneous wound healing," J. Biol. Chem. 277, 33284–33290 (2002).

170   G. Pani R. Colavitti, B. Bedogni, R. Anzevino, S. Borrello, J. Waltenberger and T. Galeotti, "Reactive oxygen species as downstream mediators of angiogenic signaling by vascular endothelial growth factor receptor-2/KDR," J. Biol. Chem. 277, 3101–3108 (2002).

171   S.J. Park S.O. Yoon, S.Y. Yoon, C.H. Yun and A.S. Chung, "Sustained production of H(2)O(2) activates pro-matrix metalloproteinase-2 through receptor tyrosine kinases/phosphatidylinositol 3-kinase/NF-kappa B pathway," J. Biol. Chem. 277, 30271–30282 (2002).

172   Yu Yang Ming Yang, Sui Zhang and Andrew M. Kahn, "Insulin-Stimulated Hydrogen Peroxide Increases Guanylate Cyclase Activity in Vascular Smooth Muscle," Hypertension (42), 569-573 (2003).

173   K. M. Mohazzab H. A. Omar, M. P. Mortelliti and M. S. Wolin, "O2-dependent modulation of calf pulmonary artery tone by lactate: potential role of H2O2 and cGMP," Am J Physiol Lung Cell Mol Physiol 264, L141-L145 (1993).

174   Chantale Lapierre Ja! nos G. Filep, Silvana Lachance and John S. D. Chan, "Nitric oxide co-operates with hydrogen peroxide in inducing DNA fragmentation and cell lysis in murine lymphoma cells," Biochem. J. 321, 897-901 (1997).

175   David A.Wink Roberto Pacelli, John A. Cook, Murali C. Krishna, William DeGraff, Norman Friedman, Maria Tsokos, Amram Samuni, and James B. Mitchell, "Nitric Oxide Potentiates Hydrogen Peroxide-induced Killing of Escherichia coli," The Journal of Experimental Medicine 182, 1469-1479 (November 1995).

176   Etelvino J.H. Bechara Paolo Di Mascio, Marisa H.G. Medeiros, Karlis Briviba, Helmut Sies, "Singlet molecular oxygen production in the reaction of peroxynitrite with hydrogen peroxide," FEBS Letters 355, 287-289 (1994).

177   Zhi-Jian Chen et al, "A realistic brain tissue phantom for intraparenchymal infusion studies," Journal of neurosurgery 101 (2) (2004).

178   Hirokazu Kato and Tetsuya Ishida, "Development of an agar phantom adaptable for simulation of various tissues in the range of 5-40 MHz," Phys. Med. Biol. 32 (2), 221-226 (1987).

179   Wu A Dobrynin D, Kalghatgi S, Park S, Shainsky N, Wasko K, Dumani E, Ownbey R, Joshi S, Sensenig R, Brooks A, "Live Pig Skin Tissue and Wound Toxicity of Cold Plasma Treatment," Plasma Medicine 1 (1), 93-108 (2011).

180   V. and Dobrynin Gostev, D., presented at the 3rd International Workshop on Microplasmas Greifswald, Germany, 2006 (unpublished).

181   Dobrynin D Chakravarthy K, Fridman G, Friedman G, Murthy S, Fridman A, "Cold Spark Discharge Plasma Treatment of Inflammatory Bowel Disease in an Animal Model of Ulcerative Colitis," Plasma Medicine 1 (1), 3-19 (2011).

182   T Shimizu and G E Morfill T Nosenko, "Designing plasmas for chronic wound disinfection," New J. Phys. 11 (2009).

183   Eric Robert Marc Vandamme, Sebastien Dozias, Julien Sobilo, Stephanie Lerondel, Alain Le Pape, Jean-Michel Pouvesle "Response of Human Glioma U87 Xenografted on Mice to Non Thermal Plasma Treatment
" Plasma Medicine 1 (1), 27-43 (2011).

184   Eric Robert Marc Vandamme, Sabrina Pesnel, Emerson Barbosa, Sébastien Dozias, Julien Sobilo, Stéphanie Lerondel, Alain Le Pape, Jean-Michel Pouvesle1, "Antitumor Effect of Plasma Treatment on U87 Glioma Xenografts: Preliminary Results," Plasma Processes and Polymers 7 (3-4), 264–273 (2010).

185   M.H.h. K. Oehmigen, R. Brandenburg, Ch. Wilke, K.-D. Weltmann, and T.v. Woedtke, "The Role of Acidification for Antimicrobial Activity of Atmospheric Pressure Plasma in Liquids," Plasma Process. Polym. 7 (3-4), 250–257 (2010).

186   J.-A. Domínguez-Rosales M. Rojkind, N. Nieto and P. Greenwel, "Role of hydrogen peroxide and oxidative stress in healing responses " Cellular and Molecular Life Sciences 59 (11), 1872-1891 (2002).

187   S. Malarvizhi Shanthi Prince, K. C. Aditya SreeHarsha, Anand Bhandari, Ankit Dua, presented at the Proceedings of the 2nd Biennial IEEE/RAS-EMBS International
Conference on Biomedical Robotics and Biomechatronics, Scottsdale, AZ, USA, October 19-22, 2008 (unpublished).

188   Steven A. Hackworth Laura E. Riley, Christopher Henry, Mingui Sun, Robert J. Sclabassi, David Hirsch, presented at the Bioengineering Conference, 2007. NEBC '07. IEEE 33rd Annual Northeast Long Island, NY 10-11 March 2007 (unpublished).

189   Harvey Diehl and Richard Markuszewski, "Studies on fluorescein—VII: The fluorescence of fluorescein as a function of pH " Talanta 36 (3), 416-418 (1989).

190   Harvey Diehl and Richard Markuszewski, "Studies on fluorescein—II: The solubility and acid dissociation constants of fluorescein in water solution," Talanta 32 (2), 159-165 (1985).

191   Harvey Diehl, "Studies on fluorescein—VIII: Notes on the mathematical work-up of absorbance data for systems with single and multiple dissociations, the limitations of the conventional logarithmic treatment, and the dissociation constants of fluorescein," Talanta 36 (7), 799-802 (1989).

192   Naomi Horchak-Morris Harvey Diehl, Alta J. Hefley, Linda F. Munson and Richard Markuszewski, "Studies on fluorescein—III : The acid strengths of fluorescein as shown by potentiometric titration," Talanta 33 (11), 901-905 (1986).

193   Monique M. Martin and Lars Lindqvist, "The pH dependence of fluorescein fluorescence," Journal of Luminescence 10 (6), 381-390 (1975).

194   S. Cheruthazhekatt, M. Cernak, P. Slavicek, and J. Havel, "Gas plasmas and plasma modified materials in medicine," Journal of Applied Biomedicine 8 (2), 55-66 (2010).

195   G. E. Morfill, M. G. Kong, and J. L. Zimmermann, "Focus on Plasma Medicine," New Journal of Physics 11 (2009).

196   F. Massines, N. Gherardi, N. Naude, and P. Segur, "Recent advances in the understanding of homogeneous dielectric barrier discharges," European Physical Journal-Applied Physics 47 (2) (2009).

197   M. Laroussi, "Low-Temperature Plasmas for Medicine?," Ieee Transactions on Plasma Science 37 (6), 714-725 (2009).

198   N. Y. Babaeva and M. J. Kushner, "Intracellular electric fields produced by dielectric barrier discharge treatment of skin," Journal of Physics D-Applied Physics 43 (18) (2010).

199   Z. Cao, Q. Nie, D. L. Bayliss, J. L. Walsh, C. S. Ren, D. Z. Wang, and M. G. Kong, "Spatially extended atmospheric plasma arrays," Plasma Sources Science & Technology 19 (2) (2010).

200   J. P. Sarrette, S. Cousty, N. Merbahi, A. Negre-Salvayre, and F. Clement, "Observation of antibacterial effects obtained at atmospheric and reduced pressures in afterglow conditions," European Physical Journal-Applied Physics 49 (1) (2010).

201   T. Nosenko, T. Shimizu, and G. E. Morfill, "Designing plasmas for chronic wound disinfection," New Journal of Physics 11 (2009).

202   X. Lu, Z. Xiong, F. Zhao, Y. Xian, Q. Xiong, W. Gong, C. Zou, Z. Jiang, and Y. Pan, "A simple atmospheric pressure room-temperature air plasma needle device for biomedical applications," Applied Physics Letters 95 (18) (2009).

203   D. Staack, B. Farouk, A. Gutsol, and A. Fridman, "Stabilization of the ionization overheating thermal instability in atmospheric pressure microplasmas," Journal of Applied Physics 106 (1) (2009).

204   A. Bekstein, M. Yousfi, M. Benhenni, O. Ducasse, and O. Eichwald, "Drift and reactions of positive tetratomic ions in dry, atmospheric air: Their effects on the dynamics of primary and secondary streamers," Journal of Applied Physics 107 (10) (2010).

205   H. Rauscher, O. Kylian, J. Benedikt, A. von Keudell, and F. Rossi, "Elimination of Biological Contaminations from Surfaces by Plasma Discharges: Chemical Sputtering," Chemphyschem 11 (7), 1382-1389 (2010).

206   M. Yousfi, A. Bekstein, N. Merbahi, O. Eichwald, O. Ducasse, M. Benhenni, and J. P. Gardou, "Basic data for atmospheric pressure non-thermal plasma investigations in environmental and biomedical applications," Plasma Sources Science & Technology 19 (3) (2010).

207   G. Malovic, N. Puac, S. Lazovic, and Z. Petrovic, "Mass analysis of an atmospheric pressure plasma needle discharge," Plasma Sources Science & Technology 19 (3) (2010).

208   Q. Xiong, X. P. Lu, K. Ostrikov, Y. Xian, C. Zou, Z. Xiong, and Y. Pan, "Pulsed dc- and sine-wave-excited cold atmospheric plasma plumes: A comparative analysis," Physics of Plasmas 17 (4) (2010).

209   A. Shashurin, M. N. Shneider, A. Dogariu, R. B. Miles, and M. Keidar, "Temporary-resolved measurement of electron density in small atmospheric plasmas," Applied Physics Letters 96 (17) (2010).

210   G. Y. Park, Y. J. Hong, H. W. Lee, J. Y. Sim, and J. K. Lee, "A Global Model for the Identification of the Dominant Reactions for Atomic Oxygen in He/O-2 Atmospheric-Pressure Plasmas," Plasma Processes and Polymers 7 (3-4), 281-287 (2010).

211   Y. Xian, X. Lu, Z. Tang, Q. Xiong, W. Gong, D. Liu, Z. Jiang, and Y. Pan, "Optical and electrical diagnostics of an atmospheric pressure room-temperature plasma plume," Journal of Applied Physics 107 (6) (2010).

212   T. Sato, S. Ochiai, and T. Urayama, "Generation and transport mechanisms of chemical species by a post-discharge flow for inactivation of bacteria," New Journal of Physics 11 (2009).

213   A. Helmke, D. Hoffmeister, N. Mertens, S. Emmert, J. Schuette, and W. Vioel, "The acidification of lipid film surfaces by non-thermal DBD at atmospheric pressure in air," New Journal of Physics 11 (2009).

214   J. van Dijk, G. M. W. Kroesen, and A. Bogaerts, "Plasma modelling and numerical simulation," Journal of Physics D-Applied Physics 42 (19) (2009).

215   E. H. Leach, "Experimental Termal Burns, Eepecially the Moderate Temperature Burn," Exp Physiol 32 (1), 67-86 (1943).

216   T. Suzuki, T. Hirayamaa, K. Aiharab and Y. Hirohatab, "Experimental studies of moderate temperature burns," Burns 17 (6), 443-451 (1991).

217   AL Bloom, "Physiology of blood coagulation," Pathophysiology of Haemostasis and Thrombosis 20 (1), 14-29 (1990).

218   KG Mann, "Biochemistry and physiology of blood coagulation," Thrombosis and haemostasis 82 (2), 165 (1999).

219   VI Zarnitsina, FI Ataullakhanov, AI Lobanov, and OL Morozova, "Dynamics of spatially nonuniform patterning in the model of blood coagulation," Chaos: An Interdisciplinary Journal of Nonlinear Science 11, 57 (2001).

220   W Dzwinel, K Boryczko, and DA Yuen, "A discrete-particle model of blood dynamics in capillary vessels," Journal of colloid and interface science 258 (1), 163-173 (2003).

221   DN Ku, "Blood flow in arteries," Annual Review of Fluid Mechanics 29 (1), 399-434 (1997).

222   MJ Conlan, JW Rapley, and CM Cobb, "Biostimulation of wound healing by low-energy laser irradiation A review," Journal of clinical periodontology 23 (5), 492-496 (1996).

223   CP Kiritsy, AB Lynch, and SE Lynch, "Role of growth factors in cutaneous wound healing: a review," Critical Reviews in Oral Biology & Medicine 4 (5), 729 (1993).

224   AJ Singer and RAF Clark, "Cutaneous wound healing," New England journal of medicine 341 (10), 738 (1999).

225   I Langmuir, "Oscillations in Ionized Gases," Proceedings of the National Academy of Sciences of the United States of America 14 (8), 627-637 (1928).

226   G. G. Ginsberg, A. N. Barkun, J. J. Bosco, J. S. Burdick, G. A. Isenberg, N. L. Nakao, B. T. Petersen, W. B. Silverman, A. Slivka, and P. B. Kelsey, "The argon plasma coagulator," Gastrointestinal Endoscopy 55 (7), 807-810 (2002).

227   S.U. Kalghatgi, G. Fridman, M. Cooper, G. Nagaraj, M. Peddinghaus, M. Balasubramanian, V.N. Vasilets, A. Gutsol, A. Fridman, and G. Friedman, "Mechanism of Blood Coagulation by Nonthermal Atmospheric Pressure Dielectric Barrier Discharge Plasma," IEEE Transactions on Plasma Science 35 (5, Part 2), 1559-1566 (2007).

228   M. Laroussi, O. Minayeva, F. C. Dobbs, and J. Woods, "Spores Survivability After Exposure to Low-Temperature Plasmas," Plasma Science, IEEE Transactions on 34 (4), 1253-1256 (2006).

229   M Vandamme, E Robert, S Pesnel, E Barbosa, S Dozias, J Sobilo, S Lerondel, A Le Pape, and JM Pouvesle, "Antitumor Effect of Plasma Treatment on U87 Glioma Xenografts: Preliminary Results," Plasma Processes and Polymers 7 (3-4), 264-273 (2010).

230   WA Dorsett-Martin, "Rat models of skin wound healing: A review," Wound Repair and Regeneration 12 (6), 591-599 (2004).

231   JI Weitz, "A novel approach to thrombin inhibition* 1," Thrombosis Research 109, S17-S22 (2003).

232   M Elg, S Carlsson, and D Gustafsson, "Effects of agents, used to treat bleeding disorders, on bleeding time prolonged by a very high dose of a direct thrombin inhibitor in anesthesized rats and rabbits," Thrombosis Research 101 (3), 159-170 (2001).

233   G Fridman, A Shereshevsky, MM Jost, AD Brooks, A Fridman, A Gutsol, V Vasilets, and G Friedman, "Floating Electrode Dielectric Barrier Discharge Plasma in Air Promoting Apoptotic Behavior in Melanoma Skin Cancer Cell Lines," Plasma Chemistry and Plasma Processing 27 (2), 163-176 (2007).

234   J.P. Watson, *et al.*, "*Colonoscopic Argon Plasma Coagulation for Benign and Malignant Rectal Tumours* " Gut 40, Th156 (1997).

235   J.J. Vargo, "*Clinical Applications of the Argon Plasma Coagulator* " Gastrointestinal Endoscopy 59 (1), 81-88 (2004).

236   M K Bennett J P Watson, S M Griffin, K Matthewson, "The tissue effect of argon plasma coagulation on esophageal and gastric mucosa," Gastrointestinal endoscopy 52 (3), 342-345 (2000).

237   H.G. and S.W. Crawford Colt, "*In Vitro Study of the Safety Limits of Bronchoscopic Argon Plasma Coagulation in the Presence of Airway Stents* " Respirology 11 (5), 643-647 (2006).

238   E. Stoffels, *et al.*, "*Plasma Needle: A Non-Destructive Atmospheric Plasma Source for Fine Surface Treatment of (Bio)Materials*," Plasma Sources Science and Technology 11 (4), 383-388 (2002).

239   K.M. Anderson, *et al.*, "*Free Radicals and Reactive Oxygen Species in Programmed Cell Death* " Medical Hypotheses 52 (5), 451-463 (1999).

240   G.G. Ginsberg, *et al.*, "*The Argon Plasma Coagulator* " Gastrointestinal Endoscopy 55 (7), 807-810 (2002).

241   I.E. Kieft, *et al.*, "*Electric Discharge Plasmas Influence Attachment of Cultured Cho K1 Cells* " Bioelectromagnetics 25 (5), 362-368 (2004).

242   I.E. Kieft, M. Kurdi and E. Stoffels "*Reattachment and Apoptosis after Plasma-Needle Treatment of Cultured Cells* " Plasma Science, IEEE Transactions on 34 (4), 1331-1336 (2006).

243   McCarty Sonnenberg A., D. J. and Jacobsen, S. J., "Geographic variation of inflammatory bowel disease within the United States," Gastroenterology 100 (1), 143-149 (1991).

244   A. J Wakefield, Ekbom, A., Dhillon, A. P., Pittilo, R. M., and Pounder, R. E., "Crohn's disease: pathogenesis and persistent measles virus infection," *Gastroenterology* 108 (3), 911-916 (1995).

245   R. B. Sartor, "Pathogenesis and immune mechanisms of chronic inflammatory bowel diseases," *Gastroenterology* 92 (12 Suppl), 5S-11S (1997).

246   Besedin E Misyn F, Gostev V, Komkova O, "Experimental Studying of Bactericidal Action of Cold Plasma", in *Diagnostics and Treatment of Infectious Diseases* (Petrozavodsk, Russia, 2000).

247   Besedin EV Misyn FA, Komkova OP, Gostev VA, "Experimental Investigation of Bactericidal Influence of ''Cold'' Plasma and Its Interaction with Cornea", in *Diagnostics and Treatment of Infectious Diseases* (Petrozavodsk, Russia, 2000).

248   I.V. Reshetov, R.K. Kabisov, A.B. Shekhter, A.V. Pekshev, and M.V. Maneilova, "*The use of a "Plason" air-plasma apparatus for coagulation and NO-therapy in plastic reconstructive surgery for oncologic patients*," Annals of Plastic, Reconstructive and Aesthetic Surgery 4, 24-38 (2000).

249   A.B. Shekhter, R.K. Kabisov, A.V. Pekshev, N.P. Kozlov, and Y.L. Perov, "*Experimental and clinical validation of plasmadynamic therapy of wounds with nitric oxide*," Bulletin of Experimental Biology and Medicine 126 (2), 829-834 (1998).

250   A.B. Shekhter, V.A. Serezhenkov, T.G. Rudenko, A.V. Pekshev, and A.F. Vanin, "*Beneficial effect of gaseous nitric oxide on the healing of skin wounds*," Nitric Oxide-Biology and Chemistry 12 (4), 210-219 (2005).

251   Babb R., "Intestinal gas (Medical Information)," West J Med 127, 362-363 (Oct. 1977).

252   H. S. Cooper, Murthy, S. N., Shah, R. S., Sedergran, D. J., "Clinicopathologic study of dextran sulfate sodium experimental murine colitis. ," *Lab Invest* 69 (2), 238-249 (1993).

253   Pravda J., "Radical induction theory of ulcerative colitis," World J Gastroenterology 11 (16), 2371-2384 (2005).

VITA

Appointments
2007 – 2011   Graduate research fellow, Electrical and Computer Engineering Department, College of Engineering, Drexel University
2002 – 2007   Research fellow, Research and Educational Center "Plasma", Petrozavodsk State University, Russia

5 most significant publications:

1. Physical and Biological Mechanisms of Direct Plasma Interaction with Living Tissue, D Dobrynin, G Fridman, G Friedman, A Fridman, New J. Phys. 11 (2009) 115020 (26pp).

2. Direct and Controllable Nitric Oxide Delivery into Biological Media and Living Cells by a Pin-to-Hole Spark Discharge (PHD) Plasma, D Dobrynin, Krishna Priya Arjunan, Alexander Fridman, Gary Friedman, Alisa Morss Clyne, *J. Phys. D: Appl. Phys.* 44 (2011) 075201

3. Cold Plasma Inactivation of Bacillus cereus and Bacillus anthracis (Anthrax) Spores, Dobrynin, D.; Fridman, G.; Mukhin, Y.V.; Wynosky-Dolfi, M.A.; Rieger, J.; Rest, R.F.; Gutsol, A.F.; Fridman, A.; IEEE Transactions of Plasma Science, 38 (8), 2010, 1878 – 1884

4. Cold Spark Discharge Plasma Treatment of Inflammatory Bowel Disease in an Animal Model of Ulcerative Colitis, Kalyan Chakravarthy, Danil Dobrynin, Gregory Fridman, Gary Friedman, Sreekant Murthy, Alexander Fridman, Plasma Medicine Journal 1 1, 2011, 3-20

5. Live Pig Tissue and Wound Toxicity of Cold Plasma Treatment, Danil Dobrynin, Sameer Kalghatgi, Sin Park, Natalie Shainsky, Kimberly Wasko, Gregory Fridman, Ari Brooks, Gary Friedman, Alexander Fridman, Plasma Medicine Journal 1 1, 2011, 93-108

Professional memberships
• International Society of Plasma Medicine (founding member) March, 2009 – present
• Institute of Electrical and Electronic Engineers (IEEE) January, 2010 – present

Reviewer/referee for Journals
• Institute of Electrical and Electronic Engineers, Transactions on Plasma Science (IEEE TPS)
• Plasma Medicine Journal
• Journal of Applied Physics